STRATHCLYDE INSTITUTE OF PHARMACY & BIOMEDICAL SCIENCES

University of Strathclyde Science

Observation of the impact of reactive oxygen species-inducers on the metabolomes of pulmonary artery smooth muscle cells and retinal pigment epithelial cells

By

Abdulwahab A. S. Alamri

A Thesis Submitted in Fulfillment of the Requirements for the Award of Degree of Doctor of Philosophy in Strathclyde Institute of Pharmacy and Biomedical Sciences at the University of Strathclyde

2019

Declaration

'I declare that, except where specifically indicated, all the work presented in this report is my own and I am the sole author of all parts.'

Signed: _____

Date: _____

Acknowledgements

I wish to express my sincerest gratitude to Allah for providing me with health, commitment and patience to complete my PhD studies. I am deeply grateful to my principal supervisor, Dr David G Watson, for his immense support, continuous encouragement and motivation throughout my PhD studies. My thanks also extend to our collaborator Dr Xinhua Shu from Glasgow Caledonian University.

Particular thanks are owed to all my friends and colleagues in SIPBS for their support during my study.

I also wish to offer my sincere gratitude to my parents for their emotional support and prayers and to my brothers and sister for their encouragement. I am grateful to my wife and my kids for their patience, support and love.

Finally, I wish to thank the Saudi government represented in Hail University for sponsoring my PhD study.

Table of Contents

List of Figures

List of Tables

List of abbreviation

AMD	Age-related macular degeneration
ATP	Adenosine Triphosphate
CI	Confidence interval
CV-ANOVA	Cross Validated ANOVA
CVD	Cardiovascular diseases
GSH	Glutathione
GSSG	Glutathione disulphide
G3P	Glyceraldehyde 3-phosphate
GAPDH	Glyceraldehyde 3-phosphate dehydrogenase
DR	Diabetic retinopathy
HG	High glucose (25 mM glucose)
KO	Knockout cell type
LC	Liquid Chromatography
LC-MS	Liquid Chromatography-Mass Spectrometry

LG/NG	Normal glucose (5 mM glucose)
HG	High glucose (25 mM glucose)
m/z	Mass to Charge Ratio
mM	Millimolar mmol/l
MDA	Malondialdehyde
NADH	Nicotinamide Adenine Dinucleotide
NADPH	Nicotinamide adenine dinucleotide phosphate
OPLS-DA	Orthogonal Partial Least Squares Discriminant Analysis
OxLDL	Oxidized low-density lipoprotein
PAH	Pulmonary arterial hypertension
PASMC	Pulmonary artery smooth muscle cells
PCA	Principal Component Analysis
PPP	Pentose phosphate pathway
ROS	Reactive Oxygen Species
RPE	Retinal pigment epithelial cells

RSD	Relative Standard Deviation
SIMCA	Soft-Independent Modelling of Class Analogy
TSPO	Translocator Protein 18 kDa
VIP	Variable Importance in the Projection
WT	Wild-type

Papers published and posters presented

Papers

1. Alamri A, Burzangi AS, Coats P, Watson DG. Untargeted Metabolic Profiling Cell-Based Approach of Pulmonary Artery Smooth Muscle Cells in Response to High Glucose and the Effect of the Antioxidant Vitamins D and E. Metabolites [Internet]. 2018 Nov 30;8(4).

2. Alamri A, Biswas L, Watson D, Shu X, Alamri A, Biswas L, et al. Deletion of TSPO Resulted in Change of Metabolomic Profile in Retinal Pigment Epithelial Cells. Int J Mol Sci [Internet]. 2019 Mar 19;20(6):1387.

Posters

1. Alamri A, Watson DG, editors. Metabolomics profiling of pulmonary artery smooth muscle cells treated by nitric oxide donors. Scottish Metabolomics network meeting; 2016; Inverness.

2. Alamri A, Watson DG, editors. Effect of High glucose (25 mM) as oxidative stress inducer on the pulmonary artery SMCs. Scottish Metabolomics network meeting; 2017; Glasgow.

Abstract

Background: Endogenous and exogenous reactive oxygen species (ROS) inducers cause intracellular metabolic modifications leading eventually to serious diseases. Overproduction of ROS is associated with many diseases including diabetes, diabetic retinopathy and cardiovascular diseases (CVD). Exposing of different cell types to oxidative agents impair the cell redox status by primarily inducing the excessive generation of superoxide that is enzymatically converted to other forms of oxidative agents causing cell damage. The hyperglycaemia that occurs due to diabetes mellitus causes high ROS production. Identification of reliable markers that indicate metabolic alteration due to oxidative stress could enable a better understanding of many diseases in terms of diagnosis and treatment with therapeutic targets.

Aim: To identify the main metabolic markers that are influenced by ROS in pulmonary artery smooth muscle cells (PASMCs) and retinal pigment epithelial cells (RPE) in-vitro. To investigate the impact of anti-oxidant agents in attenuating the modifications that may appear due to the high production of ROS.

Study design and methodology: biological cell samples were prepared and collected for each of the four included studies based on the intervention of each study whether it is the impact of hyperglycaemia with or without vitamin as antioxidants and the impact of TSPO protein deletion. In the first study, PASMCs were exposed to diabetic-like conditions and either supplemented or not supplemented by anti-oxidant agents. In the following study, PASMCs were also

examined under hyperglycaemia in normoxic or hypoxic conditions. In the two other following studies, we investigated the impact of oxidised low density lipoprotein (OxLDL) and hyperglycaemia on the TSPO knockout and wildtype RPE cells. All studies were carried out utilizing high-performance liquid chromatography-mass spectrometry. We used untargeted metabolic profiling to detect comprehensive metabolic alterations that occurred intracellularly due to our interventions. MzMatch software was used to identify the metabolites present; multivariate and univariate analyses were employed to determine the most reliable metabolites as biomarkers for oxidative stress.

Results: The outcomes established that high glucose influences cell proliferation and enhances oxidative stress. The general metabolomics results show the induction of carbohydrate metabolism accompanied by activation of the pentose phosphate pathway (PPP) to boost the generation of NADPH as an antioxidant product. Amino acids were also disturbed while some of them were up-regulated and some others were down-regulated. Lipids were frequently the most influenced pathway suggesting that the cell membrane was damaged by ROS induction. Purines and pyrimidines, in addition, were influenced consequently due to the changes occurring in PPP metabolism.

Conclusion: These hypothesis-free metabolomics profiling studies have identified intracellular metabolites in PASMCs, and RPE cells which are differentially sensitive to the hyperglycaemia or oxidative stress inducers and may be useful to initiate

hypothesises about markers that can help to prevent or cure diseases where oxidative stress plays a role.

Chapter one

General introduction

1 Introduction:

1.1 The impact of oxidative stress on cellular metabolism

1.1.1 General background

Living organisms produce Reactive Oxygen Species (ROS) as a result of normal cellular metabolism. Reactive oxygen species (ROS) are molecules derived from oxygen, characterised by an unpaired electron in their outer orbital (1). At moderate concentrations, they act normally in the physiological cell processes, but at elevated concentrations, they produce hostile alterations to cellular components, such as lipids, proteins, and DNA which lead to the development of various diseases (2–4). Oxidative stress occurs when the formation of ROS surpasses the capability of the antioxidant defence mechanisms and the imbalance between oxidant/antioxidant occurring toward oxidants due to excessive production of ROS or depletion of antioxidants. Living organisms have incorporated antioxidant systems involving enzymatic and non-enzymatic antioxidants that regularly mop up the ROS to protect the cells from oxidative damage. However, in pathological circumstances, the antioxidant systems can be damaged.

Oxidative stress is described by a change of cell redox state towards a more oxidised environment verified by more pro-oxidant molecules than antioxidant, the effect of which is a growth in autoxidation and molecular impairment (5,6). Although at

present it is widely accepted that oxidants play an important role in cell signalling and consequent adaptive responses, the proportion of the positive impact or the negative consequences of oxidants is still controversial subject (7–9). Moreover, factors like the cause of ROS production, the time span of exposure to oxidants and personal characteristics all could contribute to impact the signalling cascade leading to a significant disturbance in the adaptive response (10).

High levels of ROS are related to oxidative stress and play a role in some disease pathogenesis including type II diabetes mellitus (T2DM) and cardiovascular diseases (CVD) (11,12). It also plays a key role in many other pathological disorders, including cancer, neurological disorders, (13–15) atherosclerosis, hypertension, ischemia/perfusion (16–18), acute respiratory distress syndrome, idiopathic pulmonary fibrosis, chronic obstructive pulmonary disease (19), and asthma (20). ROS cause cellular damage by oxidizing nucleic acids, proteins, and membrane lipids leading to alterations in the gene expression of antioxidant enzymes, stress-response genes, and cytokines.

ROS include free radicals, such as superoxide (O2-), hydroxyl radical (OH-), nitric oxide (NO), lipid radicals (LOO-), which have unpaired electrons with oxidising effects. They also include hydrogen peroxide (H_2O_2), hypochlorous acid (HOCl) and peroxynitrite (ONOO-). ROS includes free radicals and non-radicals. Molecules having one or more unpaired electrons and so giving reactivity to the molecule are called free radicals. A non-radical is created when two free radicals share their unpaired electrons. Free radicals are highly reactive components according to a spin

state that each electron has which at any time can be either positive or negative (21).

1.1.2 Source of ROS:

The mitochondrial electron transport chain (ETC) is part of normal cellular metabolism and is able to generate reactive species by firmly regulate enzymes such as Nitric Oxide Synthase (NOS) and NADPH oxidase, xanthine oxidase and xanthine dehydrogenase (22). Intracellular reduction of molecular oxygen produces superoxide (O2· –), hydrogen peroxide (H_2O_2) and hydroxyl radicals (HO·). Superoxide is the primary free radical that is formed from the univalent reduction of molecular oxygen (23) and is produced in the mitochondria throughout energy transduction reactions (24). The superoxide radical enters in a chain of "self-propagating" reactions leading to the formation of new radicals including hydrogen peroxide, hydroxyl, peroxyl, alkoxyl ascorbyl, singlet oxygen, as well as nitrogen radicals such as peroxynitrite (25). Other intracellular sources that may produce superoxide are NADPH, oxidases of phagocytes, 5-lipoxygenase and xanthine oxidase.

In addition to these endogenous sources of reactive species, there are exogenous sources that may further increase the large endogenous oxidant load. Exogenous mediators include chemical carcinogens, UV and ionizing radiations. Moreover, bacterial and viral infections trigger the production of reactive oxygen (ROS) and nitrogen (RNS) species (26)

1.1.3 Physiology of reactive species:

It is crucial to maintain cellular redox balance via oxidants and antioxidant equilibrium to preserve the cell's health. ROS keep the cell redox state within the physiological limits under normal conditions via effective enzymatic and non-enzymatic defence mechanisms. Enzymatic factors such as glutathione reductase and superoxide dismutase and non-enzymatic factors such as Vitamin E and C prevailing in living organisms play an intrinsic role as antioxidants (27). Glutathione (GSH) is the most important endogenous antioxidant which is abundant in the cytosol, mitochondria and the cell nucleus. It is synthesized by the successive enzymatic reactions of glutathione synthetase and rate limiting enzyme (glutamate-cysteine ligase). In the cell nucleus, GSH preserves the redox state of thiol groups (R-SH) of proteins essential for the restoration and expression of DNA. Moreover, it acts as a cofactor for numerous de-toxifying enzymes such as glutathione peroxidase and glutathione transferase, involved in the process of amino acid transport through the plasma membrane, serves as a scavenger of OH· and superoxide, de-toxifies H_2O_2 and lipid peroxides and supports in the restoration of vitamins C and E (28). Because of these actions, enzymatic and non-enzymatic anti-oxidant components modulate the balance status of oxidant/antioxidant reactions and therefore conserve the accurate balance between favourable and damaging impacts of free radicals due to redox regulation.

There are several signalling pathways that respond to redox imbalance of the cell including platelet-derived growth factor (PDGFs), cytokines, interleukins, mitogen-

activating protein kinases (MAPKs), transforming growth factor (TGF). ROS endogenous levels regulate these pathways by acting on various levels in “signal transduction cascades” and, consequently, modulate the proliferation, differentiation and cell division (22). Expression of genes stimulated by redox mechanisms and adjusting proliferation, apoptosis and cell differentiation mutate by these reactive species (29). Hence, interruption of that balance transmits oxidative stress, and so, these reactive species will interfere with the physiological functions of cells directly by disrupting lipids, proteins and carbohydrates or indirectly through mutations as a result of DNA base modification (30).

1.1.4 Implications of oxidative stress:

Overproduction of reactive species as discussed previously ultimately influence living organisms and long-term exposure to ROS leads to cell damage. Cardiovascular diseases, diabetes and neurodegeneration, are the most common consequences of increased DNA oxidation.

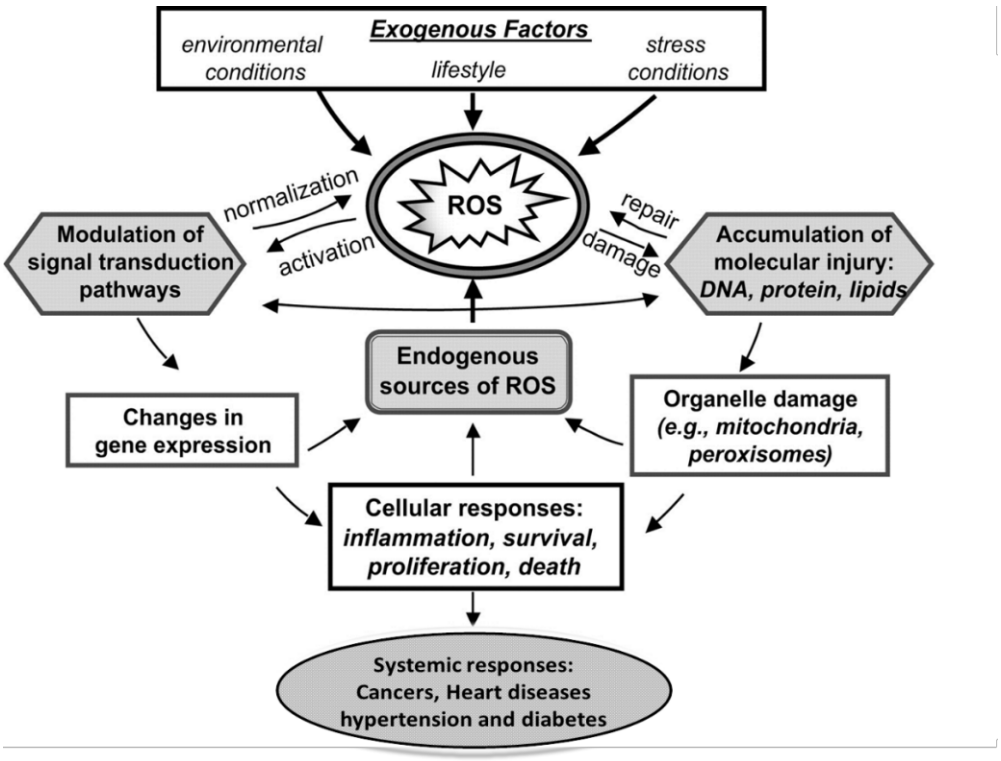

Figure 1-1: Summary of the proposal by which ROS could initiate and contribute to undesired systemic responses.

1.1.4.1 Effects of Oxidative Stress on DNA:

Reactive species can lead to DNA alterations in several manners, including single- or double-stranded DNA breaks, pyrimidine, purine, mutations, and cross-linking with proteins. These DNA alterations are applicable to cardiovascular, ageing, neurodegeneration, carcinogenesis, and autoimmune diseases as oxidation of DNA modifies the sequence of numerous nucleotides along with the alteration of bases. Endogenous and exogenous ROS factors that cause DNA lesions involved in many diseases pathogenesis are able to produce free radicals able to bind with thiol groups of the amino acids. 8-Hydroxyguanosine (8-OHG) formation is the best-

identified marker of DNA damage occurring due to oxidative stress and is a significant biomarker for carcinogenesis, cardiovascular diseases and some other pathogenic states (3,28,31). It is formed due to the attack of ROS at the C-8 position of 2- deoxyguanosine and is also known to be the product of pro-mutagenic base modification.

Provider regions of genes have sequences for transcription factors. These transcription factors–binding sites are comprised of guanine-cytosine (G-C) sequences that are susceptible to oxidative attack. 8-OHG formation modifies the enzyme-catalysed methylation of cytosine that is significant for the regulation of gene expression (22). Even though such modification is high in oxidative stress, "base excision repair" provides a restoration mechanism and DNA breaks due to oxidant injury can easily be tolerated by cells. However, when DNA replication takes place prior to the restoration of this altered base (8-OHG) that will result in trans version mutations of (G-C) to thymine and adenine (T-A) that are correspondingly found in genes whose dysfunction is involved in the genesis of cancer.

Cysteine residue oxidation could form reversible mixed disulphides between protein thiol groups (−SH) and low molecular weight thiol (GSH). Oxidative attack of Proteins leads to oxidative cleavage, loss of histidine residues and formation of protein centred alkyl R·, alkoxyl RO· and alkyl peroxyl ROO· radicals. Formation of these oxidised side chain amino acids cause loss of protein catalytic vigour and proteins become more susceptible to proteolytic degradation (32).

1.1.4.2 Effect of oxidative stress on the lipids:

Reactive species can cause significant damage to the lipid components of cell membranes, mitochondrial membranes, endoplasmic reticulum membranes and nuclear membranes leading to an overall decline in membrane integrity (33). Lipids are vulnerable targets of ROS because of their molecular structures contain abundant reactive double bonds (34). Reactive species can encourage lipid peroxidation and interrupt the lipid membrane bilayer that may deactivate membrane-bound receptors and enzymes leading to loss of membrane fluidity and elasticity, permeability, impaired cellular functioning, and even cell lysis. Lipid peroxidation appears as a result of a series of reactions starting with a single extracted hydrogen from an unsaturated fatty acid. The extraction of the hydrogen counteracts the original radical and forms a lipid radical which integrates with oxygen to produce a very unstable lipid peroxyl radical (LOO•) which then further reacts with nearby fatty acids in a self-propagating process of lipid peroxidation (35).

Within cell membranes, ROS oxidise polyunsaturated free-fatty acids (PUFA) and increase in turn the formation of lipid peroxides and generate other ROS such as peroxyl (ROO-) or hydroperoxides (ROOH) and substances such as malondialdehyde (MDA) (33).

Lipid peroxidation products such as MDA, isoprostanes and 4-hydroxynonenal are identified among significant oxidative stress biomarkers and are able to deactivate various cellular proteins by protein cross-link formation. MDA is a reactive carbonyl

compound known to be mutagenic, atherogenic and carcinogenic. Its reaction with lysine residues forms lysine–lysine cross-links which have been detected in the apolipoprotein B (apoB) fragment of oxidized low-density lipoprotein (OxLDL) and has been hypothesized that it disrupts the interaction between OxLDL and macrophages and thereby enhances atherosclerosis (36).

In addition to causing cell membrane impairment lipid peroxidation also changes the intracellular liquids, minimizing the calcium transport in the endoplasmic reticulum, influencing mitochondrial function, cell modifications and causing deficiency of proteins and enzymes (37). Therefore, lipid peroxidation provides two main paths for oxidative damage. Firstly, in the generating and increasing of lipid-derived ROS which form radical products which react with, lipids, proteins, carbohydrates and DNA (37). Secondly, the oxidation of membrane-bound lipids leads to a reduction in the membrane integrity, making cellular components accessible to attack from pathogens and other ROS inducers.

1.1.4.3 Effect of oxidative stress on protein

ROS can react with amino side chains of proteins or their molecular backbone (38). Potent ROS react spontaneously and non-specifically with proteins, but the impact of less potent ROS may be restricted via individual protein structure, redox potential and availability of oxidizable sites (39). So, amino acid such as methionine and cysteine with side chains that are rich in electrons are at high danger of oxidation (40). ROS-protein reactions may form new reactive species and/or instant modification to proteins may happen.

The impacts of protein oxidation can be harming making proteins unable to function efficiently and leading to their destruction. Harmed proteins, in turn, influence intracellular pathways and play a key role as a causative factors to various disorders including Alzheimer's disease (AD), rheumatoid arthritis, diabetes, sepsis, chronic renal failure, and respiratory distress syndrome (41). If the proteolytic systems that mediate the process of protein degradation do not function appropriately, modified proteins may accumulate in the cell and engage in the progression of pathological conditions. Different studies demonstrate how several types of ROS-induced protein alteration occur via the loss of sulfhydryl (−SH) groups among other modifications including the formation of carbonyls, disulphide crosslinks, methionine sulfoxide, and dityrosine cross-links (42–44). Loss of protein sulfhydryl groups could be prompted via different ROS species and is reported amongst the most immediate response to an increase in the oxidative stress level (42). Sulfhydryl group loss has a functional consequence leading to protein misfolding, catalytic suppression, diminished anti-oxidative efficiency, and loss of specific functions such as albumin binding to the heavy metals and sulphur-containing amino acids (45).

1.1.4.4 Cell signalling

Inter and intra-cellular signalling is part of a complex system of communication that mediates cell functions and initiating a variety of cellular activity including cell death, cell growth, up and down-regulation of genes and proteins, cell proliferation, muscular contraction and relaxation and differentiation and nerve transmission (46–48). Cell signalling appears in response to alteration or signal, launched by

ligand binding to a receptor, which may be intra or extracellular. This could trigger an impact, such as an alteration in cell membrane permeability, activate receptor kinases or activate regulatory proteins. ROS can react with membrane receptors and changing intermediates in cell transduction pathways and altering the signal response consequently (49). This could happen immediately by ROS reaction with other molecules associated with signalling cascades (50). For instance, the human protein tyrosine phosphatases are enzymes that contribute to the regulation of numerous signalling molecules (51). These contain a functioning site which is vulnerable to reversible alteration by hydrogen peroxide (49). Consequently, phosphorylation catalysed via protein tyrosine phosphatases can be mediated by hydrogen peroxide. As a result of ROS signalling, modification in gene expression and protein up-regulation could lead to cell adaptations (52).

1.2 High glucose "diabetic-like conditions" and reactive oxygen species

Diabetes is a chronic metabolic disorder characterized by elevated plasma glucose levels (generally fasting plasma glucose (FPG) is ≥126 mg/dL) due to the defects in insulin secretion or insulin action or both. The chronic hyperglycaemia of diabetes induces several pathophysiological complications including cardiovascular abnormalities, neural retinal and renal diseases (53–55). There are two types of diabetes: diabetes type 1 known or insulin-dependent diabetes mellitus (IDDM) and diabetes type 2 or non-insulin-dependent diabetes mellitus (NIDDM). Type 1 diabetes is principally triggered via cellular-regulated autoimmune destruction of

the pancreatic cells (β-cells) and accounts for about 5–10% of diabetic patients. On the contrary, type 2 diabetes is described by insulin resistance with a proportional shortage of insulin and accounts for 90–95% of diagnosed cases (56).

1.2.1 Diabetic induce ROS

It has been demonstrated that a variety of tissues produce ROS under high glucose conditions (57). Accumulated evidence illustrating that the metabolic dysregulation of diabetes via different mechanisms causes mitochondrial superoxide overproduction (58,59). These pathways underlying hyperglycaemia-induced diabetic vascular damage including induction of glucose flux via the polyol pathway, the excess formation of intracellular advanced glycation end-products (AGEs), increased the expression of the AGEs receptor and its activating ligands, stimulation of protein kinase C (PKC), and over promotion of the hexosamine pathway. However, clinical studies (60,61) failed to demonstrate any clinical progress when only one of these mechanisms was suppressed which could assist the theory stated that all these mechanisms might be stimulated by a single upstream incident: the overproduction of mitochondrial ROS (58,62).

A specific inhibitor that has been used in cell culture or animal models to inhibit aldose reductase activity, AGE formation, receptor for AGE ligand binding, PKC activation, and hexosamine pathway flux was able to improve various diabetes-induced abnormalities (63–66). In addition, the abnormalities of all these pathways were rapidly corrected when the glucose level was restored to the normal level which complicates the explanation of hyperglycaemic memory phenomena. This

demonstrates that all of these different pathogenic mechanisms stem from a hyperglycaemia-induced process, specifically overproduction of superoxide via the mitochondrial electron-transport chain. Superoxide is the first form of oxygen free radical that is converted later to other further reactive oxygen species able to damage cells (67).

Under normal conditions, electron transfer complexes I, III and IV are responsible for proton pump outwards to the intermembrane space, creating a proton gradient that initiatives ATP synthase (Complex V) because the protons pump back into the matrix via the inner membrane (see figure 1-2).

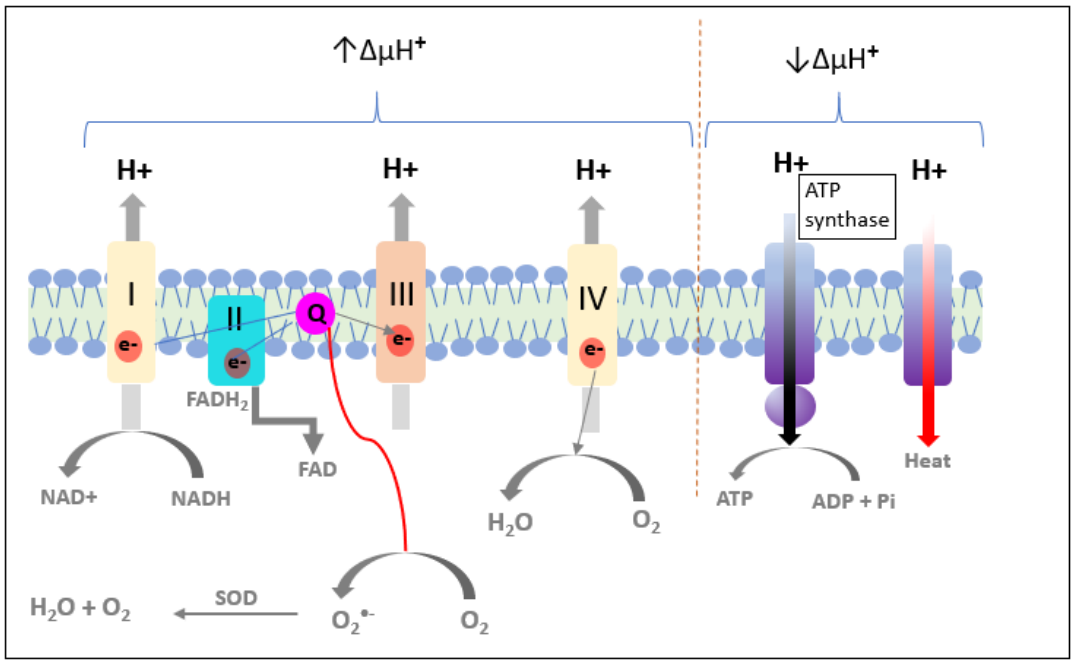

Figure 1-2: Production of ROS by the mitochondrial electron transport chain.

NADH and $FADH_2$ as main electron donors are produced through the tricarboxylic acid (TCA) cycle. The flow of the donated electrons (e−) through the electron-transport chain in the inner mitochondrial membrane drives H+ ions into the intermembrane space. When the voltage gradient is high due to increased flux of electron donors, more superoxide is generated. (Adapted From (68))

On the contrary, in diabetic conditions with intracellular hyperglycaemia, there is extra glucose-derived pyruvate being oxidized in the Krebs cycle inducing the outflow of electron donors (NADH and $FADH_2$) into the electron transport chain. Consequently, the voltage gradient over the mitochondrial membrane increases until it reaches a critical threshold. Then, electron transfer via complex III is blocked (69), increasing the electrons to back up to coenzyme Q, which gives the electrons one at a time to molecular oxygen, thus generating superoxide (see figure 1-2). The isoform of superoxide dismutase enzyme in the mitochondria degrades this oxygen free radical to hydrogen peroxide (H_2O_2), which is thereafter converted to H_2O and O_2 by other enzymes. Intracellular hyperglycaemia of arterial endothelial cells in culture has been demonstrated to increase superoxide production necessarily by increasing the voltage across the mitochondrial membrane above the critical threshold (70). It has also been established that hyperglycaemia-induced overproduction of ROS causes dynamic alteration in mitochondrial morphology. In the vascular endothelium, neither increased fatty acid oxidation nor hyperglycaemia increases ROS nor stimulates any of the mechanisms when either the mitochondrial membrane voltage gradient is suppressed by uncoupling protein 1 (UCP-1) or when the formed superoxide is degraded by superoxide dismutase (SOD) (71). While it is obvious that the mitochondria are essential for the promoting of hyperglycaemia-induced superoxide formation, considerable evidence suggests that this, conversely, may trigger a number of other superoxide generating mechanisms that could increase the main destructive effect of hyperglycaemia. These mechanisms include NADPH oxidases, redox imbalance, and uncoupled eNOS.

Overexpression of SOD was found to preserve the cardiac mitochondria against oxidative damage, enhances respiration and normalizes mass in diabetic mitochondria (72). It also prevents the diabetic heart from undergoing morphological alterations and totally standardizes contractility in diabetic cardiomyocytes (73).

Inhibition of glyceraldehyde 3-phosphate dehydrogenase (GAPDH) plays a key role in hyperglycaemia-induced mitochondrial superoxide production and to activate the mechanism of polyol pathway flux, the formation of advanced glycation end products (AGEs), activation of protein kinase C (PKC) and hexosamine pathway flux. GAPDH catalyses the conversion of glyceraldehyde 3-phosphate (G3P) to 1,3 bisphosphoglycerate as a sixth step in the glycolysis and drives the process towards the TCA cycle. Inhibition of this enzyme by hyperglycaemia-induce ROS, increases the upstream level of all the glycolytic intermediates. Accumulation of (G-3P), as a consequence of GAPDH inhibition, activates the AGEs pathway and PKC pathway directly. It activates the AGEs pathway because methylglyoxal as a -major intracellular AGE precursor- is formed from glyceraldehyde-3 phosphate. G3P also formed diacylglycerol the activating cofactor for the classic isoforms of protein kinase. Inhibition of GAPDH increases the level of early pathway glycolytic intermediates including glucose and fructose 6-phosphate (F6P) which, in turn, activates the polyol pathway via glucose conversion to sorbitol and activates the hexosamine pathway where F6P converts to uridine diphosphate (UDP)–N acetylglucosamine (68).

Use of UCP-1 or MnSOD to prevent mitochondrial overproduction of superoxide in hyperglycaemic cells helps to protect against GAPDH inhibition. When the GAPDH enzyme was inhibited by antisense DNA in normal glucose conditions, its level was found to be reduced to the level of hyperglycaemic conditions. In addition, inhibition of that enzyme in the normal glucose conditions was also found to activate the pathways that were elevated to the same extent as promoted by hyperglycaemia (74).

The ability of cells to resist oxidative stress damage is determined by the bulk of a selection of antioxidant defence systems, among which reduced glutathione (GSH) is the most abundant available within cells. GSH is a tripeptide made from glutamate, cysteine, and glycine in binary steps catalysed by “γ-l-glutamyl-l-cysteine: glycine ligase” and glutathione synthetase. Its physiological functions including its role as a potent defence mechanism against oxidative stress in addition to affecting the regulatory pathway of cellular signalling which has made it a subject of interest for many researchers (75). Moreover, GSH homeostasis plays an important role in different processes including the mediating of cellular proliferation, apoptosis and the post-transcriptional modification of proteins through S-glutathionylation. Nevertheless, dysfunction of GSH homeostasis was found to contribute to the pathobiology of neurodegenerative disorders, pulmonary and cardiovascular diseases, as well as the chronic age-related diseases (76,77). GSH exists in two forms: reduced glutathione GSH and oxidized form (GSSG) while the comparative amounts of each define the redox status of a cell. The cell ratio of GSH/GSSG at rest is 100:1 whereas this ratio is reduced to be about 10:1 when cell

is exposed to oxidative stress (78). Imbalance or qualitative and quantitative changes of the GSH/GSSG ratio are considered as a marker of oxidative damage (22). Glutathione peroxidase (GPx) regulates the enzymatic oxidation of GSH and leads to GSSG formation, while GSH is intracellularly restored by glutathione reductase (GR) in an NADPH-dependent process (79). Physiologically, the activity of GR and the accessibility of NADPH are essential to maintain the molar proportion of GSSG:GSH at about 1:100 to 1:1000 (80). However, during oxidative stress or when GR activity is reduced due to GAPDH deficiency for example, then, GSSG accumulates, and the GSH/GSSG ratio is impaired (81).

Importantly, NADPH plays a critical role as reaction cofactor to convert oxidized glutathione GSSG into two molecules of reduced glutathione GSH (82). Therefore, the dysregulation or depletion of NADPH via the polyol pathway, for example, may influence the redox states of GSH. Moreover, the PPP acts as an oxidative defence in the cells by producing NADPH. Oxidative stress induces the enzyme known as glucose-6-phosphate dehydrogenase (G6PD) which acts as the rate-limiting enzyme of the PPP (83). Stimulation of this enzyme induces the PPP to produce further NADPH to attenuate the increase of oxidative stress states.

1.2.2 Hypoxia and ROS

Hypoxia is a situation that occurs when a body or a part of the body has insufficient oxygen supply at the tissue level. This can arise due to environmental circumstances such as a decrease in atmospheric pressure due to high altitude (84), throughout exercise (85) or due to pathological situations (86,87). Acute or chronic hypoxic

exposure has been linked to an increase in ROS production, lipid peroxidation and DNA oxidation (88,89). After three weeks living at high altitude, a noticeable induction of oxidative damage was found, consistent with a reduction in antioxidant enzymes GSH and SOD (89). Likewise, staying at high altitude for 44 days lead to a substantial increase in hydrogen peroxide (90).

An increase in ROS levels is frequently observed during hypoxia, despite a reduction in the oxygen flux to the mitochondria and blood vessels (91). The production of mitochondrial and non - mitochondrial ROS in hypoxia mainly occurs as a consequence of a reductive state due to the accumulation of reducing equivalents observed during the absence of oxygen (92). The subsequent increase in free electrons increases the potential for reductive reactions, as seen with the formation of superoxide from oxygen through enzymatic and non - enzymatic mechanisms (91). Complex III in the mitochondrial electron transport chain of cell mitochondria has been indicated as a principal source of ROS in hypoxia (93).

1.2.3 Diabetic complications

As illustrated previously, diabetic states or hyperglycaemia increase oxidative stress which leads to the disturbance of many relative metabolites and pathways. Prolonged exposure to elevated glucose in the blood circulation affects the blood vessels that may start to get damaged, and this can lead to serious heart, renal and retinal complications (94–96). Evidence suggests that hyperglycaemia causes the excessive production of the ROS of vascular cells as agents of the oxidative stress involved in the pathogenesis of subsequent cardiovascular complications (97).

Under hyperglycaemic conditions, the resulting complications are either macrovascular complications include accelerating cardiovascular disease, or microvascular complications include eye disease, kidney disease and neural damage. Diabetes increases the risk of cardiovascular diseases in which it has been shown that the subjects with diabetes have a risk of myocardial infarction (MI) equal to that of non-diabetic subjects who have had the incidence of MI previously (98). Cardiovascular diseases account for a high percentage of mortality among diabetes patients (99), and diabetes subjects are at threefold higher risk of getting MI compared to a control population (100). Many studies, in addition, exhibited an association between diabetic and pulmonary hypertension (101–103).

Diabetes can also impair the retina cells causing what it knew by diabetic retinopathy (DR). DR is a microvasculopathy characterized by serum leaks of microvasculature, increased vascular permeability, and loss of capillaries in the early stage of disease (104). Diabetic retinopathy progresses over several years, and almost all type 1 diabetes patients (105), and the majority of type 2 diabetes (106) reveal some retinal lesions at some point after 20 years of the disease. Study of meta-analysis including 35 studies conducted over the world between 1980 and 2008, predicted the global incidence of DR to be 35.4% among diabetes patients (107).

Fluctuations in hemodynamic are correlated with changes in the systemic blood pressure and the blood pressure within the kidney, have been reported to arise early in diabetes. Diabetic kidney disease (DKD) is a considerable complication that

takes place in 20% to 40% of all diabetics (108). Due to the high prevalence of diabetes disease globally while it is predicted to affect about 8% of the population by the end of the coming 15 years (109). It has been estimated that more than 40% of diabetes subjects will DKD (110), including a significant number who may develop end-stage kidney disease needing renal replacement therapies.

1.2.4 Antioxidants

The human body has a variety of antioxidants that act to counterbalance the impact of oxidants. These antioxidants either enzymatic such as SOD. Catalase, glutathione peroxidase, glutathione transferase, thioredoxin and peroxiredoxin or non-enzymatic such as GSH, vitamin A, C and E (28). NADPH bioavailability is critical for enzymatic antioxidant as a reducing equivalent. NADPH preserves the active form of catalase and is used as a cofactor by GSH reductase to restore GSH from glutathione oxidized form. Intracellular NADPH, in contrast, is obtained by the NADP+ reduction via glucose-6-phosphate dehydrogenase, the first and rate-limiting enzyme of the PPP, through the conversion of glucose-6-phosphate to 6-phosphogluconolactone. Therefore, NADPH production and GAPDH play a critical role in the determination of the cytosolic GSH level, and so they can be considered as important regulatory antioxidant enzymes.

The non-enzymatic antioxidant vitamin C provides aqueous phase antioxidant capacity mainly by scavenging oxygen-containing free radicals. It transforms free radicals of vitamin E back to vitamin E. It has been shown that its plasma levels

decrease with age (111). In the hydrophobic interior of the cell membrane, the lipid soluble vitamin E is the main defence against oxidant-induced membrane injury.

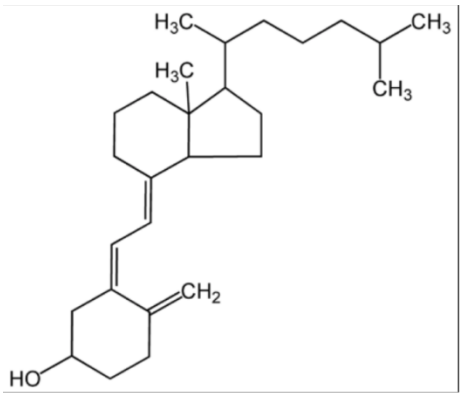

Vitamin D (Cholecalciferol)

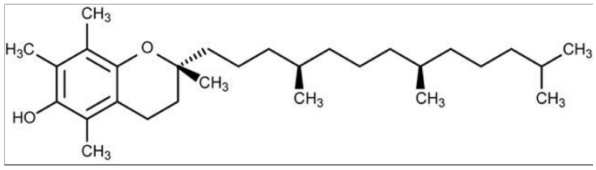

Vitamin E (Alpha-tocopherol)

Figure 1-3: The chemical structures of vitamin D and E

α-Tocopherol is the ultimate active form of vitamin E and the principal cell-bound membrane antioxidant. Vitamin E stimulates cancer cell apoptosis and obstructs free radical formation (112). Vitamin D active form, which is either in the form of vitamin D3 (cholecalciferol) or vitamin D2 (ergocalciferol), is also a lipid-soluble vitamin that is metabolized to cholecalciferol and has antioxidant properties among many different biological effects. There is evidence demonstrating that the deficiency of vitamin D is associated with many different diseases (113–115). Vitamin D contributes to the avoidance of many chronic diseases such as CVD, diabetes and kidney diseases by controlling of oxidative stress via several mechanisms including the induction of enzymes involved in the antioxidant defence system such as GSH peroxidase and SOD and also suppressing the expression of

NADPH oxidase (116). However, the impact of vitamin D as antioxidant still controversial and needs further investigation.

1.2.5 In-vitro culture model

Cell culture is an aseptic culture of prokaryotic and eukaryotic cells in a completely controlled environmental condition. Cells in the cell culture maintained in an artificial environment contain suitable media prepared with nutrients, growth factor, gases and the treatment if applicable and monitored mostly by automated system. So, the main advantage of the cell culture system is the control of physiochemical environment in the culture system. Models of cell culture are important tools for understanding the pathways of cells disturbed during processes of disease. So, it seems to be critical to observed ROS-mediated damage resulting from ROS produced and retained within the cells. The use of cell culture helps to understand the pathophysiological processes and metabolic modification that may occur due to the induction of ROS generation. The culture models for the current project were oxidatively stressed using media with elevated glucose level “hyperglycaemic condition”, hypoxia conditions, by using oxidized low-density lipoprotein (oxLDL) agent and/or deletion of TSPO protein. Given that these conditions going to influence the oxidative stress in treated cells, the agents of vitamin D and vitamin E were also used to examine their action as antioxidants.

The present study established used cell culture models of retinal pigment epithelial cells (RPEs), and pulmonary artery smooth muscle cells (PASMCs) and the effects of treatments were investigated using metabolomics techniques. Metabolomics of cell

cultures can be used to identify pathological biomarkers and metabolic pathways that produce such biomarkers. Cell metabolomics analysis has several potential applications and benefits comparing to other models being used currently in the postgenomic era.

1.3 Metabolomics

Metabolomics is one of the recently established sciences interested in the study of low molecular weight organic and non-organic metabolites in biological systems (mammalian cells, tissues or bio fluids) focusing on the study and detection of the complete set of small molecules metabolites which represent the intermediate or end products of the cellular process. Metabolomics is defined as the unbiased, inclusive detection and quantification of the total metabolome in a certain environment with high selectivity and sensitivity analytical techniques (117). Metabolomics along with other “omics” such as proteomics and genomics has arisen along with a better understanding of the complications of different diseases and a desire for their comprehensive evaluation.

Metabolic profiling/metabolomics could provide an immediate and robust indication of the cell physiology. Cells and tissues have a unique “metabolomics fingerprint” that contains cell-specific information and represents a specific biological process so, any change of that metabolite may lead to an alteration in the biological system. Metabolomics has a promising future for early diagnosis and understanding of various diseases pathogenesis and potentially to help develop current therapy or establish a new therapeutic target. Over the past several years,

there was a noticeable rise in the detection of the metabolites biomarkers that were involved in human diseases as a marker or initiating new drug therapy. A better understanding of the molecular level in biological systems may improve early diagnosis and prognosis of specific diseases, especially when combined with genomics and proteomics information (118). Recent reports illustrate the ability of the proteomics and genomics to identify known and unknown biomarkers of pulmonary hypertension and other morbidity diseases such as cancer (119,120). The advantage of metabolomics is represented in its ability to detect hundreds of metabolites which reveal an effective method for managing altered biochemistry. According to the Human Metabolome database, there are more than 15000 measurable metabolites in the human body, and around 700 metabolic and disease pathway diagrams have been described. Moreover, changes of metabolite concentrations are often increased which makes the detection of metabolite profiles a reasonably sensitive and accurate measurement of biological status in comparison to those of gene expression or protein levels (121,122).

In the metabolomics research, the analysis of the sample must be accomplished with an unbiased method, operating a robust and reproducible technique also preserving extraordinary levels of accuracy and sensitivity.

1.3.1 Applications of Metabolomics:

Within a living cell, metabolomics enables the investigation and detection of endogenous biochemical reaction products, elucidating information on the

particular metabolic pathways and revealing connections among different pathways that operate within the living cell.

Cell metabolomics relies on four sequential phases: (a) reliable preparation and extraction of samples, (b) profiling techniques able to identify low-weight molecules (Metabolites) such as NMR or mass spectrometer (c) pattern recognition approaches (example: MzMine, MzMatch) and bioinformatics data analysis (example: SIMCA-P), (d) metabolite identification resulting in putative biomarkers and molecular targets.

1.3.2 Approaches to metabolome analysis

Metabolic profiling studies of different disease conditions or treatments can be based on targeted, semi-targeted or un-targeted metabolomics (123). Semi-targeted metabolomics analysis varies from untargeted method since it needs to confirm the structures of the identified metabolites in the sample. In turn, the fully targeted method already defined the metabolites prior to sample analysis and the procedure is adjusted to give high precision, accuracy and selectivity for the metabolite being targeted, making the targeted approach substantially quantitative. Therefore, the targeted method employs the results that are initially generated from untargeted or semi-targeted studies to justify using robust techniques involving authentic standards. Ultimate identification of the significant biomarkers via targeted metabolomics assist in providing a definitive conclusion about their biological relevance in relation to the hypothesis initiated in the first place based on the untargeted method.

Untargeted approaches of metabolic profiling can identify up to thousands of metabolites with restricted or no previous knowledge of the metabolite profile in a given sample. During this technique, samples are analysed, and the subsequent data evaluated using obtainable tools. In turn, the results achieved allow the researcher to originate a hypothesis rely on the substantial interpretations obtained from the data. This approach involves a lot of metabolites some of which are not detected and certainly even those detected occasionally cannot all be confirmed as this would demand an enormous number of standards which is expensive and some of them might not be obtainable.

As an apparently new and emerging field, metabolomics studies became promising due to improvement in the analytical techniques and informatics tools which have enabled easy and quick analysis of complex samples to produce massive quantities of data which can be evaluated and demonstrated using different software and online based tools. These technologies recently applied in the plant, environmental and mammalian systems with the purpose of recognizing a novel biomarkers and elucidating possible biological mechanisms resulting from different treatments or genetic alterations (123)

1.3.3 Analytical platforms

Nuclear magnetic resonance spectroscopy (NMR) and mass spectrometry (MS) are two well-known methods used in the study of metabolomics whether for profiling, un-targeted or targeted metabolomics (124). These techniques have been improved to include the different requirements for different aims of a study. Early

development of metabolomics depends on nuclear magnetic resonance spectroscopy (NMR), which is restricted by low resolution for singular metabolites and the narrow variety of analytes identified. However, mass spectrometry has become increasingly applied to this area (125,126). An analytical technique that sort ions depending on their mass or weight is known as mass spectrometry (MS) which give a measurement of the particular composition of a certain sample. The high ability and sensitivity of mass spectrometry made it an important method to detect and quantify metabolites in a variety of samples. The LTQ Orbitrap innovation (127) was the foremost technology discovered to have high and consistent mass accuracy combined with the fast scanning mandatory for compatibility with chromatographic systems (128).

1.3.3.1 Mass spectrometer (MS)

High-resolution MS detects the elemental composition compounds in a sample based on their atomic configuration and their charge state (118). So, identifying unknown compounds in a sample is one of the most important mass spectrometer advantages. The mass spectrometer works by converting individual molecules into small ions so that they can be moved about and controlled by external electric or magnetic fields. Mass spectrometers separate compounds relying on a property defined as the “mass-to-charge ratio” (129). Identify an unknown compounds need to be ionized at first, and then progressed through magnetic or electric fields in order to calculate the mass of ion depending on parameters such as the quantity of deflection initiated by the field or the time that molecules need to pass through a

certain distance (130). The separated ions exposed to the field will then undergo the same degree of deflection if they have a similar mass to charge ratio.

The combination of high-performance liquid chromatography (HPLC) and mass spectrometry (MS) allows comprehensive structural information to be obtained on the metabolites which are changed in a certain sample due to a specific intervention. Though liquid chromatography separates mixtures of multiple components, mass spectrometry identifies individual components through high molecular specificity and detection sensitivity. The benefits of combining chromatography with mass spectrometry are in reducing ion suppression effects and the ability to differentiate between isomers.

HPLC and MS devices are primarily incompatible; therefore, the LC-MS system requires an interface that competently transfers the separated compounds from the HPLC column into the MS ion source (131). It is impossible to immediately inject the eluate from the HPLC column into the MS source, so the interface is designed in such a system to offer sufficient vaporization and spraying of the liquid, sample ionization, elimination of the additional solvent vapour, and extraction of the ions into the mass analyser. Electrospray ionization (ESI) and atmospheric pressure chemical ionization (APCI) systems are the most widely used interfaces.

1.3.4 ZIC-pHILIC zwitterionic hydrophilic interaction liquid chromatography column.

Reversed phase (RP) HPLC combined to mass spectrometry, has been applied sufficiently to separate a wide variety of non-polar compounds; however, ionic and polar compounds demonstrate little or no retention on traditional RP columns. Some most important compound classes in metabolomics like carbohydrates, amino acids and nucleotides are poorly retained by reversed phase columns but properly separated and retained by hydrophilic interaction liquid chromatography especially ZIC-pHILIC. Hydrophilic interaction chromatography was initially employed to separate polar analytes such as amino acids and pharmaceuticals instead of RP-HPLC with a low-aqueous/high-organic mobile phase (132). HILIC retains compounds using partitioning between an organic mobile phase and a hydrophilic stationary phase while the elution is driven by increasing the water content in the mobile phase. The retention mechanism of HILIC relies on the water surface layer (pseudo-stationary phase) associated with a zwitterionic or polar surface coating on the column. The fundamental feature of the zwitterionic coating in HILIC columns is its overall neutral charge and its capability to separate both positive and negatively charged molecules via charge interaction with the analytes. HILIC chromatography has become increasingly common due to the superior separation efficiency for polar compounds contrasting to RP-HPLC due to favourable mass transfer via the low viscosity of organic mobile phases. In addition, the appropriateness of HILIC chromatography for LC-MS is due to the enhancement of ionisation efficiency which is more efficient in lower viscosity mobile phases. The increasing demand for the

analysis of polar biochemicals including proteins, oligosaccharides, drugs analysis over the past years has led to the advancement of the HILIC technique (133).

Traditionally, it is favourable to use two chromatographic runs using reverse phase and hydrophilic interaction liquid chromatography to separate polar and non-polar compounds in a particular sample. However, this increases the difficulty of the preparation of the sample (132). In addition, samples need to be run on two separate columns repeatedly which leads to increased analysis time and complicates the data analysis.

1.3.5 Mass spectrometric Ionization

There are many different ionization techniques which can be interfaced with the chromatography for analysis. Electron ionization (EI) known formerly as electron impact ionization was first described in 1918 for the detection of the mass to charge ratio of several components (134). EI is compatible with gas chromatography (GC) separation only; however, it cannot be conjugated with liquid chromatography (LC) because it is not possible to introduce solvent into the instrument and maintain high vacuum. The most frequently used technique with liquid chromatography is electrospray Ionisation (ESI). This technique uses electrospray to produce ions when a liquid passing through a capillary tube is exposed to a strong electric field to generate an aerosol. The primary molecules are initially introduced into the spectrometer ionisation source to be ionized and acquire a positive or negative charge. ESI is one of the most frequently used methods of ionization in metabolomics, and it is a favourable ionization technique for HPLC-MS for many

reasons. It efficiently ionizes compounds in the liquid phase and can generally be used for both small molecules (<1,000 amu) and large molecules like proteins. In addition, it is a soft ionization technique; thus it does not prompt a substantial fragmentation of the molecular ions. The disadvantage of using ESI that its ionization efficiency is critically influenced by the presence of salts so that the chromatography methods are limited to use volatile buffers like formic acid, ammonium acetate or ammonium formate.

There are two ion modes of ESI known by negative ion electrospray ionisation (NIESI) and positive ion electrospray ionisation (PIESI). Amino acids are one class of biochemicals that can be detected in both modes which can obtain a positive or negative charge as their side chain include amine and hydroxyl groups. PIESI is highly sensitive for the compounds that contain amine groups whilst being unable to ionise polar acid groups like Krebs cycle acids and neutral sugars that can easily be detected via NIESI. Molecular ions can also form adducts with ingredients in the mobile phase and also with other abundant metabolites. For example, the most popular adducts in positive mode appear with acetonitrile, methanol, ammonia and sodium, while negative mode adducts appear with formic acid, acetic acid and chloride. Additionally, using a strong organic solvent mobile phase enhance the evaporation of droplet and form gas phase ion, which then promote the efficient of compounds ionisation in ESI and also decreases adduct formation (135). On the other hand, in addition to the environmental contamination, the content of an abundant matrix component when the sample for example infused directly into the instrument reduces the efficiency of ESI ionisation. Moreover, co-eluting

metabolites can cause ion suppression when they compete for charging, and low electron or proton affinity metabolites are disturbed or not detected at all.

1.3.6 Ion separation and detection methods

Once the ions are introduced into the ion source, they will be separated subsequently based on their mass to charge ratio (m/z) using a mass analyser. The ions then have to be physically detected according to the ion current striking a photo or electron multiplier or by orbital frequencies being detected as an image current. Mass spectrometer detects metabolites by the measurement of molecular mass that can give a molecular formula at high mass accuracy (< 1 ppm), if a high-resolution trap like an Orbitrap is used, or can carry out structure elucidation by producing fragmentation mass spectra.

Metabolite identification with high sensitivity and resolution is desired at all events. However, it is challenging to obtain both goals in a single MS detection mode because as a universal rule higher resolution leads to lower sensitivity and vice versa. Different types of mass analyser techniques are applied in metabolomics including single quadrupole MS or tandem MS/MS, each of which has different sensitivity and resolution performance. A single quadrupole provides complex data if combined with a good chromatographic system and gives a basic LC-MS system with a reasonable cost but does not deliver accurate mass measurement or fragmentation. Triple quadrupole (Tandem MS) delivers the highest sensitivity, so it is widely applied to analyse drugs and their metabolites and has the ability to fragment the analytes. Quadrupole instruments drawback is their low resolution

which is about 0.5 amu. An ion trap is less sensitive than quadrupole but able to provide multiple fragmentations and provide more details about the structure of the compound.

The single stage MS configurations include the Orbitrap, the quadrupole (Q), linear ion trap (LIT), quadrupole ion trap (QIT), time of flight (TOF) and Fourier transform ion cyclotron resonance (FTICR). The quadrupole and ion trap provide high sensitivity but low resolution while the Orbitrap, TOF, and FTICR provide high mass resolution. Tandem configurations include triple quadrupole (TQ), triple-quadrupole ion trap (QTrap), linear-quadrupole ion trap-Orbitrap (LTQ-Orbitrap), and quadrupole-TOF (Q-TOF). Due to their outstanding sensitivity and selectivity, QTrap and TQ analysers are the widely prevalent MS spectrometers linked to LC and are used in targeted metabolic studies. Q-TOF and LTQ-Orbitrap analysers are appropriate for untargeted metabolic screening and metabolite identification (including isomer analysis) due to their higher mass-resolving power. A key technological innovation was the invention of the LTQ Orbitrap Fourier Transform mass spectrometer (FTMS) (136) that presents consistent and very high mass accuracy in combination with rapid scanning essential for compatibility with chromatographic systems (128) and also fragmentation.

1.3.7 Data extraction and Analysis

LC/MS data are in 3D-matrix form (m/z, retention time, intensity). Many softwares can be used to process these data and deconvolve them into a matrix of detected peaks the perform metabolite identification (ID), with a peak response for

metabolites determined. The software must be able to align retention times and accurate masses that drift due to the order of injections. Different types of tools can also be used to process the data in the way that is designed by instrument companies like ThermoFisher SIEVE or the free open access software like MZmine (137), MzMatch (138) and IDEOM (139). MzMatch and IDEOM were the only software used in the current project.

Metabolomic approaches generate huge quantities of data and that need to be processed using either commercial or non-commercial software to identify the metabolites in particular. MzMatch is open access and platform tool. Raw LC/MS data are managed via converting of instrument-specific data format to XCMS using Centwave for peak selecting and mzMatch is used for noise filtering, peak detection and alignment; then identification is ultimately carried out by IDEOM. The statistical language used in MzMatch and Ideom as the background is known as “R”. It enables mzMatch to analyse more than 100 LC/MS data files from different groups of experiments. Retention time database updated in each run by RT calculator uses the Quantitative Structure-Retention Relationships (QSRR) approach to properly predict retention times based on the identified retention times of authentic standards and the physicochemical nature of the interactions of the analytes with the stationary phase (139).

With the improvement in the analytical methods, numerous metabolite peaks are generated from a biological sample. Displaying and interpreting a metabolomics differentiation in a certain experiment is interesting but needs a robust multi- and

univariate statistical approach to detect consistent biomarkers. To reduce data, the multivariate statistical tool should be used to separate bio fluids samples into “treated” and “control” populations relying on the alterations of numerous metabolites before it processed.

1.3.8 Multivariate and univariate analysis

Recent advances in the analytical technologies are enhancing our ability to obtain more data from biological experiments. So, there is an urgent need for rapid and precise statistical and bioinformatic software that enables us to deal with the complexity and volume of the data generated by metabolomic studies.

Recent advances in high data-density analytical techniques provide great hope for the development of medical diagnostics in the near future. Genomics, proteomics and metabolomics give a comprehensive description of the biological processes for each individual. Linking the huge quantity of data obtained to numerous different persons and their current or even future phenotype is an inappropriate task for classical multivariate statistics. The datasets generated from metabolomics techniques very often violate the requirements for classical multivariate analysis (MVA) (such as multiple regressions, N must be greater than K, the K variables should be noise-free and uncorrelated, and the X-matrix should be complete. For MVA, K can be much larger than N, the K variables can be multicollinear and the X-matrix noisy and incomplete. An alternative statistical approach was developed in the early part of this century by Hermann Wold and colleagues which can overcome these problems. This approach, called multivariate analysis (MVA), has the ability to

revolutionise medical diagnostics in a wide range of diseases. It opens up the prospect to the current systems that diagnose many different diseases simultaneously, and even make prognoses about the future diseases that an individual may suffer from (140).

This module of data analysis consists of two steps, multivariate analysis followed by univariate analysis. The multivariate step includes two phases, firstly, pattern recognition using the unsupervised model in order to visualise and to get an overview of the data and to ensure that it does not contain any outliers, secondly, biomarker identification followed by model validation to certify predictive ability. Prior to starting the steps of data visualisation and biomarkers identification, data should be pre-processed.

1.3.9 Data pre-processing.

1.3.9.1 Transformation

Transformation is applied to normalize the data when individual variables depart from the normal distribution. Thus, transformation enhances the residual distribution of data to make it more normal which in turn effectively helps to eliminate outliers (141). Many forms of data transformations can be used, including log2, log10, inverse, neglog, etc., based on the data nature. This can be detected and examined using normal probability plots (141).

(Figure 1-3) below demonstrate the observations in plot B are located on the straight line with R2 =0.975 after log2 transformation compared to the

untransformed observations in plot A which deviate from the straight line with R2 =0.934.

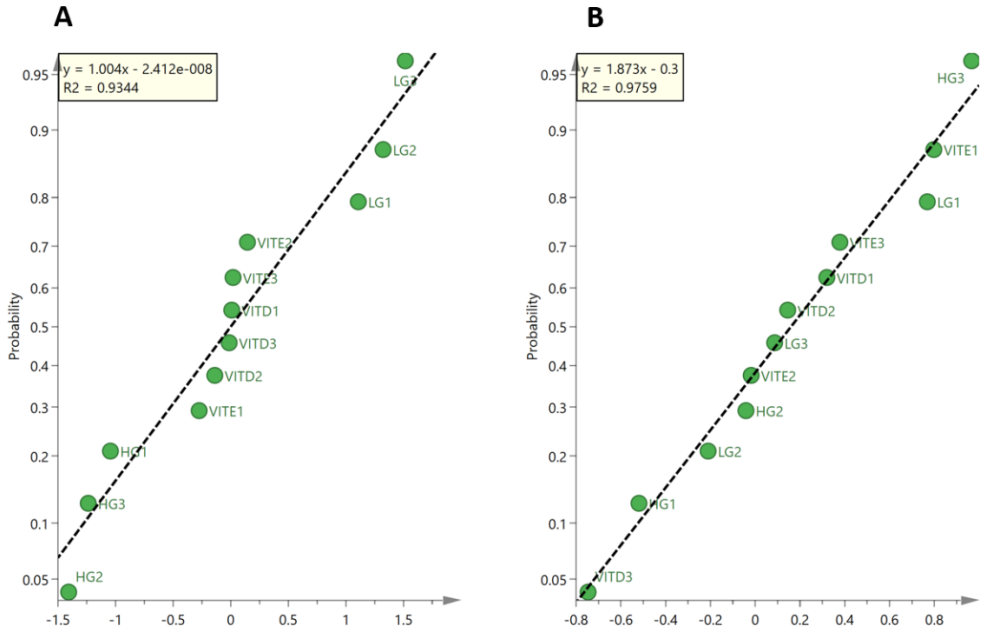

Figure 1-4: Normal probability plot of residuals.

The plot is displaying the residuals standardized on a double log scale on y-axis vs standard deviation on the x-axis. Observations lying outside the –4 or +4 standard deviations are outliers. The regression line to assess the normality of the observations. (A) Untransformed variables (B) log2 transformed variables

1.3.9.2 Scaling

The statistical analysis highly focuses on high-intensity metabolites and gives less importance to the lower intensity metabolites. However, the importance of these smaller intensity metabolites must not be ignored as they might have a higher biological impact. Scaling is regularly used in metabolomics to solve this issues (142) and can be performed via different approaches including: [1] Mean centring, i.e., by taking the average of each variable and subtracting it from the intensity of the

variable in each row; [2] Univariate scaling, i.e., by the calculating standard deviation of each variable (column) and dividing it by the intensity of the variable in each row (sample); [3] Auto scaling, which is a combination of univariate scaling and mean centring. Auto-scaling is preferred when variables have different units. But it may increase the effect of noisy variables on the analysis. To reduce such undesirable effects, [4] Pareto scaling is recommended. Pareto scaling takes the square root of the standard deviation of each variable in a column and divides it by the intensity of the variable per row. Pareto scaling is more popular when dealing with spectroscopic data (142), and this was the approach that we used throughout the study. [5] Block weighting, is another scaling technique where a variable in each row is multiplied by 1/(kblock)1/2, where kblock = number of variables in that block. This technique is ideal in combination with univariate scaling when variables with different units are analysed, and a block of variables with large values will dominate over smaller value blocks (141), for instance, systolic blood pressure (mmHg) and height (m).

1.3.10 Data visualisation and biomarker identification

Metabolomics produces a very large amount of data based on the analysis of sets of biological samples. So, we need to find potential relationships or significant distinction between different samples or group observations; the larger the amount of information to be analysed, the larger the difficulty and complexity of obtaining the associated biomarkers will be. It will be practically unattainable to correctly observe and analyse the data without appropriate statistical software. Therefore, it

is essential to employ sufficient statistical methods that promote the probability of identifying any possible similarities or differences between samples, by reducing the high input space dimensionality of the data to a small number.

To categorise the samples into groups of analogous characteristics, which can give an initial insight into the investigation condition, statistical methods such as Principal Components Analysis (PCA) can be used. Samples are classified into a group with similar characteristics different from those in other groups. No data about the groups is known beforehand, and no assumptions are required concerning the group into which a sample may be classified. These unsupervised pattern recognition techniques aim to reduce the amount of data complexity and afterwards present the samples clustering pattern of the data in a graphical form (143).

PCA is an unsupervised model used to display how variables cluster with no regard to which group the observation belonged to (144). Analysts used it primarily as the main tool for data reduction to extract expressive information (145). This carried out by combining variables that associate with each other into a few components. The higher the correlation between variables is the smaller the number of components that will be needed with components < observations, without losing a vital amount of the total variation of the data (143). PCA is usually utilized as the first step of metabolomics data analysis (144,146) in order to visualize the data and detect outliers.

PCA offers insight about the dataset, but it does not link the phenotype of an individual or a sample to the measured parameters. Partial least squares-discriminant analysis (PLS-DA) performs a PCA analysis on the Y-matrix (observations/samples) to yield a small number of components and then constructs a series of components from the X-matrix (descriptors/variables/metabolites) which elucidate the maximum variance in these Y components.

Orthogonal partial least squares - discriminant analysis (OPLS-DA) is an extension of PLS-DA model but has an advantage over the PLS-DA that it can separate variation in X that correlates to Y (horizontally) called predictive variation, and also separate variation in X that is uncorrelated to Y (orthogonal) (see figure 1-4). OPLS-DA is more powerful method that is applied to observe the difference between groups (144). It helps to detect the consistent biomarkers that have a robust correlation with separation between groups (146) and relate certain diseases or interventions to a disturbance in metabolic pathways (147) and thus assist in increasing our understanding of the pathophysiology and possible future therapeutic targets.

The excellence of (OPLS-DA) model is assessed by R2 (the goodness of fit) and Q2 (the goodness of prediction), in addition to the p-value of the model (P CV-ANOVA) and cross-validation procedures that determine the degree of model significance (148). These measurements are known as quality parameters (149).

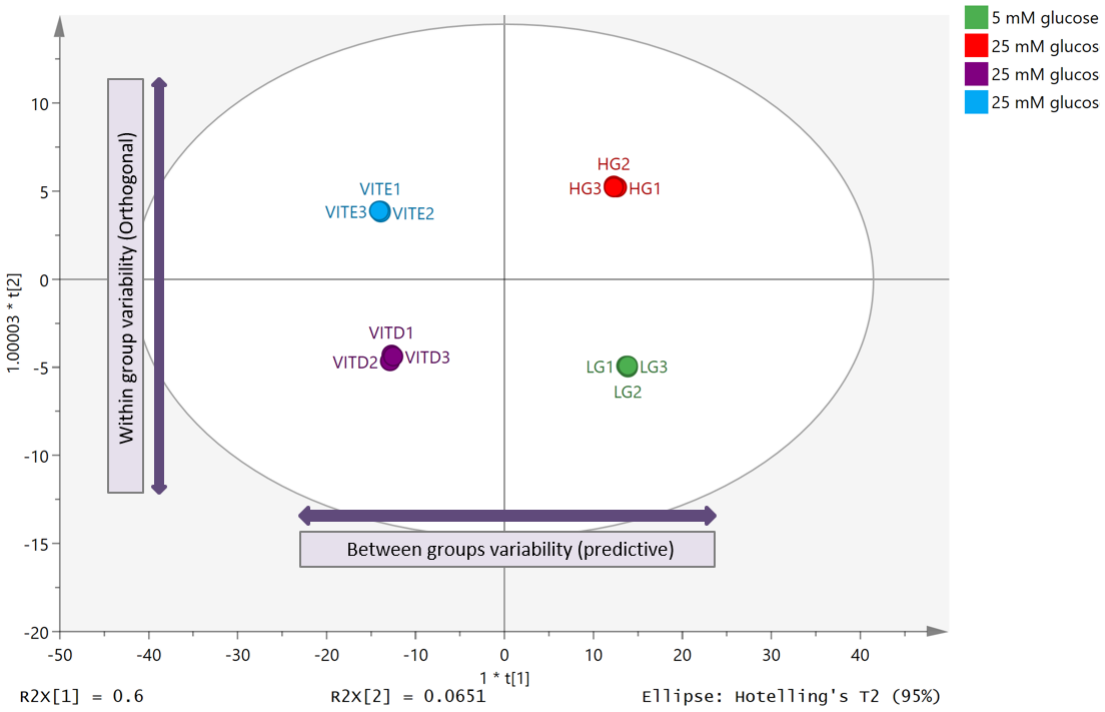

Figure 1-5: Orthogonal Partial Least Square Discriminant Analysis (OPLS-DA) score plot.

The OPLS-DA score plot shows biological samples of pulmonary artery smooth muscle cells exposed to high glucose level (red), normal glucose (green), high glucose + vitamin D (purple) and high glucose + vitamin E (light blue). The figure shows the clear separation between the four groups horizontally (predictive), and vertically (orthogonal). The model explains 71% of the predictive variation -between groups- and 22% of the orthogonal variation -within the group.

1.3.11 Model validation

Cross-validated ANOVA (CV-ANOVA) is one of the validation tests for the supervised model using CV-ANOVA that examines the variation predicted by the model against H_0 hypothesis of equal cross-validated predictive residuals around the mean (150). A model with P CV-ANOVA < 0.05 is valid. Another validation test can be used known as a permutation test. In this test, the R2 and Q2 parameters obtained from the original model are compared to the new permuted R2 and Q2; this process can

be repeated to generate new quality parameters. The new parameter's value created from the process of permutation should all be lower than the original values, or the regression line of the predictive model should cross the horizontal zero line (141) (see figure 1-5).

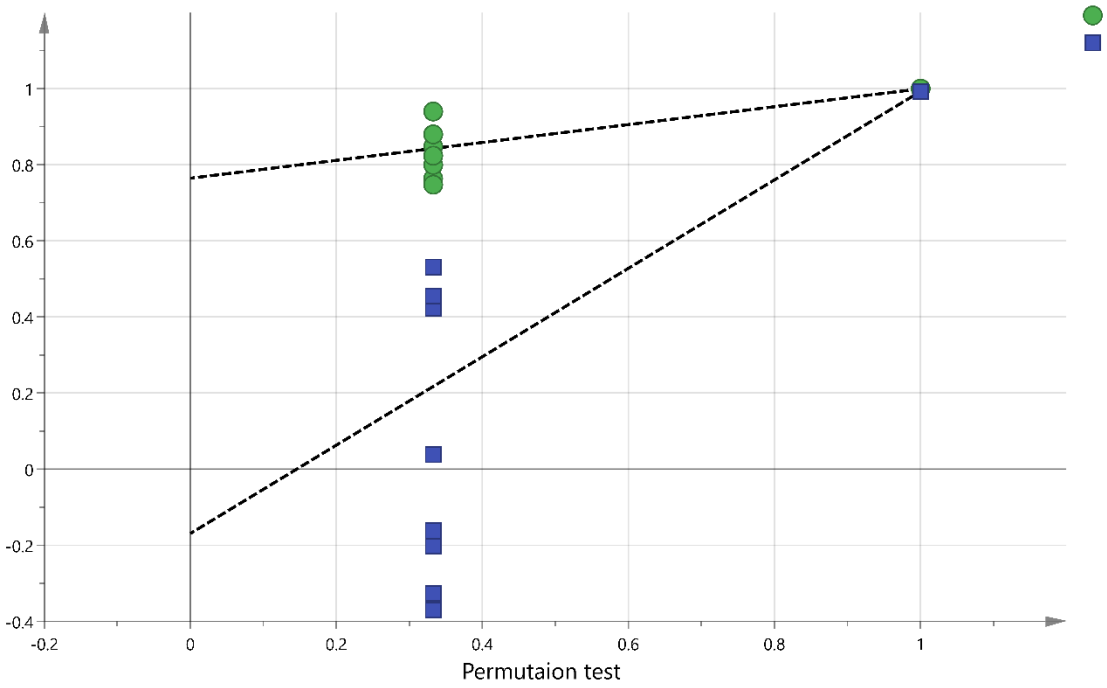

Figure 1-6: Permutations test.

The plot shows, the vertical axis gives the R2Y and Q2Y -values of each model. The horizontal axis represents the correlation coefficient between the original Y, which has correlation 1.0 with itself, and the permuted Y. If the supervised model has valid predictive ability, the R2Y and Q2Y of the real model are always bigger than the corresponding values of the models fitted to the permuted responses.

1.3.12 Variable importance in the projection (VIP)

This test observes the contribution of every individual metabolite by the estimate and ranks its importance in the projection and usually used for variable selection during metabolomics (143). Metabolites of VIP value > 1 have a high contribution in

the model, and those with VIP ≤ 1 are considered less significant (141,151). Each metabolite has (VIPpred) value representing its contribution to the difference between groups of comparison and (VIPortho) represent its contribution to the difference within the group. We are obtaining VIP by dividing the value of VIPpred by the value of VIPortho a metabolite with high VIPpred, and low VIPortho values are sensitive and specific.

1.4 Aims and Objectives

The work within this thesis aims to explore the metabolomics response to oxidative stress. It will consider the metabolic alterations that occur due to exposing cells to ROS inducers and consider the factors that may affect ROS generation under certain circumstances.

To achieve this, metabolic differences will be profiled based on the differentiation between control conditions and different interventions or between two comparisons. The project will also investigate the effect of supplementation with the anti-oxidant agents of vitamin D & E into the culture medium.

The individual aims and objectives for each of the four studies included within this thesis are outlined below:

Study one

A) Aim: To study the effect of high glucose (hyperglycaemia) on the ROS and cell proliferation of pulmonary artery smooth muscle cells (PASMCs) in the presence and absence of antioxidants.

A) Objective: To measure cell proliferation assay and ROS with or without vitamin D & E supplementation.

B) **Aim**: To investigate the metabolomics response of PASMCs to hyperglycaemic conditions in the presence and absence of antioxidants.

Objective: To measure intracellular metabolites, using a metabolomics platform, in samples obtained from in vitro cells exposed to normal and high glucose level and with or without vitamin D & E supplementation.

Study two

A) Aim: To consider the effect of hypoxic hyperglycaemia on the reactive oxygen species and cell proliferation of pulmonary artery smooth muscle cells (PASMCs) in the presence and absence of antioxidants.

A) Objective: To measure cell proliferation assay and reactive oxygen species with or without vitamin D supplementation.

B) Aim: To investigate the metabolomics response of PASMCs to a hypoxic hyperglycaemic environment in the presence and absence of antioxidants.

Objective: To measure intracellular metabolites, using a metabolomics platform, in samples obtained from in vitro cells exposed to normal and high glucose level under hypoxic conditions and with or without vitamin D supplementation.

Study three

Aim: To investigate the metabolomics response of retinal pigment epithelial cells to the oxidized low-density lipoprotein and the impact of protein translocator protein TSPO deletion.

Objective: To measure intracellular metabolites, using metabolomics platform, in samples obtained from in vitro RPE cells for control and treated groups of both cell types (Wildtype and Knockout).

Study Four

Aim: To investigate the metabolomics response of retinal pigment epithelial cells to hyperglycaemic conditions in the presence and absence of antioxidants.

Objective: To measure intracellular metabolites, using a metabolomics platform, in samples obtained from in vitro RPE cells for hyperglycaemia and normoglycaemia groups of both cell types (Wildtype and Knockout).

Chapter two

Method and material

2 Methodology

2.1 Materials:

Table 2-1: Materials, solvents, chemicals, tools and instruments used for the experiments

Weymouth, F12, DMED Dulbecco's Modified Eagle Medium	Obtained from Gibco Life Technologies (Thermofisher, Paisley).
TrypLE Express	Obtained from Gibco Life Technologies (Thermofisher, Paisley).
Fetal Bovine Serum (FBS) growth factor	Obtained from Lonza, Verviers, Belgium.
Pulmonary Artery Smooth Muscle Cells passage 1-7 (PASMCs)	Obtained from the pulmonary artery of Sprague-Dawley rats in PBU at Strathclyde University
Penicillin-streptomycin	Obtained from Gibco Life Technologies (Thermofisher, Paisley).
ARPE-19 (ATCC® CRL-2302™)	Obtained from American Type Culture Collection (ATCC), Virginia, USA. Cell line derived in 1986 from the normal eyes of a 19-year-old male who died from head trauma in a motor vehicle accident.
Cell culture flasks 25, 75 ml	SIGMA-ALDRICH, (Irvine UK)
Glucose	Obtained from Sigma (Dorset, UK)
Vitamin D & E	Obtained from Sigma (Dorset, UK)
Dimethyl sulfoxide (DMSO)	Obtained from Sigma Life Science (Dorset, UK)
Acetonitrile HPLC grade	Fisher Scientific, (Leicestershire UK)
Methanol HPLC grade	Fisher Scientific, (Leicestershire UK)
Distilled water	Fisher Scientific, (Leicestershire UK)
Column: The experiment applied using ZIC	Hichrom, Reading, UK

pHILIC column 150 mm X 3.0 mm i.d. and 5 µm particle size.	
Liquid Chromatography-mass spectrometer (LC_MS): Accela High-Performance liquid chromatography with Orbitrap Exactive	Thermo Fisher Scientific (Bremen, Germany)
Phosphate buffer saline (PBS)	Obtained from Gibco Life Technologies (ThermoFisher, Paisley).
Ammonium carbonate	Obtained from Sigma (Dorset, UK)
Analytical Standards	Obtained from Sigma (Dorset, UK)

2.2 Method:

2.2.1 Preparation of artery smooth muscle cells samples:

2.2.1.1 Cell Culture

The project involved the study of pulmonary artery smooth muscle cells (PASMCs) and retinal pigment epithelium ARPE-19.

1. (PASMCs) were isolated from the vessel that carries deoxygenated blood from the heart to the lungs. Pulmonary arteries were harvested and dissected from Sprague-Dawley rats and cleaned independently under aseptic conditions. Small rings of the vessels were transferred into 25 cm^2 flasks that were filled with culture media. PASMCs were plated in a mixture of F-12 medium, Weymouth's medium supplemented by 5% penicillin 5000 units, streptomycin 5mg/ml in order to avoid any bacterial growth and 10% fetal bovine serum (FBS). Primary cells were cultured under standard normoxic conditions at 37° C in a 21% O_2, 5% CO_2 incubator for up

to three weeks until the cells became 70-80% confluent (Figure 2.1), and then the cells were transferred into a T-75 flask.

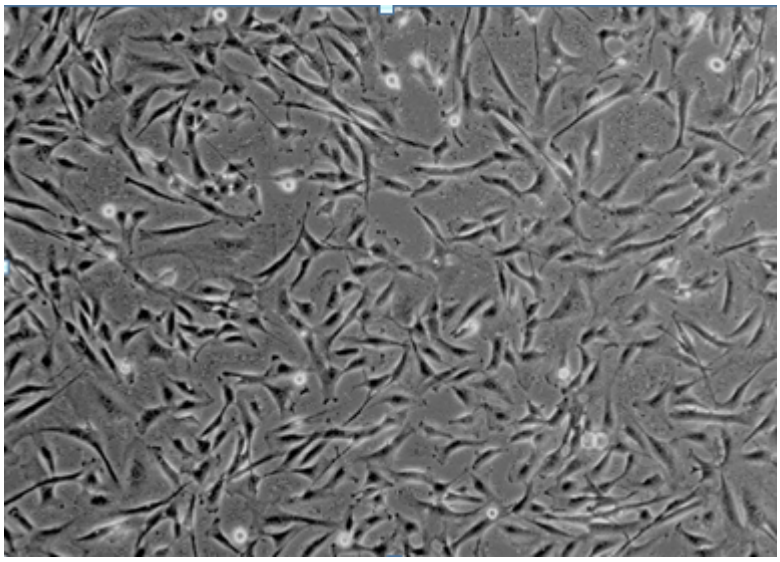

Figure 2-1: PASMCs microscopic image Picture illustrates microscopically capture of pulmonary artery smooth muscle cells of approximately 80% confluent (152).

2. ARPE-19 obtained from ATCC were maintained in DMEM/F-12 medium (1:1) and supplemented by 10% FBS, 5% penicillin-streptomycin and 0.26% Sodium bicarbonate. Cells were cultured under standard conditions at 37° C in a 21% O_2, 5% CO_2 incubator until the cells became 70-80% confluent before they were prepared for cell sub-culture or experiments.

2.2.1.2 Passaging

Once the cells culture became confluent, passaging of cells was carried out in order to keep the cells in the logarithmic growth phase. Media was removed, and the culture was rinsed with sterile PBS to ensure removal of all dead cells.

Trypsinization: appropriate amount of TrypLE^{TM} express was added, enough to cover the surface of the cells in order to detach cells from the flask's surface and they were placed at 37°C in incubators for about 10 minutes. Once the cells detached, complete media was added to quench the Tryple express, and the cells were transferred to a 15 ml centrifuge tube and centrifuged at 1500 r.p.m for 2 minutes. The supernatant was discarded, 1 ml of complete media was added, and the pellet was re-suspended gently till a good cell suspension was achieved for passaging. To allocate the cells into a new passage, equal amounts of counted cell suspension was pipetted into the new flasks prepared with media. Sub-culturing passage ratio was 1:3 or 1:4 depending on the experimental protocol. For PASMCs passages 2 to 7 were used for experiments while passages 30-35 were used in ARPE-19. For experiments, cells were cultured in 6 well plates or 25 ml flasks at a density of $8x10^5$, $2.4x10^6$ respectively.

2.2.2 Cell treatment and extraction

Confluent flask of a minimum of $1x10^6$ cells was used in the experiments. Every extraction condition was prepared in four biological replicates. Cells were cultured with various conditions and the drug at the indicated final concentrations, with their corresponding vehicle as controls and incubated for the appropriate time.

The cells were trypsinized as described previously, quenched with media and counted to determine the volume of the extraction solution (methanol: acetonitrile: water 5:3:2). Extraction volume was normalized based on the cell count of each group and a ratio of 1mL: $1x10^6$ cell was added. Cells were then placed on ice after

adding an appropriate volume of extraction buffer. Cells were then scraped, and cell lysates mixed on a mixer rotor at 1440 (r.p.m) for 12 minutes at 4^{o}C, before they were then centrifuged at 15300 r.p.m. for 15 min at 0°C. The supernatant was collected and stored for further analysis using LC-MS. Mixtures of authentic standard metabolites samples were also injected in order to facilitate the identification of metabolites.

2.2.3 Liquid chromatography-mass spectrometer conditioning

2.2.3.1 Mobile phase solutions for ZIC-pHILIC chromatography

All mobile phase solutions were freshly prepared and were kept at room temperature for up to 72 hours. Aqueous mobile phase A is 20mM ammonium carbonate buffer, pH 9.2 the Organic mobile phase B is HPLC-grade acetonitrile. The column used is a ZIC-pHILIC column (L150 × I.D. 4.6 mm, 5µm, polymeric bead support) (153).

2.2.3.2 HPLC setup

The HPLC was fitted with the appropriate mobile phase components. The auto-sampler needle and sample syringe were flushed with the syringe wash solution (Methanol: Water, 1:1). The system was initially purged, successively, with 100% of each of mobile phase (B followed by A) at a flow rate of 5 ml/min for 5 min in each case. The purge valve was then closed, and the selected HPLC column was conditioned with 50% of mobile phase B at a flow rate of 0.3 ml/min for 10 min. The operating pump pressure was continuously monitored to ensure that it was below

2,000 p.s.i. chromatographic separations were performed on ZIC-pHILIC by applying two separate linear gradients over a specific time using the mobile phases described in sections 2.2.3.1 at a flow rate of 0.3ml/min (See Table 2-2). The MS was operated in a positive/negative polarity switching mode. While on the instrument, samples were kept on a vial tray which was set to a constant temperature of 4˚C to avoid any possible degradation of samples.

Table 2-2: Gradient elution program applied for ZIC-pHILIC in LC-MS analysis

Time (min)	Mobile phase A%	Mobile phase B %	Flow rate (ml/min)
0	20	80	0.3
30	80	20	0.3
31	92	8	0.3
36	92	8	0.3
37	20	80	0.3
46	20	80	0.3

2.2.3.3 Orbitrap Exactive MS setup

LC-MS was performed with an Accela HPLC pump connected to an Exactive (Orbitrap) mass spectrometer from Thermo Fisher Scientific (Bremen, Germany). In the experiment, the quality of data was ascertained by using standard mixtures run with each set of samples to assess parameters such as peak width, height, retention time, and chromatographic resolution. The relative standard deviations (RSDs) of these parameters were checked to ensure that they did not vary by more than 20-

30% for each of the standards. The retention time shifts in the data obtained at the beginning and at the end of a given sequence were expected not to be more than 0.5 min. When this condition was violated, the HPLC system was checked for any leaks before the use of a new column was considered. If any defects were found in the instrument, the analysis was postponed until the system was serviced. Instrument sensitivity was assessed weekly, and any residues in the ion source chamber were removed to maintain enhanced sensitivity. This was done by sonicating the sample cone and the ion transfer capillaries in a 50:50 (vol/vol) methanol/water solution for 15 min. The MS was tuned and calibrated in accordance with the manufacturer's specifications using the Thermo Calmix standard solutions. The signals of acetonitrile dimer (2xACN+H) m/z 83.0604 and m/z 195.03765 for caffeine were used as lock masses for positive (PIESI) mode, and m/z 91.0037 (2 x formate-H) was used as a lock mass for negative (NIESI) mode, during each analytical run. The MS accuracy was tested using standard analytes with intensities between 10^4 and 10^7 to check mass accuracy. The calibrant peaks were checked to make sure that the mass deviations were less than 3 ppm; otherwise, the instrument was recalibrated to correct the mass errors. The spray voltage used was 4.5 kV for positive mode and -4.0 kV for negative mode. The temperature of the ion transfer capillary was 275 °C, and the sheath and auxiliary gases were set at 50 and 17 arbitrary units, respectively. The full scan range was 75 to 1200 m/z for both positive and negative modes with settings of AGC target and resolution as Balanced and High (1E6 and 50,000), respectively. The resulting data

were recorded using the Xcalibur 2.1.0 software package (Thermo Fisher Scientific, Bremen, Germany).

2.2.4 Data extraction, processing and analysis:

2.2.4.1 MzMatch and IDEOM

All raw data files (Xcalibur format) were manually placed into folders according to the study groups. Then data were converted to (mzXML) files while being split into positive and negative polarity using the mzMatch split function. Afterwards, split XCMS files were run through R and, utilizing the centwave function, peaks were selected, and each individual file converted to the peakml format. The settings for the centwave function employed were: mass deviation from scan to scan (< 2) ppm, the range for baseline peak width (minimum 5 seconds and maximum 100 seconds), Signal to Noise ratio (3), prefilter intensity (1000), and Mzdiff (0.001). This was always followed by running mzMatch to match peaks from each sample to produce a single dataset and group individual peakml files together.

Furthermore, the noise filter, RSD filter, intensity filter and detection filter were run to remove irreproducible signals (139). Parameter settings for the mzMatch filters were: mass deviation from sample to another is (5 ppm), and RT deviation is (0.5 min). If there was a considerable shift in retention times, the signal intensities would not be comparable, and the datasets would not make sense. MzMatch filtrations also consider: [1] RSD filter (0.5), where peak reproducibility is measured by the RSD of peak intensities for each group of replicates; [2] noise filter (0.8), while peak shape was evaluated by CoDA-DW score (0-1); [3] intensity filter (1000),

where features are removed if no sample has a peak above the intensity threshold; and, [4] detection filter (3), when peaks must be present in a minimum number of samples. In addition, mzMatch fills the gap for peaks which may fall off during the process. Finally, IDEOM is used to filter the data additionally, and the metabolites subsequently are identified and compared (139).

IDEOM is a Microsoft Excel template supported for automated data processing of high-resolution LC-MS data obtained from untargeted metabolomics studies. In IDEOM, further noise filtration was done, and the authentic chemical standard is matched with a sample metabolite. It is essential to update DB through retention times using a list of retention times from authentic standards (≈180 standards) run with each experiment; this list is created using Toxid (which is an automated compound identification tool that dramatically simplifies processing of LC/MS data and identifies compounds according to retention time and chemical formula). The retention time calculator also uses physiochemical properties (depending on the functional group and chemical formula of compounds) in the DB sheet to predict retention times based on a multiple linear regression model with the authentic standards. The retention time calculator uses the Quantitative Structure-Retention Relationships (QSRR) approach to predict retention times based on the known retention times of authentic standards and the physicochemical nature of the interactions of analytes with columns that determine retention times (154). Accurate identification of putative metabolite requires more filtration of mzMatch files. The blank run with the study group to filter all intensities must be greater than that in the solvent blanks to remove contaminants. Other filters for noise, such as

RSD, intensity and detection filters, are repeated. Chromatography filters, shoulder peak filter and duplicate peak filter, are also applied in IDEOM. Identification of metabolites is performed by matching the accurate mass (accurate mass error for mass identification with DB < 3ppm is suitable for formula identification from a biochemical database with unique entries in DB of 97%) and retention time (RT for identification of authentic standards is 5%) of detected metabolite peak to metabolites in the database. Final lists of identified and rejected peaks are annotated with confidence level from 0 to 10 (10 = most confident) according to the identification of each metabolite; confidence < 5 is rejected as false identification and metabolites matched with the retention times of authentic standards are identified metabolites and highlighted yellow.

2.2.4.2 Databases used for identification

Table 2.2: The databases used for metabolite identification

KEGG Kyoto Encyclopaedia of Genes and Genomes	http://www.genome.jp/kegg/
HMDB Human Metabolome Data Base	http://www.hmdb.ca/
METACYC Metabolic Pathway Database	http://metacyc.org/
LIPID MAPS	http://www.lipidmaps.org/

2.2.5 Metabolomics profiling and biomarker detection

2.2.5.1 Statistical application used

Multivariate analysis SIMCA-P software v.14 (Umetrics AB, Umeå, Sweden) was utilized to process and visualise data, for biomarker identification, diagnostics and validation (151). Metaboanalyst 3.0 (www.metaboanalyst.ca) (155) and Microsoft Excel 2010 were employed for univariate analysis.

2.2.5.2 Data processing and pre-treatment

Prior to multivariate analysis, LC-MS data were log-transformed (to base 2), and then Pareto scaled for variance so that the responses for each variable were centred by subtracting its mean value and then dividing by the square root of its standard deviation. The RSD of each metabolite was also calculated based on the reading of the pooled sample that was run repeatedly throughout the experiment while metabolites with RSD higher than 20-30% were excluded before the data was examined by SIMCA-P.

2.2.5.3 Data visualisation and biomarkers identification

Before LC-MS data was modelling, Hotelling's T2 and DModX limits were applied to determine samples outliers that may affect the model. Sample if so, were then removed from the model when it was above 99% red line (action limit) of Hotelling's T2 or if they exceeded the 95% orange line (warning limit) of Hotelling's T2 plus Dcrit (critical limit) of DModX (141).

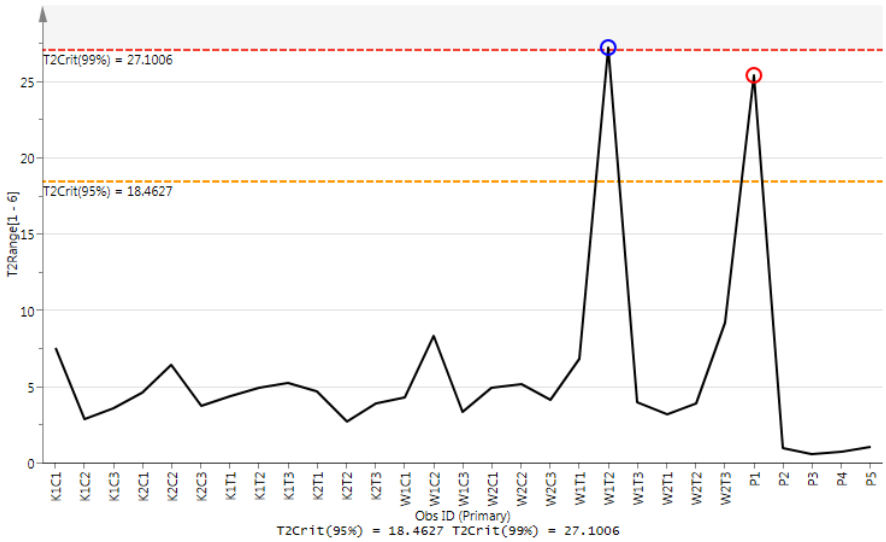

Figure 2-2: Hotelling's T2 test that helps to determine outliers in a model

Unsupervised modelling using PCA was applied to find out how observations clustered based on their metabolic composition regardless of their group classification (144,145). On the other hand, a supervised model OPLS-DA was employed to observe the variances between groups disregarding the systemic variation (144). VIP was also utilized to evaluate the contribution of each variable in the detected metabolomics change to a given model compared to the rest of the variables (141,156). VIP divided into VIPpred, which characterize the contribution of a metabolite to the difference between groups compared to other metabolites, and VIPortho, which designates the influence of a metabolite to variability within group compared to other metabolites in the same model. The average VIP is equal to 1; thus a variable with VIP > 1 has more influence to explain y and vice versa (141). The 95% confidence interval (CI) for each metabolite was considered based on a jack-knife of uncertainty which estimates the prediction error rate based on the cross-validation rule used (157). Metabolites were then filtered based on their p-values

and 95% CI so that all metabolites with p-values > 0.05 and/or 95% CIs crossing the zero point were filtered out.

2.2.6 Diagnostics and validation

R2 and Q2 were used as diagnostic tools for supervised and unsupervised models. The R2 characterizes the percentage of variation described by the model while Q2 represents the percentage of variation in response to cross-validation (144). In the process of cross-validation SIMCA-P, by default, leaves out 1/7th of the data, and then examines the appropriateness of the cross-validation by plotting Y observed vs Y predicted. The R2 value of the regression line in the plot signifies the strength of the association between the observed and predicted Y values; the closer to unity, the stronger is the association. The R2 value was used to choose the number of latent variables (orthogonal axis) (142). Model validity was also considered using cross-validated ANOVA (CV-ANOVA) which corresponds to H^0 hypothesis of equal cross-validated predictive residuals of the supervised model in comparison to the variation around the mean (150).

Table 2-3: CV-ANOVA of OPLS-DA supervised model as a validation test

Model	SS	DF	MS	F	p	SD
Total corr.	66	66	1			1
Regression	39.3221	18	2.18456	3.93056	7.63573e-005	1.47803
Residual	26.6779	48	0.555789			0.745513

2.2.7 Putative biomarkers detection workflow:

1. Following analysis by SIMCA-P, metabolites were filtered based on their p-values and 95% CI of mean difference; if a metabolite had a p-value > 0.05 and/or it's 95% CI crossed 0, then it was filtered out.

2. All significant metabolites were processed using Metaboanalyst in order to get FDR corrected p-values and if the metabolite had an FDR > 0.05 it was filtered out.

3. VIP -occasionally- employed to selected metabolites following FDR adjusted p-value and 95% CI but not before.

Chapter three

Untargeted Metabolic Profiling of Pulmonary Artery Smooth Muscle Cells in Response to High Glucose and Effect of Antioxidant Vitamins D and E

---

3 Untargeted Metabolic Profiling of Pulmonary Artery Smooth Muscle Cells in Response to High Glucose and the Effect of the Antioxidant Vitamins D and E.

3.1 Introduction

Pulmonary artery hypertension is a disease characterized by an increase in mean pulmonary arterial pressure by more than 25 mmHg and is characterized by vasoconstriction and vascular obstruction. This, in turn, increases pulmonary vascular resistance and right ventricular failure. Various factors contribute to pulmonary hypertension, so it is difficult to understand the mechanisms that initiate and develop the disease. Although knowledge of disease pathogenesis and treatment has greatly improved, the mortality rates are still high among PAH patients (158) and survival of patients is significantly influenced despite the classification of the disease (159,160). Clinical diagnosis and treatment of PAH depend on the disease classification based on "updated clinical classification of pulmonary hypertension" while a comorbid condition such as hyperglycaemia has not been taken into consideration yet (161). The UK and Ireland, pulmonary hypertension registry data, show that more than 20% of PH patients above 50 years old had diabetes (101). These data associated with the combined data of four pulmonary hypertension centres assessed diabetes mellitus for those who were newly diagnosed with PH and found that 107 out of 415 pulmonary hypertension patients had diabetes (102,103). In addition, mortality was found to be higher among diabetic pulmonary hypertension patients comparing to non-diabetic patients (102) indicating that hyperglycaemia could adversely contribute to the PAH patients survival. Another study was investigating the survival of PAH patients with

and without diabetes mellitus (DM) found that DM patients had 10 years of lower survival than PAH patients without DM (103).

Since other studies (162,163) that found glucose intolerance, insulin resistance and metabolic syndrome were influenced in PAH, it can be hypothesized that hyperglycaemia could disturb the metabolic pathway of PASMCs leading to medial hypertrophy, fibrosis, proliferation, increased vessel thickness, vascular inflammation and remodelling leading eventually to right ventricular failure.

The current study aimed to examine the alteration of the metabolomic profile that occurs in the pulmonary artery smooth muscle cells following an increase in glucose concentration and to examine the effect of anti-oxidant treatment with Cholecalciferol-D3 (vitamin D) or tocopherol (vitamin E) on the metabolomics of PASMCs during diabetic-like conditions.

Evidence indicates that high glucose level stimulates overproduction of reactive oxygen species (ROS) in vascular cells which considered to be a strong contributor to the oxidative stress involved in the pathogenesis of subsequent complications in cardiovascular diseases (97). Sustained exposure to elevated glucose levels enhances the production of reactive species in the heart and macrovascular system and stimulates, in turn, fatty acid oxidation (97). Overproduction of ROS by the mitochondria due to more glucose being oxidized in the TCA cycle drives the mechanisms responsible for tissue damage (68). Superoxide ($O_2\bullet^-$) is the primary form of mitochondrial free radical that transforms into other reactive species leading to cell damage (164).

Overproduction of reactive species ultimately influences living organisms as they interfere with cell DNA, lipids and proteins leading to mutation due to negative gene-environment interactions (28). Cardiovascular diseases, diabetes and neurodegeneration, are the most common consequences of increased DNA oxidation. Increased lipid and protein oxidative damage in diabetes patients are associated with disease complications (165)-(166).

Glutathione (GSH) is an important and abundant endogenous antioxidant that preserves the redox state of thiol groups (R-SH) of proteins essential for the restoration and expression of DNA. It serves as a scavenger of OH• and superoxide, de-toxifies H_2O_2, lipid peroxides and supports the recycling of vitamins C and E (167). A decrease in the cellular concentration of reduced GSH and glutathione metabolism impairment as a result of a reduction in cysteine and glycine the precursors necessary to synthesize glutathione has been correlated with diabetes (168),(169). Chronic hyperglycaemia produces oxidative stress via the competition between glutathione reductase and aldose reductase for NADPH resulting in decreased GSH restoration from its oxidized form and decreased ratio of NADPH/NADP+ (75).

ROS also obstruct glycolytic enzymes like glyceraldehyde 3-phosphate dehydrogenase, phosphofructokinase-1 and pyruvate kinase M2. Proportionally, glycolytic inhibition diverts glycolysis towards the PPP oxidative arm to generate NADPH that recycles oxidized glutathione as an antioxidant response to the oxidative stress (see figure 3-1 and 3-2).

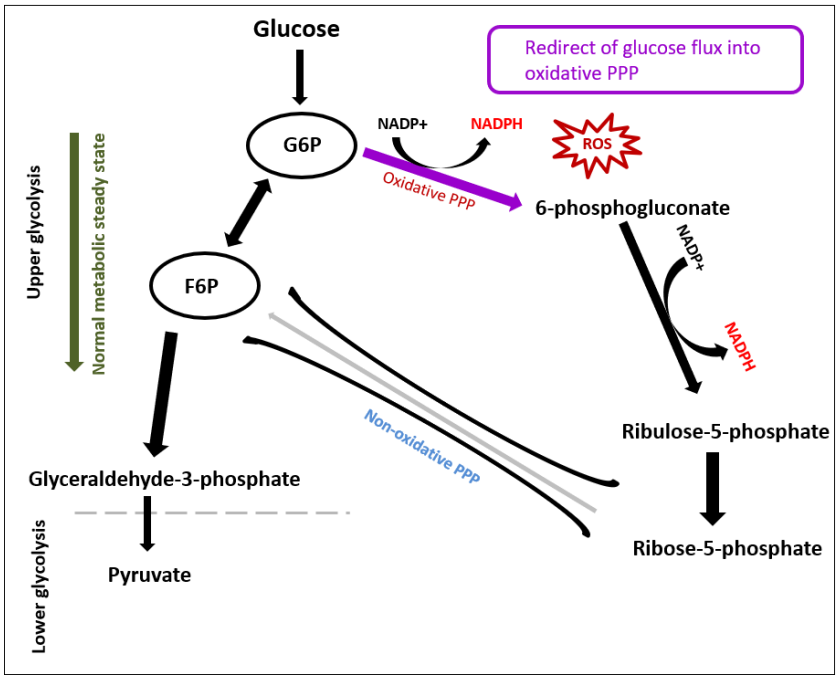

Figure 3-1: ROS impact on glycolysis metabolism

The rerouting of glucose flux into PPP due to oxidative stress. Glycolysis was encouraged while activation of PPP by reactive oxygen species enhances the production of NADPH from NADP+.

A decrease in the GSH/GSSG ratio has been reported as an oxidative stress marker. A study stated that serum glutathione of diabetes patients was found to contain lower levels of GSH compared to control subjects (170).

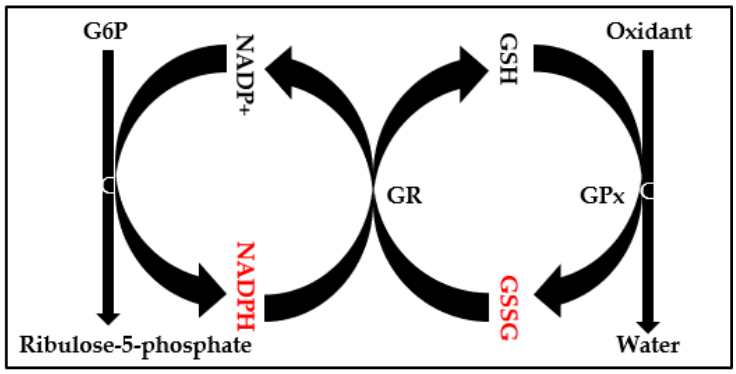

Figure 3-2: recycling of GSSG by NADPH in the presence of GR

The oxidative branch of the PPP is a major supplier of NADPH for glutathione recycling. Reduction of glutathione disulphide to glutathione via glutathione reductase needs NADPH to be completed. Thus, GSSG:SGH and NADPH:NADP+ ratios are impaired due to oxidative stress

ROS, in addition, can damage proteins causing loss of protein catalytic activity and drive them to become more susceptible to proteolytic degradation (32).

Lipids also are vulnerable targets of ROS as their molecular structures have abundant reactive double bonds (34). Reactive species cause lipid peroxidation and disrupt the lipid bilayer, and this may deactivate membrane-bound receptors and enzymes leading to loss of membrane fluidity, elasticity, permeability, impaired cellular function and cell lysis. Lipid peroxidation leads to products such as malondialdehyde (MDA), isoprostanes and 4-hydroxynonenal. These have been identified as significant oxidative stress biomarkers and are able to deactivate various cellular proteins by the formation of protein cross-links.

MDA is a reactive carbonyl compound known to be mutagenic, atherogenic and carcinogenic. Its reaction with lysine residues forms lysine–lysine cross-links which

have been detected in apolipoprotein B (apoB) fragments of oxidized low-density lipoprotein (OxLDL) and has been hypothesized to interrupt the interaction between OxLDL and macrophages and thereby enhance atherosclerosis (36).

3.1.1 Antioxidants:

Vitamin D & E have been shown to have antioxidant properties (171). Serum levels of 25-hydroxyvitamin D are found to be deficient among type 2 diabetic patients (172,173). Animal models and clinical trial studies have demonstrated the ability of vitamin D to reduce oxidative markers (174,175). Vitamin E is a lipid-soluble antioxidant and scavenges lipid radicals. It has been shown that the incidence of primary major coronary events among subjects who received vitamin E is decreased by 4% compared to a control group receiving placebo and the incidence was decreased by 8% (176). However other trial studies indicated that the efficacy of vitamin E in reducing the number of major cardiovascular incidents did not influence total mortality (177,178). The current study aimed to investigate the role of both vitamin E and D as antioxidants and to examine their effects on the smooth muscle cell metabolome in the presence of high glucose media.

3.2 Materials and Methods:

3.2.1 Cell culture:

Rat pulmonary artery smooth muscle cells (PASMCs) were obtained, harvested and incubated as described previously in sections 2.2.1.1 and 2.2.1.2. In addition, condition of each group was prepared as following (1) 25 mM glucose for high

glucose media “diabetic-like condition” (HG); (2) 5 mM glucose for normal glucose media (LG); (3) 25 mM glucose + physiological concentration of vitamin D cholecalciferol (80 ng/ml) (VITD); and (4) 25 mM glucose + physiological concentration of vitamin E α-tocopherol (9 μg/ml) (VITE).

3.2.2 Cell Viability:

PASMCs were seeded at an intensity of 14×10^4 cells/well in 25 cm^2 flask supplemented with 10% BCS DMEM overnight allowed to attach. Next, cells were washed with free media and cultured in 5% BCS for 72 hrs with appropriate glucose and antioxidant concentration based on our intervention and condition of each group. By the end of the incubation period, cells were harvested, suspended, and counted using a haemocytometer cell counting chamber. 10% trypan blue was used to detect viable cells.

3.2.3 PASMC Proliferation Assay:

Confluent PASMC were trypsinized, placed in DMEM supplemented with 10% (BCS), and seeded into 24-well flasks at cell intensity of $2x10^4$ per well. After 24 hours, cells were washed by free media and quiesced with 0.1% BCS for 24 hrs. Cells were then cultured in 5% BCS for 72 hrs with appropriate glucose concentration and antioxidant concentration based on our intervention and the conditions for each group. During the final 6hrs of the assay, [^{3}H-thymidine] aqueous solution (GE Healthcare®) was added to each well. In order to prepare assay samples, media

were discarded, and cells rinsed by cold 1 ml PBS 10 minutes and treated 4 times with 1 ml 10% (w/w) trichloroacetic acid (TCA, Sigma). Afterwards, 250 µL 0.1% sodium hydroxide/Sodium lauryl sulphate (SDS) was added into each well. The sample was transferred to a scintillation vial, and 2 ml of Emulsifier-safe™ scintillation fluid was added to the scintillation vial of each sample before they mixed well prior to measuring the radioactive counts using a scintillation counter.

3.2.4 Reactive oxygen species experiment:

PASMCs were seeded at 5×10^3 cells per well in 96-well plates supplemented with 10% BCS DMEM for 24 hrs allowed to attach. Media then was discarded, and cells washed by free media, followed by the addition of 5% BCS DMEM media for 72 hrs with appropriate glucose and antioxidant concentration based on the intervention and conditions for each group. During the final 30 minutes of the assay, 2.0 µL of dihydroethidium (DHE) or 10 µL of 2', 7'-dichlorofluorescein (DCF) was added to each well, and the cells were placed for 30 minutes in the dark before fluorescence microscopy was performed. DHE or DCF are fluorogenic dyes that measure the quantity of ROS superoxide or hydrogen peroxide respectively.

3.2.5 Metabolic profiling sample preparation:

In an appropriate number of replications, cells were cultured with various conditions at indicated final concentrations, with their corresponding vehicle only controls and incubated for 72 hours. Afterwards, samples were prepared and

collected as previously described in section 2.2.2. The supernatant was collected and placed in -20° for further liquid chromatography-mass spectrometer analysis (LC/MS). During the run, the temperature of the autosampler was maintained at 4 °C. Mixtures of standard biochemicals (Sigma-Aldrich, Poole, UK) and the pooled (QC) sample were injected throughout analysis run in order to simplify metabolites identification and to assess the method stability and reproducibility. QC sample was prepared by taking equal aliquots (10 µl) from all samples and placing into one HPLC vial.

3.2.6 Samples analysis (LC/MS)

The analysis was carried out on an Accela HPLC system interfaced to an Exactive Orbitrap mass spectrometer using a hydrophilic interaction liquid chromatography (HILIC) column (ZIC-pHILIC, 150 x 4.6 mm, 5 µm particle size). The samples were loaded and run on the system as described in section 2.2.3

3.2.7 Data extraction, analysis and biomarker identification.

Described in section 2.2.4 and 2.2.5

3.3 Results:

3.3.1 Effect of high glucose media alone, with Vitamin D, or with Vitamin E on cell viability:

Prior to cell extraction preparation for LC/MS, the high and normal glucose cultured cells and the treated cells were counted using trypan blue exclusion at the end of the 72 hours experimental period (Figure 3-3). This demonstrated that viable cell numbers were substantially increased by the high glucose culture medium (14.9% ± 0.67% vs LG). Treating PASMCs with vitamin E or vitamin D decreased cells number almost to the level of the normal glucose medium (by 11.5% ± 0.4% or by 10.1% ± 2.3% vs HG), respectively.

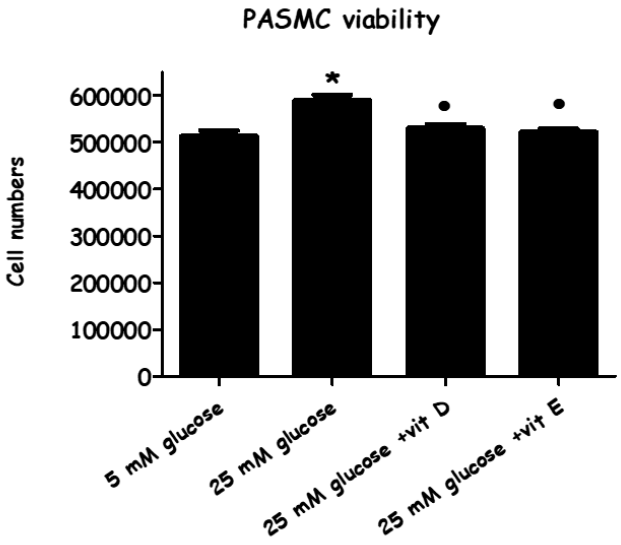

Figure 3-3: The effect of vitamin D / vitamin E in high glucose-induced PASMC proliferation

Cells were cultured with normal glucose (5 mM) and high glucose (25 mM) for 72 h. Vitamin D (80 ng/ml) and Vitamin E (9 µg/ml) were added immediately along with the high glucose incubation. Cells were stained with trypan blue dye, and the viable cells were counted after 72 h. Each value represents the mean ± SEM from 4 independent experiments. *p <0.05 vs. cells cultured in normal glucose (5mM) media. ●p <0.05 vs HG stimulated cells. ANOVA one way followed by Tukey's comparison test was performed.

3.3.2 Effect of high glucose media alone, with Vitamin D, or with Vitamin E on PASMCs proliferation:

The proliferative capacity of high glucose media and the combined effects of high glucose with vitamin D/ or with vitamin E on cell proliferation were assessed by the [^{3}H] thymidine incorporation assay. High glucose media increased DNA synthesis in PASMCs by (14.4% ± 3.19% vs LG) while Vitamin D and vitamin E were significantly able to suppress DNA synthesis of cells cultured in high glucose by (5.3% ± 2.8% and

15.6% ± 4%, vs HG) respectively (Figure 3-4). Cell counting and proliferation quantification showed that cells cultured at matching density and examined (counting or assayed) at the same time point of 72 hrs, PASMCs in HG media steadily revealed a noticeably superior proliferation rate.

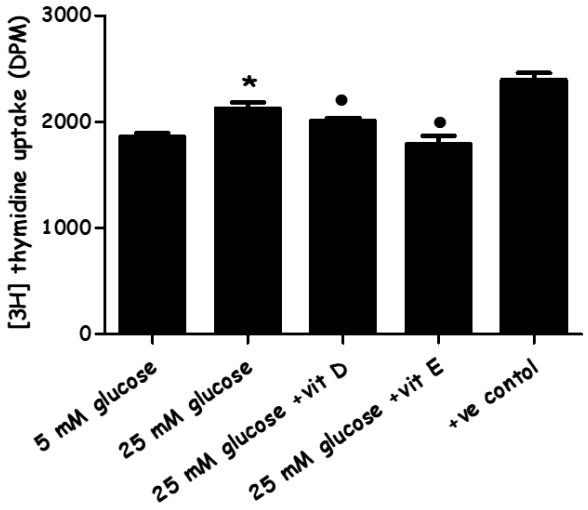

Figure 3-4: The effect of Vitamin D and Vitamin E on high glucose-induced [3H] thymidine uptake by PASMCs

Quiesced cells were cultured in LG (5 mM) or HG (25 mM) for 72 h. Vitamin D (80 ng/ml) and vitamin E (9 µg/ml) were added immediately along with high glucose incubation. [3H]-thymidine incorporation assay was performed for the evaluation of DNA synthesis (as an index of cell proliferation). Radioactive counts were measured in disintegrations per minutes (DPMs) ± SEM. *p <0.05 vs. cells cultured in normal glucose (5mM) media. ●p <0.05 vs. high glucose cultured cells (n=4). (+ve) control: cells placed in the culture of the ordinary environment with no adjusted glucose and 10% bovine serum.

3.3.3 Evaluation of oxidative stress

Measurement of ROS was carried out to determine whether or not the high concentration of glucose in the culture media enhanced ROS activity within the cells. In addition, ROS levels were also evaluated following the combined effects of HG media supplemented with vitamin D / or with vitamin E.

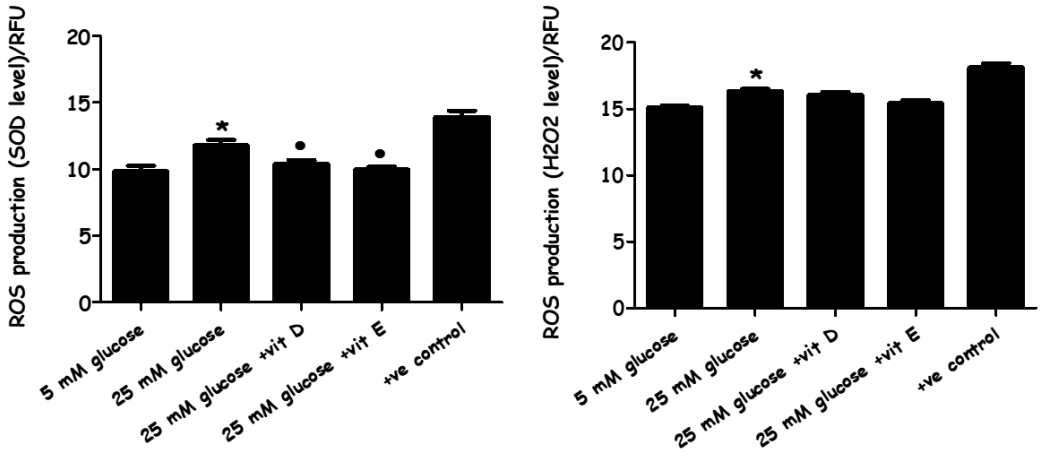

Figure 3-5: The effect of high glucose media alone, with Vitamin D, and with Vitamin E on ROS production

PASMC cells were incubated with normal (5 mM) and high glucose (25 mM) for 72 h. Vitamin D (80 ng/ml) and vitamin E (9 µg/ml) were added immediately along with high glucose incubation. Superoxide ($O_2^{\bullet-}$) levels and hydrogen peroxide (H_2O_2) levels were detected by (DHE) and (DCF) fluorescence compound, respectively. *p <0.05 vs unstimulated cells (n=4). *p <0.05 vs. cells cultured in LG (5mM) media. ●p <0.05 vs HG cells n=4). +ve controls are superoxide or hydrogen peroxide.

Intracellular Superoxide ($O_2^{\bullet-}$) levels and hydrogen peroxide (H_2O_2) release within the PASMCs were measured by DHE and DCF, respectively. The results showed that

PASMCs cultured in HG media significantly generated higher ROS (Superoxide and H_2O_2) levels in comparison to cells cultured in LG media. Interestingly, adding vitamin D or E to the high glucose-cultured cells significantly reduced the intracellular superoxide levels while no effect was noticed on hydrogen peroxide. So, they were able to reduce the primary ROS product ($O_2^{\bullet-}$) but not the secondary ROS product (H_2O_2) (Figure 3-5), thus suggesting that the two ROS are not necessarily linked.

3.3.4 Metabolomics:

LC/MS analysis carried out where the samples were prepared, injected and data afterwards extracted and processed to identify all biochemicals (metabolites) markers changed by HG media comparing to control LG media. Then, the impact of adding vitamin D and vitamin E on HG media were also measured on those altered metabolites. Triplicate samples were prepared for each group in duplicate experiments, and only consistent metabolites alterations were listed.

3.3.4.1 Quality control samples (Pooled):

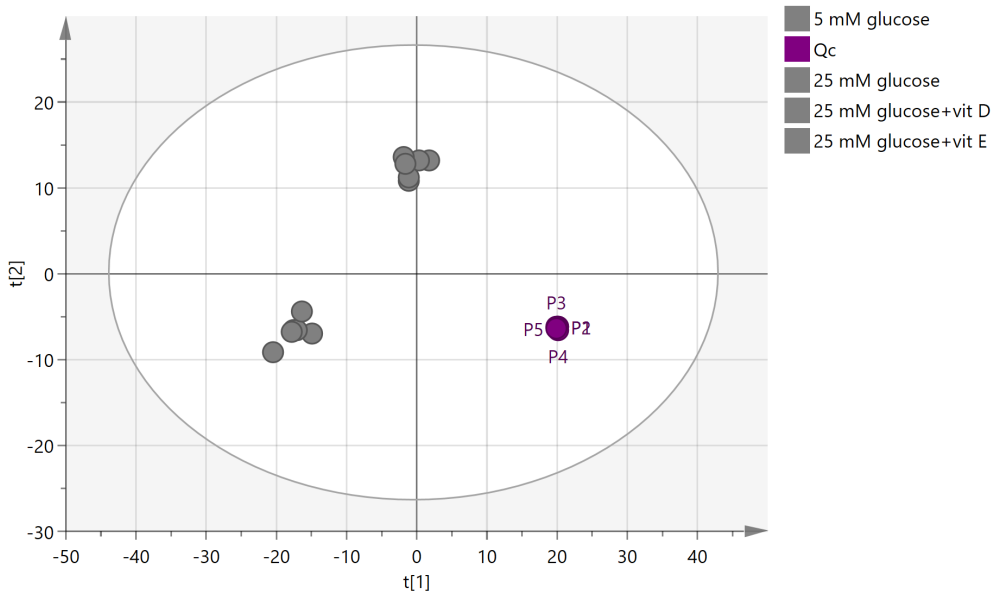

Figure 3-6: principal components analysis PCA score plot for Qc (pooled) cell extract samples of (PASMCs).

P1, P2, P3, P4 and P5 represent the quality control sample frequently runs throughout the experiment.

To measure the precision of the instrument, the relative standard deviation (RSD) was calculated based on the reading of the pooled samples which were injected five times during the course of the run and clustered together in the PCA plot (Figure 3-6). RSD was calculated based on total intensities in each sample, and an RSD of 19.58% was obtained. RSD was then calculated individually for each putative metabolite in the pooled samples, and the highest RSD was for Oxoglutarate (138%) followed by Ornaline (91%) while glutamine had the lowest RSD value of (0.076 %). The precision of these values clearly indicates that any metabolic differences

between groups cannot be due to instrumental factors alone. Metabolites with RSD higher than 20% were excluded before the model was fitted by using (SIMCA-P).

3.3.4.2 Visualization and biomarkers identification:

PCA was employed to observe the possible presence of outliers, groups, similarities and other patterns in the data. Afterwards, OPLS-DA was used to understand the differences between groups and to identify the biomarkers that distinguish one group from another.

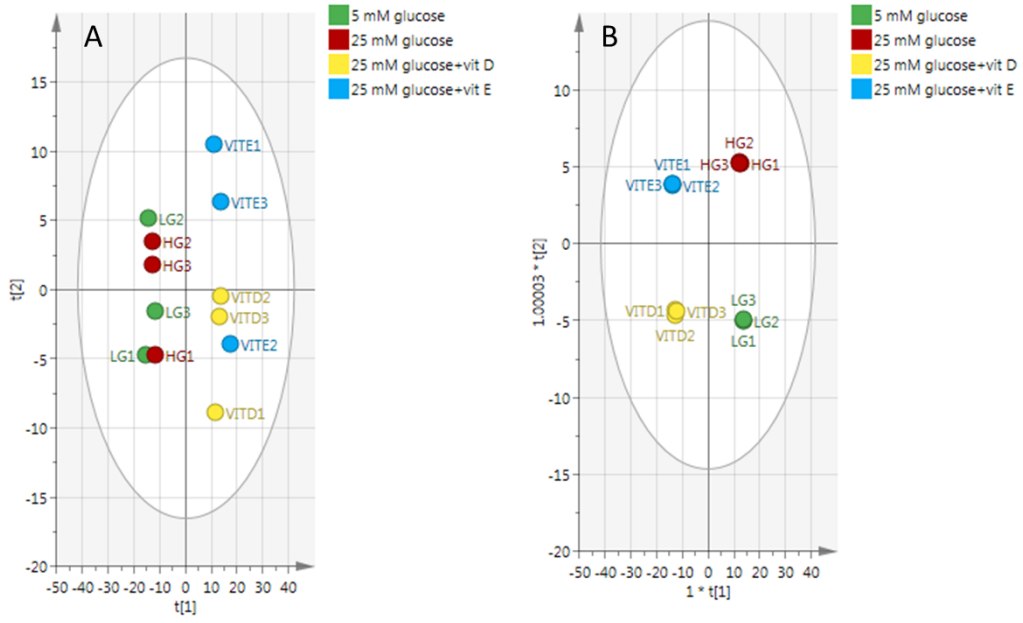

Figure 3-7: PCA and OPLS-DA models for 12 samples of 4 different groups

(A) PCA plot, (B) OPLS-DA plot for groups of normal glucose (5 mM glucose), high glucose (25 mM glucose), vitamin D and vitamin E. The plot shows the distribution of 12 samples based on the reading of 549 putative metabolites.

The PCA plot in figure (3-7 A) shows separation between groups of cells cultured in vitamin D & E and another two groups cultured in high and normal glucose alone. No clear separation can be seen between LG and HG groups (Figure 3-7 A). However, clustering became clearer when OPLS-DA analysis was applied.

The OPLS-DA model shows a clear clustering pattern while each group was able to gather as can be seen in (figure 3-7 B). Even though samples were clustered, and goodness of prediction was high at 0.99, and the model fit was good (72% predictive, 23% orthogonal) The CV-ANOVA of the model (P = 0.885) indicated that model was not valid (Table 3-1).

Table 3-1: display the validity of the model shown in figure 3-7 B where P value above 0.05

Model	SS	DF	MS	F	P. value	SD
Total corr.	33	33	1			1
Regression	27.15	30	0.905	0.465028	0.885	0.9514
Residual	5.840	3	1.946			1.3952

3.3.4.3 Effect of high glucose media:

In order to identify the markers that distinguish HG and LG groups, a new model was built comparing only samples cultured in LG and HG. The data then were filtered based on CV ANOVA, 95% CI and VIP values, of each 549 features as described in (Figure S1 Section 10.1). This workflow highlighted 80 metabolites that distinguished the HG from LG. The included metabolites have p values < 0.05, 95% CI not including 0 value, RSD < 20% in the pooled samples and VIP values > 1.

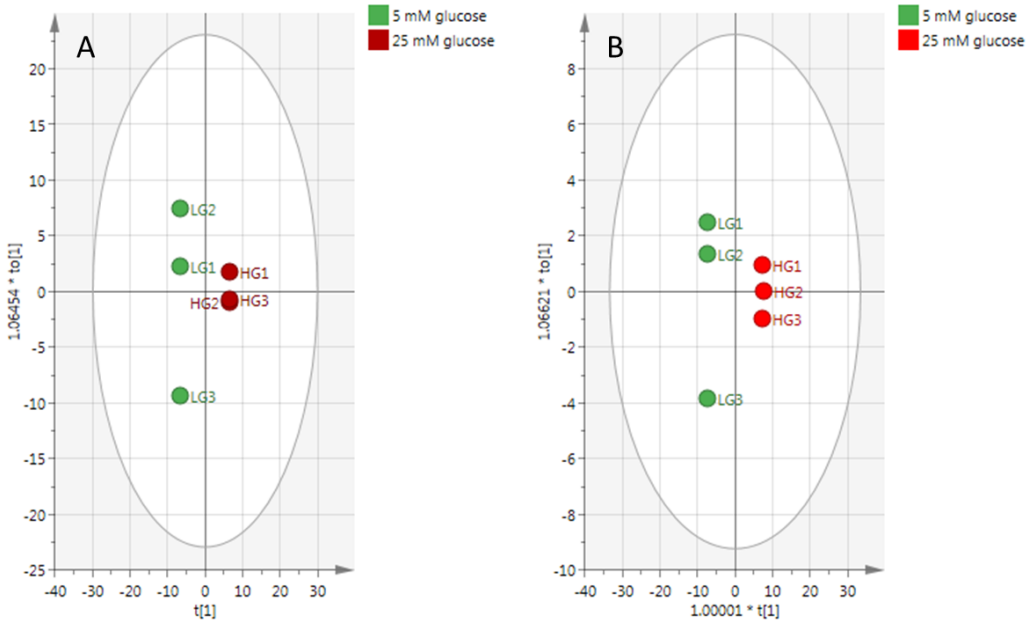

Figure 3-8: OPLS-DA model comparing HG to LG

OPLS-DA score plots showing the effect of high glucose media compared to normal glucose media on the pulmonary artery smooth muscle cells. (A) Based on the reading of 549 features. (B) Based on the reading of 80 significant markers affected by hyperglycaemic media.

Figure 3-8 A shows the clustering of the samples in the model based on 549 metabolites where the model fits 89% of the data (30% predictive, 59% orthogonal and CV-ANOVA *P*= 0.0954). Plot (B) was then rebuilt based on the reading of 80 significant biomarkers where the model was able to fit 86% of the data (80% predictive, 6% orthogonal and CV-ANOVA *P*= 0.0141).

Several lipids and lysolipids fell significantly due to high glucose indicating that the cell membrane composition was affected. Some amino acids were influenced too especially lysine degradation and biosynthesis while in addition oxidized glutathione (GSSG) as oxidative damage marker increased and reduced glutathione (GSH) was

decreased. Glycolysis metabolites were influenced as well when particularly the pentose phosphate oxidative pathway was activated due to high glucose flux into that pathway. In addition, NADH was slightly increased while Acetyl-CoA and TCA acids were not influenced suggesting that lower glycolysis pathway was not as active as the upper glycolysis pathway. ATP was decreased which may indicate it was consumed in cell division since the cell growth increased when the PASMCs were cultured in HG media. Also, the majority of nucleotides metabolites were influenced by the conditions specifically the pyrimidine pathway that might be enhanced due to activation of the pentose phosphate pathway (PPP).

3.3.5 Antioxidants:

Metabolic profiling illustrated that using vitamin D & E attenuated the oxidative stress that occurred through exposing of PASMCs to HG.

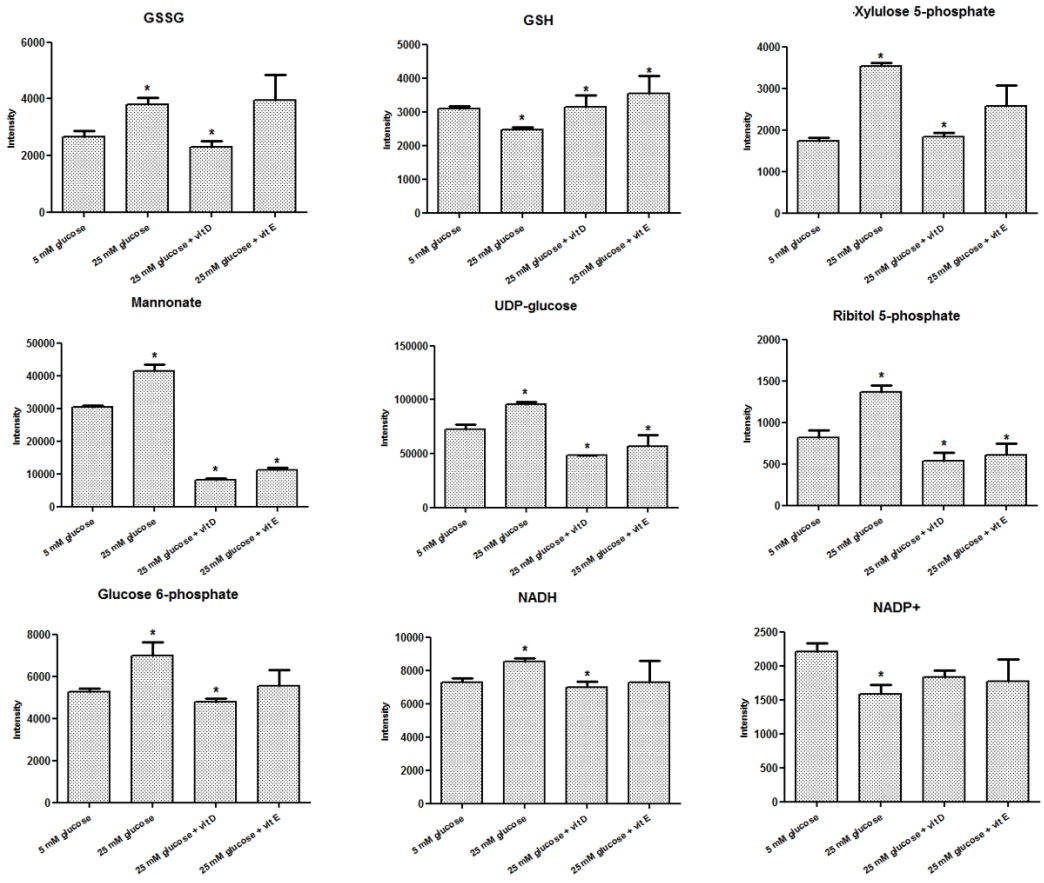

Figure 3-9: sugar Metabolites changes among different groups

Changes occurred among selected metabolites due to different interventions. Most of the glutathione haemostasis and PPP metabolites influenced by hyperglycaemia responded to antioxidants and preserved the normal levels. Pentose phosphate specifically was attenuated via vitamin D & E suggesting that NADPH re-cycling was decreased. (*)(CV-ANOVA < 0.05).

Many of the metabolites see (Table S1 section 10.1) that were altered by HG were restored to control levels when plasma concentrations of either vitamin D or E were added. Glycolysis metabolites which were enhanced by HG only showed no enhancement when the antioxidants were used with HG samples. This effect also can be seen in oxidized and reduced glutathione where particularly vitamin D helps

to preserve normal status. Many of lipids including fatty acids and glycerophospholipids (GPL) were decreased by HG, but the antioxidants were not effective in restoring GPL metabolites. Nucleotide metabolites generally increased due to HG while antioxidants were able to restore most of them to around normal levels.

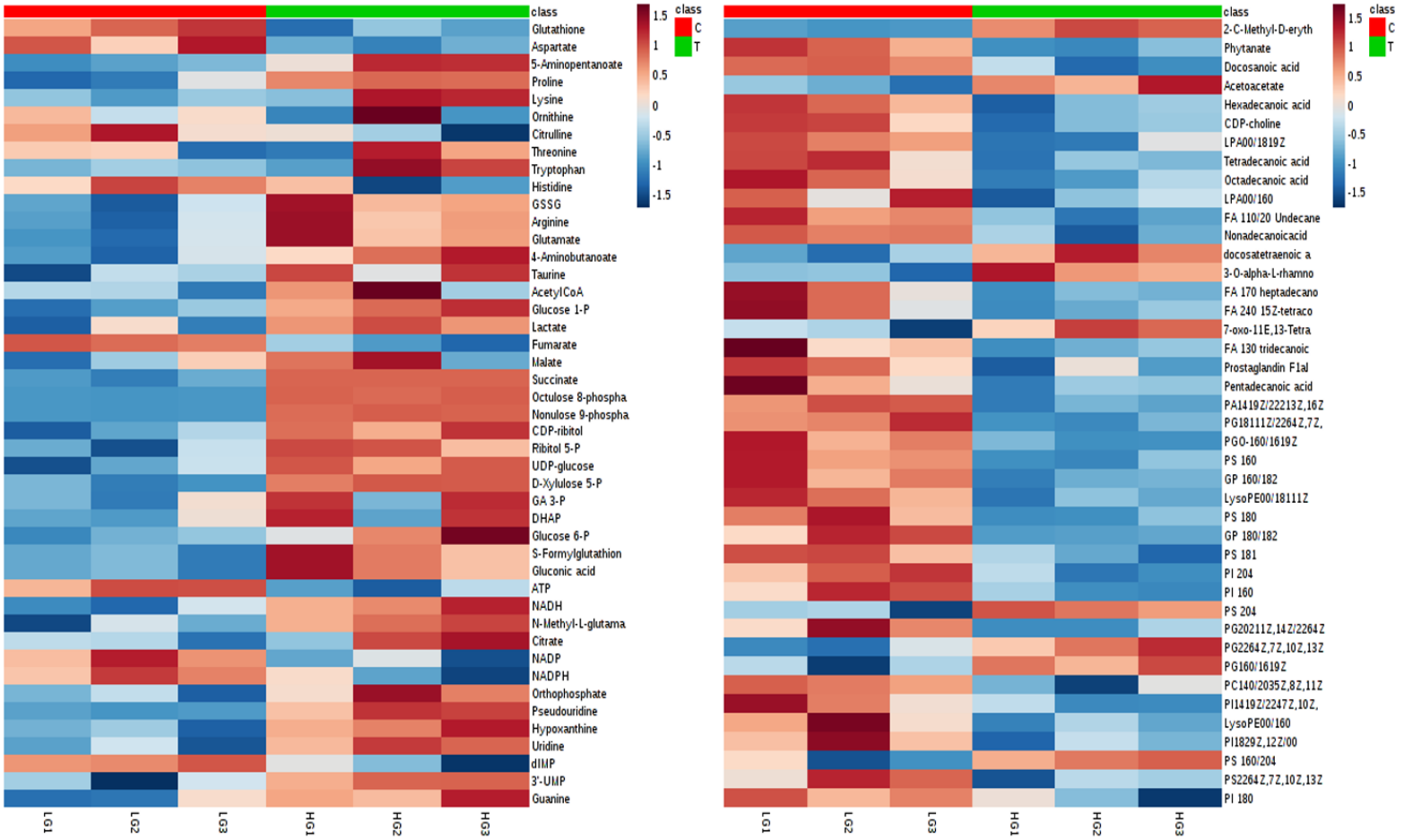

Figure 3-10: Heatmap showing alterations in metabolites between HG and LG. Row: represents the metabolite; Column: represents the samples group (red: normal glucose; green: high glucose); The colour key specifies the metabolite intensity: lowest: dark blue; highest: dark red

3.4 Discussion

High glucose (HG) is an important cause of cardiovascular disease which acts via various mechanisms to enhance ROS accumulation which, successively, cause cellular impairment that is strongly involved in diabetes complications. ROS can immediately damage cellular components including proteins, carbohydrates, lipids, DNA and subsequently affect the metabolic pathways resulting in a shift of the PASMC phenotype from the contractile phenotype to a synthetic (hyper-proliferative/apoptotic resistant) phenotype and initiate cell proliferation and migration (179). While in turn, some clinical studies found inadequate provision for the use of antioxidants in diabetes (180–182) others demonstrate the advantages of antioxidant usage in the prevention of diabetic cardiovascular complications (183–185).

The current study was designed to determine the impact of HG on PASMC proliferation and ROS generation and focused on the abnormal changes in the cellular metabolome and investigating the effect of adding the antioxidants vitamin D or E in order to prevent cell proliferation and the oxidative damage caused by ROS generation which could be induced by stimulating the PASMCs with HG medium.

The data obtained from the cell viability assay demonstrated a significant increase in the PASMCs number by increasing the glucose concentration to 25 mM. This result is compatible with the results of the [^{3}H]-thymidine incorporation assay which indicates that cell proliferation was increased in response to HG as both increases in

total cell numbers and DNA synthesis was observed. Cell proliferation was significantly induced when cells exposed to HG for 72 hrs while, in turn, adding vitamin D or E to HG media succeeded in inhibiting cell proliferation. These results link with many studies carried out on animal and human cellular models (186–188) indicating that HG medium enhances pulmonary arterial smooth muscle cell proliferation via different pathways. In contrast, the antioxidants, particularly vitamins D & E have been found to suppress VSMCs proliferative activity (189–191) through different mechanisms.

The current results also showed that HG medium not only induced cell proliferation but also elevated ROS levels including both superoxide (O_2^-) and H_2O_2 levels. Vitamin D inhibited the overexpression of O_2^- in high glucose-stimulated cells but not H_2O_2 while vitamin E was able to suppress both O_2^- and H_2O_2 levels. Vitamin D is well known to promote scavenging of ROS and diminishes reactive species formation in diabetic mice by suppression of NADPH oxidase gene expression (192,193). In an experiment carried out on diabetic mice, vitamins D & E decreased lipid peroxidation and promoted superoxide dismutase (SOD) activity (194). Alpha-tocopherol (vitamin E) inhibited the prevalence of peroxidation originating from reactive species preventing undesired lipid oxidation (195).

In the current experiment adding physiological concentration of vitamin E and vitamin D to the stimulated cells had a favourable effect on most of the altered metabolites. A total of 549 metabolites were profiled in both positive and negative modes by LC-MS while only 80 metabolites were found to distinguish HG samples

from LG in a valid OPLS-DA model. Samples treated with vitamin E or vitamin D were also compared to the HG group to examine their impact as antioxidants. The impact of the antioxidants on the 80 metabolites that distinguished the LG from HG were only considered. Vitamin E and vitamin D restored many of the metabolites affected by HG to the levels observed in LG (figure 3-9).

Glycolysis: Glucose metabolism fluctuation plays an important role in increasing cellular oxidative stress and vascular remodelling of PAH in diabetic patients (196,197). In the current study, although increased levels of glucose-1-phosphate G1-P and glucose-6-phosphate G6-P were observed as well as increased levels of glyceraldehyde 3-phosphate (G3P) and dihydroxyacetone phosphate (DHAP) in HG compared to LG, Vitamin D and vitamin E had such a significant effect in lowering these metabolites. HG samples revealed higher levels of gluconate, CDP-ribitol, ribitol 5-phosphate, UDP-glucose and Xylulose 5-phosphate, indicating that the glucose flux was redirected toward the PPP. The shift of glucose flux towards the PPP is compatible with increased cell proliferation reflecting an increased requirement for nucleotides. Stimulation of smooth muscle cells leads to the activation of the PPP in order to increase the production of NADPH from NADP+ as part of an antioxidant mechanism. However, it would seem that the flux through the PPP is via a non-oxidative route into sedoheptulose phosphate since the levels of NADPH are reduced possibly as a result of excessive ROS generation as evidenced by an increase in GSSG levels (198). The elevation of the non-oxidative route into sedoheptulose phosphate is underlined by the elevation of compounds putatively

identified as octulose and nonulose phosphates which could be formed via the action of transaldolase on fructose, ribose phosphates and two fructose phosphate molecules respectively. Interestingly, phosphoglycerate was not increased by HG which might further re-enforce the view that there was a diversion of glucose into the PPP upstream of these metabolites. HG samples exhibited a slight increase in the NADH level which indicates that the Krebs cycle was not significantly inhibited and suggested that other pathways like the polyol pathway may be induced by hyperglycaemia. TCA cycle acids mainly were not increased by HG with a decrease of citric acid and increase of fumaric acid. Lactate, in addition, was slightly increased which could also indicate that there was some conversion of pyruvate to lactate rather than acetyl CoA "Warburg effect". Accumulation of G3P was significantly increased in the HG samples indicating that excessive ROS generation might inhibit the conversion of most of G3P via the glycolysis process into pyruvate. N2-(D-1-Carboxyethyl)-L-lysine (CL) is a product of the reaction of methylglyoxal (MG) with lysine residues in proteins which occurs in diabetes and has been proposed to be linked to cardiovascular disease and indicates increased levels of MG. MG has been shown to inhibit glyceraldehyde phosphate dehydrogenase (GAPDH) thus causing the accumulation of G3P and diversion of glucose into the PPP (199). Reaction with NADP+ and H_2O in the presence of CL dehydrogenase forms L-lysine, NADPH and pyruvate. In the HG samples accumulation of CL pointed to inhibition of that reaction. Vitamin D and vitamin E appear to have a direct effect in promoting the degradation of CL. Antioxidants showed no impact on G3P that was upregulated by

HG media. These findings confirm that the upper glycolysis and PPP were strongly affected by HG but not the lower glycolysis and TCA cycle.

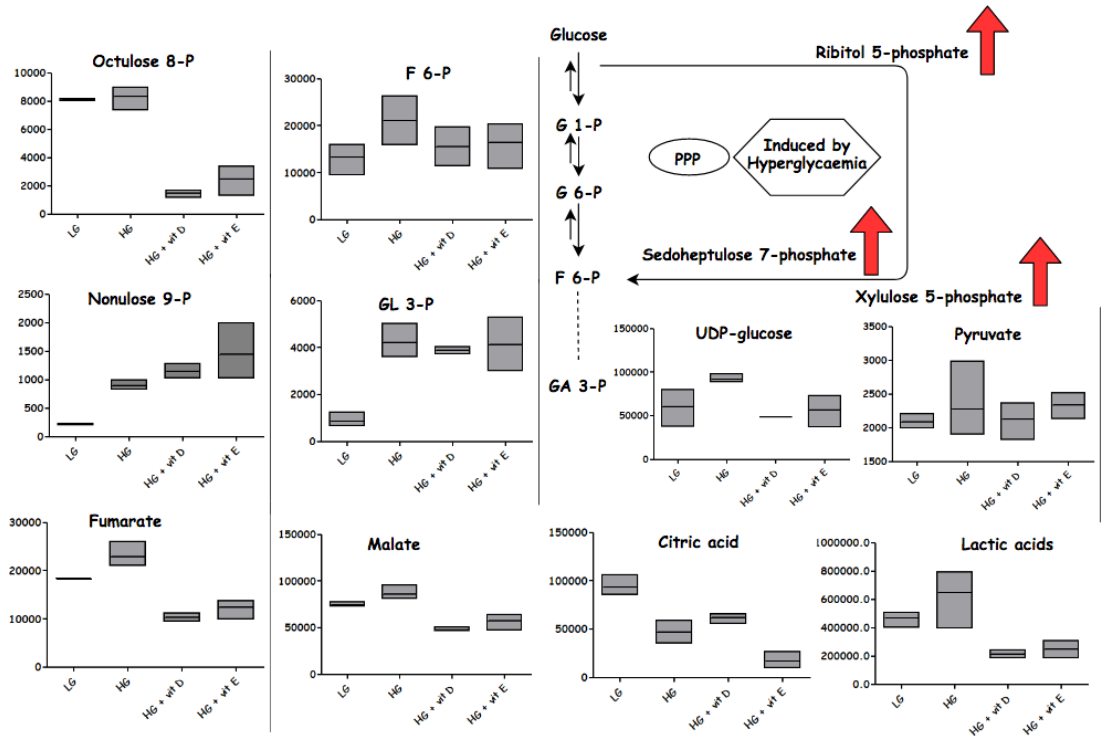

Figure 3-11: Some metabolites responses to the experiment conditions

Metabolites affected by different condition normoglycemia (LG), hyperglycaemia (HG), (HG) with vitamin D or vitamin E. column figures display the average intensities of specific metabolite in different conditions. G1-P: glucose 6-phosphate; G6-P: glucose 6-phosphate; GA 3-P: Glyceraldehyde 3-phosphate; F6-P: fructose 6-phosphate.

Under HG, the cells appear to produce glycogens with UDP-glucose (their precursor) and sugar dimers, tetramers and pentamers being increased indicating that the cells have the capacity for glucose storage. ATP levels were lowered by HG indicating that increased energy was consumed which may correlate with increased cell proliferation. These findings agree with different studies which have indicated that high glucose produces oxidative stress, disturbed glucose metabolism and impaired

the most substantial source of energy “electron transport chain” activity causing ETC dysfunction (200). Vitamin D or E attenuates many of metabolites induced by HG. Vitamin D decreased the level of GSSG and increased the level of GSH, and this was mirrored by a further fall in NADPH in comparison with HG since it is consumed as a co-factor in the conversion of GSSG to GSH. Correspondingly GSH levels increase in the HG samples treated with vitamin D. GSSG levels also increase in the vitamin E treated samples but without GSH or NADPH falling suggesting a different mechanism for conserving GSH compared with vitamin D. HG is believed to diminish GSH synthesis which is reported in diabetic patients (201). Increasing GSSG formation is associated with the excessive generation of free radicals as a marker of oxidative stress which is believed to be elevated in diabetes and PAH (202). Despite the decrease in ATP when antioxidants were added, NADH and NADP+ were restored almost to their normal level.

Amino acids: they were generally disturbed with no clear pattern while aspartate downregulation may indicate an inhibition of the conversion of aspartate to pyruvate which has been demonstrated previously in a metabolomics-based study of pulmonary arterial hypertension (203). Citrulline and histidine were also downregulated while almost all other amino acids were not significantly affected apart from glutamate and N2-(D-1-Carboxyethyl)-L-lysine that were increased by HG. In addition, N6-acetyllysine and aminopentanoate were influenced indicating that the lysine degradation pathway might be activated in order to promote the biosynthesis of acetoacetyl-CoA. Although small changes of amino acids appeared

due to HG, vitamins D & E were able to inhibit some of the induced changes such as those for glutamate, N2-(D-1-Carboxyethyl)-L-lysine and aminopentanoate.

Lipids: Metabolic profiling of induced PASMCs showed an alteration of lipid pathways by HG. However, there was no clear pattern with some lipids especially fatty acids being upregulated and some being downregulated by HG. The clearest effect of vitamin D and vitamin E appeared to be in promoting levels of the polyunsaturated fatty acids linoleic acid, eicosatrienoic acid, docosatetraenoic and docosatrienoic acid. This might indicate some protection of these acids against oxidation. Cardiovascular diseases were associated with changes in lipid metabolism and accordingly alterations in lipid profiles (204). Other studies carried out on Alzheimer's disease revealed significant decrease in long-chain glycerophosphocholines PC(36:5; 38:6 and 40:6), sulphatides (205,206), and increases of very long chain LPCs(32:0 and 34:0) (207). Vitamin E is an effective antioxidant reserve lipid preventing most of the lipid oxidation (208). Vitamin D was first identified to work as an antioxidant in 1993 when it was shown that it at the ability to prevent lipid peroxidation in the cell membrane (172). However, our results demonstrated a narrow impact on specific lipids that could show a positive response to the antioxidants suggesting that they might help to prevent some of the undesired modifications occurring on the lipid metabolites due to HG.

Nucleotides: HG-induced pyrimidine and purine pathway metabolites and increased intracellular content of uridine, pseudouridine, 3'-UMP, guanine, and hypoxanthine. PPP influences nucleotide metabolites that are believed to modulate smooth

muscle cell proliferation. Cell culture studies on artery SMCs derived from human and rat showed that mononucleotide polyphosphates like ATP and UTP stimulate SMC proliferation (209). In vitro and in vivo studies reported that increases of the intracellular content of uridine correlated with an increase in insulin resistance (210) (211). Vitamins D and E have a marked effect on lowering uridine levels under HG. A study investigated biochemical oxidative markers and found that hypoxanthine plasma concentration was elevated (212) among patients with obstructive sleep apnoea syndrome as a disease characterized by the increase of oxidative stress (213) in comparison to normal subjects. However, hypoxanthine has also been found to inhibit the proliferation of smooth muscle cells, while both antioxidant vitamins were found to highly increase hypoxanthine levels in the current experiment.

3.5 Conclusion:

Sustained exposure to hyperglycaemia causing metabolic disruption of pulmonary artery smooth muscle leads to cellular damage and could contribute to pulmonary hypertension via enhancing the generation of free radicals and promoting the proliferation of PASMCs which eventually results in a narrowing and remodelling of the pulmonary arteries and pulmonary hypertension. Therapeutic stabilization and restoration and targeting of pulmonary arterial smooth muscle cell function via antioxidants treatment could be beneficial for improving the redox status related to diabetic and cardiovascular deterioration. Based on that and in consistent with the importance of avoiding ROS produced by hyperglycaemia causing cardiovascular

disease as a complication, antioxidants may assist in reducing the oxidative damage via reacting with free radicals to scavenge them or indirectly by suppressing the free radical generating enzymes or promoting intracellular antioxidant enzyme activity which all could slow the proliferation of PASMCs. Antioxidants vitamin D & E thus can be considered to maintain the redox state of PASMCs in the presence of elevated glucose conditions in an in-vitro setting.

3.7 Limitations and future prospects:

Our findings were directly linked to the cell-based work which is focused on the medial smooth muscle cell, particularly which may not be applied in an in-vivo setting. Inflammatory processes and immune system impacts were not taken into account. Thus, the reported responses in our hyperglycaemic (diabetic-like) cell culture model might differ from the hyperglycaemic responses in an in-vivo setting. Therefore, it would be valuable to investigate the current study observations on an animal model. In addition, further increases in glucose levels and vitamins concentration might be considered in the future studies to produce biomarkers which could be used in human studies.

Chapter Four

Combination impact of hyperglycaemia and hypoxia on pulmonary artery smooth muscle cells metabolome in presence of Cholecalciferol-D3: Untargeted metabolomics-based study

---

4 Combination impact of hyperglycaemia and hypoxia on pulmonary artery smooth muscle cells metabolome in presence of Cholecalciferol-D3: Untargeted metabolomics-based study

4.1 Introduction

In the previous chapter, the impact of hyperglycaemia as a key aspect of diabetes effects on PASMCs was demonstrated in-vitro. Hyperglycaemia-induced mitochondrial ROS changing, in turn, the cellular metabolic processes and increasing smooth muscle cell proliferation. An increase in the proliferative capacity of PASMCs may be attributed to increased production of vascular endothelial growth factor induced by hypoxia caused by vessel narrowing with the consequent reduction in perfusion that occurs at an early stage after the onset of diabetes (214). Hyperglycaemia moreover is supposed to target endothelial cells as an initial consequence of diabetes-inducing endothelial cellular hypoxia which in combination with mitochondrial ROS overproduction would consistently cause hyperglycaemic damage (215). Hyperglycaemia in vivo have a “hypoxia-like” effect that is enhanced via endothelial cell activity and might contribute to the smooth muscle cellular alteration (214). The current study investigated the impact of a combination environment of both 25 mM glucose media (hyperglycaemia) and 3% O_2 (hypoxia) on the PASMCs based on the hypothesis suggest that hyperglycaemia created an environment of hypoxia in the vasculature cells. Oxygen is an essential substrate in the glycolysis process as it is needed to convert NADH to ATP via the

terminal respiratory chain. Under hypoxic conditions, it might be that glycolysis would be promoted rather than the TCA cycle.

Uncontrolled diabetes induces mitochondrial ROS and causes further metabolic dysfunction of different pathways including the polyol pathway, methylglyoxal, hexosamine and protein kinase C (PKC). Glucose is converted to sorbitol due to elevation glucose above the glycolytic capacity of cells. This leads to ROS generation via NADH in the presence of NADH oxidase and plays an important role in diabetes complications (216). Accumulation of glyceraldehyde 3-phosphate well known to be one of the consequences of hyperglycaemia due to inhibition of glyceraldehyde 3-phosphate dehydrogenase (GAPDH) by ROS (217). Accumulation of this metabolite along with glycolysis metabolism upstream increases the formation of methylglyoxal (MGO) and advanced glycation end-products (218).Stimulation of these pathways including polyol and methylglyoxal activate PKC which is associated with hyperglycaemia and has been found to be involved in various diabetic complications (60). Hypoxia, on the other hand, induces pulmonary vascular remodelling and has been demonstrated to directly enhance cell proliferation in some in-vitro studies while no change was found in some others (219–221). However, the exact mechanism for the effects of hypoxia is still not fully reported yet. It is also well known that hypoxia impacts PASMC glycolysis by shifting pyruvate towards lactate rather than the TCA cycle in what is known as the "Warburg effect". Overall remodelling pathways affected by both hypoxia and hyperglycaemia were the focus of interest.

4.2 Materials and Methods

4.2.1 Cell culture

PASMCs were obtained, harvested and dissected in aseptic conditions as has been described in sections 2.2.1.1 and 2.2.1.2. Cells were then supplemented by 10% bovine calf serum (BCS), 5% penicillin and streptomycin in a mixture of 1:1 F-12 DMEM and cultured at 37° C in a 21% O_2, 5% CO_2 incubator. Depending on the experiment condition of each group, cells were cultured either in 1. High glucose media (25 mM) "diabetic-like condition" in a hypoxic chamber (3% O_2) or normoxic (21% O_2). 2. Normal glucose media (5 mM) in a hypoxic chamber (3% O_2) or normoxic (21% O_2). 3. 25 mM glucose + physiological concentration of vitamin D cholecalciferol (80 ng/ml) in hypoxic chamber (3% O_2) or normoxic (21% O_2).

4.2.2 PASMC Proliferation Assay

PASMCs were placed in DMEM media supplemented by 10% (BCS) and seeded into 24-well flasks at cell intensity of $2x10^4$ per well. After 24 hours, cells were washed by free media and quiesced with 0.1% BCS for 24 hrs. Cells were then cultured in 5% BCS for 72 hrs in compatible with the intervention and condition of each group (hypoxic samples were moved for normoxia and placed in hypoxia incubator at last 24 hrs). Samples were then prepared according to the procedure described in section (3.3.3)

4.2.3 Reactive oxygen species experiment

PASMCs were seeded at 5×10^3 cells per well in 96-well plates supplemented with 10% BCS DMEM for 24 hrs allowed to attach. Media then was discarded, and cells washed by free media, followed by the addition of 5% BCS DMEM media for 72 hrs with regard to our intervention and condition of each group. Reactive oxygen species were then measured based on the methodology designated in section (3.3.4)

4.2.4 Metabolic profiling sample preparation

In an appropriate number of replications, cells were cultured with various conditions at indicated final concentrations and incubated as described previously. Metabolomics samples were prepared and stored as described in section 2.2.2. Samples afterwards run on the liquid chromatography-mass spectrometer using the standard lab method and conditions described in section 2.2.3. Mixtures of standard metabolites and pooled quality control (QC) sample were injected in each analysis run in order to facilitate the identification and to evaluate the stability and reproducibility of the analytical method. QC sample was obtained by taking equal aliquots from all the samples and placing them into the same HPLC vial.

4.2.4.1 Samples analysis (LC/MS)

Samples analysis carried out on an Accela HPLC system interfaced to an Exactive Orbitrap mass spectrometer by hydrophilic interaction liquid chromatography (p-HILIC) using the procedure explained in section 2.2.3

4.2.4.2 Data extraction, analysis and biomarker detection

Explained in sections 2.2.4 and 2.2.5

4.3 Results

4.3.1 PASMCs oxidative stress status was influenced by combined conditions (Hyperglycaemic media and hypoxia)

ROS were measured when PASMCs exposed to hyperglycaemic medium in the hypoxic chamber. In addition, the effect of vitamin D (Cholecalciferol-D3) on ROS when supplemented to the hypoxic elevated glucose media was also measured.

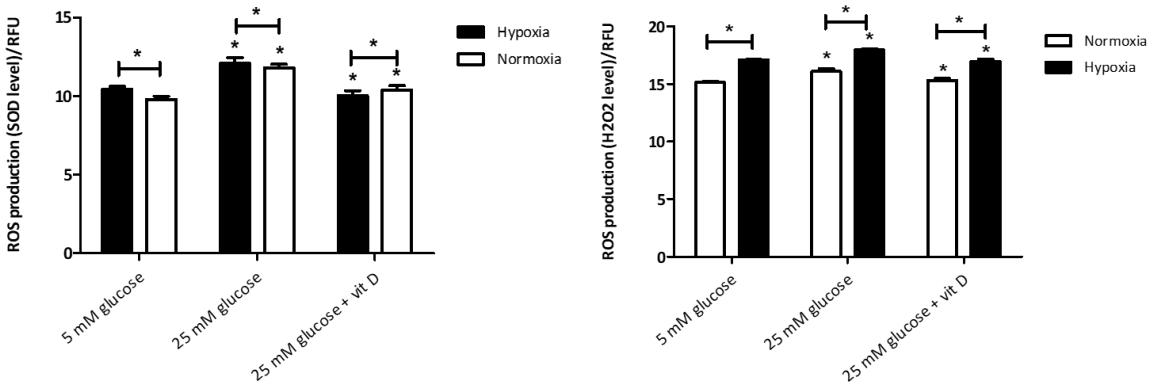

Figure 4-1: ROS production of different groups

The effect of hypoxia companied with high glucose media with and without Vitamin D on ROS production. The figure also demonstrates normoxic samples in comparison. PASMCs were incubated for 72 h where the hypoxic samples left in a 3 % O_2 chamber for 24 h. Vitamin D (80 ng/ml) was added immediately along with the high glucose incubation. Superoxide (O2.-) levels and H_2O_2 levels were detected by (DHE) and (DCF) fluorescence compound, respectively). * p <0.05 (T-test) of comparison variables whether among hypoxia of both SOD and H2O2 or comparing them to the normoxia condition.

Intracellular O2.- and H_2O_2 levels produced in PASMCs were detected using (DHE) and (DCF). (Figure 4-1) demonstrates that hypoxic high glucose (HHG) media influenced the PASMCs to yield more ROS rather than hypoxic normal glucose samples (HNG). PASMCs under HHG condition increased the production of O2.- to about 10% and H_2O_2 to about 9%. It also shows that hypoxia-induced ROS under HG and NG while cells exposed to 3 % O_2 generated more ROS than in NG, HG or HG supplemented with vitamin D. Adding vitamin D to the HG media with and without hypoxia attenuated redox state of superoxide and hydrogen peroxide by about 4% and 5% respectively.

4.3.2 Combination impact of hypoxia and hyperglycaemia on PASMCs proliferation activity

The proliferative effect of hypoxia on control, HG and HG media supplemented by vitamin D on PASMCs proliferation was assessed by a [3H] thymidine incorporation assay in comparison with normoxia.

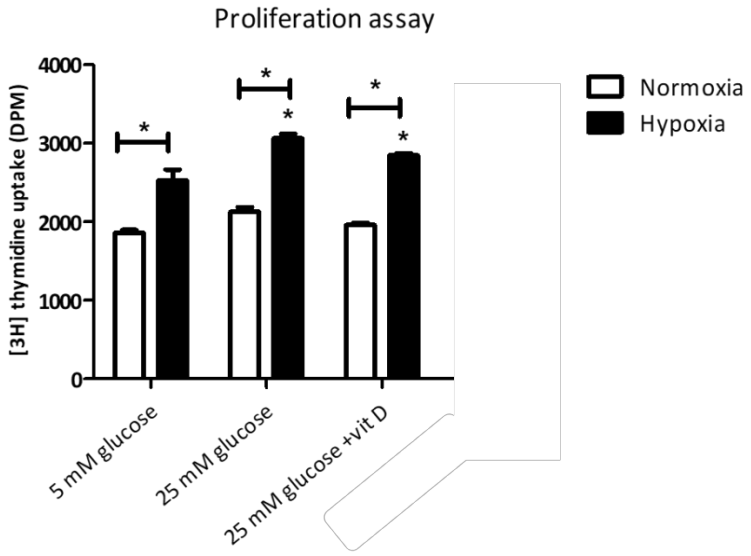

Figure 4-2: Proliferation assay of the hypoxic and normoxic condition in different conditions

The effect of Vitamin D on hypoxic high glucose-induced [3H] thymidine uptake by PASMCs. Quiesced cells were cultured with normal (5 mM) and high glucose (25 mM) for 72 h (hypoxic samples transferred to 3% O2 Chamber in the final 24 h). Vitamin D (80 ng/ml) was added immediately along with high glucose incubation. [3H]-thymidine incorporation assay was performed for the evaluation of DNA synthesis (as an index of cell proliferation). Experiments were conducted in quadruplicate. Radioactive counts were measured in disintegrations per minutes (DPMs) ± SEM. * p <0.05 (T-test) of comparison variables whether among hypoxia conditions of proliferation assay or comparing each condition to the same one of normoxic.

It is obvious that HG media accompanied by 3% O_2 increased DNA synthesis of PASMCs increasing the proliferation ability of cells by about 20% which in turn

reverted to a normal level when 80 ng/ml cholecalciferol-D3 was used. The result also illustrates that hypoxia under all conditions was able to increase cell proliferation in comparison with normoxia.

Oxidative stress and the proliferation capability of PASMCs were slightly influenced by the combination HHG. Cholecalciferol-D3, in addition, might help to suppress unwanted reactions initiated due to exposing cells to such stressor factors.

4.3.3 PASMCs under HHG conditions have distinctive metabolomic biomarkers

Further study was carried out on PASMCs with the aim of obtaining the metabolic fingerprint in order to enhance the current understanding of biological changes appearing in response to external oxidative stress factors. Using LC/MS analysis samples were prepared, injected and data afterwards extracted, processed and analysed to detect metabolites influenced by HHG comparing to HNG and HHG supplemented by vitamin D.

4.3.3.1 Metabolomics data extraction, processing, analysis and markers identification

Data were extracted using Xcalibur 2.1 as explained in section 2.2.4 and converted to numeric files via MzMatch. Data were then normalized using log 2 transformation, and an RSD was calculated based on pooled sample readings prior to data examined using multivariate analysis application (SIMCA-P 14.1). Based on the RSD that evaluates the precision of the instrument, 84 metabolites with values above 30% were excluded.

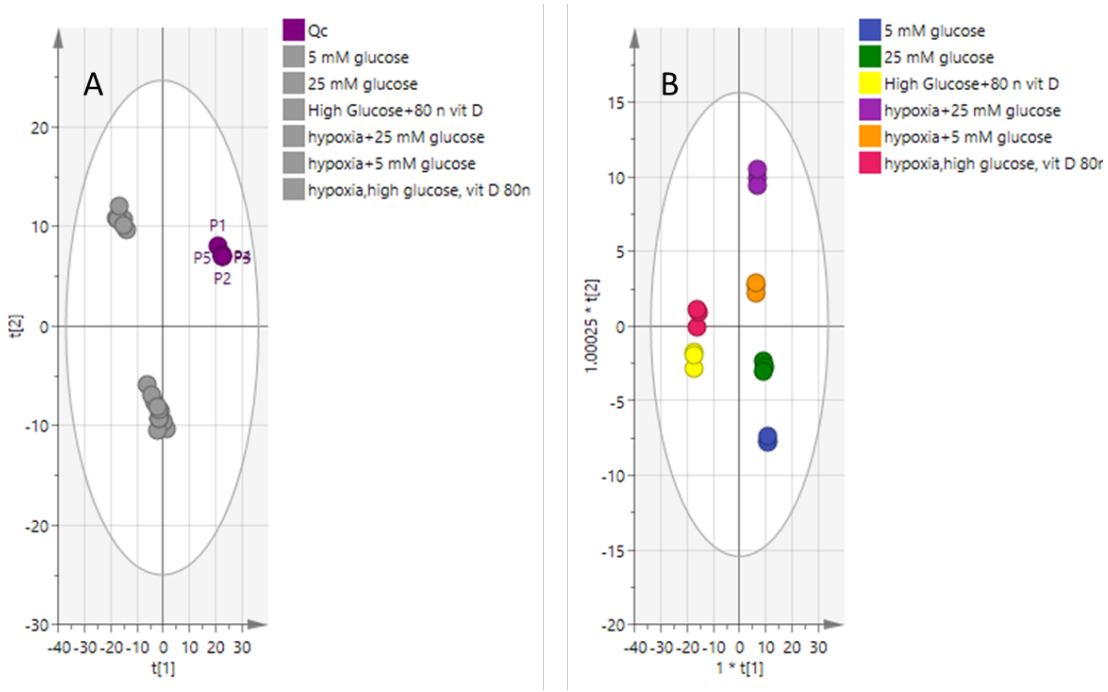

Figure 4-3: QC sample PCA model and the OPLS-DA model for 6 groups involved in the experiment

(A) Shows pooled (Qc) samples clustering indicates to analytical stability so that the differences between groups will not be due to instrumental factors alone. There are five repeated reading for one sample were prepared by taken 10 µl of each sample and were injected to be run after every set of samples. (B) OPLS-DA supervised model to display the pattern of samples distribution in the model. The plot exhibits the distribution of 18 samples based on the reading of 548 putative metabolites.

It is clear that there is a marked difference in the metabolic profiling of different groups (Figure 4-3 B). Even though samples were well clustered, and the goodness of prediction was high of 0.99, and the model fit was good where about 89% of model was explained (72% predictive, 16% orthogonal), the model gave a CV-ANOVA of (P = 0.567) demonstrating that model is not valid

Table 4-1: CV-ANOVA that represent the model validity where only $p < 0.05$ considered to be valid

Model	SS	DF	MS	F	p	SD
Total corr.	85	85	1			1
Regression	59.2557	60	0.987595	0.959042	0.567561	0.993778
Residual	25.7443	25	1.02977			1.01478

4.3.3.2 Metabolic profiling of hypoxic 25 mM glucose (hyperglycaemia), 5 mM glucose (control) and 25 mM glucose supplemented by cholecalciferol-D3

Putative metabolites that discriminate each group from others were identified using a Student's t-test, 95% confidence interval and VIP of each comparison individually. Results revealed that out of 548 putatively identified compounds, 81 metabolites were found to be significantly changed in HHG PAVSMCs compared to HNG cells with P value < 0.05, 95% CI not including 0 value, RSD ≤ 30% and VIP > 1. In order to study the impact of cholecalciferol-D3, only those metabolites significantly altered by HHG were considered.

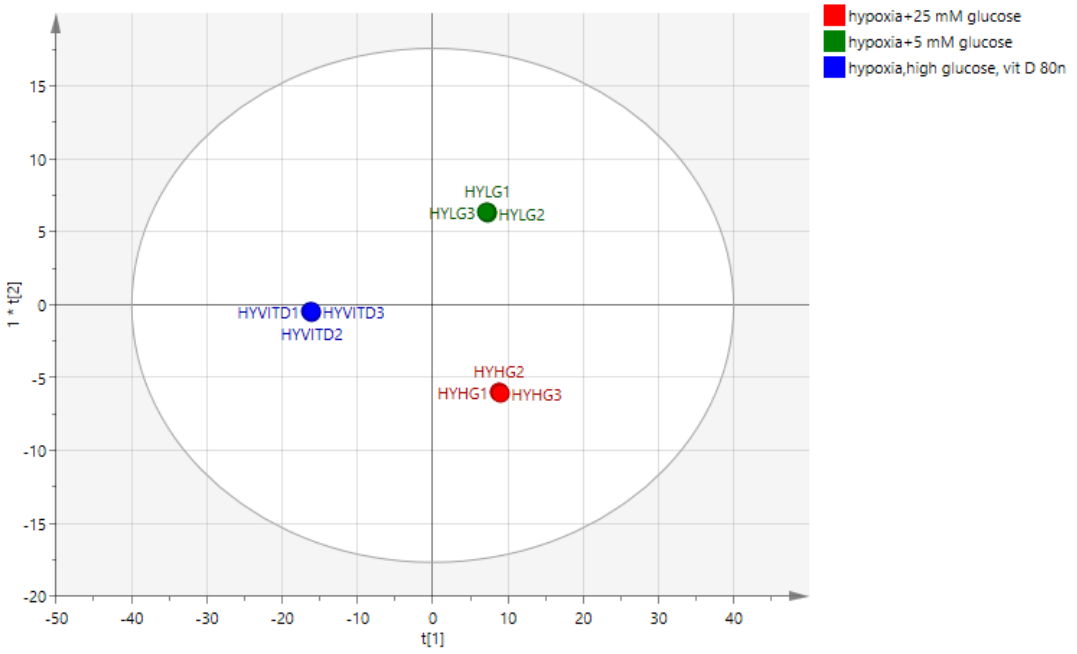

Figure 4-4: OPLS-DA score plot for 9 samples of different 3 groups

OPLS-DA score plot displays the distribution of groups samples based on the reading of 548 metabolites. The figure illustrates the clustering of the samples in the model of total metabolites while model fit 94% of the data (71% predictive, 23% orthogonal and CV-ANOVA P= 0.603).

Model validation prior to the obtaining of significant metabolites shows that the model was not valid. However, model significance was examined again once it was rebuilt based on the reading of 81 significant biomarkers and demonstrated valid model with CV-ANOVA of (P = 4.26E-005) and a permutation test indicated that model was not spurious.

Table (4-2) shows the list of significantly altered metabolites including amino acids, glycolysis metabolites, lipids and nucleotides that distinguish HHG from HNG.

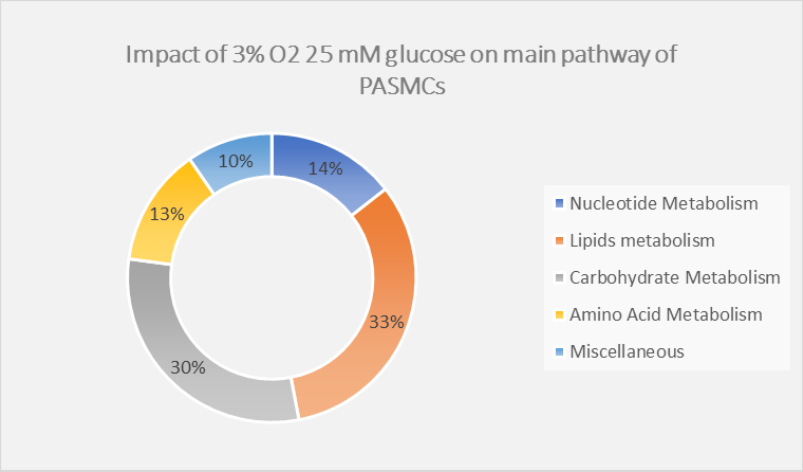

Figure 4-5: Percentage of different metabolic pathways contributes to the discrimination between groups.

It demonstrates the percentage of metabolites out of the total number of metabolites affected in the various pathways impacted by hypoxia hyperglycaemia and vitamin D. It determined based on the number of metabolites detected in each pathway.

Fatty acids and lipids represented the most affected pathways affected by HHG conditions demonstrating that cell membrane and cell permeability might be impaired by treatment. Increases in carnitine metabolites were observed following the exposure of cells to HHG conditions. Increases in levels of carnitines might indicate decreased transport of these intermediates in the mitochondria due to fatty acid metabolism being impaired by a lack of oxygen which is required to convert the NADH produced by fatty acid beta-oxidation into ATP. NADH was found to accumulate in the hypoxic conditions.

Glycolysis metabolites were influenced as well when particularly the PPP oxidative pathway was stimulated due to glucose being redirected into that pathway. Moreover, upregulation of NADH companied by CoA and Acetyl CoA increases

possibly indicate a slowing of the TCA cycle. This was also supported by the accumulation of upper glycolysis intermediates like glucose 6-phosphate and glucose 1-phosphate.

Oxidized glutathione (GSSG) as oxidative damage marker was increased although the levels of GSH were not affected.

Vitamin D, on the other hand, minimized HHG impact on PASMCs while most of the influenced metabolites restore to its normal level as in HNG sample

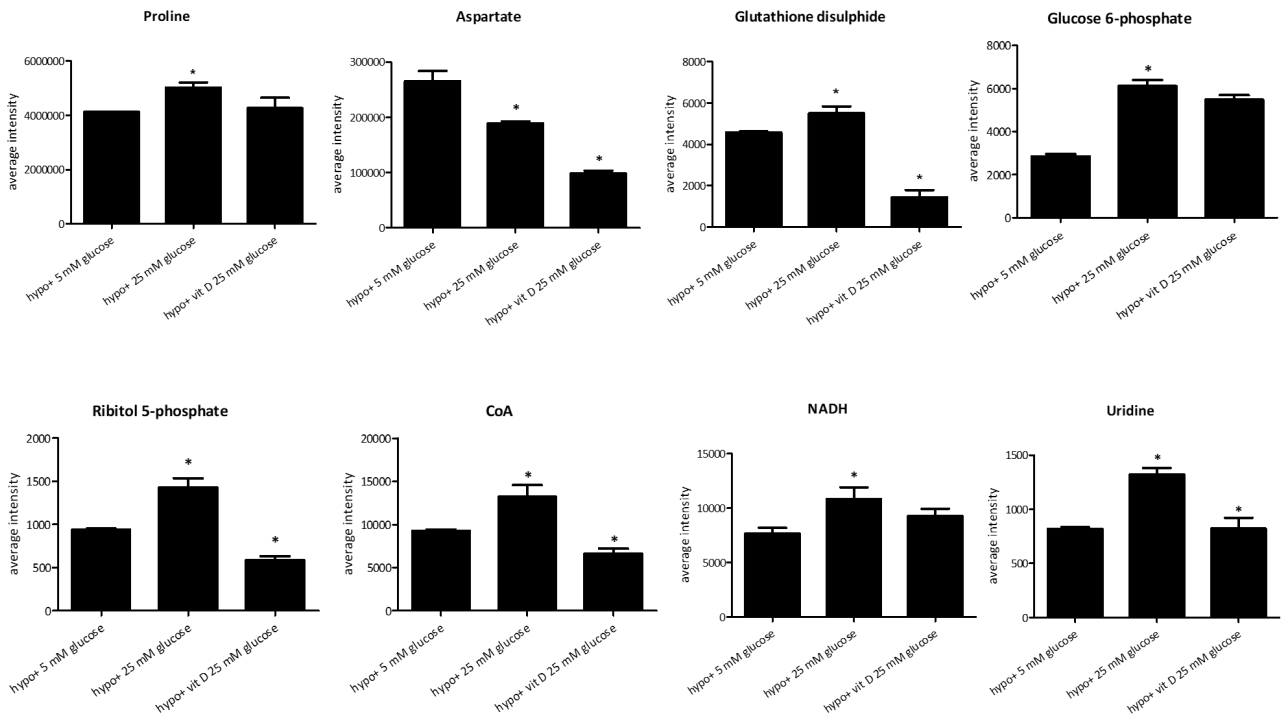

Figure 4-6: Some metabolites that influenced by the condition.

Examples of different metabolites average intensity at different conditions of hypoxic normal, high and high glucose supplemented by vitamin D. metabolites intensities tended to be restored to control levels when vitamin D was added.

Table 4-2: List of significant altered putative metabolites that affected by hypoxia hyperglycemia and supplemented by vitamin D.

Mass	RT	Putative metabolite	-/+	Hypoxia 25 mM/5 mM glucose		Hypoxia vitamin D/25 mM glucose	
Miscellaneous				P. value	Ratio	P. value	Ratio
246.09	10.16	5-6-Dihydrouridine	-	0.023	1.28	<0.001	0.29
223.11	13.33	N-acetyl -D- glucosaminitol	-	0.007	1.46	ns	1.18
246.05	13.48	Glycerophosphoglycerol	-	0.005	1.52	0.001	1.55
185.00	10.83	Serine O-sulfate	-	0.021	0.74	ns	1.17
181.04	12.42	Methionine sulfone	+	0.030	0.79	ns	1.09
Glutathione homeostasis							
307.08	14.58	Glutathione*	-	0.001	1.01	0.010	1.24
612.15	17.99	Glutathione disulphide*	-	0.045	1.20	0.006	0.26
744.09	17.55	NADPH*	-	0.008	1.20	0.020	0.75
743.08	17.61	NADP+*	-	0.025	0.86	ns	1.01
230.02	16.70	Xylulose 5-phosphate*	-	0.000	1.94	ns	0.99
232.03	16.46	Ribitol 5-phosphate	-	0.004	1.53	0.001	0.41
335.08	14.56	S-Formylglutathione	+	0.002	1.26	0.000	0.17
Amino Acids							
131.07	14.93	Creatine*	+	0.010	1.10	0.000	0.63
219.07	14.94	O-Succinyl-L-homoserine	-	0.024	1.51	0.003	0.48
145.11	4.55	4-Trimethylammoniobutanoate	+	0.009	1.36	0.006	0.60
101.08	13.34	Betaine aldehyde	+	0.016	1.34	ns	1.03
103.06	15.79	4-Aminobutanoate *	+	0.014	1.22	0.001	1.56

115.06	12.93	Proline *	+	0.007	1.22	ns	0.85
133.04	15.85	Aspartate*	+	0.009	0.71	0.000	0.52
109.02	15.45	Hypotaurine*	+	0.005	1.21	0.000	0.44
117.08	11.26	5-Aminopentanoate	+	0.015	1.51	0.000	0.32
Sugar metabolism							
566.06	17.48	UDP-glucose*	-	0.002	1.28	<0.001	0.65
290.04	17.22	Sedoheptulose 7-phosphate	-	<0.001	3.15	ns	1.03
537.08	17.65	CDP-ribitol*	-	0.037	1.72	0.020	0.78
260.03	17.93	Glucose 1-phosphate*	-	0.012	1.38	ns	0.84
259.02	17.82	Fructose 6-phosphate*	-	0.009	1.39	0.021	0.78
178.07	11.22	Glucosamine	-	0.015	1.51	0.000	0.29
258.05	15.45	Glucosamine 6-phosphate	-	0.020	3.07	ns	1.31
89.02	10.29	(R)-Lactate	-	0.006	0.87	0.011	0.85
827.27	18.53	Maltopentaose	-	0.044	3.09	ns	1.04
665.20	18.08	Maltotetraose	-	0.000	6.12	ns	0.95
503.17	14.66	Maltotriose	-	0.040	1.21	ns	0.96
87.01	7.49	Pyruvate*	-	ns	0.85	ns	0.79
168.99	16.31	DL-Glyceraldehyde 3-phosphate	-	0.001	2.61	0.011	0.79
181.08	14.31	Sorbitol	-	0.277	0.80	ns	1.32
191.02	19.66	Citrate*	-	0.031	1.65	ns	0.80
117.02	16.33	Succinate*	-	0.004	0.87	0.014	1.13
115.00	15.82	Fumarate*	-	0.274	1.02	0.009	0.70
133.01	17.31	Malate*	-	0.023	0.97	0.011	0.74
196.06	15.07	Gluconate	-	0.003	2.23	0.001	0.32
255.71	14.50	CoA*	-	0.027	1.43	0.007	0.50

260.03	16.82	Glucose 6-phosphate*	-	0.000	2.14	ns	0.90
809.12	12.95	Acetyl-CoA*	+	0.027	1.17	0.017	0.78
665.13	14.13	NADH*	-	0.047	1.42	ns	0.86
Fatty Acids and lipids							
257.10	14.54	sn-glycero-3-Phosphocholine	-	0.014	1.17	0.000	0.25
210.16	4.12	[FA (13:2)] 3E,5E-tridecadienoic acid	+	0.005	2.79	ns	0.81
215.12	7.47	2-Amino-9,10-epoxy-8-oxodecanoic acid	+	0.015	1.41	0.032	0.66
399.33	4.32	[FA] O-Palmitoyl-R-carnitine	+	0.000	1.39	0.015	0.81
501.29	4.24	LysoPE(0:0/20:4(5Z,8Z,11Z,14Z))	-	0.028	0.70	ns	1.36
811.54	3.56	[PS (18:0/20:4)]	-	0.038	1.65	0.039	0.72
842.51	3.48	PG(20:4(5Z,8Z,11Z,14Z)/22:6(4Z,7Z,10Z,13Z,16Z,19Z))	-	0.034	1.21	0.002	0.63
809.52	3.57	PS(18:1(9Z)/20:4(5Z,8Z,11Z,14Z))	-	0.035	1.33	0.002	0.53
720.49	3.52	PG(16:0/16:1(9Z))	-	0.029	1.68	ns	0.84
834.52	3.58	PI(16:0/18:2(9Z,12Z))	-	0.032	1.23	0.002	0.57
765.57	3.74	PC(18:3(6Z,9Z,12Z)/P-18:1(11Z))	+	0.006	1.38	ns	0.89
723.52	3.69	PE(18:3(6Z,9Z,12Z)/P-18:1(11Z))	+	0.040	1.34	0.001	0.48
753.53	3.77	[PC (14:0/20:4)]	+	0.045	1.19	0.005	0.39
812.68	3.80	SM(d18:1/24:1(15Z))	+	0.007	1.61	0.022	0.26
702.57	3.87	N-(hexadecanoyl)-sphing-4-enine-1-phosphocholine	+	0.023	1.42	0.000	0.40
810.66	3.92	SM(d18:2/24:1)	+	0.030	1.83	0.021	0.57
741.61	3.53	N-(docosanoyl)-1-beta-glucosyl-pentadecasphing-4-enine	+	0.049	1.42	ns	1.48
593.52	3.52	Diacylglycerol	-	0.037	1.47	0.039	0.74
257.16	7.46	2-Hexenoylcarnitine	+	0.015	1.26	0.009	0.70
425.35	4.30	Oleoylcarnitine	+	0.018	1.20	0.000	0.38
245.16	7.64	2-Methylbutyroylcarnitine	-	0.038	0.83	0.000	0.39

289.15	7.46	3-Methylglutarylcarnitine	+	0.002	1.25	ns	0.92
Purines and pyrimidines							
324.04	17.49	3'-UMP*	-	0.000	1.46	0.000	0.60
244.07	9.94	Uridine*	-	0.001	1.61	0.020	0.62
324.04	16.01	Pseudouridine 5'-phosphate	-	0.023	1.41	0.001	0.40
559.07	15.71	ADP-ribose	-	0.034	0.59	ns	1.24
244.07	12.27	Pseudouridine	-	0.017	1.43	0.000	0.31
347.06	14.31	3'-AMP*	-	0.047	1.35	0.008	1.82
323.05	16.10	3'-CMP*	-	0.048	1.21	0.005	0.82
404.00	17.06	UDP*	-	0.025	0.70	0.013	0.67
126.04	12.26	Thymine	+	0.005	0.86	0.000	1.27
151.05	12.64	Guanine*	+	0.001	1.42	0.000	0.19
128.06	15.04	5,6-Dihydrothymine	+	0.003	1.59	0.002	0.50
606.08	16.08	UDP-N-acetylglucosamine	-	0.016	0.89	0.000	0.44

(*) means that metabolite matches standard retention time.

Table 4-2 shows univariate assessments for all metabolites that are importantly altered due to HHG and explores, in addition, the effect of vitamin D on that modification.

Sugar metabolites stimulated by HHG were not influenced when vitamin D was added. This impact was noticed similarly on oxidized glutathione where essentially vitamin D decreases the levels which might be expected since it is known to stimulate glutathione reductase. Some lipid metabolites including fatty acids and glycerophospholipids were altered and were mainly upregulated and with some being downregulated. Vitamin D was effective in restoring most of the altered lipid metabolites. Uridine and some other nucleotides were affected by HHG were normalised when vitamin D was added.

4.3.3.3 Comparing with normoxic control

In order to assess the influence of hypoxia on the metabolomic changes of hyperglycaemic samples, we independently compared metabolomic profiling of PAVSMCs cultured in normoxic hyperglycaemic (NHG) conditions and those cultured in hypoxic hyperglycaemic (HHG) (See Table S2 section 10.2). Hypoxia was found to significantly influence 131 metabolites in hyperglycaemia environment.

Table 4-3: Summary of metabolic modification due to the intervention.

Statistical comparison	
Metabolites significantly changed	$\frac{\text{Hypoxia}}{\text{Normoxia}}$ 25 mM glucose
Total number of metabolites	131
Metabolites (↑ | ↓)	(46 | 85)

Carbohydrate intermediates like Glucose 1-phosphate, Glucose 6-phosphate, GDP-L-fructose and PPP metabolites were less influenced in comparison to normoxic hyperglycaemia. HHG, however, was accompanied by increases of ATP, CoA and NADH indicating that cells energy generating was alternatively relied on AGEs of proteins, lipids or nucleotides glycosylation and/or enhance of pentose phosphate pathway. S-Formyl glutathione precursor of formic acid that formed by oxidation of hydroxymethyl glutathione in the presence of formaldehyde dehydrogenase to generate NADH was increased among hypoxic hyperglycaemia cells. Increasing NADH:NAD+ ratio in the cytosol is associated with an increase in the glucose level (222).

Even though amino acids of HHG cells were higher than those of hypoxic normal glucose (HNG), biochemical of alanine, arginine, glycine, tryptophan and valine pathways were apparently less induced comparing to NHG suggesting that hypoxia might inhibit amino acid uptake and protein formation. Amino acids generally decreased when PASMCs were exposed to hypoxia despite the increased glucose

level. Oxidized glutathione was the only exception while GSSG intensities significantly increased as an indicator for the oxidative stress-inducing capacity of hypoxia.

We also found some fatty acids, sphingolipids, glycerophosphocholines and glycerophosphoglycerol were increased among HHG samples while some glycerophosphoethanolamines, glycerophosphoinositols and glycerophosphates components were decreased. Our findings show that HHG generally disturbed lipid metabolites when compared to NHG.

HHG comparing to NHG showed increased guanine and adenine and decreased cytosine and thymine. In general, hypoxia disturbed nucleotides.

4.3.4 The impact of hypoxia on PASMCs under the normoglycemic condition

To exhibit the impact of hypoxia on PASMCs, we observed the differences between normoxia normoglycemia (NNG) and hypoxia normoglycemia (HNG). Comparing NNG to HNG samples showing that most of the metabolites were down-regulated indicating that mitochondrial respiration of PASMCs was impaired by hypoxia. On the other hand, oxidized glutathione was significantly increased by about 2.7-fold $P = 0.0011$ in hypoxic cells comparing to normoxic cells accompanied by decreasing of NADP+. This might occur due to the induction of PPP to produce more NADPH assist in maintaining the GSSS:GSH ratio and then keep the balance of redox status. PPP intermediates mannonate, ribitol 5-phosphate and UDP-glucose were increased while other pathway metabolites like xylulose 5-phosphate, gluconate, D-

Sedoheptulose 7-phosphate and UDP-glucuronate were significantly decreased. In turn, upper glycolysis biochemicals G6-P and G1-P were reduced demonstrating inhibition of glycolysis by hypoxia. These findings along with no significant differences found in TCA components between HNG and NNG suggests that pentose phosphate was the most influenced pathway in adapting to hypoxic conditions where some of its metabolites were noticeably consumed, and others increased.

HNG slightly decreased acetyl-CoA comparing to NNG in conjunction with a slight decrease in pyruvate and no change of TCA acids apart from citrate which was not statistically significant due to the variance within normoxia samples. In addition, surprisingly lactate was not affected by hypoxia which is inconsistent with other hypoxia studies of PASMCs that demonstrated a Warburg-like effect when pyruvate tend to convert mainly to lactate rather than acetyl CoA. Triose phosphate was slightly increased by hypoxia compared to normoxia, and there was a small increase in lipid accumulation. Hypoxia, in addition, increased levels of some fatty acids which might be expected since mitochondrial respiration is required for their metabolism.

4.4 Discussion:

Culture conditions applied to this experiment were designed based on previous work on the pulmonary artery smooth muscle primary cells exposed to

hyperglycaemic conditions and supplemented with or without antioxidants in normoxia (21% O_2).

Direct comparison of cells grown under condition of HHG and HNG showed an increase in the reactive oxygen species of PASMCs cultured in the HHG accompanied by induction of DNA synthesis. On the other hand, a difference when the HHG and HNG were compared showed that hypoxia promoted ROS formation and the synthesis of DNA and thus cell proliferation.

The study presented that exposure to HHG for 72 hrs causes substantial metabolic alterations. The main aim of this study was to identify prospective biomarkers affected by combination environment of hypoxia (3% O_2) and hyperglycaemia (25 mM glucose) on PASMCs and assess the effects of adding the physiological amount of vitamin D the sample.

HHG elevated increased metabolites in the upper glycolysis pathway and significantly influenced the pentose phosphate in comparison to hypoxic normal glucose HNG while no ultimate changes were noticed in TCA or oxidative phosphorylation metabolites apart from citric acid which increased by 1.65-fold P= 0.031. Lactic acid was not increased by HHG providing further indication of that glycolysis has not been diverted by the Warburg effect where pyruvate is reduced by NADH to lactate. PPP intermediates like Xylulose 5-phosphate, ribitol 5-phosphate and sedoheptulose 7-phosphate were also elevated. PPP enhancement was previously demonstrated to be correlated with diabetes mellitus and hypoxia

while glucose redirection towards the pentose phosphate PPP is favourable to increased cell proliferation and thus increased nucleotides demand (223). Metabolome profiling demonstrated an increase of maltotetraose, maltopentaose and maltotriose indicating that the cells have the capacity for glucose storage. This may elucidate the reason why TCA metabolites were not increased significantly while upper glycolysis and PPP influenced. Another pathway attributed to this could be the polyol pathway after hyperglycaemia encouraged the cell to activate mass balance reaction when glucose reduced to sorbitol to be converted to fructose. When cells are exposed to elevated glucose exceeding the capacity of glycolysis could address, glucose then will be reduced to sorbitol via NADPH following by oxidizing of sorbitol to fructose via NAD which leads to decrease the pool of NADPH and NAD components that are essential cofactors in redox reactions. Fortunately, though, PPP stimulation significantly helps to maintain the NADPH level.

ATP was not significantly increased by HHG comparing to HNG although glycolysis was induced by HHG. Glycolysis yields more ATP when it was stimulated via NADH oxidation by electron transport chain (ETC) even though the Krebs cycle was not highly induced. In addition, two equivalents ATP also produced through the upper glycolysis process. DNA synthesis was increased by HHG suggests that energy was consumed in the process of cells proliferation.

Our results are in agreement with different researchers studying the impact of hyperglycaemia on macro, and microvascular activation of protein kinase, polyol and hexosamine pathways (224) (225). Inhibition of GAPDH due to overexpression

of superoxide activates those pathways. In addition, advanced glycation end products (AGEs) which are proteins or lipids that are glycated as an effect of uncontrolled sugars levels could initiate or worsen diabetes (226) (see figure 4-7). Lipids like low-density lipoprotein (LDL) and proteins such as collagen of many cells types are directly impaired by AGEs especially those of artery wall cells and lead to modifying wall stiffness and elasticity (227).

Diabetes mellitus and hypoxia believed to increase methylglyoxal (MGO) glycolysis by-products inducing oxidative stress as a consequence of modification of arginine and lysine residues of intracellular proteins. Glycated proteins disturb cellular stability and boost the mitochondrial ROS manifestation and thus promoting posterior glycation modification (228).

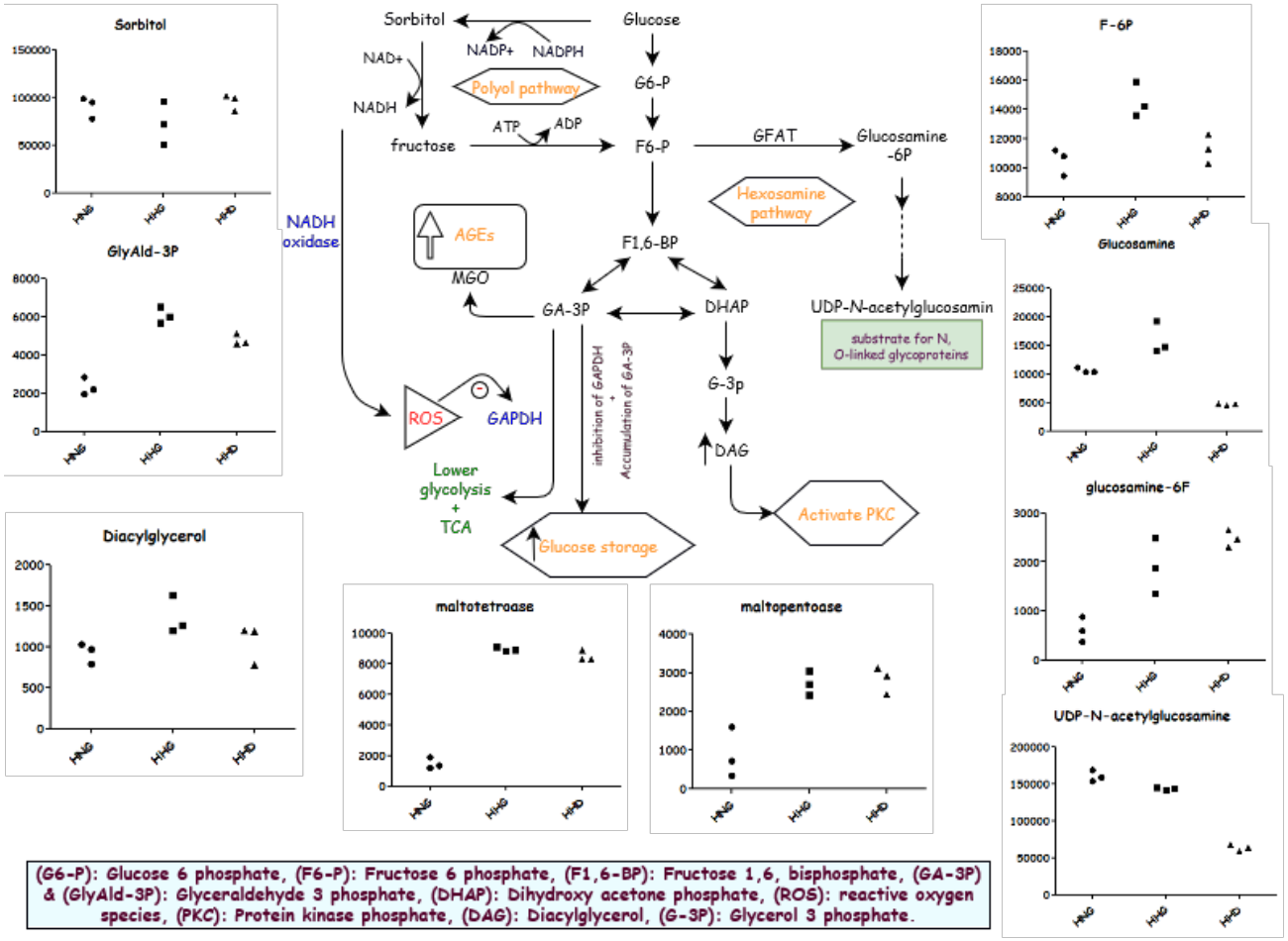

(G6-P): Glucose 6 phosphate, (F6-P): Fructose 6 phosphate, (F1,6-BP): Fructose 1,6, bisphosphate, (GA-3P) & (GlyAld-3P): Glyceraldehyde 3 phosphate, (DHAP): Dihydroxy acetone phosphate, (ROS): reactive oxygen species, (PKC): Protein kinase phosphate, (DAG): Diacylglycerol, (G-3P): Glycerol 3 phosphate.

Figure 4-7: Glycolysis metabolism influenced by HHG

Glucose redirection into the polyol pathway has been related to the complications of diabetes through numerous possible pathways. Polyol pathway when glucose is reduced to sorbitol and then oxidized to fructose converted to (F6-P) by hexokinase decreases, in turn, NADPH and NAD+. NADH oxidase oxidizing NADH generates reactive oxygen species (ROS), which can damage the membranes of mitochondria. Also, the hexosamine pathway which is further converted F6-P to glucosamine-6-phosphate produces UDP-N-acetylglucosamine as end product used as a substrate for N,O-linked glycoproteins. GlyAld-3P accumulation along with DHAP might lead to the formation of methylglyoxal (MGO). The incessant interconversion of GA3-P to DHAP leads to associated transfer of electrons from reduced cytosolic NADH to mitochondrial oxidized FAD, which would produce high membrane potentials and suppression of the electron transport chain. They also induced the formation of advanced glycation end-products. In addition, DHAP conversion to diacylglycerol activates protein kinase C (PKC).

4.4.1 Formation of Methylglyoxal (MGO)

Although methylglyoxal cannot be detected via our analysis methodology -mass lower than 75 g/mol- it is believed to be induced via exposure to an elevated glucose environment (229). Accumulation of glyceraldehyde 3-phosphate (G-3P) via the inhibitory impact of ROS on GAPDH in addition to the upstream accumulation of glycolysis metabolites produces more MGO. It instantly reacts with nucleic acids in addition to arginine and lysine residues forming AGEs that lead to mitochondrial decline and overproduction of ROS (230). MGO has a direct impact on mitochondrial respiration and enhances the alteration of specific mitochondrial proteins (231). Vitamin D, on the other hand, was able to inhibit the accumulation of G3P when hypoxia hyperglycaemia samples were supplemented by Cholecalciferol-D3 compared to HHG which might occur as a consequence of the capability of vitamin D to restore NADH and NADPH to their normal level.

4.4.2 Activation of the hexosamine pathway

Metabolic profiling of HHG PASMCs shows that glucose flux through the hexosamine pathway is enhanced via fructose 6-phosphate being converted to glucosamine that leads finally to the formation of uridine Phosphate-N-acetylglucosamine/hexosamine. Glucosamine is increased by about 1.5-fold while glucosamine 6-phosphate is increased by about 3-fold, P= 0.015 & P= 0.020 respectively. This was also combined with decreased in UDP-N-acetylglucosamine where it might be consumed to produce the end product N,O-linked glycoproteins.

Glucose shunting into the hexosamine pathway is considered to be one of the complications of diabetes and is known to initiate insulin resistance and/or atherosclerosis. Modification of N,O-linked glycoproteins has been connected to a variety of gene transcriptional factors and alteration of vascular smooth muscle cells (232). A study found that inhibition of glutamine:fructose-6-phosphate aminotransferase (GFAT) enzyme suppressed converting of F-6P to glucosamine and decreased the influence of hyperglycaemia to increase transcription of transforming growth factor (TGF) that mediates a signalling pathway for cell proliferation and differentiation and plasminogen activator inhibitor-1 (PAI-1) which is correlated with atherosclerosis (233). Vitamin D was able to decrease the effect of HHG on glucosamine levels, but glucosamine-6P was increased accompanied by a significant decrease of UDP-N-acetylglucosamine. This may suggest that vitamin D caused accumulating of glucosamine-6P which suppressed the formation of UDP-N-acetylglucosamine.

4.4.3 Diacylglycerol (DAG):

Diacylglycerol levels were increased when PASMCs were cultured in the HHG environment (Table 4-2). GAPDH inhibition by HHG leads to the accumulation of the upstream glycolysis intermediate G-3P which also can be converted to DAG. DAG amount has been found to be elevated in diabetes patients at vascular tissues of aorta and heart (234). Vascular cells culture studies showed that total DAG levels are raised in tissues exposed to elevated glucose conditions (235,236). It also has been illustrated that DAG levels of vascular smooth muscle cells can be increased by

hyperglycaemia via boost DAG de novo synthesis through intermediates of glycolysis (237). DAG consequently mediates activation of protein kinase C. Vitamin D attenuates the impact of HHG on DAG restores the levels to close to the hypoxic normoglycemia levels.

4.4.4 Protein kinase C (PKC):

Stimulation of polyol levels that generates ROS increases MGO and diacylglycerol since G3P accumulation, directly and indirectly, activates PKC. PKC activation of vascular smooth muscle cells is associated with sustained exposure to hyperglycaemia and is well recognised to contribute to multiple diabetic complications including hemodynamic changes, vascular contractility, vascular permeability, cell adhesion, proliferation, differentiation and gene expression (238), (239). In addition, in vitro study found that activation of PKC via hypoxia-induced pulmonary artery smooth muscle cell proliferation (240).

4.4.5 Amino Acids

Metabolic profiling of amino acids as mentioned earlier showed that HHG increased most of them apart from aspartate that only showed to be decreased in compared to HNG. Arginine and proline metabolites were observed to be significantly increased by about 1.22-fold in HHG group. Similarly, serine and threonine metabolism O-Succinyl-L-homoserine, creatine and betaine aldehyde were also detected increased by 1.50, 1.10 and 1.34 folds respectively. Lysine metabolites 5-aminopentanoate and 4-trimethyl ammoniobutanoate were increased by 1.50 and

1.36-folds respectively. A study was carried out newly to diagnose diabetics in comparison to controls found that amino acids were mainly increased in diabetics apart from histidine and glutamine (241). Disturbance of amino acid levels due to the various metabolic and hormonal modifications as a consequence of diabetes. Stimulation of amino acids via elevated glucose exposure encourages them to enter via pyruvate or acetyl CoA into the Krebs cycle to yield more energy molecules. PASMCs that were cultured in high glucose media supplemented by vitamin D had lower amino acid levels.

4.4.6 Lipids

Lipids are metabolised into their component glycerol and fatty acids. The current study showed that the fatty acids tridecadienoate and oxo decanoate in the HHG group were higher than control by 2.79 & 1.41-fold and *P*= 0.005 & 0.015 respectively compared to HNG. Despite the significant difference between groups of HNG, fatty acids were generally decreased and with some being increased. Determination of free fatty acids among type 1 diabetic patients shows higher levels in comparison to controls (242). A previous study showed that fatty acids were down-regulated in human placenta from women with gestational diabetes mellitus (GDM) comparing to a control group (243). Lipid accumulation was apparent in both studies being affected by G3P accumulation and GAPDH inhibition.

The current results showed higher levels of glycerophospholipids in the HHG group suggesting that there was lipid accumulation due to conversion of G3P and DHAP. A

change in the cellular lipid composition would definitely impact the cell energy production and influence in turn the cell damage.

Ceramides and sphingolipids were also found to be influenced by high glucose and have significant effect in the diabetes pathogenesis and its accompanying complexity. Increased levels of sphingosine and ceramide metabolites indicate that they were highly increased in HHG comparing to HNG which is in agreement with a variety of studies observing the role of sphingolipids in diabetes (244,245).

4.4.7 Nucleotides

The PPP oxidative arm generates 5 carbon sugars that supply nucleotide biosynthesis backbone. Metabolic profiling of nucleotides shows increasing at most of the metabolites including uridine, dihydrothymine, UMP, guanine, pseudouridine and AMP. Association between hyperglycaemia and elevated levels of uridine, for example, have been identified previously (246). Nucleotide demands for DNA replication are essential for cell proliferation in addition to the influence of PPP and induce pyrimidine and purine synthesis. Along with the fact that cell division is NADPH dependent (247) inducing of PPP mainly contribute to increased cell proliferation and DNA synthesis. Vitamin D was able to attenuate the impact of high glucose on PPP and consequently restore most of the nucleotides close to control levels.

4.4.8 Pulmonary arterial hypertension

Numerous studies believe that the cellular process underlying pulmonary hypertension is due to the "Warburg effect" which occurs with the potential involvement of hypoxia inducing factor (HIF) which similar to the process occurring in cancer cells. Metabolic profiling of pulmonary artery smooth muscle cells cultured in a HHG environment could not determine the glycolytic shift towards lactic acid "Warburg effect". However, apparently, glycolytic disturbance was initiated via hypoxia hyperglycaemia combined by overproduction of ROS. These factors are widely known to participate in pulmonary artery smooth muscle cell remodelling, differentiation and proliferation (248). In addition, to the fact that hyperglycaemia could initiate and develop PAH as it has demonstrated in the previous chapter, diabetes could also promote hypoxia like effect augmented in turn abnormal cellular processes. Metabolic alterations including an increase of TCA malate and fumarate, acylcarnitine, nucleotides, decrease of steroids and phosphatidylcholines were observed in plasma samples when PAH patients were compared control subjects (249). Therefore, monitoring of the factors like hyperglycaemia that might cause matching metabolites modification could positively assist in preventing PAH onset due to hyperglycaemia.

4.4.9 Vitamin D

Taking into consideration the results for oxidative stress, DNA synthesis (proliferation assay) and metabolic profiling of PASMCs, adding vitamin D to the

HHG vitamin D appeared to reverse most of the undesirable effects in vitro. However, the clinical benefit of using vitamin D generally to improve diabetes and/or cardiovascular performance is still debatable. Further in-vitro and in-vivo studies need to be carried out to demonstrate whether vitamin D might help to prevent metabolic alterations resulting from hypoxia hyperglycaemia in PASMCs.

Chapter Five

Deletion of the translocator protein gene (TSPO) results in changes of metabolomic profile in retinal pigment epithelial cells

---

5 Deletion of translocator protein (TSPO) results in changes of metabolomic profile in retinal pigment epithelial cells

5.1 Introduction:

AMD is a cumulative chronic disorder of the central retina and a principal cause of blindness worldwide. AMD is characterized by the accumulation of focal (Drusen) and diffuse extracellular (basal) deposits in the macula lutea, among the adjacent Bruch's membrane and the retinal pigment epithelium (RPE). These deposits might lead to retinal dysfunction and subsequent RPE death correlated with loss of photoreceptor (250). Deposition of lipids influences Bruch's membrane leading to hydraulic conductivity and macromolecular permeability which is assumed to impair the metabolism of the retina. Existence of apolipoprotein, cholesterol and cholesteryl ester deposits beneath the RPE cells was reported in AMD patients linking irregular cholesterol transport to the progression of the disease (251). Cholesterol is mainly removed from the cells by reverse cholesterol transport (RCT) mechanism by which high-density lipoprotein (HDL) returns surplus cholesterol to the liver for either storage or excretion. The first step of RCT is cholesterol efflux.

RPE cells are well known to support photoreceptors cell with certain functions like waste and nutrient transport, in addition to phagocytosis and handling of the photoreceptor outer segment shedding process. RPE cells are responsible for cholesterol efflux and uptake which is eventually processed and delivered as HDL

like particles to HDL receptors on the photoreceptor cells; RPE cells also transport cholesterol to the sub-RPE space for clearance through the choriocapillaris (252,253). In AMD disease, there is a development of lipid accumulation in extracellular tissue separating the retina from blood supply known by Bruch's membrane (254,255). Lipid disposition is believed to be via the retina as the predominant source and derives from residues of photoreceptor outer segments degradation (256). Therefore, RPE cells act as the main site of cholesterol and other lipid transportation through different proteins to the inner and outer side of the retina

TSPO is an 18 kDa protein localized to the outer mitochondrial membrane. It is one of the complex proteins involved in the mitochondrial cholesterol trafficking and believed to mediate several of functions including neuroinflammation, mitochondrial homeostasis and apoptosis (257). It has been demonstrated that TSPO is strongly expressed in human and mouse RPE cells and participated in mediating cholesterol efflux from RPE cells (253). The study also found a significant increase of cholesterol uptake and accumulation of RPE/-TSPO comparing to wildtype confirming eventually that TSPO deletion impaired cholesterol efflux and lipid transport of retinal cells. In the current study, analyses were employed on retinal pigment epithelial cells (RPE) from wild and knockout (*TSPO*$^{-/-}$ RPE) types treated by Oxidized Low Density Lipoprotein (OxLDL) to detect key metabolic changes associated with oxidative stress generated by OxLDL on retinal cells in the presence and absence of TSPO.

A comprehensive understanding of the metabolic pathways of RPE cell pathogenesis could be highly beneficial for enhancing new therapeutic targets and providing disease prognosis. The current study implements untargeted metabolic profiling to identify the most fundamental pathways for retinal homeostasis that might help to provide a better understanding of metabolic perturbation and might have broad clinical importance for retinal degeneration therapy. Various of metabolomics studies were carried out to find biomarkers distinguishing patients from healthy subjects for different eyes diseases including AMD, keratoconus (258), retinal detachment (259), diabetic retinopathy (260,261) and anterior uveitis (262).

Different metabolic pathways were identified in these studies that were carried out mainly in plasma, urine and, tears samples. The identified pathways included amino acids, aminoketones, carbohydrates, carnitines, catecholamines and derivatives, hydroxy acids, keto acids, phospholipids and nucleotides.

5.2 Methods and material

5.2.1 Metabolic profiling:

5.2.1.1 Sample preparation

The TSPO knockout and wildtype of ARPE-19 cell line was given to us by Dr Xinhua (Glasgow Caledonian University) (253). Wildtype and TSPO Knockout cells were seeded in a six-well plate ($6x10^5$ cells/well) and grown for 24h at 37^oC in an incubator with 5% CO2. The cells were treated with oxLDL for 24h. Afterwards, culture media were removed, and adherent cells were washed with phosphate-

buffered saline (PBS) at 37°C. Cooled (-20°C) extraction cocktail of methanol/acetonitrile/water at ratio 50:30:20 was used to extract variety of polar and non-polar putative metabolites. Samples were then prepared stored and analysed as described previously in sections 2.2.2 and 2.2.3. Mixtures of authentic standard metabolites (263) and pooled quality control (QC) sample were injected in order to facilitate the identification and to evaluate the sensitivity and reproducibility of the analytical method. Pooled sample (QC) was prepared by obtaining 10 µl from each sample and aliquoted in separate LC/MS analysis vial. It was run frequently throughout the experiment after every three samples. The five readings of pooled (QC) sample provide fundamental evidence of the analysis efficiency. Relative standard deviation (RSD) was calculated based on those reading for each metabolite. The metabolites of RSD < 30% were only included. Authentic standards are run with the samples in the same experiment to help with the confirmation of the metabolite by matching the retention time (RT) of that metabolite in the samples and the standard.

5.2.1.2 Liquid Chromatography Mass Spectrometer (LC/MS) Analysis

Samples were run on UPLC/MS as described in section 2.2.3

5.2.1.3 Data extraction and processing

Data were extracted and treated as described in section 2.2.4

5.2.1.4 Statistical Analysis and biomarker identification

Biomarkers were detected in procedure demonstrated earlier in section 2.2.4 and 2.2.5

5.3 Results

5.3.1 Principle Component Analysis (PCA) and Orthogonal Projections to Latent Structures discriminant analysis (OPLS-DA)

Samples of wildtype and TSPO knockout cells with or without oxLDL treatment were prepared and injected into the LC-MS, the data was afterwards extracted and processed to detect metabolites which were different between wildtype and TSPO knockout cells or between oxLDL treated and untreated cells. Initially, system stability was examined by running pooled QC samples throughout the experiment frequently after every three samples. Pooled samples were clustered together in the PCA plot (Figure S3) section 10.3, indicating reasonable system stability and high precision. Moreover, relative standard deviation (RSD) values were calculated based on total intensities in each of the pooled samples, and total RSD of 19.58% was obtained. Metabolites with RSD values higher than 30% were excluded. Clustering of QC samples (P1, 2, 3, 4 and 5) reflected good sensitivity where the extra assessment of RSD was used to ensure that differences between samples were based on the intervention not due to instrumental factors.

Quantitative metabolomics was employed by applying metabolite extraction and identification workflow to categorize metabolic alterations due to treating of

wildtype and RPE/-*TSPO* cells with oxLDL and comparing them to the control of each type. Common markers distinguishing the groups are listed based on the *t*-test reading. Fold change ratios were calculated for each metabolite for each comparison. Metabolites with significant changes in the comparisons were listed in Table S3 (section 10.3).

The wildtype cells without the treatment of oxLDL (WTC), wildtype cells with the treatment of oxLDL (WTT), *TSPO* knockout cells without the treatment of oxLDL (KOC) and *TSPO* knockout cells with the treatment of oxLDL (KOT) were evaluated by PCA model.

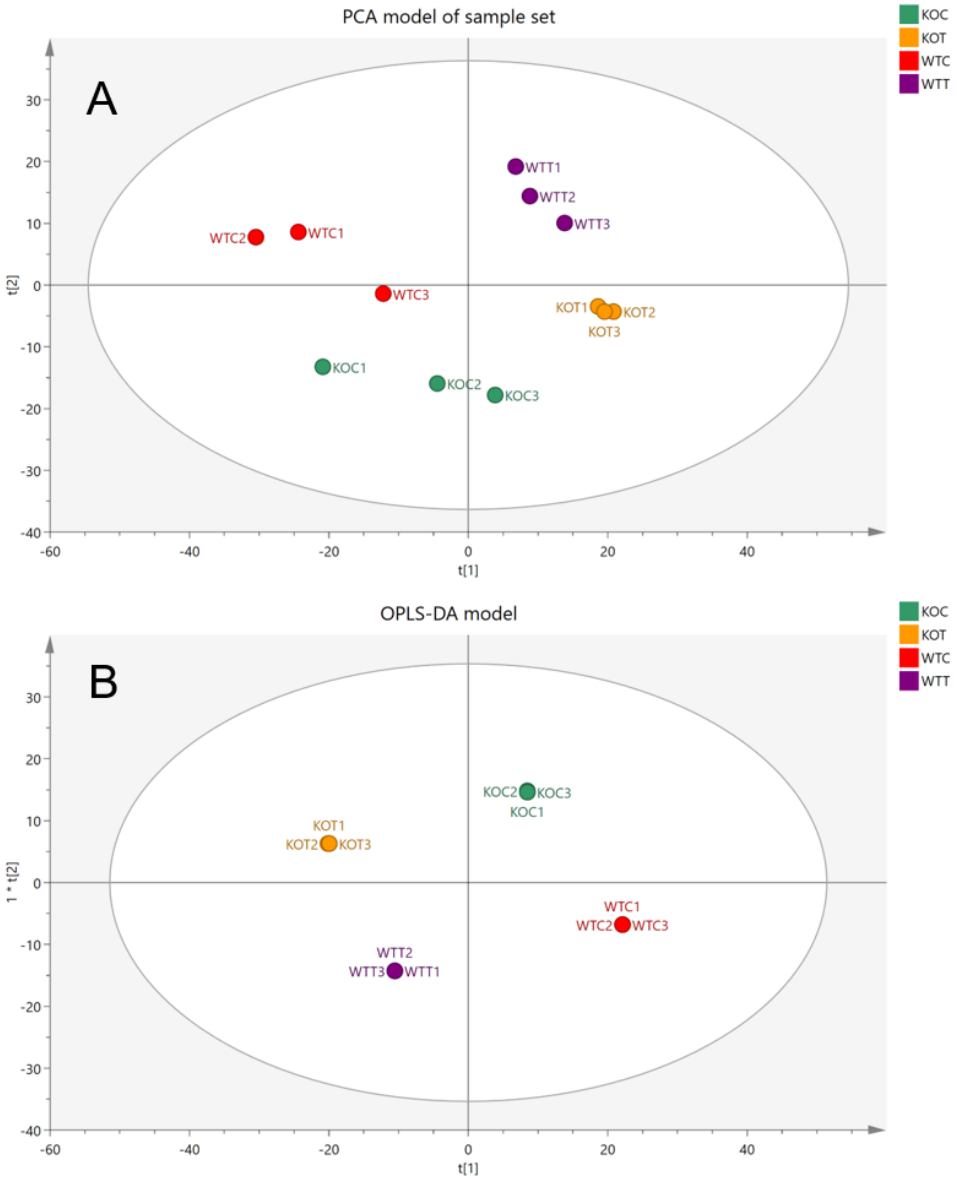

Figure 5-1: PCA and OPLS-DA model for 12 samples of 4 different groups

(**A**) Represent Principal components analysis (PCA) plots of four different groups: WTC, wildtype control cells without treatment of oxLDL; WTT, wildtype cells treated with oxLDL; KOC, *TSPO* knockout control cells without treatment of oxLDL; KOT, TSPO knockout cells treated with oxLDL. (**B**) OPLS-DA score plots the samples according to their classification coloured based on their group and the reading of 1106 putative metabolites.

Score plots demonstrated clear separation and clustering of each group showing the difference of metabolic profiles between different groups (Figure 5-1 A). In

addition, an OPLS-DA supervised model was used to highlight the differences between groups and to examine the effect of the intervention (Figure 5-1 B). The model evaluation parameters, R^2=0.99 and Q^2=0.71, indicated that the OPLSDA model was reliable and valid. The current model built based on the total reading of 1106 metabolites and show a clear separation between the four different groups. However, we could not detect the discrimination features that separate each group from others in a model of four groups. Therefore, subsequentially new models were built based on the total reading of 1106 metabolites to compare every two different groups in a separate model. The newly built models were comparing oxLDL-treated *TSPO* knockout (KOT) to oxLDL-treated wildtype (WTT), untreated *TSPO* knockout (KOC) group compared to the untreated wildtype (WTC) group, oxLDL-treated TSPO knockout (KOT) compared to untreated *TSPO* knockout (KOC) group, and oxLDL-treated wildtype (WTT) group compared to the untreated wildtype (WTC) group. This assists in detecting the statistically significant metabolites that contribute to the discrimination between two certain groups. Outcomes of these comparisons provide a better understanding about the differences between wildtype and *TSPO* knockout RPE cells in terms of the metabolic modifications occurred due to oxLDL treatment and TSPO deletion.

5.3.2 The lipid Pathway Was Most Affected

Based on all the identified metabolites, lipids were the most significantly influenced metabolites in response to the stress raised due to TSPO deletion and/or the treatment with oxLDL representing 51% of total affected metabolites, followed by

amino acid metabolism pathways 19%, and the nucleotide metabolism pathway is the least affected 8% (Figure S2) (section 10.3). OxLDL treatment greatly increased the levels of long-chain acylcarnitines in both *TSPO* knockout and wildtype cell metabolites (Table S3) section 10.3. While the levels of oxidised fatty acids in KOC and WTC cells were similar, there was a very large increase in the levels of some fatty acids and particularly oxidized fatty acids (Figure 5-2), possibly resulting from oxLDL treatment and this might be attributed to the oxLDL which could be contributing these components to the cell extracts.

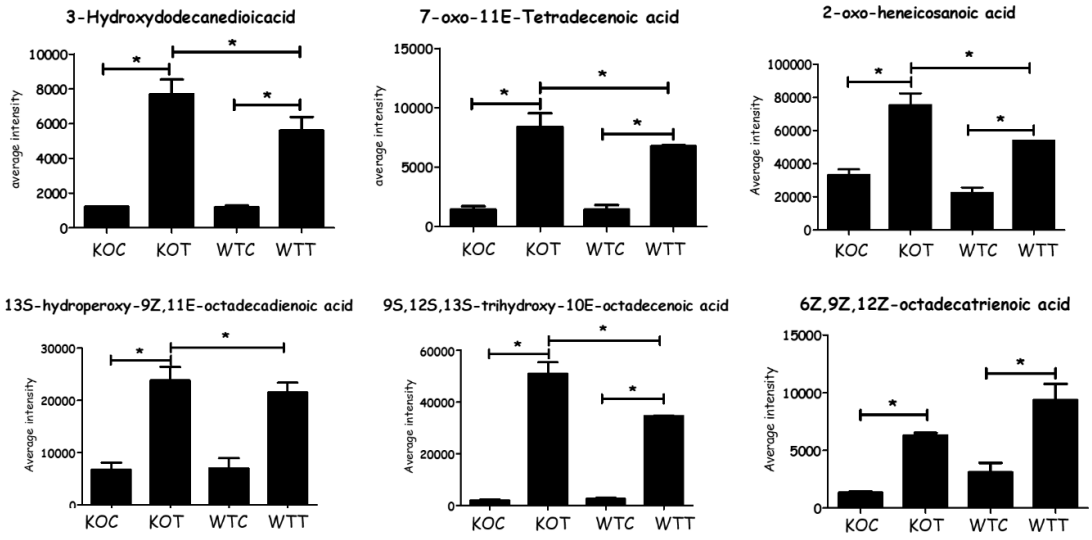

Figure 5-2: impact of OxLDL on fatty acids of wild and knockout RPE cells

Significant changes in some fatty acids as a consequence of oxLDL treatment at different groups. * Comparison indicates that different is significant with $p < 0.05$. KOT: *TSPO* knockout cells with the treatment of oxLDL; KOC: *TSPO* knockout cells without the treatment of oxLDL; WTT: Wildtype cells with the treatment of oxLDL; WTC: Wildtype cells without the treatment of oxLDL. Error bar is the standard error of the mean (SEM)

Lipids were strongly affected by the treatments. There are differences in the phospholipid between WT and KO cells. Figure (5-3) indicates that four ether lipids are more abundant in the WT cells in comparison to the KO cells. There were marked effects on the range of phospholipids resulting from oxLDL treatment on both RPE and RPE/-TSPO. Many of these lipids were of low abundance such as the phosphatidyl glycerol lipid PG 44:12 and PC lipids 40:7 and 42:7 (Table S3 section 10.3), but also some high abundance lipids were affected such as PC 34:2 (Figure 5-3). Figure 5-3 shows a heatmap for the 30 most abundant lipids extracted from the cells. The second most abundant lipid a PC with 36 carbons in the acyl chains and 2 units of unsaturation was decreased after treatment, as well as a PC lipid with 32 carbon atoms and 0 unsaturation, while an abundant lipid PC34:2 was increased after treatment. Since these lipids are abundant, this perhaps indicates some major remodelling of the cell membrane in response to oxidative stress. There are interesting differences in the less abundant lipids with several ether lipids being markedly increased and some lipids with highly unsaturated chains being decreased which is possibly indicative of oxidative stress while others were increased (Table S3 section 10.3). In particular, a glycolipid with 44 carbon atoms in its acyl chains and 12 units of unsaturation is decreased in the treated samples. It is likely that this lipid is substituted with two docosahexaenoic acid chains and such lipids are known to serve an important function in the retina (263).

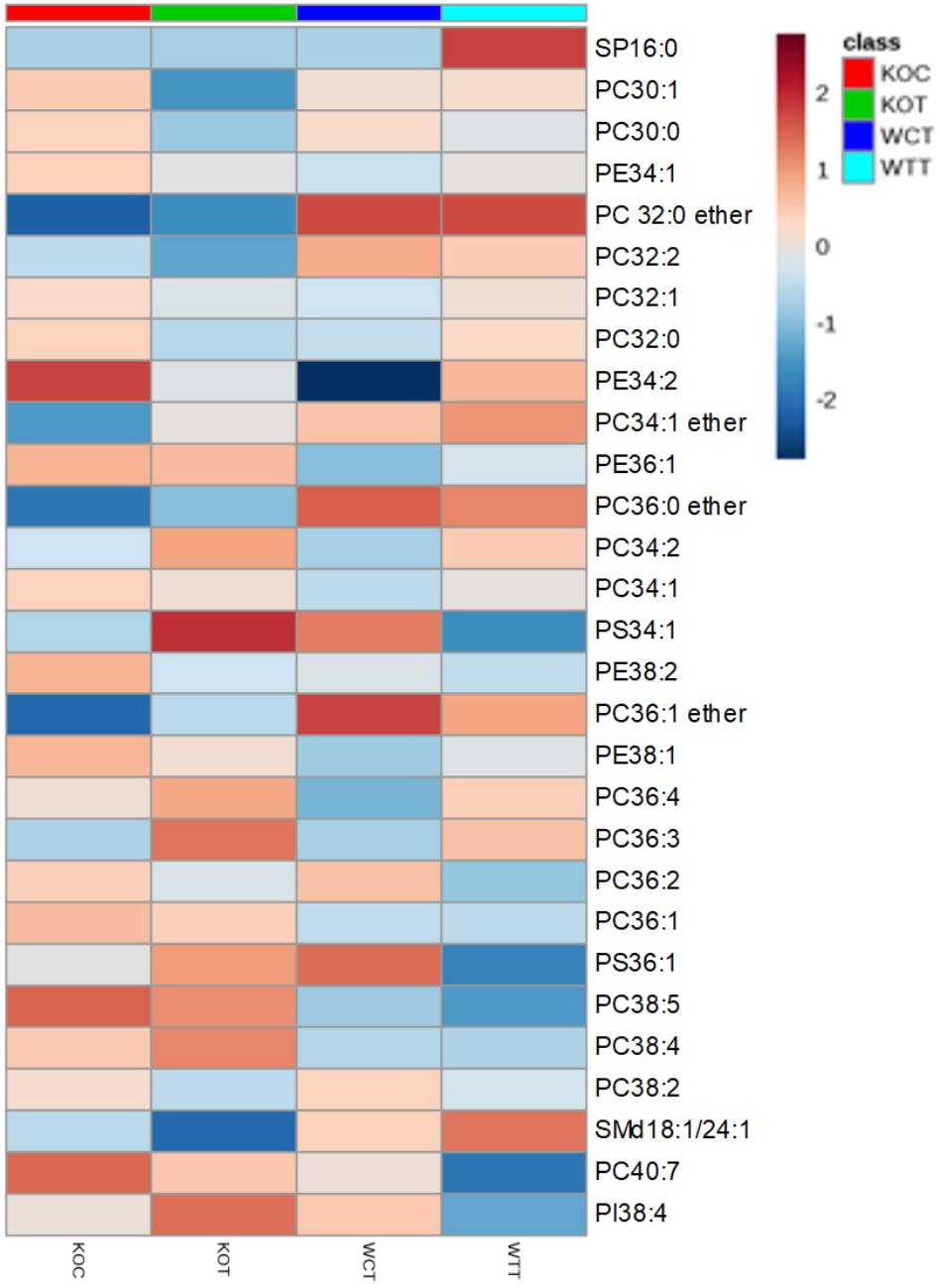

Figure 5-3: Lipid metabolism alteration of 30 metabolites in different condition

The relative intensity of 30 most abundant lipids extracted from different groups. Colour represents the average intensity of group samples for each metabolite. Colour scale of highest value coloured in dark Red and the lowest value coloured in dark blue. KOT: *TSPO* knockout cells with the treatment of oxLDL; KOC: *TSPO* knockout cells without the treatment of oxLDL; WTT: Wildtype cells with the treatment of oxLDL; WTC: Wildtype cells without the treatment of oxLDL.

5.3.3 Metabolic changes in glucose metabolism

Several glycolytic metabolites were elevated in RPE/-TSPO cells compared to wildtype cells. Deletion of TSPO influenced metabolites of the pentose phosphate pathway RPE/-TSPO cells demonstrated higher levels of ribose 5-phosphate and gluconate 6-phosphate than wildtype. An increased level of the TCA cycle component, cis-aconitate, was observed in KOC compared to WTC conditions, while citrate was lower in wildtype cells than that of TSPO knockout cells. NADH and ATP levels were higher in the KOC cells, possibly indicating a faster metabolic rate in these cells. This suggests that TSPO deletion mainly causes increased glucose metabolism, which was obvious when KOC was compared to WTC (Figure 5-4).

Glucose metabolism (glycolysis, TCA cycle and pentose phosphate pathway) was also affected by TSPO deletion and oxLDL treatment (see figure 5-4). Glycolysis metabolites, fructose 6-phosphate (F6P) and gluconic acid, were significantly increased in WTT compared to WTC. F6-P, on the contrary, was not notably changed in KOT when compared to that of KOC, but gluconic acid was significantly increased in KOT compared to KOC. Glyceraldehyde 3-phosphate (G3P) accumulated due to oxLDL treatment only in TSPO knockout cells. OxLDL treatment decreased pyruvate in both wildtype and TSPO knockout cells. The PPP metabolites, ribose 5-phosphate and gluconate 6-phosphate, were slightly increased when wildtype and TSPO knockout cells were treated by oxLDL in comparison to

untreated controls. Thus, both wildtype and knockout cell types exposed to oxLDL showed an ability to compensate for oxidative stress by producing increased levels of NADPH. The TCA metabolites (cis-aconitate and succinate) were also induced by oxLDL treatment, and this was accompanied by an increase in the generation of NADH, ATP and creatine phosphate, which forms in order to export ATP, formed from the terminal respiratory chain, out of the mitochondria. However, the other TCA component, citrate, was significantly decreased in oxLDL treated cells when compared to untreated cells and this could be explained by citrate also being utilised to produce NADPH, which is formed via the action of isocitrate dehydrogenase. Thus, both cell types respond to oxidative stress by up-regulating energy production and oxidative defence. Therefore, although KOC cells suffer from underlying oxidative stress, their ability to mount a defence against additional oxidative stress is not impaired. OxLDL treatment decreases pyruvate of both types. The PPP metabolites, ribose 5-phosphate and gluconate 6-phosphate, were slightly increased when wild and knockout cells treated by oxLDL.

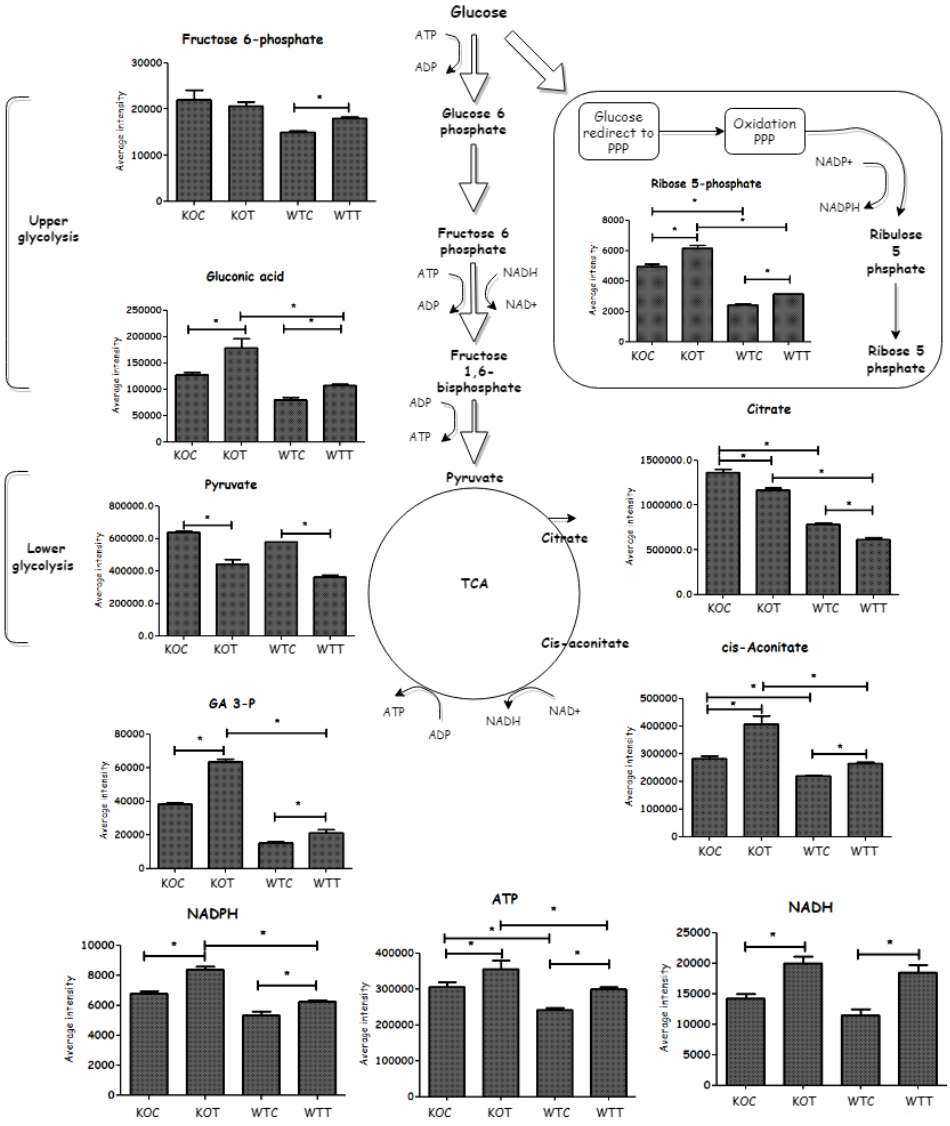

Figure 5-4: Alterations of carbohydrates metabolism among different metabolites in different conditions

Schematic representation of glycolysis, pentose phosphate pathways and TCA cycle. It is clarifying how glycolysis was induced by treatment increasing ATP generating. Included column figures demonstrate metabolites average intensity of different groups Glucose flux into oxidation PPP reflects the impact of *TSPO* knockout and oxLDL treatment in RPE cells. NADPH provided insight into redox status of cells while various factors play an important role in its synthesis and consuming. * In comparison indicates that different is significant with corrected $p < 0.05$. KOT: *TSPO* knockout cells with the treatment of oxLDL; KOC: *TSPO* knockout cells without the treatment of oxLDL; WTT: Wildtype cells with the treatment of oxLDL; WTC: Wildtype cells without the treatment of oxLDL. Error bar is the standard error of the mean (SEM)

5.3.4 Metabolic Changes in Amino Acid Metabolism

When comparing WTC and KOC, number of amino acids and amino acid metabolites were altered. In the arginine pathway, there was a slight decrease in arginine, which may reflect an increased requirement for creatine and creatine phosphate in the KOC cells; both proline and N-acetyl glutamate, which are potential precursors of arginine, were elevated in KOC. Taurine and one of its precursors, cysteic acid, were elevated in KOC compared to WTC; taurine is an important antioxidant. Amino acid metabolism was disturbed by oxLDL treatment in both wildtype and TSPO knockout cells where some metabolites were up-regulated, and some others were down-regulated (Figure 5-6 and Table S3 section 10.3). Among 27 metabolites detected, 5 metabolites decreased, 16 increased and 6 were not changed when comparing KOT to KOC, and almost similar alterations were observed in WTT compared to WTC. On the other hand, 12 amino acid metabolites were found to be increased in KOT compared to WTT, and two metabolites were significantly decreased. Creatine, cysteate, 3- sulfino-L-alanine, phosphocreatine, alanine, creatinine and N-Acetyl-L-glutamate were the most influenced metabolites by oxLDL in wildtype and TSPO knockout cells, although they were induced in KOT and KOC more so than WTT and WTC. Serine and arginine were significantly decreased by oxLDL in both wildtype and knockout cells and were also reduced in knockout cells compared to wildtype cells with or without oxLDL treatment. Carnitine is synthesized from lysine side chains and has a role in transporting the long chain fatty acid into mitochondria.

Carnitine metabolites were markedly increased in oxLDL treated wildtype and TSPO knockout cells compared to untreated cells (Figure 5-5).

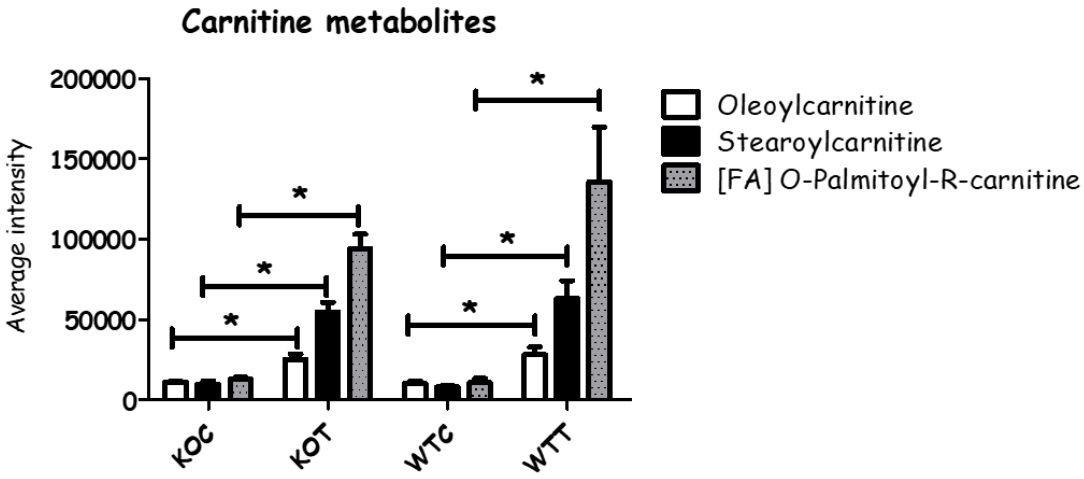

Figure 5-5: Some carnitine metabolites were changed between different groups.

KOT: *TSPO* knockout cells with the treatment of oxLDL; KOC: *TSPO* knockout cells without the treatment of oxLDL; WTT: Wildtype cells with the treatment of oxLDL; WTC: Wildtype cells without the treatment of oxLDL. * In comparison indicates that different is significant with corrected $p < 0.05$. Error bar is the standard error of the mean (SEM)

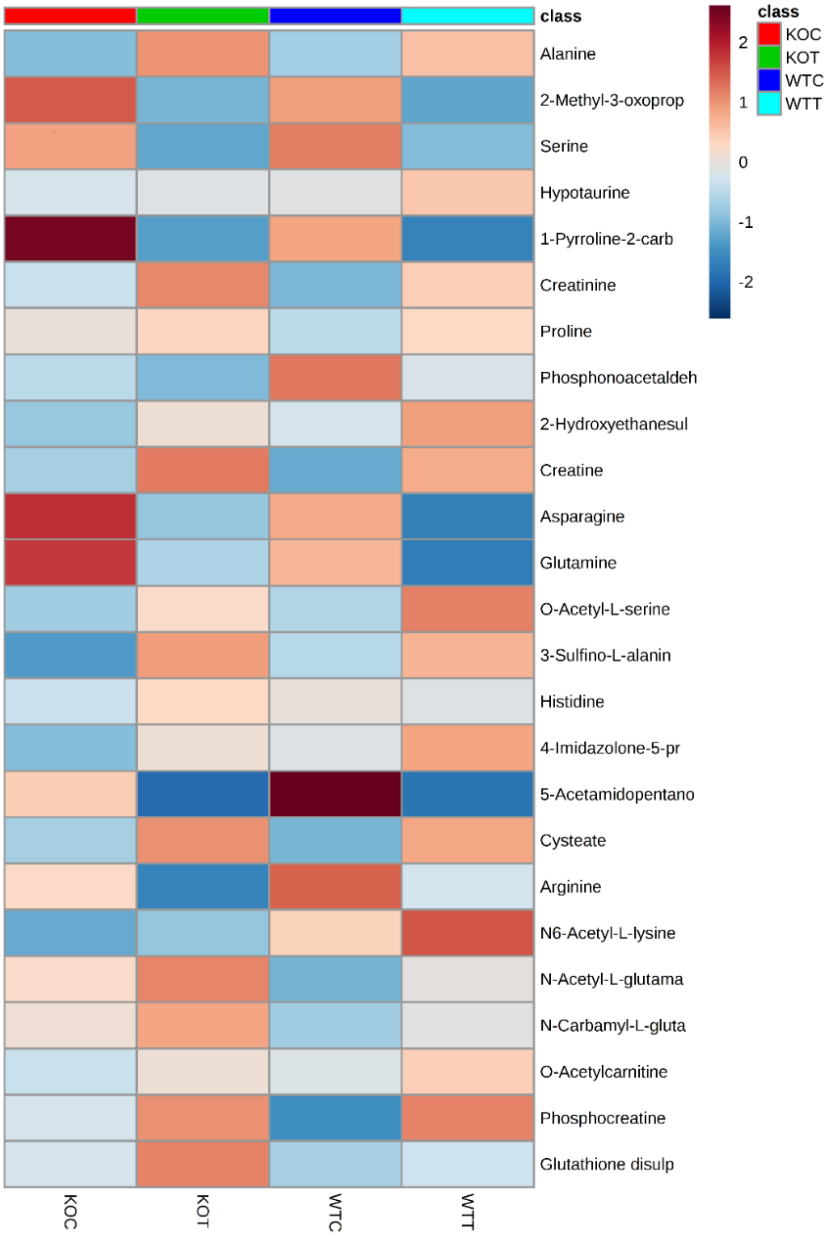

Figure 5-6: Heatmap for amino acids alterations among different groups

Heatmap of amino acid metabolites that significantly altered due to OxLDL treatment. It also displays how metabolites were influenced in different groups. Colour scale of highest value coloured in dark Red and the lowest value coloured in dark blue. KOT: *TSPO* knockout cells with the treatment of oxLDL; KOC: *TSPO* knockout cells without the treatment of oxLDL; WTT: Wildtype cells with the treatment of oxLDL; WTC: Wildtype cells without the treatment of oxLDL.

5.3.5 Metabolic Changes in Nucleotide Metabolism

Metabolic profiling of some purine metabolites demonstrated that adenosine monophosphate (AMP) was induced by oxLDL in both wildtype and knockout cells (Figure 5-7). It also showed a slight increase of inosine in KOT compared to KOC, but no difference between WTT and WTC was observed. The levels of hypoxanthine and xanthine were significantly increased in knockout cells compared to wildtype cells; however, hypoxanthine showed no statistical difference neither between WTT and WTC nor between KOT and KOC. Xanthine, on the other hand, was significantly decreased when either wildtype or knockout cells were treated with oxLDL. Uric acid was notably increased in oxLDL treated cells compared to untreated cells. It was also higher in WTC than KOC (Figure 5-7).

Pyrimidines pathway components such as thymine and 5,6-dihydrothymine were significantly influenced by oxLDL treatment. They showed higher levels even among KOT and KOC more than WTT and WTC respectively. Thymine is well known to be broken into 3-aminoisobutyric acid at the last step of pyrimidine degradation that eventually enters the TCA cycle. 3-aminoisobutyrate, however, was not affected by oxLDL or by TSPO deletion while no difference was observed between any of the comparisons. Cytosine and 5-methylcytosine were downregulated by oxLDL treatment and also decreased among knockout cells compared to wildtype cells with or without oxLDL treatment (Table S3 section 10.3).

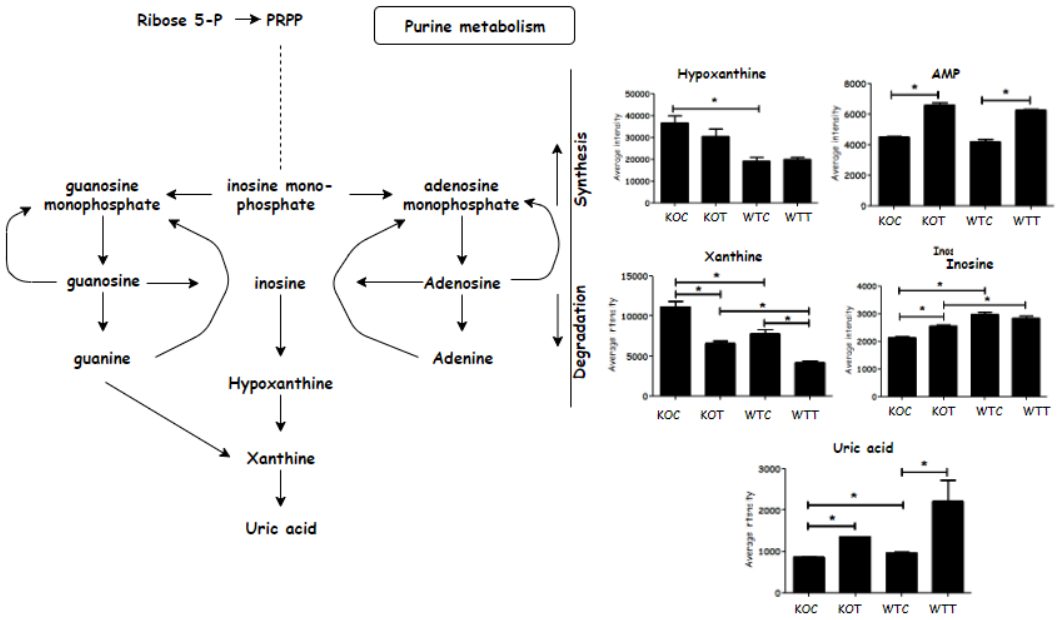

Figure 5-7: effect of interventions on the purine's metabolism

Figure show purine metabolites that were altered due to oxLDL treatment. AMP: adenosine monophosphate; PRPP: Phosphoribosyl pyrophosphate. KOT: *TSPO* knockout cells with the treatment of oxLDL; KOC: *TSPO* knockout cells without the treatment of oxLDL; WTT: Wildtype cells with the treatment of oxLDL; WTC: Wildtype cells without the treatment of oxLDL. * In comparison indicates that different is significant with corrected $p < 0.05$. Error bar is the standard error of the mean (SEM)

5.3.6 Increased Oxidative Stress in OxLDL-treated Cells

TSPO deletion and oxLDL treatment have been reported to induce reactive oxygen stress (ROS) production in RPE cells (253). Reduced glutathione is converted to form oxidized glutathione disulphide (GSSG) in the presence of hydrogen peroxide and glutathione peroxidase. A higher GSSG level was detected in oxLDL-treated cells when compared to untreated cells; TSPO knockout cells produced more GSSG compared to wildtype cells, with or without oxLDL treatment. NADPH is required to

reduce GSSG back to GSH in the presence of glutathione reductase. The increased level of NADPH was not sufficient to counteract an increase in GSSG in the KOC and KOT cells. However, GSH levels were not significantly affected in the KOC and KOT cells (Figure 5-8). Therefore, TSPO knockout cells generally demonstrated a higher oxidative stress response due to an imbalance of GSSG and GSH

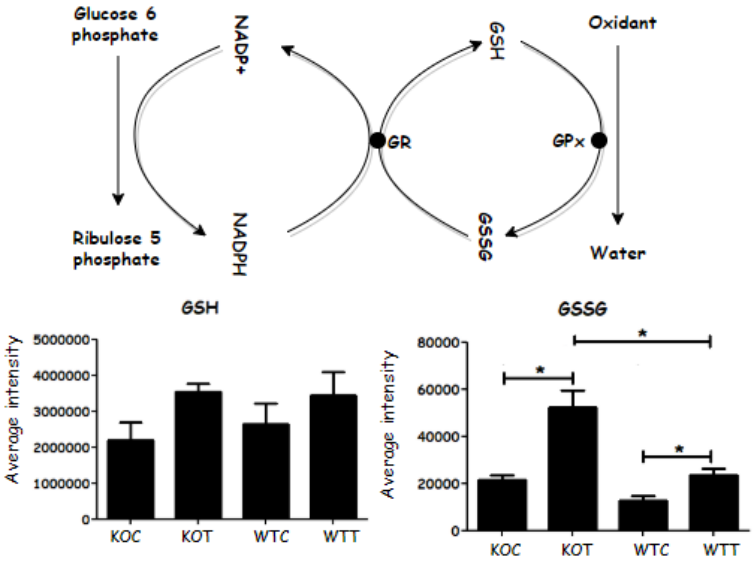

Figure 5-8: The responses of glutathione oxidized and reduced forms to the interventions

Oxidized glutathione (GSSG) convert to reduced form in existence of NADPH that gives proton and converted to oxidized form NADP+. GSSG increased significantly when knockout cells were treated by OxLDL. GSH: glutathione; GSSG: glutathione disulphide; GR: glutathione reductase; GPx: glutathione peroxidase. KOT: *TSPO* knockout cells with the treatment of oxLDL; KOC: *TSPO* knockout cells without the treatment of oxLDL; WTT: Wildtype cells with the treatment of oxLDL; WTC: Wildtype cells without the treatment of oxLDL. * Comparison indicates that difference is significant with $p < 0.05$. Error bar is the standard error of the mean (SEM)

5.4 Discussion

In this study, LC/MS metabolomics approach was used to quantitatively investigate metabolite changes in wildtype and *TSPO* knockout RPE cells, with or without oxLDL treatment. The data demonstrate dysregulation of different metabolic pathways affected by TSPO knockout oxLDL treatment. Our observations revealed higher intracellular levels of carnitine, fatty acids, glycerophospholipids, eicosanoids, sphingolipids and glutathione homeostasis metabolites when either wildtype or *TSPO* knockout cells were treated with oxLDL compared to untreated cells.

In *TSPO* knockout cells the clearest effect on metabolism in comparison with wildtype was increased oxidative stress, as evidenced by an increased level of GSSG in the cells. Associated with this was an increase in phosphogluconate, a major source of NADPH, which is required to recycle GSSG back into GSH. NADPH levels were also slightly elevated in the knockout cells, but GSH level was not affected, indicating that the compensatory increase in NADPH allowed normal levels to be maintained. In addition, the antioxidants, carnosine and homocarnosine, were increased in the knockout cells, and so provided a reduction in oxidative stress. The taurine biosynthesis pathway is also affected by oxLDL treatment, and this pathway can provide another mechanism for countering oxidative stress. The exact function of TSPO remains unknown, although it has been associated with cholesterol transport and regulation of oxidative stress, and, therefore, knockout of the gene could promote oxidative stress (257).

Oxidative stress is a hallmark of retinal degeneration despite results from different studies being inconsistent with regard to the association of age-related changes in oxidative markers in RPE cells (264). The major effect of oxLDL on both wildtype and knockout cell is to increase the markers of oxidative stress, including GSSG, phosphogluconate and NADPH. Thus, wildtype cells appear to behave in a similar way to the untreated knockout cells, and in the treated knockout cells, the pathways that indicate oxidative stress are further increased, consistent with early studies which showed that loss of TSPO resulted in increased ROS production in RPE and steroidogenic cells (253).

There is an indication that the glycolysis is up-regulated in knockout cells with G-3P, glucose 6-phosphate (F-6P), fructose phosphate, fructose bisphosphate and phosphoglyceric acid being increased in knockout cells compared to wildtype cells. In addition, some TCA cycle metabolites, citrate and aconitic acid were also elevated. Linked to this is a slight elevation of ATP and NADH, and a marked increase in creatine phosphate (CPi, Table S3 section 10.3), which is required for exporting ATP derived from the electron transport chain out of the mitochondrion (265). In addition, creatine, the precursor of CPi, and creatinine, its breakdown product, were also elevated. Altogether this suggests that energy metabolism is up-regulated in the knockout cells, possibly in order to counteract the effects of oxidative stress. The glycolysis pathway is believed to generate about 50% of ATP in the retina (266). Studies have been carried out in vivo to investigate the impact of inducing glycolysis in RPE cells and found that neighbouring photoreceptors

degenerated as a consequence (267). A less expected effect is that several acylcarnitines were up-regulated by oxLDL treatment in both knockout and wildtype cells. The most marked elevations were in the long chain acylcarnitines, stearoyl and palmitoyl carnitine, and this suggests an increase in fatty acid β-oxidation in order to derive more energy metabolites, and potentially, NADPH. Carnitine conjugation is required in order for the fatty acids to enter the mitochondria. It has been observed that aged retinal cells lose some of their capacity for energy metabolism, which makes them less able to adapt to the oxidative stress (268).

As previously established, TSPO deletion deteriorates cholesterol efflux and enhances lipid accumulation in cells (253). Knockout of TSPO in steroidogenic cells (MA-10 Leydig cell line) also resulted in increased uptake and oxidation of fatty acid (269). In the current study, lipid metabolism was the most affected pathway, with about 51% of all identified metabolites. There were differences in the lipid composition between the KOC and WTC cells, with the WTC cells having a greater abundance of ether lipids. Ether lipids, with a double bond adjacent to the oxygen to which they are bonded, are known as plasmalogens and have been found to be important in myelination, with glycolipids in myelin containing up 70% plasmalogens (270). Amongst the abundant lipids, some are increased, and some are decreased by oxLDL treatment, suggesting remodelling of the cell membrane to counteract oxidative stress. There were also marked effects on the lipid composition resulting from oxLDL treatment amongst less abundant lipids. Some lipids were enriched by the treatment, and some were depleted. The depleted lipids

include some very long-chain lipids, such as PG44:12. Such lipids are typically found in the retina where docosahexaenoic acid is abundant and it is incorporated into lipids typically containing two docosahexaenoyl chains. Low levels of docosahexaenoic acid have been associated with retinitis pigmentosa (271). Long chain unsaturated fatty acids within lipids are susceptible to oxidative damage, and there are four lipids with unsaturation >7 that were depleted in both KOC and WTC cells by oxLDL treatment. Numerous studies have emphasized the influence of lipid modification in RPE cells on the metabolic processes of the retina (272–274). As RPE cells process and recycle the lipids from lipid-rich photoreceptor outer segments (POS) throughout life to maintain visual function, RPE cell lipid disturbance will subsequently affect photoreceptors, leading to further visual dysfunction due to lipid accumulation and lipid peroxidation products (275). Even though lipid accumulation may not harmfully influence RPE cell function, in combination with oxidative stress over time, it could lead to the formation of lipid peroxidation products, such as malondialdehyde (MDA) (276). Lipid progressive accumulation will also stress the RPE, which in turn induces cell apoptosis that is known to be the initial process of AMD disease (277). Particularly, significant dysregulation was mainly found in the glycerophospholipids, the major component of cell membranes, which is enriched in neural membranes. In addition to their importance for providing membrane fluidity and structural stability, glycerophospholipids, along with sphingolipids, appear to play a fundamental role in generating and expanding oxidative stress in neurologic disorders (278). They were also found to play an

essential role in neural cell proliferation, differentiation, and apoptosis. RPE cell membrane impairment due to phospholipid dysregulation emphasizes the importance of the role of lipids in AMD and other neurodegenerative diseases. A study carried out by Suzuki et al. revealed that oxidized phosphatidylcholine levels in the photoreceptors and RPE of the human macular area increased with age (279). Higher intense immunoreactivity for oxidized phospholipids was noticed among eyes with AMD than in normal eyes. Application of sub-retinal oxidized phospholipids was reported to induce choroidal neovascularization in mice (280). From the current results, it is difficult to see a clear trend, with some lipids being up-regulated and some were down-regulated. One group of lipids where there is a clear up-regulation is in the sphingolipids. Two ceramides were higher in knockout cells and increased in both knockout and wildtype cells following oxLDL treatment. It has been observed that sphingomyelins are hydrolysed to ceramides in response to oxidative stress, which then acts as mediators of oxidative stress (281). Observing the differences of lipid metabolites between knockout and wildtype revealed a disturbance of fatty acids, ceramide/sphingosine lipids and glycerophospholipids, and inducing oxidative stress. This is correlated with a metabolomics study carried out on AMD patients, which reported significant changes, especially in plasma lipid metabolism, compared to control subjects (282). In that study, among 87 significant metabolites that differed between AMD patient samples and controls, most were involved in lipid metabolism, including fatty acids, diacylglycerols, phosphatidylcholines and phosphatidylinositol.

Our observations relate to cell-based work on retinal pigment epithelial cells, which might not be principally relevant to an in vivo setting. Impacts of neighbouring cells of photoreceptors, in addition to the inflammatory and immune systems, cannot be taken into account. Accordingly, the metabolic modification described in our RPE cell culture model may vary from an in vivo setting based on the same intervention. Therefore, it is fundamental to examine the current study findings on an animal model, such as a *TSPO* knockout mouse model. In addition, the limited number of authentic standards, which are often not available, restricted our ability to confirm all involved metabolites, particularly lipids. Thus, quite a number of compounds were only identified to MSI level 2. Independent biological replicates would be required to fully confirm the observations made. In further in vivo and in vitro work, it might be useful to look at the effect of added anti-oxidants on the metabolic shifts observed in the current work. In addition, it would be important to gain more understanding of the structures of the lipids in these cell lines. The ether lipids seem particularly abundant, and this requires confirmation.

5.5 Conclusions

The most consistent changes in KO cells and oxLDL treated KO and WT cells were with regard to increased glycolysis and an increase in indicators of oxidative stress such as GSSG which were either increased by TSPO knock out or by treatment with oxLDL. Thus, regardless of the effect that TSPO knock out might have on cholesterol transport, the major effect of protein knockout might cause tissue damage via oxidative stress. This is underlined by the fact that the effect of oxLDL is able to

promote similar metabolic changes in WTC that are observed in the KO cells without treatment. In the KO cells treatment with oxLDL further promotes the metabolic changes that were produced by the gene knock out. The changes in the lipids in the treated KO and WT cells are too variable to propose a clear mechanism. It is evident that there are differences in the phospholipid profiles of the KO and WT, but it is difficult to link these to a disease mechanism since lipids are both up and down-regulated by treatment. In contrast, several markers of oxidative stress are clearly upregulated in KOC and KOT, and WTT. It is clear from the response of both the KO and WT cells to oxLDL treatment that both cells are able to counter oxidative stress by maintaining GSH levels and increasing levels of antioxidants such as urate, carnosine and homocarnosine. The cells do this by upregulating their metabolism particularly with respect to glycolysis, the pentose phosphate pathway and fatty acid β-oxidation.

Chapter six

Metabolic profiling of retinal pigment epithelial cells in response to high glucose with or without vitamins D and the impact of TSPO deletion

---

6 Metabolic profiling of retinal pigment epithelial cells in response to high glucose with or without vitamins D and the impact of TSPO deletion

6.1 Introduction

RPE cell functions are essential to maintain the retina and photoreceptor cells integrity and health. The main functions of RPE include nutrients transportation, light absorption, shedding of photoreceptor membranes phagocytosis and the secretion of numerous factors for the retinal structural integrity, RPE controls sub-retinal fluids which are critical for the maintenance of photoreceptor stimulation (283). Although chronic hyperglycaemia causes diabetic retinopathy in many diabetic patients, the exact mechanism of disease onset is still not fully understood. Moreover, the impact of hyperglycaemia on the RPE is not entirely clear. Indeed, the proliferation of RPE cells due to elevated glucose levels is still controversial (284,285).

High glucose is well known to induce the oxidative stress in retinal cells modifying the signalling in the sorbitol and protein kinase C pathways (285–287). Even though RPE can combat against stressors, its impairment due to hyperglycaemia will eventually damage its essential functions.

Oxidative stress develops and accelerates retinal diseases like diabetic retinopathy (DR), age-related macular degeneration (AMD) and glaucoma. An increase in ROS

generation could lead to morphological and functional damages in the RPE, cells, and retinal ganglion cells (RGCs) (288).

Many diabetes-induced metabolic abnormalities are involved in disease and seem to be inspired by oxidative stress elevation. Superoxide increase is considered as one of the most pathogenesis of diabetic complications which is related to elevated glucose and associated with the other metabolic abnormalities.

Metabolomics has been previously used to profile the metabolic changes due to diabetic retinopathy (260,261). Chen et al. found 11 biomarkers distinguishing moderate non-proliferative diabetic retinopathy samples from type 2 diabetics without diabetic retinopathy. The study reported a significant increase in the PPP that mediates NADPH generation. It also showed increases of thymidine, cytosine and cytidine while the high value for cytidine's specificity and sensitivity indicated that it could be a valuable biomarker of diabetic retinopathy. However, these findings were limited to a population of Singaporeans and South Indian ancestry (261). The other metabolomics study reported a lower plasma level of arachidonic acid and linoleic acids among patients with proliferative diabetic retinopathy in comparison to controls (260). Decreases of these metabolites were related to increase levels of circulating pro-inflammatory agents such as interleukin-1 receptor antagonist (IL-1RA) and Interleukin 6 (IL-6) (289).

On the other hand, antioxidants have revealed positive action on retinopathy progression. Although antioxidants are widely used in a variety of chronic diseases,

better clinical trials are necessary to provide stronger evidence for the effects of antioxidants in the retinopathy progression in diabetic patients.

TSPO is an 18 kDa protein localized in the outer membrane of RPE cells mitochondria which provide an essential role in mediating several functions of retina cells including cholesterol trafficking. TSPO knockout from RPE cells led to metabolic dysregulation as demonstrated previously when knock cell type was compared to the wild type. TSPO, in addition, mediates the performance of mitochondrial energy-dissipating systems as a reaction to oxidative stress (290) that could be raised due to a high glucose environment. TSPO expression was reported to be reduced in adipocytes from obese and diabetic subjects in comparison to a healthy group (291). Decreases of this protein led to impaired glucose uptake and adipogenesis. These findings suggest that therapeutic targeting of TSPO protein may provide a new prospect to a new treatment strategy to help to attenuate diabetic complications.

The current study aims to examine the impact of high glucose level media (HG) “diabetic like effect” on the retinal pigment epithelial cells with and without vitamin D supplementation as anti-oxidant. It also studies the metabolic alterations of RPE/-TSPO cells due to HG media in comparison to normoglycemia (NG) conditions and HG in RPE wildtype cells.

6.2 Method and material

6.2.1 Metabolic profiling:

6.2.1.1 Sample preparation

RPE cells were prepared and incubated as described previously in sections 2.2.1.1 and 2.2.1.2. Wildtype cells were either exposed to high glucose media 25 mM; normal glucose media 5 mM; or high glucose media supplemented by vitamin D cholecalciferol (80 ng/ml). To profile the impact of TSPO deletion on hyperglycaemic RPE cells, we cultured the TSPO/-RPE cells in normal and high glucose media and compared them to wildtype cells cultured in the same conditions.

Afterwards, culture media were removed, and adherent cells were washed with PBS at 37°C. A cooled (-20°C) extraction cocktail of methanol/acetonitrile/water at ratio 50:30:20 was used to extract a variety of polar and non-polar putative metabolites. Samples were then prepared stored and analysed as described previously in sections 2.2.2 and 2.2.3. Mixtures of authentic standard metabolites and pooled quality control (QC) sample were injected in order to facilitate the identification and to evaluate the sensitivity and reproducibility of the analytical method. A pooled sample (QC) was prepared by obtaining 10 µl from each sample and aliquoted in separate LC/MS analysis vial.

6.2.1.2 Liquid Chromatography Mass Spectrometer (LC/MS) Analysis

Samples were run on UPLC/MS as described in section 2.2.3

6.2.1.3 Data extraction and processing

Data were extracted and treated as described in section 2.2.4

6.2.1.4 Statistical Analysis and biomarker identification

Biomarkers were detected in procedure demonstrated earlier in section 2.2.

6.3 Result:

6.3.1 Hyperglycaemic RPE cells with or without vitamin D

6.3.2 QC samples

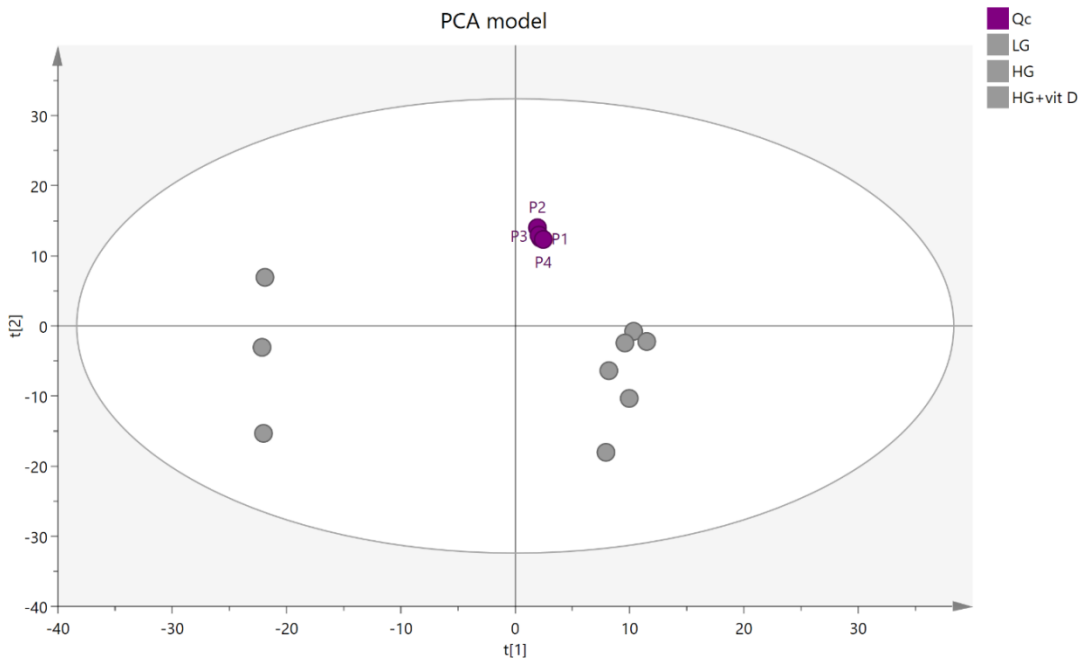

Figure 6-1: PCA score plot of the pooled sample (Qc)

PCA score plot for QC (pooled) cell extract samples of ARPE cells representing the quality control sample runs throughout the experiment.

Figure 6-1 shows the clustering of pooled samples (QC) compared to the rest of the cell extract samples. To quantify the precision of the measurements, the relative standard deviation (RSD) of 4 pooled readings was calculated based on total intensities in each sample, and an RSD of 21.6% was obtained. RSD was also calculated for each of the putative biomarkers in the pooled samples, and the highest RSD was for L-Cysteinylglycinedisulfide (112%) followed by MES (76%) while

the lowest RSD was for [PI (16:0)] (0.14%). The precision of these values clearly indicates that any metabolomic differences between groups cannot be due to instrumental factors alone. Metabolites with RSD higher than 20% were excluded before the model was fitted by using SIMCA-P.

6.3.3 Data visualization and biomarkers identification:

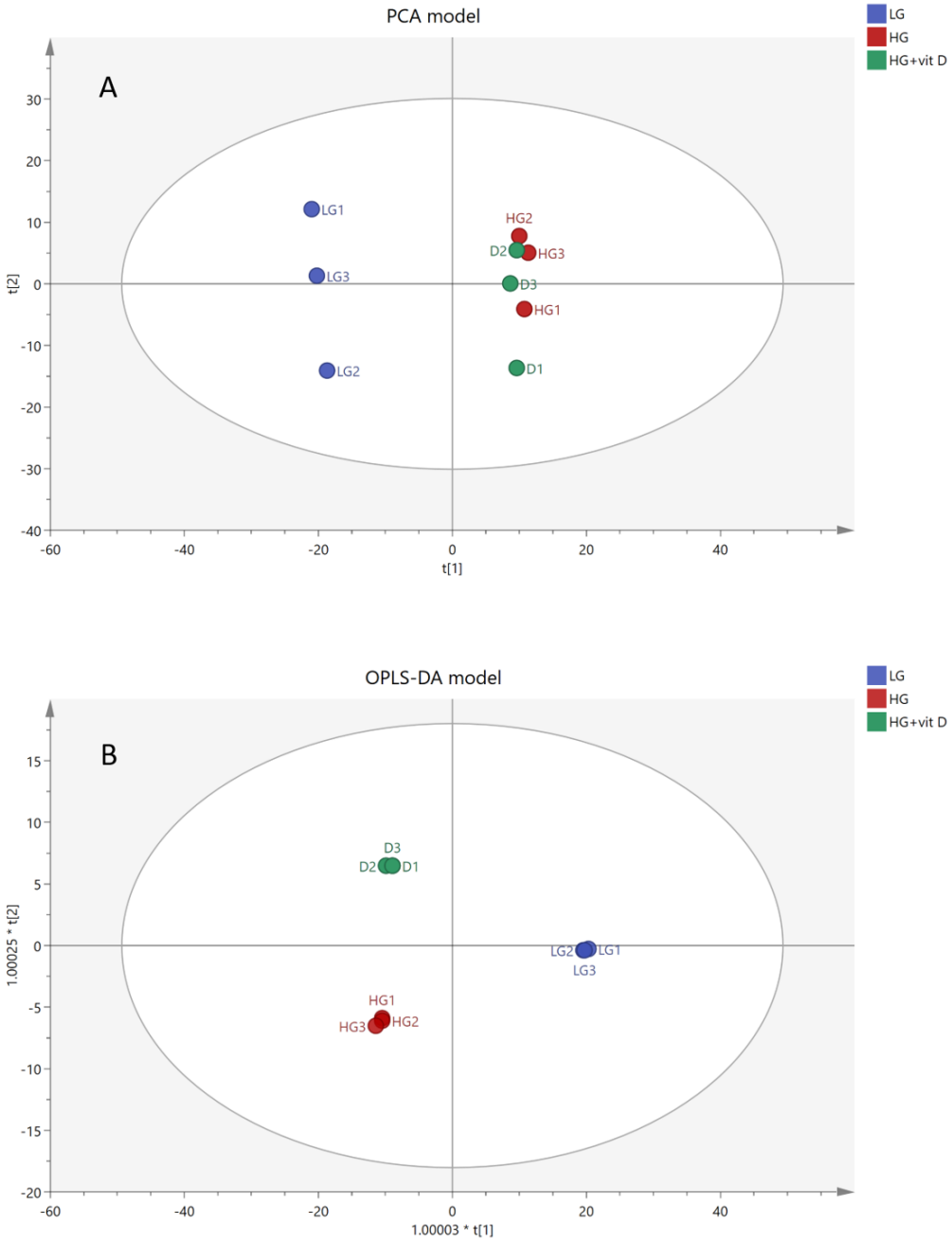

Figure 6-2: PCA model and OPLS-DA model for samples plotting of different groups

(A) (PCA) plot for three different groups**.** NG (5 mM glucose), HG (25 mM glucose), vitamin D 80 ng/ml added to HG (25 mM glucose + Vit D). (B) OPLS-DA score plots the samples according to their classification coloured based on their group**.** The plots show the distribution of 9 samples based on the reading of 1042 putative metabolites of three groups.

Figure 6-2 (A) was created to examine the possible presence of outliers, groups, similarities and other patterns in the data. PCA plot figure was capable of separating HG with and without vitamin D from NG. However, it fails to separate HG with and without vitamin D from each other. To understand the differences between the groups, it is advisable to do SIMCA classification or a PLS-DA/OPLS-DA.

To examine the effect of HG media as a stressor on the RPE cells, an OPLS-DA model was built based on all putative biomarkers which were measured in the samples (triplicate of each group). Discrimination between the groups occurred when the OPLS-DA model was fitted as shown in figure 6-2 (B).

The OPLS-DA model consists of two predictive x-score components; component t[1 , 2] and two orthogonal x-score components to t[2]. Predictive t[1-2] explaining 58% of the predictive variation in x, to orthogonal t[1,2] explaining 23.5% of the orthogonal variation in x, R^2X (cum) = 0.82, R^2Y (cum) = 1, R^2 (cum) = 0.99, Goodness of prediction Q^2 (cum) = 0.747. *P* CV ANOVA= 0.330. However, this model could not identify the metabolites that distinguish groups from each other. Therefore, we need to compare HG to LG separately and then HG compare to vitamin D HG to detect biomarkers contributing to the distinction between each comparison.

In order to detect the significant metabolites among all included metabolites, each comparison has been investigated separately. Statistically significant metabolites that were found to be different between hyperglycaemia and normoglycaemia were only considered as biomarkers.

6.3.4 Biomarker identification

6.3.4.1 HG induces oxidative stress in RPE cells in comparison to NG.

Table 6-1: Metabolites alteration of different pathways affected by HG and vitamin D.

Statistical comparisons						
Statistically significant metabolites		*Amino Acids*	*Carbohydrates*	*Lipids*	*Purines*	*Pyrimidines*
HG/LG	265	42	19	171	8	13
	Metabolites (↑ | ↓)	32 | 10	17 | 2	47 | 124	3 | 5	10 | 3
Vitamin D/ HG	71	9	5	32	0	2
	Metabolites (↑ | ↓)	3 | 6	2 | 3	30 | 2	0	2
Numbers of metabolites restored by vitamin D		6 out of 9	2 out of 5	25 out of 32	None	2 out of 2

Table 6-1 shows that lipid metabolism was the most influenced pathway due to HG followed by amino acids, glycolysis and nucleotides respectively. Disturbance of metabolites was clear among different pathways apart of glycolysis biomarkers where about 90% of sugar metabolism components were increased. Nucleotide metabolites were changed in the purine pathway while the metabolites of the pyrimidine pathway were mostly up-regulated.

6.3.4.1.1 Amino acids metabolism

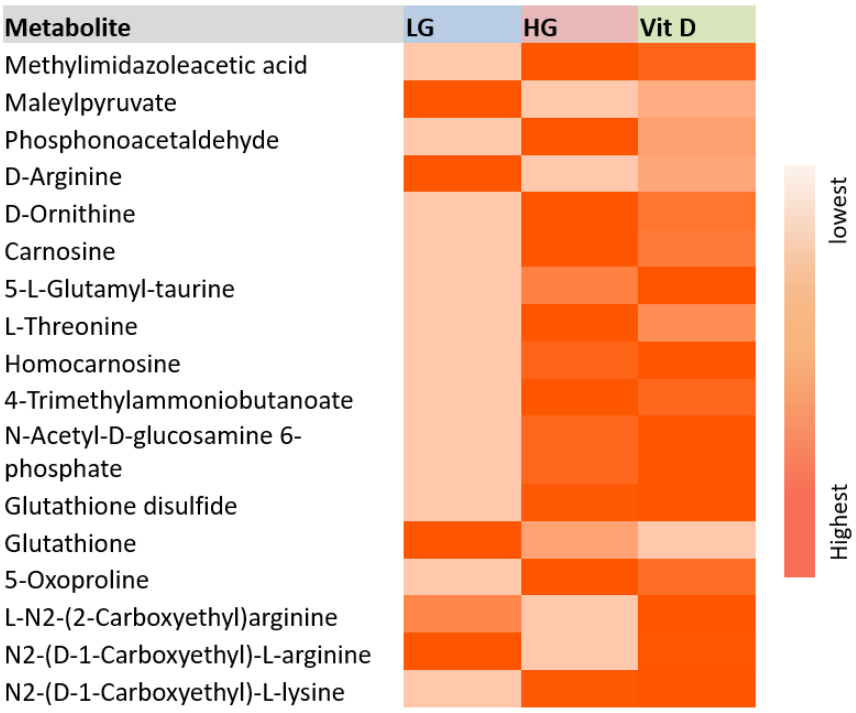

Figure 6-3: Heatmap for amino acids metabolites that significantly change between groups.

Heatmap visualizing the alteration of amino acids by HG comparing to LG and the impact of adding vitamin D. Raw: represents the metabolite; Column: represents the average of samples in each group. The colour key specifies the metabolite intensity: lowest: light orange; highest: dark orange

Metabolic profiling of RPE cells shows that HG significantly upregulates 32 and down-regulates 10 amino acids while the addition of vitamin D was able to affect 9 of them significantly, 3 metabolites were increased, and 6 decreased in comparison to HG samples. Comparing to NG samples, HG samples exhibited a higher level of homocarnosine, glutathione disulphide and ornithine. Vitamin D was not effective in restoring those metabolites close to the normal level when it was supplemented with HG samples. In contrast, vitamin D helps to restore some other amino acids

influenced by HG including maleylpyruvate, phosphonoacetaldehyde, arginine, carnosine, oxoproline and threonine.

6.3.4.1.2 Sugar metabolism

Several carbohydrate metabolites were influenced in response to the stress raised due to RPE cells exposed to HG. Nineteen sugar metabolites were significantly influenced by HG in which 17 increased and 2 decreased. Five of those altered biochemicals also responded to vitamin D supplementation where 2 metabolites increased and 3 decreased. Glucose 1-phosphate and PPP components were induced accompanied by enhancement of amino sugar, nucleotides and ascorbate 6-phosphate. ATP along with NAD including (NAD+ and NADH) were considerably increased and this could indicate both increased glycolysis and increased flux through the TCA cycle.

In HG the PPP metabolites ribulose-5-phosphate and sedoheptulose 7-phosphate were elevated. This is in line with the very large elevation in glyceraldehyde 3-phosphate (G-3P) due to inhibition of glyceraldehyde 3-phosphate dehydrogenase and the consequent build-up of polyol metabolites, as can be seen here in the form of elevated sorbitol levels and increased flux into the PPP pathway. Increased flux through PPP should increase NADPH production as a cellular antioxidant mechanism. Surprisingly current results show it was decreased suggesting that NADPH was readily utilized to maintain redox states reducing the oxidized form of glutathione.

Table 6-2: The response of carbohydrate metabolites to hyperglycaemia and their response to adding of vitamin D

Pathway	Met name	HG/NG		Vit D/ HG	
		P. value	Ratio	P. value	Ratio
Pentose phosphate pathway	UDP-glucuronate	5.4	0.002	1.2	ns
	2-Deoxy-D-ribose 1-phosphate	16.6	0.044	1.1	ns
	Sedoheptulose 7-phosphate	4.7	0.000	1.0	ns
	UDP-glucose	4.4	0.001	1.0	ns
Amino sugar metabolism	UDP-N-acetyl-D-glucosamine	29.4	<0.001	1.2	ns
	CMP-N-acetylneuraminate	2.4	0.004	1.1	ns
Oxidative phosphorylation	ATP	2.2	<0.001	0.9	0.02
	NADH	3.0	0.002	1.0	ns
	ADP	1.6	0.013	1.1	ns
	NAD+	1.9	0.010	1.0	ns
Glycolysis	Fructose 6-phosphate	0.0	4.237	0.6	ns
	Lactate	1.4	0.013	0.9	ns
	Acetyl-CoA	1.2	0.002	1.0	ns
	D-Glucose 1-phosphate	5.4	<0.001	1.1	0.01
	Sorbitol	3.5	0.006	1.0	ns
	GL-3P	75.3	<0.001	1.1	ns
	Octulose 8 phosphate	5.2	0.003	1	ns

Oxidized glutathione (GSSG) was slightly elevated when cells were exposed to HG in comparison to NG which might cause NADPH to decrease. In addition, increases in the levels of carnosine and homocarnosine by HG demonstrate the capability of elevated glucose media to influence anti-oxidant mechanism of RPE cells.

In addition, UDP-N-acetyl-D-glucosamine was significantly induced by HG which may suggest that the hexosamine pathway was activated. Glucose flux into the

hexosamine pathway is considered to be one of the diabetes complications that is known to initiate insulin resistance. UDP-N-acetyl-D-glucosamine formed as a consequence and this is thought to modify the transcription factor Sp1 by O-NGlcNAcylation. Vitamin D, in turn, was not effective in attenuating the impact of hyperglycaemia on most of carbohydrate pathway metabolites.

6.3.4.1.3 Nucleotide metabolism

Several of pyrimidine metabolites were increased by HG probably due to activation of the PPP (Table S4 section 10.4). Pyrimidine increase via glucose shift towards PPP could be due to the high demand of nucleotides necessary for cell production. Supplementation of vitamin D, however, was able to decrease the impact of HG on thymine and pseudo-uridine 5'-phosphate. Purine metabolites, on the other hand, were disturbed while guanosine diphosphate (GDP) and guanosine triphosphate (GTP) were increased by HG. This might occur due to salvage pathway activation through guanine and guanosine rather than de novo synthesis. Influence of guanosine also known to be an anti-oxidant mechanism increasing as a defence mechanism against the damage of cell DNA by oxidative stress factors.

6.3.4.1.4 Lipids metabolism

HG influenced 171 lipid metabolites comparing to NG (Table S4 section 10.4). 124 metabolites decreased among those altered components, and 47 were increased. On the other hand, vitamin D has an impact on 32 of altered lipid metabolites in which 30 increased and 2 decreased.

HG significantly induced sphingosine and most of glycerophosphoglycerols lipids pathways. Fatty acids (FA) appeared to be disturbed while 5 FA metabolites were increased and 12 decreased by HG. Four metabolites of 43 glycerophosphocholines were increased while the rest were decreased. All included metabolites of glycerophosphoinositols were also decreased by HG comparing to NG. These demonstrated that HG could impact the cell membrane transit and permeability and such effects believed to occur when cells are exposed to oxidative stress (292,293).

6.3.5 Metabolomics different between hyperglycaemic wild RPE and (RPE/-TSPO) types

To examine how RPE cells of both types of wild and RPE/-TSPO respond to diabetic-like conditions, we investigated the untargeted metabolic alteration of RPE cells cultured in HG and NG. Triplicates of each group were prepared. Knockout cells were also cultured in the same conditions.

6.3.5.1 Visualization:

A PCA model was created to examine the possible presence of outliers, groups, similarities and other patterns in the data. In addition, An OPLS-DA was used to understand the differences between groups and to examine the effect of the intervention.

6.3.5.1.1 PCA-X:

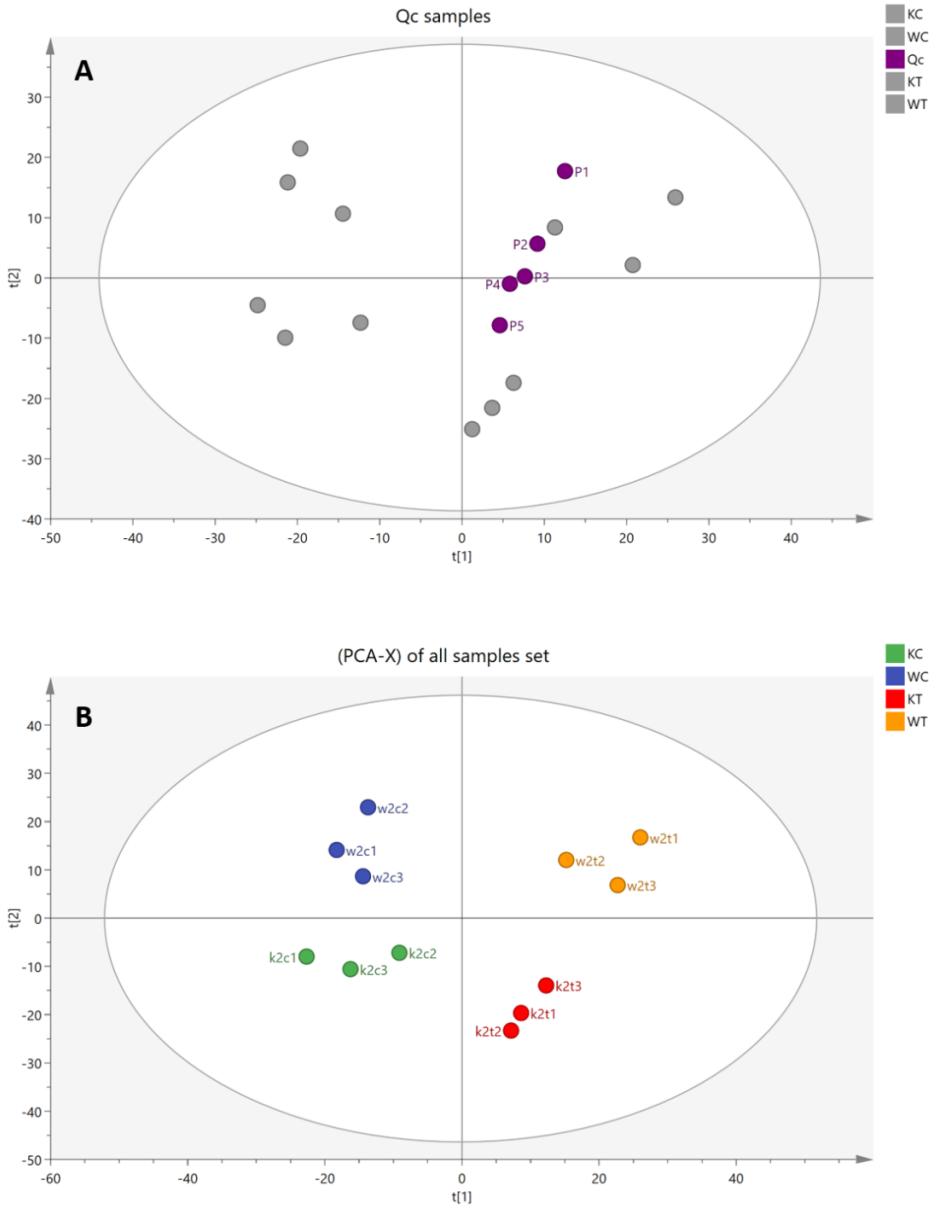

Figure 6-4: Qc and samples PCA score plots

(A) PCA score plot for QC (pooled) cell extract samples of hyperglycaemic RPE cells wild and knock out types. P1, P2, P3, P4 and P5 represent the quality control sample runs throughout the experiment. (B) Principal components analysis (PCA) plot for four different groups, wild control, knock out control (5mM glucose), wild and knock out high glucose (25mM glucose). The plots show the distribution of 12 samples based on the reading of 1267 putative metabolites of four groups.

Pooled samples were run after every 3 samples and clustered in PCA plot showing good system stability (Figure 6-4 A). The RSD was calculated for 5 pooled samples where and an RSD of 20.11% was obtained. Metabolites with RSD higher than 20% were excluded.

The unsupervised model shows a pattern where samples of each group plot closed to each other and separate from different groups (Figure 4-B). In order to understand the differences between different groups, an OPLS-DA test carried out.

6.3.5.2 Data analysis and biomarker identification:

6.3.5.2.1 OPLS-DA

New model built for all data set to investigate the significant markers that distinguished each group from others.

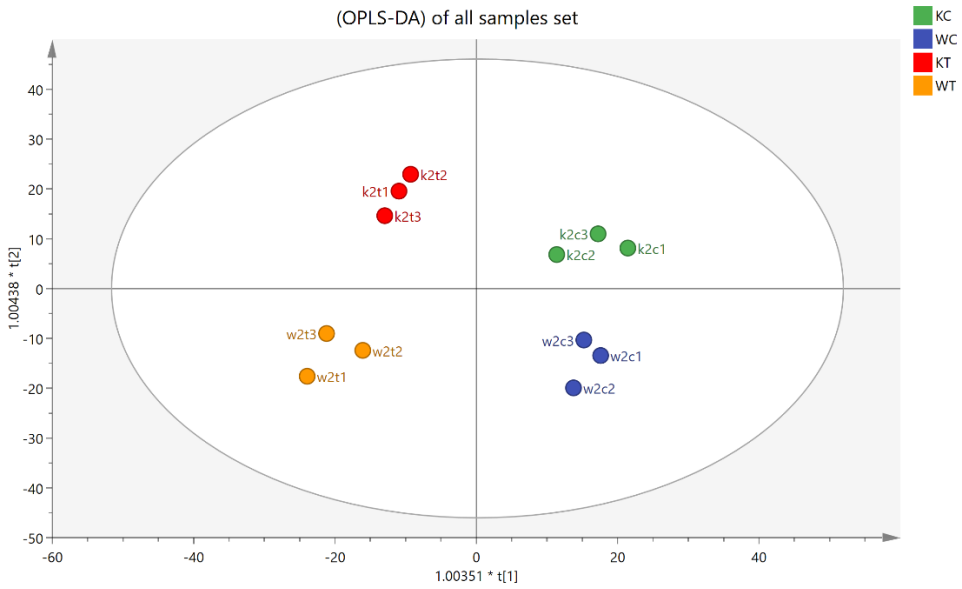

Figure 6-5: OPLS-DA score plot for 12 samples of 4 different groups

OPLS-DA score plots the samples according to their classification and coloured based on their group based on the reading of 1267 putative metabolites.

The valid and significant model was obtained with CV-*ANOVA= 0.016* consisting of three predictive x-score components; component t[1-3] and two orthogonal x-score components to t[2] was obtained. Predictive t[1-3] explaining 61% of the predictive variation in x, to orthogonal t[1-2] explaining 25% of the orthogonal variation in x, R2X (cum) = 0.86, R2Y (cum) = 1, R2 (cum) = 0.992, Goodness of prediction Q2 (cum) = 0.85

The present study focused on the differences between knockout and wild types in the HG condition and how knockout influenced by "HG in comparison to WT. Data afterwards were filtered according to CV-ANOVA test of each comparison, 95% confidence interval, VIP and RSD obtained from pooled samples.

Table 6-3 Metabolites that were altered significantly due to exposing of wild and knock out ARPE cells to NG or HG.

Mass	RT	Metabolite Name	Knock out hg/ng		High glucose k/w		Normal glucose k/w	
			Ratio	P.value	Ratio	P.value	Ratio	P.value
Miscellaneous								
243.15	5.3	Tiglylcarnitine	0.34	<0.001	0.53	<0.001	0.31	<0.001
245.16	5.1	Isovalerylcarnitine	0.19	<0.001	0.76	0.049	0.67	0.002
188.08	10.3	N-Acetylglutamine	0.51	0.012	1.45	0.050	4.33	0.003
173.11	7.3	N-Acetyl-L-leucine	0.28	0.004	1.56	0.124	6.71	0.005
172.01	13.9	sn-glycerol-1-phosphate	2.13	0.011	2.35	0.004	2.53	0.011
231.15	5.8	Isobutyryl-L-carnitine	0.19	0.001	0.23	0.001	0.44	0.011
117.12	39.8	2-Methylcholine	1.33	0.035	0.70	0.004	0.48	0.016
197.08	8.5	N-Acetyl-L-histidine	0.24	0.010	0.59	0.447	2.67	0.033
304.09	17.4	N-Acetyl-aspartyl-glutamate	0.36	<0.001	0.61	0.007	0.91	0.038
245.16	7.4	2-Methylbutyroylcarnitine	0.21	<0.001	0.86	0.543	0.75	0.063
427.37	4.1	Stearoylcarnitine	3.35	0.003	2.00	0.004	0.77	0.465
171.03	15.9	serinol phosphate	8.04	<0.001	1.68	0.003	1.11	0.492
Amino acids								
398.14	15.9	S-Adenosyl-L-methionine	0.75	0.021	0.29	<0.001	0.17	<0.001
161.07	9.3	O-Acetyl-homoserine	0.55	<0.001	1.81	0.017	3.08	0.004
165.08	9.6	Phenylalanine	0.24	<0.001	0.50	0.035	1.59	0.005
115.06	28.3	Proline	2.87	0.013	2.59	0.049	2.00	0.005

175.05	14.9	N-Acetyl-L-aspartate	0.47	<0.001	0.75	0.019	0.75	0.006
246.13	13.6	N2-(D-1-Carboxyethyl)-L-arginine	7.80	<0.001	0.48	0.005	1.12	0.036
246.13	17.0	L-N2-(2-Carboxyethyl)arginine	13.25	0.001	0.94	0.637	4.53	0.012
180.04	7.3	2-Hydroxy-3-(4-hydroxyphenyl) propenoate	13.62	<0.001	1.48	0.029	0.69	0.016
190.06	17.0	N-Carbamyl-L-glutamate	1.48	0.029	1.56	0.037	1.30	0.037
217.14	22.8	beta-Alanyl-L-lysine	1.84	0.011	0.42	<0.001	0.70	0.050
133.04	17.2	Aspartate	0.58	0.034	0.45	0.010	0.78	0.050
174.10	15.4	N-Acetylornithine	0.38	0.031	0.36	0.011	1.26	0.517
145.11	9.1	3-Dehydroxycarnitine	0.60	0.004	0.75	0.039	0.89	0.523
117.08	12.0	Valine	0.23	0.001	0.36	0.028	1.10	0.700
174.11	28.6	Arginine	0.32	0.016	0.30	0.035	0.95	0.886
102.03	8.8	2-Methyl-3-oxopropanoate	0.03	0.027	0.30	0.019	0.51	0.947
Glycolysis/PPP/OXPHOS								
612.15	17.6	Glutathione disulphide	0.13	<0.001	1.54	0.267	8.46	0.010
307.08	14.2	Glutathione	0.74	0.027	0.67	0.014	0.67	0.015
566.06	16.8	UDP-glucose	0.69	0.041	0.74	0.131	1.40	0.002
182.08	13.6	Sorbitol	2.59	0.013	1.29	0.040	3.91	0.012
90.00	18.6	Oxalate	0.55	0.002	0.42	0.002	0.59	0.015
340.00	18.9	beta-D-Fructose 2,6-bisphosphate	17.22	<0.001	1.34	0.171	1.44	0.020
607.08	15.3	UDP-N-acetyl-D-glucosamine	2.93	0.005	0.72	0.162	0.87	0.031
174.02	18.7	cis-Aconitate	1.91	<0.001	1.12	0.150	1.17	0.032
767.11	13.7	CoA	0.47	<0.001	0.84	0.085	0.78	0.041
134.02	16.6	(R)-Malate	1.55	0.007	1.32	0.041	0.84	0.054
116.01	15.0	Fumarate	0.48	0.003	0.75	0.008	0.78	0.103
90.03	14.5	Lactate	0.92	0.341	0.69	0.088	0.53	0.004

276.03	18.3	6-Phosphogluconate	18.94	<0.001	1.57	0.094	1.50	0.133
260.03	16.2	Fructose 6-phosphate	6.58	<0.001	1.14	0.166	1.60	0.150
150.05	11.2	Ribulose	2.54	0.044	0.96	0.826	1.64	0.195
88.02	8.3	Pyruvate	7.00	<0.001	1.78	0.020	1.74	0.223
170.00	16.5	Glyceraldehyde 3-phosphate	97.14	<0.001	1.11	0.278	2.01	0.234
176.03	16.0	Ascorbate	5.09	0.003	2.83	0.011	1.31	0.296
118.03	14.1	Succinate	0.47	0.037	0.48	0.007	0.97	0.872
230.02	16.0	Ribose 5-phosphate	18.89	<0.001	0.95	0.680	1.00	0.945
537.08	17.0	CDP-ribitol	2.06	0.021	1.03	0.571	1.04	0.977
427.03	15.3	ADP	1.58	0.046	0.70	0.166	1.65	0.040
665.12	13.3	NADH	3.58	0.002	0.79	0.176	0.83	0.125
210.07	13.0	Sedoheptulose	3.94	<0.001	0.71	0.016	1.27	0.239
507.00	16.9	ATP	0.58	0.009	1.25	0.133	0.94	0.322
Fatty Acid and Lipid Metabolites								
215.06	15.4	sn-glycero-3-Phosphoethanolamine	1.23	0.030	1.46	<0.001	1.93	0.001
169.05	13.7	Phosphodimethylethanolamine	0.57	0.004	0.50	<0.001	0.55	0.001
125.02	15.1	Taurine	0.69	<0.001	0.92	0.481	1.66	0.002
436.26	4.1	LPA(0:0/18:1(9Z))	0.47	0.016	1.91	0.040	2.62	0.053
231.15	8.0	O-Butanoylcarnitine	0.40	<0.001	0.53	<0.001	0.64	0.001
103.06	26.6	(S)-2-Aminobutanoate	0.61	0.041	0.50	0.012	0.68	0.011
217.13	9.0	O-Propanoylcarnitine	0.46	<0.001	1.23	0.070	0.80	0.016
171.09	4.9	N-Butyryl-L-homoserine lactone	0.50	0.032	0.58	0.039	1.74	0.121
188.14	4.4	[FA hydroxy(10:0)] 3-hydroxy-decanoic acid	0.74	0.023	0.82	0.045	1.06	0.662
102.07	4.6	ethyl propionate	0.24	0.009	0.65	0.046	0.59	0.797
649.43	4.0	PC(16:0/9:0(CHO))	2.59	0.007	3.20	0.008	1.42	0.012

864.57	3.4	PI(14:0/22:1(11Z))	1.66	0.039	1.78	0.028	0.77	0.082
507.33	4.2	LysoPE(0:0/20:1(11Z))	1.53	0.032	2.89	0.002	2.30	0.103
789.55	3.5	PS(18:0/18:1(9Z))	1.94	0.005	1.58	0.021	0.65	0.174
745.56	3.6	[PC (15:0/18:1)] 1-pentadecanoyl-2-(11Z-octadecenoyl)-sn-glycero-3-phosphocholine	1.76	0.007	1.47	0.004	1.24	0.223
481.32	4.2	[PC (15:0)] 1-pentadecanoyl-sn-glycero-3-phosphocholine	1.60	0.002	1.85	0.004	1.15	0.384
841.66	3.6	PC(16:1(9Z)/24:1(15Z))	2.55	0.005	1.52	0.017	0.75	0.409
733.56	3.6	[PC (16:0/16:0)] 1-hexadecanoyl-2-hexadecanoyl-sn-glycero-3-phosphocholine	1.69	0.014	1.39	0.001	0.84	0.413
717.53	3.6	[PC (15:0/16:1)] 1-pentadecanoyl-2-(9Z-hexadecenoyl)-sn-glycero-3-phosphocholine	1.68	0.014	1.61	0.005	1.13	0.436
773.59	3.6	PC(15:0/20:1(11Z))	2.04	0.020	1.58	0.021	1.20	0.474
729.57	3.6	PC(15:0/P-18:1(11Z))	1.93	0.008	1.97	0.008	0.91	0.508
845.62	3.4	PS(18:0/22:1(11Z))	1.68	0.008	1.69	0.045	1.06	0.537
886.56	3.4	PI(16:0/22:4(10Z,13Z,16Z,19Z))	1.67	0.014	1.77	<0.001	0.92	0.607
721.51	3.7	PE(18:4(6Z,9Z,12Z,15Z)/P-18:1(11Z))	4.76	0.005	1.34	0.046	0.80	0.859
814.69	3.7	SM(d18:0/24:1(15Z))	1.77	<0.001	1.55	0.009	0.77	0.185
Purines/pyrimidines								
324.04	15.2	UMP	5.02	<0.001	0.94	0.731	1.89	0.007
363.06	17.0	GMP	6.90	<0.001	0.80	0.340	0.54	0.008
403.02	17.5	CDP	1.88	0.045	1.31	0.317	1.39	0.008
347.06	13.6	AMP	12.22	<0.001	0.33	0.005	0.46	0.009
443.02	18.4	GDP	2.10	0.038	0.97	0.887	1.88	0.025
126.04	11.5	Thymine	1.58	0.044	0.53	0.009	0.83	0.165
404.00	17.0	UDP	0.74	0.030	1.26	0.033	1.19	0.258

559.07	15.0	ADP-ribose	0.68	0.030	2.35	0.015	6.88	0.363

Table 6.3 shows the most significant differences between the responses of KO and WT to HG. Carbohydrates were the most significant metabolites influenced in response to the stress raised due to RPE/-TSPO cell being exposed to 25 mM glucose media. Pentose phosphate pathway was induced in response to high glucose in both KO and WT cells. The effect of HG on the PPP in these cells are much more marked than those observed for PASMCs shown in chapter 3. Glucose-6-phosphate converts to 6-phosphogluconate in the oxidative phase of the PPP. TSPO deletion appears to have a marked effect on the PPP when the KO cells are exposed to high glucose. There is a large increase in 6-phosphogluconate in response to HG, and this indicates that the cells are well adapted to producing NADPH. The WT cells are similarly adapted. Like the WT cells, there are large elevations in the upper glycolysis pathway metabolites in the KO cells suggesting inhibition of glyceraldehyde 3-phosphate dehydrogenase (GAPDH) with the effects in RPE both KO and WT being more marked than in the PASMCs. In addition, the advanced glycation product carboxy ethyl arginine was markedly increased in both KO cells under HG. The effect on stimulating hexosamine metabolism was also marked. Krebs' cycle components were disturbed by HG in which fumarate, oxalate, succinate decreased and cis-aconitate and malate increased although it is difficult to read anything into this. Pyruvate was significantly increased by high glucose with no change noticed in lactic acid suggesting that TCA cycle might be influenced consequently. In addition, NADH found to be increased by HG while ATP surprisingly decreased which may indicate it was consumed in the cell growth. The KO cells

under HG show small increase in ATP compared to wild type. Glutathione disulphide was decreased when KO cells were exposed to HG. However, comparing KO to the WT displays higher GSSG level accompanied by an increase in NADPH confirming that TSPO deletion increases oxidative stress in RPE cells generally despite that HG decreasing GSSG in KO in comparison to NG.

Disturbance of amino acids, lipids and nucleotides pathways elucidated the impact of HG on RPE/-*TSPO* cells. However, the amino acids in KO cells exposed to HG were not influenced as much as those of WT. Most of the amino acids show higher levels among KO cells comparing to WT in NG conditions.

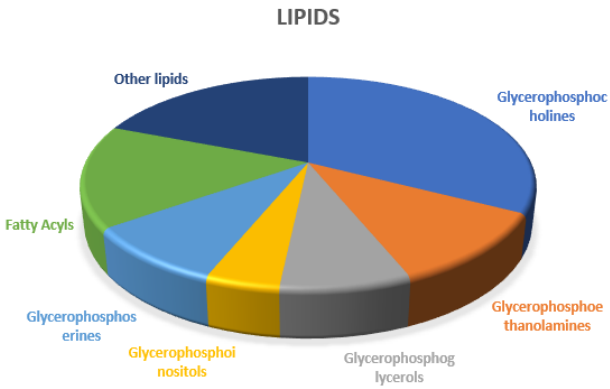

Lipids	Change of KO hg/ng	
Glycerophosphocholines	Decreased	3
	No different	11
	Increased	15
Glycerophosphoethanolamines	Decreased	2
	No different	0
	Increased	8
Glycerophosphoglycerols	Decreased	2
	No different	0
	Increased	5
Glycerophosphoinositols	Decreased	3
	No different	0
	Increased	1
Glycerophosphoserines	Decreased	5
	No different	0
	Increased	3
Fatty Acyls	Decreased	13
	No different	0
	Increased	1
Other lipids	Decreased	7
	No different	0
	Increased	10

Figure 6-6: lipid alterations between high and normal glucose level of RPE/-TSPO cells.

The response of lipids among different lipid pathways. It shows the number of metabolites the increased, decreased or not affected by the elevated glucose in knockout cell types

Lipids, on the other hand, were mainly influenced more in KO when they exposed to elevated glucose comparing to wild type cells. Figure 6.6 above shows a total of 89 lipid metabolites influenced by HG in the KO cells while in turn, HG influenced 36 lipid metabolites in the WT. This might elucidate the important role of TSPO protein in mediating lipid metabolism in the RPE cells.

6.4 Discussion

The present study carried out general metabolic profiling of the impact of HG on the RPE cells in the presence and absence of vitamin D. This enhanced the understanding of the impact of diabetic condition on the metabolism of these cells and provided understanding of the benefits of vitamin D supplementation to

prevent unwanted metabolic modifications that may occur due to HG. It also reveals the metabolic difference between wild and TSPO knockout types of RPE exposed to HG.

6.4.1 Hyperglycaemic RPE and vitamin D supplementation

We observed that oxidized glutathione was increased and accompanied by NADPH consumption even though the PPP was induced by HG. This suggests that RPE cells activate the PPP to attenuate the impact of ROS. Increasing of homocarnosine by HG also increases antioxidant levels contributes to diminishing oxidative stress associated with HG.

Diabetic retinopathy (RD) as a complication of diabetes mellitus (DM) was reported previously to be associated with oxidative stress (68,292). Prolonged exposure to HG induces ROS production that in turn enhance various of pathways including polyol pathway, advanced glycation end products (AGEs) pathway, the hexosamine pathway, the protein kinase C (PKC) pathway and causes inhibition of GAPDH (293). We found that sugar metabolites including glycolysis, PPP and amino sugar metabolism were highly induced indicating that these pathways might be influenced. Krebs cycle components, on the other hand, were not noticeably increased although ATP and NADH were increased by 2.2-fold and 2.9-fold respectively comparing to NG.

Our findings are consistent with the results of other studies which demonstrated that elevated glucose induced the sorbitol pathway to convert glucose to fructose

and increased the triose phosphate pool (294,295). In the first step of the sorbitol pathway glucose is reduced to sorbitol in which NADPH is oxidized to NADP+. In the second step, sorbitol is oxidized to fructose accompanied by NAD+ being reduced to NADH that eventually inhibits GAPDH contributing to excessive production of ROS. This can be seen obviously by the significant accumulation of G3P due to GAPDH inhibition. NADPH depletion occurs despite increased flux through the PPP that is supposed to increase its pool and could be affected by the influence of the sorbitol pathway thus affecting levels of oxidized glutathione. Hyperglycaemia, in addition, redirects glucose efflux into the PPP increases, in turn, the triose phosphate known to be associated with oxidative stress initiated by elevated glucose exposure (296). Increasing of octulose 8 phosphate along with the accumulation of G3P indicates that hyperglycaemia may drive the RPE cells to the glucose storage. However, there is less evidence of this than in the PASMCs where glycogens were observed. Moreover, lactate-pyruvate ratio impairment provides an indicates of mitochondrial redox imbalance. Lactate increases suggesting that a “hypoxia-like” effect might implicate on RPE cells exposed to HG. Further experiments are needed to investigate whether RPE cells rely on the Warburg effect to yield energy under HG or not.

Activation of the hexosamine pathway increases the production of transforming growth factor-beta (TGF-beta1) that causes the development of diabetic nephropathy. Amino sugars that were found influenced by HG could indicate increasing levels of TGF-beta1 and activation of protein kinase C (PKC). Long-

lasting activation by HG of PKC enzymes has been correlated with different vascular modifications including contractility, permeability, cell growth and apoptosis (60). Accumulation of G3P due to hyperglycaemia stimulates the accumulation of the upstream metabolite fructose 6-phosphate to be converted into the hexosamine pathway instead of glycolysis increasing UDP-N-acetyl-D-glucosamine that produces the end product N,O-linked glycoproteins. The inhibition of glutamine fructose-6-phosphate aminotransferase (GFAT) enzyme suppresses the conversion of F6-P to glucosamine and reduces the effect of HG to increase the transcription of transforming growth factor TGF that regulates the signalling pathway of cell proliferation and differentiation and plasminogen activator inhibitor-1 (PAI-1) (233). In addition, elevated glucose leads to increased flux through the biosynthetic pathway of hexosamine, resulting in an increase of post-translational modification of serine/threonine residues of proteins by O-linked β-N-acetylglucosamine (O-GlcNAc). O-GlcNAcylation mediates several nuclear and cytoplasmic proteins in a pattern comparable to protein phosphorylation (297). Signalling modification of O-GlcNAc has been involved in diabetes pathogenesis and can play a significant role in diabetic retinopathy pathogenesis.

It is widely known that purine metabolism can be firmly related to the progression of diabetic microvascular complications and high glucose levels have been found to modify the purinergic system of retinal cells (298). Although several purines were decreased when RPE cells cultured in HG media, clinical samples from diabetic retinopathy patients showed that adenosine, xanthine and uric acid as the end

product of purine metabolism were increased in comparison to control subjects (299). An in-vitro study carried out on new born Wistar rat retina cells also illustrated that adenosine protein receptors were influenced by elevated glucose levels in comparison to controls (300). On the other hand, hyperglycaemia was found not to induce RPE cell proliferation significantly (284) therefore; pyrimidine metabolites increased following PPP activation may not be related to the cell growth demand. However, a study carried out on two rat strains demonstrated that elevated glucose-induced RPE cells proliferation in the late first week and in the second and third weeks before cell growth significantly decreases in comparison to a control (285). In the current experiment where extractions were collected after 72 hours of cells cultured in HG may reflect the outcomes of the second study.

Lipid metabolism, in addition, was reduced by HG in which most of the affected lipids were down-regulated. The strongest effect of elevated glucose appeared to be in influencing sphingosines which might suggest that some of these lipids have antioxidant properties.

Published review focused on the lipid metabolism of retina among diabetic retinopathy demonstrated how elevated glucose disturbed fatty acids (301). A metabolic profiling of retina lipid and diabetic influence changes showed that hyperglycaemia induced particular modifications in retinal lipid metabolism (302). Dysregulation of glycerophosphocholines and glycerophosphoinositols indicated that hyperglycaemia damaged cell membranes and could impair cells permeability and signalling. Hyperglycaemia was previously found to significantly reduce RPE cell

capability to transport fluid and boost the fluid accumulation and reduced ARPE-19 cell line membrane permeability (303).

Vitamin D supplementation in the present experiment exhibited a narrow impact on the dysregulated pathways. This included effects on 6 amino acids, 3 sugar metabolites, 25 lipids and 2 pyrimidines that showed a positive response to the antioxidants, indicating that they could of help prevent some of the unfavourable alterations due to HG. However, metabolic profiling of hyperglycaemic RPE cell samples supplemented by vitamin D did not show significant differences comparing to HG. Apart from a small change in ATP, NADPH and ascorbate 6-phosphate there was no substantial change in the other sugar metabolism that was highly influenced by HG. In addition, neither oxidized nor reduced forms of the glutathione positively responded to vitamin D, but carnosine was slightly decreased. Lipids were mostly increased in response to the anti-oxidants maintaining these metabolites closed to the control level.

Elevated glucose induces excessive production of ROS enhancing the oxidative stress of RPE cells as described previously. Vitamin D demonstrated protective ability against oxidative stress in different cell lines and tissues (304). It was also effective to prevent disease progression of the early and late stage of age-related macular degeneration (305). Therefore, a comprehensive evaluation of vitamin D beneficial to protect RPE against oxidative stress initiated by HG needs further investigation.

6.4.2 Hyperglycaemic RPE and RPE/-TSPO

RPE/-TSPO cells exhibit higher oxidative stress in response to HG as they have a higher level of GSSG than wild type. This was obvious even in NG where our result displayed an increased GSSG level in KO in comparison with WT. Pyruvate was increased in WT in response to HG and also in KO but in higher levels than in wild type which may lead to a stronger effect on the TCA cycle. ATP increased in KO cells, but in contrast, NADH was decreased which might be due to a less active TCA cycle. Lactate was unchanged by HG in both KO and WT indicating that the Warburg effect was not induced by HG.

Lipids were increased in KO compared to WT. The deletion of *TSPO* the responsible protein for lipid transport might be expected to dysregulate cell lipids. As formerly confirmed, TSPO deletion deteriorates the efflux of cholesterol and stimulates lipid accumulation in RPE cells (252). Several studies have highlighted the impact of lipid dysregulation on RPE cells specifically on the metabolic processes of the retina (272–274). RPE cells play an essential role in processing and recycling the lipids from photoreceptor outer segments (POS) -the lipid-rich layer- throughout life to preserve visual function, therefore; lipid dysregulation would affect photoreceptors leading to further visual dysfunctions due to lipid accumulation and lipid peroxidation products (275). Lipid accumulation only might not be damaging but in combination with oxidative stress could form lipid peroxidation products such as malondialdehyde (MDA) (276).

Chapter seven

General Discussion and conclusion

7 General Discussion and conclusion

The work involved in this thesis observed the comprehensive role of ROS in the metabolic changes in response to oxidative factors in cell culture. Four studies were included in which the role of diabetic-like conditions on pulmonary artery smooth muscle cells were examined in different groups either supplemented or not with vitamin D or vitamin E. in addition, combining hypoxia with diabetic-like conditions could be linked to the impact of hypoxic conditions that may be induced by hyperglycaemia in diabetes mellitus patients and have an impact on PASMCs metabolism. Also, it was investigated whether or not vitamin D and vitamin E could attenuate undesired metabolic alterations or not. Next, we investigated the effect of TSPO deletion on RPE cells and on their response to treatment with oxidised lipoprotein. Then the impact of diabetic-like condition on wildtype and knockout RPE cells was examined. The effects of adding vitamin D to RPE cells to improve their response to oxidative stress was also observed. A variety of metabolites indicated homeostatic alterations in HG in comparison to NG. The results of this thesis propose that diabetes could induce an array of metabolomic alterations which increases oxidative stress, promote cell proliferation, promote hypoxia-like conditions and change lipid metabolism.

7.1 PASMCs

The current findings demonstrated that HG increases PASMCs cells growth and proliferation. It was induced the production of ROS. In turn, adding a biological concentration of vitamin D or E assisted in reducing most of these changes. These findings are consistent with metabolic profiling of hyperglycaemic PASMCs show significant changes in different metabolic pathways that play an important role in mediating cell proliferation and could contribute to the increased ROS. Glycolysis was induced by HG which consequently increases the cellular oxidative states that are believed to cause vascular remodelling of pulmonary arteries in diabetic patients (306). Increase of ROS generation inhibits the GAPDH enzyme preventing, in turn, the conversion of G-3P to D-glycerate 1,3-bisphosphate affecting the glycolytic breakdown of glucose as a primary energy supplier (307). We found that G-3P significantly increased indicating that GAPDH was inhibited by hyperglycaemia and the upstream metabolites of the PPP were increased. Increase of NADH suggests that hyperglycaemia may activate the sorbitol pathway which generates NADH via NAD when the sorbitol is converted back to fructose and depletes NADPH. Excessive production of intracellular ROS boosts the generation of NADPH through PPP as co-factor agent to restore the oxidized form of glutathione to reduced form in the presence of glutathione reductase. A study carried out on aortic smooth muscle cells reported that PPP is an intrinsic mechanism for the vascular remodelling and associated with hyperglycaemia (223). Exposure of PASMCs to a hyperglycaemic environment increases the level of GSSG confirming that cells redox

status was impaired. A decrease in cellular GSH concentration was previously found to be associated with hyperglycaemia (168). These findings in addition to the disturbance of other metabolic pathways especially the lipids elucidate cellular metabolic modification in hyperglycaemic PASMCs.

Targeting of the PPP in diabetic patients could assist in reducing the damage occurring due to the activation of that pathway. A reduction of G6PD, the rate-limiting enzyme in the PPP has been revealed to decrease the mortality rate due to CVDs (308). However, G6PD has a beneficial function including the ability to preserve the redox state of vascular smooth muscle cells via glutathione reductase activation. Therefore, G6PD targeting unselectively could be an inefficient approach to treat oxidative stress developed due to hyperglycaemia. Selective targeting of other contributing metabolism pathway or enzymes could reduce the cellular damage established via oxidative stress.

Supplementing of hyperglycaemic samples with vitamin D or E was showed some beneficial effects especially with some of PPP metabolites, but no favourable change was noticed in glyceraldehyde 3 phosphate that remain increase even in the presence of the antioxidants. Vitamin D also was able to restore GSSG levels among HG samples close to the level of NG. Therefore, antioxidants treatment be beneficial for improving the redox state related to diabetic and cardiovascular deterioration. Antioxidants may help to diminish the oxidative damage directly via reacting with free radicals scavenge them or indirectly by suppressing the free

radical generating enzymes or promoting intracellular antioxidant enzymes activity which could slow the proliferation of PASMCs.

Combining the hypoxia with hyperglycaemia conditions augmented the impact of ROS generation and cell proliferation on the PASMCs comparing to the HG only. Hypoxia demonstrates the ability to induce superoxide and hydrogen peroxide of PASMCs in high or normal glucose media higher than normoxia. Hypoxic PASMCs increased GSSG, NADH and some PPP metabolites increased in PASMCs indicating increased oxidative stress. Decrease of glucose 1-phosphate and glucose 6-phosphate by hypoxia were surprisingly accompanied by no changes in TCA metabolites nor ATP or NADH due to hypoxia suggesting that PPP was the most influenced pathway to adapt to hypoxia. Slight increase of some fatty acids by hypoxia could also play an important role to maintain the level of TCA metabolites and ATP close to the normoxia level.

7.2 RPE cells

Treatment of RPE cells with OxLDL increased the oxidative stress via affecting glutathione homeostasis and some other oxidative markers such as carnosine and homocarnosine in both cell types wild and knockout. The deletion of the protein responsible for cholesterol efflux (TSPO) was also impaired the redox status while homeostasis various metabolites were influenced. TSPO knockdown has been shown to cause impairment in cholesterol efflux leading to a significant increase in the production of ROS and upregulation of the expression of cytokines IL-1β and

TNFα (253). This was consistent with our findings that showed increases markers of oxidative stress including in KO cells xanthine, hypoxanthine, carnosine and homocarnosine in addition to the influence on glutathione homeostasis. Treating of KO cells with OxLDL showed a higher oxidative response in comparison to treated wildtype which illustrates the crucial role of TSPO deletion in the impairment of RPE redox state. Glycolysis was not significantly influenced by OxLDL in both cell types while TSPO deletion increases the accumulation of glyceraldehyde 3-phosphate. This may occur due to an increase of oxidative stress after TSPO knockdown and was also accompanied by increases in upstream glycolysis metabolites.

Lipids, on the other hand, were the most influenced pathway due to OxLDL and TSPO knockdown. There were marked effects on low abundance and some high abundance phospholipids resulting from oxLDL treatment. Alteration of these high abundance metabolites may lead to remodelling in RPE cell membrane resulting from oxidative stress. Another indication of oxidative stress was noticed when less abundant lipids were increased by OxLDL, and some highly unsaturated chains were decreased. Impact of lipids adaptation on RPE cells has been highlighted in many studies

In conclusion, the treated wildtype cells demonstrate a similar behaviour to the untreated knockout cells while KO cells treated with OxLDL showed further increases of oxidative stress. These findings illustrated the importance of lipid efflux via the mitochondrial cell membrane of RPE cells. The TSPO protein apparently impacted lipids metabolism inducing accumulation that is believed to play an

essential role in AMD disease. Oxidative stress enhancement, in addition, illustrated the role of RPE in the regulation of the oxidative stress response. TSPO can be one of the proteins that might contribute to enhance new treatment strategy for AMD and related eye diseases. Further work on RPE cells metabolic profiling need to be carried out to observe the significance of lipid involvement in the disease pathology.

Hyperglycaemia primarily induced oxidative stress of RPE cells via increases in oxidized glutathione while antioxidants such as carnosine and homocarnosine were also increased. Hyperglycaemia induces ROS consequently and activated the sorbitol pathway increasing NADH that ultimately inhibits GAPDH and caused an accumulation of glyceraldehyde 3 phosphates. This was also accompanied by an increase in PPP metabolites and amino sugars. TCA components, however, were not significantly increased due to hyperglycaemia which may suggest that increases of NADH and ATP may appear due to activation of other pathways like the polyol pathway and lactic acid metabolism. These changes demonstrate the oxidative damage that affected the glycolysis of retinal pigment cells raised due to hyperglycaemia.

Elevated glucose, in addition, decreased purine metabolism which has been reported to be increased among diabetic retinopathy patients. Purine metabolism can be linked to the progression of diabetic microvascular complications and hyperglycaemia is able to change the purinergic system of retinal cells (298). Pyrimidines conversely were mostly increased which might appear to be due to

induction of PPP and high demand for cell growth. However, the role of hyperglycaemia causing RPE cell proliferation is a debatable (284) (285).

The results also show modifications in the lipid metabolites while the robust effects can be seen in the influence on sphingosines indicating that some of these may have antioxidant properties. Alterations of glycerophospholipids reflect the impairment that may occur of the RPE cell membrane due to hyperglycaemia inducing ROS. Therefore, targeting of RPE lipid metabolism may contribute to reducing the impact of ROS on diabetic retinopathy and age-related macular degeneration diseases.

Our finding shows no substantial effect of adding vitamin D to the hyperglycaemic RPE cells apart from minor impacts on ATP, NADPH and some other lipids. Clinical studies have reported favourable effects of vitamin D in preventing disease progression of the early and late stage of age-related macular degeneration in addition to some other studies that also demonstrate the ability of vitamin D to protect different cell lines against oxidative stress. So, it is necessary to further evaluate the ability of vitamin D to reduce the hyperglycaemia complications on RPE.

Untargeted metabolomics screening has identified putative metabolites in biological cell samples which are differentially sensitive to hyperglycaemia or ROS inducers and may be useful if confirmed with animal model studies and clinical samples in the assessment of hyperglycaemia complications in diseases.

8 Limitations and Future Prospects

Some degree of trial was required to establish the PASMC cultures under HG conditions. However, a successful culture method was established during this work. Our findings were directly linked to cell-based work that is focused on the medial smooth muscle cell and retinal pigment epithelial cells, which may not be particularly applicable in an in vivo setting.

Impacts of neighbouring cells of endothelial or photoreceptors in addition to the inflammatory processes and immune systems impacts were not taken into account. Accordingly, the metabolic modification described in our cell culture models may vary from the ones in an in vivo setting based on the same intervention. So, it is fundamental to examine the current study findings on an animal model. In addition, the limited number of included authentic standards restricted our ability to the confirmation of all involved metabolites. This is one of the challenges of untargeted metabolomics since this approach involves a lot of metabolites some of which might not be identifiable and certainly even those identified cannot always be confirmed as this would require a large number of standards which is both expensive and some standards may not be available. The studies were also limited to a single analytical platform using LC-MS which may increase the chance of missing some biomarkers. In future studies, it would be interesting to further increase glucose levels and increase the concentrations of vitamin D to further support the observations made in this thesis.

9 References

1. Boveris A, Cadenas E, Stoppani AO. Role of ubiquinone in the mitochondrial generation of hydrogen peroxide. Biochem J [Internet]. 1976 May 15;156(2):435–44.

2. Halliwell B, Gutteridge JMC. Free radicals in biology and medicine. 1999.

3. Ari Barzilai, Ken-Ichi Yamamoto. DNA damage responses to oxidative stress. DNA Repair (Amst) [Internet]. 2004 Aug 1;3(8–9):1109–15.

4. Lyras L, Cairns NJ, Jenner A, Jenner P, Halliwell B. An Assessment of Oxidative Damage to Proteins, Lipids, and DNA in Brain from Patients with Alzheimer's Disease. J Neurochem [Internet]. 2002 Nov 18;68(5):2061–9.

5. Halliwell B. Biochemistry of oxidative stress. Biochem Soc Trans [Internet]. 2007 Nov 1;35(Pt 5):1147–50.

6. Fogarty MC, Hughes CM, Burke G, Brown JC, Trinick TR, Duly E, et al. Exercise-induced lipid peroxidation: Implications for deoxyribonucleic acid damage and systemic free radical generation. Environ Mol Mutagen [Internet]. 2011 Jan;52(1):35–42.

7. Bailey DM, Lawrenson L, Mceneny J, Young IS, James PE, Jackson SK, et al. Electron paramagnetic spectroscopic evidence of exercise-induced free radical accumulation in human skeletal muscle. Free Radic Res [Internet]. 2007 Jan 7;41(2):182–90.

8. Veal EA, Day AM, Morgan BA. Hydrogen Peroxide Sensing and Signaling. Mol Cell [Internet]. 2007 Apr 13;26(1):1–14.

9. Powers SK, Duarte J, Kavazis AN, Talbert EE. Reactive oxygen species are signalling molecules for skeletal muscle adaptation. Exp Physiol [Internet]. 2010 Jan 1;95(1):1–9.

10. Li C, Jackson RM. Reactive species mechanisms of cellular hypoxia-reoxygenation injury. Am J Physiol Physiol [Internet]. 2002 Feb;282(2):C227–41.

11. Davison GW, George L, Jackson SK, Young IS, Davies B, Bailey DM, et al. Exercise, free radicals, and lipid peroxidation in type 1 diabetes mellitus. Free Radic Biol Med [Internet]. 2002 Dec 1;33(11):1543–51.

12. Ceriello A, Motz E. Is Oxidative Stress the Pathogenic Mechanism Underlying Insulin Resistance, Diabetes, and Cardiovascular Disease? The Common Soil Hypothesis Revisited. Arterioscler Thromb Vasc Biol [Internet]. 2004 May;24(5):816–23.

13. Jenner P. Oxidative stress in Parkinson's disease. Ann Neurol [Internet]. 2003

Jan 1;53(S3):S26–38.

14. Sayre L, Smith M, Perry G. Chemistry and Biochemistry of Oxidative Stress in Neurodegenerative Disease. Curr Med Chem [Internet]. 2001 Jun 1;8(7):721–38.

15. Toshniwal PK, Zarling EJ. Evidence for increased lipid peroxidation in multiple sclerosis. Neurochem Res [Internet]. 1992 Feb;17(2):205–7.

16. Dhalla NS, Temsah RM, Netticadan T. Role of oxidative stress in cardiovascular diseases. J Hypertens [Internet]. 2000;18(6):655–73.

17. Kašparová S, Brezová V, Valko M, Horecký J, Mlynárik V, Liptaj T, et al. Study of the oxidative stress in a rat model of chronic brain hypoperfusion. Neurochem Int [Internet]. 2005 Jun;46(8):601–11.

18. Kerr S, Brosnan MJ, McIntyre M, Reid JL, Dominiczak AF, Hamilton CA. Superoxide anion production is increased in a model of genetic hypertension: role of the endothelium. Hypertens (Dallas, Tex 1979) [Internet]. 1999 Jun;33(6):1353–8.

19. Asami S, Manabe H, Miyake J, Tsurudome Y, Hirano T, Yamaguchi R, et al. Cigarette smoking induces an increase in oxidative DNA damage, 8-hydroxydeoxyguanosine, in a central site of the human lung. Carcinogenesis [Internet]. 1997 Sep;18(9):1763–6.

20. Andreadis AA, Hazen SL, Comhair SAA, Erzurum SC. Oxidative and nitrosative

events in asthma. Free Radic Biol Med [Internet]. 2003 Aug 1;35(3):213–25.

21. Halliwell B, Gutteridge JM. Oxygen toxicity, oxygen radicals, transition metals and disease. Biochem J [Internet]. 1984 Apr 1;219(1):1–14.

22. Valko M, Leibfritz D, Moncol J, Cronin MTD, Mazur M, Telser J. Free radicals and antioxidants in normal physiological functions and human disease. Int J Biochem Cell Biol [Internet]. 2007 Jan;39(1):44–84.

23. Fridovich I. Oxygen: How Do We Stand It? Med Princ Pract [Internet]. 2013;22(2):131–7.

24. Kovacic P, Pozos RS, Somanathan R, Shangari N, O'Brien PJ. Mechanism of mitochondrial uncouplers, inhibitors, and toxins: focus on electron transfer, free radicals, and structure-activity relationships. Curr Med Chem [Internet]. 2005;12(22):2601–23.

25. Fridovich I. Superoxide anion radical (O2-.), superoxide dismutases, and related matters. J Biol Chem [Internet]. 1997 Jul 25;272(30):18515–7.

26. Ivanov A V, Bartosch B, Isaguliants MG. Oxidative Stress in Infection and Consequent Disease. Oxid Med Cell Longev [Internet]. 2017;2017:3496043.

27. Stahl W, Sies H. Antioxidant defense: vitamins E and C and carotenoids. Diabetes [Internet]. 1997 Sep;46 Suppl 2:S14-8.

28. Birben E, Sahiner UM, Sackesen C, Erzurum S, Kalayci O. Oxidative stress and

antioxidant defense. World Allergy Organ J [Internet]. 2012 Jan;5(1):9–19.

29. Kitchin KT, Ahmad S. Oxidative stress as a possible mode of action for arsenic carcinogenesis. Toxicol Lett [Internet]. 2003 Jan 31;137(1–2):3–13.

30. Nikitaki Z, Hellweg CE, Georgakilas AG, Ravanat J-L. Stress-induced DNA damage biomarkers: applications and limitations. Front Chem [Internet]. 2015 Jun 2;3:35.

31. COOKE MS, Evans MD, Dizdaroglu M, Lunec J. Oxidative DNA damage: mechanisms, mutation, and disease. FASEB J [Internet]. 2003 Jul 1;17(10):1195–214.

32. Eaton JW, Qian M. Molecular bases of cellular iron toxicity. Free Radic Biol Med [Internet]. 2002 May 1;32(9):833–40.

33. Radi R, Beckman JS, Bush KM, Freeman BA. Peroxynitrite-induced membrane lipid peroxidation: the cytotoxic potential of superoxide and nitric oxide. Arch Biochem Biophys [Internet]. 1991 Aug 1;288(2):481–7.

34. Porter NA, Caldwell SE, Mills KA. Mechanisms of free radical oxidation of unsaturated lipids. Lipids [Internet]. 1995 Apr;30(4):277–90.

35. Catalá A. Lipid peroxidation of membrane phospholipids generates hydroxy-alkenals and oxidized phospholipids active in physiological and/or pathological conditions. Chem Phys Lipids [Internet]. 2009 Jan;157(1):1–11.

36. Slatter DA, Bolton CH, Bailey AJ. The importance of lipid-derived malondialdehyde in diabetes mellitus. Diabetologia [Internet]. 2000 May 2;43(5):550–7.

37. Catalá A. The ability of melatonin to counteract lipid peroxidation in biological membranes. Curr Mol Med [Internet]. 2007 Nov;7(7):638–49.

38. Davies MJ. The oxidative environment and protein damage. Biochim Biophys Acta - Proteins Proteomics [Internet]. 2005 Jan 17;1703(2):93–109.

39. Buxton G V., Greenstock CL, Helman WP, Ross AB. Critical Review of rate constants for reactions of hydrated electrons, hydrogen atoms and hydroxyl radicals (·OH/·O $^-$ in Aqueous Solution. J Phys Chem Ref Data [Internet]. 1988 Apr 15;17(2):513–886.

40. Stadtman ER, Levine RL. Free radical-mediated oxidation of free amino acids and amino acid residues in proteins. Amino Acids [Internet]. 2003 Dec 29;25(3–4):207–18.

41. Dalle-Donne I, Rossi R, Giustarini D, Milzani A, Colombo R. Protein carbonyl groups as biomarkers of oxidative stress. Clin Chim Acta [Internet]. 2003 Mar;329(1–2):23–38.

42. Stadtman ER, Berlett BS. Reactive Oxygen-Mediated Protein Oxidation in Aging and Disease. Drug Metab Rev [Internet]. 1998 Jan 22;30(2):225–43.

43. Montaner B, O'Donovan P, Reelfs O, Perrett CM, Zhang X, Xu Y-Z, et al.

Reactive oxygen-mediated damage to a human DNA replication and repair protein. EMBO Rep [Internet]. 2007 Nov 12;8(11):1074–9.

44. Peluffo G, Radi R. Biochemistry of protein tyrosine nitration in cardiovascular pathology. Cardiovasc Res [Internet]. 2007 Jul 15;75(2):291–302.

45. Shacter E. QUANTIFICATION AND SIGNIFICANCE OF PROTEIN OXIDATION IN BIOLOGICAL SAMPLES*. Drug Metab Rev [Internet]. 2000 Jan 10;32(3–4):307–26.

46. Kuo IY, Ehrlich BE. Signaling in muscle contraction. Cold Spring Harb Perspect Biol [Internet]. 2015 Feb 2;7(2):a006023.

47. Billaud M, Lohman AW, Johnstone SR, Biwer LA, Mutchler S, Isakson BE. Regulation of cellular communication by signaling microdomains in the blood vessel wall. Pharmacol Rev [Internet]. 2014;66(2):513–69.

48. Graham ES, Woo KK, Aalderink M, Fry S, Greenwood JM, Glass M, et al. M1 Muscarinic Receptor Activation Mediates Cell Death in M1-HEK293 Cells. Smeyne RJ, editor. PLoS One [Internet]. 2013 Sep 2;8(9):e72011.

49. Loh K, Deng H, Fukushima A, Cai X, Boivin B, Galic S, et al. Reactive Oxygen Species Enhance Insulin Sensitivity. Cell Metab [Internet]. 2009 Oct;10(4):260–72.

50. Thannickal VJ, Fanburg BL. Reactive oxygen species in cell signaling. Am J Physiol Cell Mol Physiol [Internet]. 2000 Dec;279(6):L1005–28.

51. Apel K, Hirt H. REACTIVE OXYGEN SPECIES: Metabolism, Oxidative Stress, and Signal Transduction. Annu Rev Plant Biol [Internet]. 2004 Jun 2;55(1):373–99.

52. Wojtaszewski JF, Nielsen P, Hansen BF, Richter EA, Kiens B. Isoform-specific and exercise intensity-dependent activation of 5'-AMP-activated protein kinase in human skeletal muscle. J Physiol [Internet]. 2000 Oct 1;528 Pt 1:221–6.

53. Leon BM, Maddox TM. Diabetes and cardiovascular disease: Epidemiology, biological mechanisms, treatment recommendations and future research. World J Diabetes [Internet]. 2015 Oct 10;6(13):1246–58.

54. Antonetti DA, Barber AJ, Bronson SK, Freeman WM, Gardner TW, Jefferson LS, et al. Diabetic retinopathy: seeing beyond glucose-induced microvascular disease. Diabetes [Internet]. 2006 Sep 1;55(9):2401–11.

55. Retnakaran R, Cull CA, Thorne KI, Adler AI, Holman RR, UKPDS Study Group. Risk factors for renal dysfunction in type 2 diabetes: U.K. Prospective Diabetes Study 74. Diabetes [Internet]. 2006 Jun 1;55(6):1832–9.

56. American Diabetes Association AD. Diagnosis and classification of diabetes mellitus. Diabetes Care [Internet]. 2010 Jan;33 Suppl 1(Suppl 1):S62-9.

57. Baynes JW, Thorpe SR. Role of oxidative stress in diabetic complications: a new perspective on an old paradigm. Diabetes [Internet]. 1999 Jan;48(1):1–9.

58. Du X-L, Edelstein D, Rossetti L, Fantus IG, Goldberg H, Ziyadeh F, et al.

Hyperglycemia-induced mitochondrial superoxide overproduction activates the hexosamine pathway and induces plasminogen activator inhibitor-1 expression by increasing Sp1 glycosylation. Proc Natl Acad Sci [Internet]. 2000 Oct 24;97(22):12222–6.

59. Nishikawa T, Edelstein D, Du XL, Yamagishi S, Matsumura T, Kaneda Y, et al. Normalizing mitochondrial superoxide production blocks three pathways of hyperglycaemic damage. Nature [Internet]. 2000 Apr 13;404(6779):787–90.

60. Geraldes P, King GL. Activation of protein kinase C isoforms and its impact on diabetic complications. Circ Res [Internet]. 2010 Apr 30;106(8):1319–31.

61. Ramasamy R, Goldberg IJ. Aldose Reductase and Cardiovascular Diseases, Creating Human-Like Diabetic Complications in an Experimental Model. Circ Res [Internet]. 2010 May 14;106(9):1449–58.

62. Nishikawa T, Edelstein D, Du XL, Yamagishi S, Matsumura T, Kaneda Y, et al. Normalizing mitochondrial superoxide production blocks three pathways of hyperglycaemic damage. Nature. 2000 Apr 13;404(6779):787–90.

63. Ganz MB, Seftel A. Glucose-induced changes in protein kinase C and nitric oxide are prevented by vitamin E. Am J Physiol Metab [Internet]. 2000 Jan;278(1):E146–52.

64. Engerman RL, Kern TS, Larson ME. Nerve conduction and aldose reductase inhibition during 5 years of diabetes or galactosaemia in dogs. Diabetologia

[Internet]. 1994 Feb;37(2):141–4.

65. Sima AA, Prashar A, Zhang WX, Chakrabarti S, Greene DA. Preventive effect of long-term aldose reductase inhibition (ponalrestat) on nerve conduction and sural nerve structure in the spontaneously diabetic Bio-Breeding rat. J Clin Invest [Internet]. 1990 May 1;85(5):1410–20.

66. Lee AY, Chung SK, Chung SS. Demonstration that polyol accumulation is responsible for diabetic cataract by the use of transgenic mice expressing the aldose reductase gene in the lens. Proc Natl Acad Sci U S A [Internet]. 1995 Mar 28;92(7):2780–4.

67. Wallace DC. Diseases of the Mitochondrial DNA. Annu Rev Biochem [Internet]. 1992 Jun;61(1):1175–212.

68. Brownlee M. The pathobiology of diabetic complications: a unifying mechanism. Diabetes [Internet]. 2005 Jun 1;54(6):1615–25.

69. Trumpower BL. The protonmotive Q cycle. Energy transduction by coupling of proton translocation to electron transfer by the cytochrome bc1 complex. J Biol Chem [Internet]. 1990 Jul 15;265(20):11409–12.

70. Korshunov SS, Skulachev VP, Starkov AA. High protonic potential actuates a mechanism of production of reactive oxygen species in mitochondria. FEBS Lett [Internet]. 1997 Oct 13;416(1):15–8.

71. Du XL, Edelstein D, Dimmeler S, Ju Q, Sui C, Brownlee M. Hyperglycemia

inhibits endothelial nitric oxide synthase activity by posttranslational modification at the Akt site. J Clin Invest [Internet]. 2001 Nov 1;108(9):1341–8.

72. Shen X, Zheng S, Metreveli NS, Epstein PN. Protection of cardiac mitochondria by overexpression of MnSOD reduces diabetic cardiomyopathy. Diabetes [Internet]. 2006 Mar;55(3):798–805.

73. Ye G, Metreveli NS, Donthi R V, Xia S, Xu M, Carlson EC, et al. Catalase protects cardiomyocyte function in models of type 1 and type 2 diabetes. Diabetes [Internet]. 2004 May;53(5):1336–43.

74. Du X, Matsumura T, Edelstein D, Rossetti L, Zsengellér Z, Szabó C, et al. Inhibition of GAPDH activity by poly(ADP-ribose) polymerase activates three major pathways of hyperglycemic damage in endothelial cells. J Clin Invest [Internet]. 2003 Oct 1;112(7):1049–57.

75. Pastore A, Federici G, Bertini E, Piemonte F. Analysis of glutathione: implication in redox and detoxification. Clin Chim Acta [Internet]. 2003 Jul 1;333(1):19–39.

76. Ballatori N, Krance SM, Notenboom S, Shi S, Tieu K, Hammond CL. Glutathione dysregulation and the etiology and progression of human diseases. Biol Chem [Internet]. 2009 Jan 1;390(3):191–214.

77. Franco R, Schoneveld OJ, Pappa A, Panayiotidis MI. The central role of

glutathione in the pathophysiology of human diseases. Arch Physiol Biochem [Internet]. 2007 Jan 10;113(4–5):234–58.

78. Chai YC, Ashraf SS, Rokutan K, Johnston RB, Thomas JA. S-Thiolation of Individual Human Neutrophil Proteins Including Actin by Stimulation of the Respiratory Burst: Evidence against a Role for Glutathione Disulfide. Arch Biochem Biophys [Internet]. 1994 Apr [cited 2018 Feb 23];310(1):273–81.

79. Monostori P, Wittmann G, Karg E, Túri S. Determination of glutathione and glutathione disulfide in biological samples: An in-depth review. J Chromatogr B [Internet]. 2009 Oct 15;877(28):3331–46.

80. Dalle-Donne I, Rossi R, Colombo G, Giustarini D, Milzani A. Protein S-glutathionylation: a regulatory device from bacteria to humans. Trends Biochem Sci [Internet]. 2009 Feb 1;34(2):85–96.

81. Wu G, Fang Y-Z, Yang S, Lupton JR, Turner ND. Glutathione Metabolism and Its Implications for Health. J Nutr [Internet]. 2004 Mar 1;134(3):489–92.

82. Berkholz DS, Faber HR, Savvides SN, Karplus PA. Catalytic cycle of human glutathione reductase near 1 A resolution. J Mol Biol [Internet]. 2008 Oct 3;382(2):371–84.

83. Tian WN, Braunstein LD, Pang J, Stuhlmeier KM, Xi QC, Tian X, et al. Importance of glucose-6-phosphate dehydrogenase activity for cell growth. J Biol Chem [Internet]. 1998 Apr 24;273(17):10609–17.

84. Sutton JR, Reeves JT, Wagner PD, Groves BM, Cymerman A, Malconian MK, et al. Operation Everest II: oxygen transport during exercise at extreme simulated altitude. J Appl Physiol [Internet]. 1988 Apr;64(4):1309–21.

85. Bhambhani YN. Muscle oxygenation trends during dynamic exercise measured by near infrared spectroscopy. Can J Appl Physiol [Internet]. 2004 Aug;29(4):504–23.

86. Garvey JF, Taylor CT, McNicholas WT. Cardiovascular disease in obstructive sleep apnoea syndrome: the role of intermittent hypoxia and inflammation. Eur Respir J [Internet]. 2009 May 1;33(5):1195–205.

87. Baldi S, Aquilani R, Pinna GD, Poggi P, De Martini A, Bruschi C. Fat-free mass change after nutritional rehabilitation in weight losing COPD: role of insulin, C-reactive protein and tissue hypoxia. Int J Chron Obstruct Pulmon Dis [Internet]. 2010 Feb 18;5:29–39.

88. Bailey DM, Taudorf S, Berg RMG, Lundby C, McEneny J, Young IS, et al. Increased cerebral output of free radicals during hypoxia: implications for acute mountain sickness? Am J Physiol Integr Comp Physiol [Internet]. 2009 Nov;297(5):R1283–92.

89. Vij AG, Dutta R, Satija NK. Acclimatization to Oxidative Stress at High Altitude. High Alt Med Biol [Internet]. 2005 Dec;6(4):301–10.

90. Heinicke I, Boehler A, Rechsteiner T, Bogdanova A, Jelkmann W, Hofer M, et

al. Moderate altitude but not additional endurance training increases markers of oxidative stress in exhaled breath condensate. Eur J Appl Physiol [Internet]. 2009 Jul 11;106(4):599–604.

91. Clanton TL. Hypoxia-induced reactive oxygen species formation in skeletal muscle. J Appl Physiol [Internet]. 2007 Jun;102(6):2379–88.

92. Bell EL, Klimova TA, Eisenbart J, Schumacker PT, Chandel NS. Mitochondrial Reactive Oxygen Species Trigger Hypoxia-Inducible Factor-Dependent Extension of the Replicative Life Span during Hypoxia. Mol Cell Biol [Internet]. 2007 Aug 15;27(16):5737–45.

93. Chandel NS, Maltepe E, Goldwasser E, Mathieu CE, Simon MC, Schumacker PT. Mitochondrial reactive oxygen species trigger hypoxia-induced transcription. Proc Natl Acad Sci U S A [Internet]. 1998 Sep 29;95(20):11715–20.

94. Sobel BE, Schneider DJ. Cardiovascular complications in diabetes mellitus. Curr Opin Pharmacol [Internet]. 2005 Apr 1;5(2):143–8.

95. Min TZ, Stephens MW, Kumar P, Chudleigh RA. Renal complications of diabetes. Br Med Bull [Internet]. 2012 Dec 1;104(1):113–27.

96. Crawford TN, Alfaro DV, Kerrison JB, Jablon EP. Diabetic retinopathy and angiogenesis. Curr Diabetes Rev [Internet]. 2009 Feb;5(1):8–13.

97. Giacco F, Brownlee M. Oxidative stress and diabetic complications. Circ Res

[Internet]. 2010 Oct 29;107(9):1058–70.

98. Haffner SM, Lehto S, Rönnemaa T, Pyörälä K, Laakso M. Mortality from Coronary Heart Disease in Subjects with Type 2 Diabetes and in Nondiabetic Subjects with and without Prior Myocardial Infarction. N Engl J Med [Internet]. 1998 Jul 23;339(4):229–34.

99. Laing SP, Swerdlow AJ, Slater SD, Burden AC, Morris A, Waugh NR, et al. Mortality from heart disease in a cohort of 23,000 patients with insulin-treated diabetes. Diabetologia [Internet]. 2003 Jun 1;46(6):760–5.

100. Domanski M, Mitchell G, Pfeffer M, Neaton JD, Norman J, Svendsen K, et al. Pulse pressure and cardiovascular disease-related mortality: follow-up study of the Multiple Risk Factor Intervention Trial (MRFIT). JAMA [Internet]. 2002;287(20):2677–83.

101. Ling Y, Johnson MK, Kiely DG, Condliffe R, Elliot CA, Gibbs JSR, et al. Changing Demographics, Epidemiology, and Survival of Incident Pulmonary Arterial Hypertension. Am J Respir Crit Care Med [Internet]. 2012 Oct 15;186(8):790–6.

102. Abernethy AD, Stackhouse K, Hart S, Devendra G, Bashore TM, Dweik R, et al. Impact of Diabetes in Patients with Pulmonary Hypertension. Pulm Circ [Internet]. 2015 Mar;5(1):117–23.

103. Benson L, Brittain EL, Pugh ME, Austin ED, Fox K, Wheeler L, et al. Impact of

diabetes on survival and right ventricular compensation in pulmonary arterial hypertension. Pulm Circ [Internet]. 2014 Jun;4(2):311–8.

104. Lutty GA. Effects of diabetes on the eye. Invest Ophthalmol Vis Sci [Internet]. 2013 Dec 13;54(14):ORSF81-7.

105. Hirai FE, Tielsch JM, Klein BEK, Klein R. Ten-Year Change in Vision-Related Quality of Life in Type 1 Diabetes: Wisconsin Epidemiologic Study of Diabetic Retinopathy. Ophthalmology [Internet]. 2011 Feb;118(2):353–8.

106. Kempen JH, O'Colmain BJ, Leske MC, Haffner SM, Klein R, Moss SE, et al. The Prevalence of Diabetic Retinopathy Among Adults in the United States. Arch Ophthalmol [Internet]. 2004 Apr 1;122(4):552.

107. Yau JWY, Rogers SL, Kawasaki R, Lamoureux EL, Kowalski JW, Bek T, et al. Global Prevalence and Major Risk Factors of Diabetic Retinopathy. Diabetes Care [Internet]. 2012 Mar 1;35(3):556–64.

108. Gheith O, Farouk N, Nampoory N, Halim MA, Al-Otaibi T. Diabetic kidney disease: world wide difference of prevalence and risk factors. J nephropharmacology [Internet]. 2016;5(1):49–56.

109. Andersen AR, Christiansen JS, Andersen JK, Kreiner S, Deckert T. Diabetic nephropathy in Type 1 (insulin-dependent) diabetes: an epidemiological study. Diabetologia [Internet]. 1983 Dec;25(6):496–501.

110. American Diabetes Association AD. Standards of medical care in diabetes--

2014. Diabetes Care [Internet]. 2014 Jan 1;37 Suppl 1(Supplement 1):S14-80.

111. Bunker VW. Free radicals, antioxidants and ageing. Med Lab Sci [Internet]. 1992 Dec;49(4):299–312.

112. White E, Shannon JS, Patterson RE. Relationship between vitamin and calcium supplement use and colon cancer. Cancer Epidemiol Biomarkers Prev [Internet]. 1997 Oct;6(10):769–74.

113. Chiu KC, Chu A, Go VLW, Saad MF. Hypovitaminosis D is associated with insulin resistance and β cell dysfunction. Am J Clin Nutr [Internet]. 2004 May 1;79(5):820–5.

114. Mitri J, Muraru MD, Pittas AG. Vitamin D and type 2 diabetes: a systematic review. Eur J Clin Nutr [Internet]. 2011 Sep 6;65(9):1005–15.

115. Wang TJ, Pencina MJ, Booth SL, Jacques PF, Ingelsson E, Lanier K, et al. Vitamin D Deficiency and Risk of Cardiovascular Disease. Circulation [Internet]. 2008 Jan 29;117(4):503–11.

116. Mokhtari Z, Hekmatdoost A, Nourian M. Antioxidant efficacy of vitamin D. J Parathyr Dis [Internet]. 2016 Jul 2;5(1).

117. Dunn WB, Bailey NJC, Johnson HE. Measuring the metabolome: current analytical technologies. Analyst [Internet]. 2005;130(5):606.

118. Kang J, Zhu L, Lu J, Zhang X. Application of metabolomics in autoimmune

diseases: Insight into biomarkers and pathology. J Neuroimmunol. 2015;279:25–32.

119. Geraci M, Meyrick B, Geraci M, Meyrick B. Genomics and Proteomics of Pulmonary Vascular Disease. In: Comprehensive Physiology. John Wiley & Sons, Inc.; 2011.

120. Tainsky MA. Genomic and proteomic biomarkers for cancer: A multitude of opportunities. Biochim Biophys Acta - Rev Cancer. 2009;1796(2):176–93.

121. Goodacre R, Vaidyanathan S, Dunn WB, Harrigan GG, Kell DB. Metabolomics by numbers: acquiring and understanding global metabolite data. Trends Biotechnol. 2004;22(5):245–52.

122. Kitteringham NR, Jenkins RE, Lane CS, Elliott VL, Park BK. Multiple reaction monitoring for quantitative biomarker analysis in proteomics and metabolomics. J Chromatogr B. 2009;877(13):1229–39.

123. Dunn WB. Diabetes - the Role of Metabolomics in the Discovery of New Mechanisms and Novel Biomarkers. Curr Cardiovasc Risk Rep [Internet]. 2013 Feb 7 [cited 2017 Nov 22];7(1):25–32.

124. Alonso A, Marsal S, JuliÃ A. Analytical Methods in Untargeted Metabolomics: State of the Art in 2015. Front Bioeng Biotechnol. 2015;3:23.

125. van Ginneken V, Verhey E, Poelmann R, Ramakers R, van Dijk KW, Ham L, et al. Metabolomics (liver and blood profiling) in a mouse model in response to

fasting: A study of hepatic steatosis. Biochim Biophys Acta - Mol Cell Biol Lipids [Internet]. 2007 Oct [cited 2017 Nov 22];1771(10):1263–70.

126. Zhen Y, Krausz KW, Chen C, Idle JR, Gonzalez FJ. Metabolomic and genetic analysis of biomarkers for peroxisome proliferator-activated receptor alpha expression and activation. Mol Endocrinol [Internet]. 2007 Sep;21(9):2136–51.

127. Makarov A, Denisov E, Lange O, Horning S. Dynamic range of mass accuracy in LTQ orbitrap hybrid mass spectrometer. J Am Soc Mass Spectrom [Internet]. 2006 Jul [cited 2019 Feb 11];17(7):977–82.

128. Kamleh A, Barrett MP, Wildridge D, Burchmore RJS, Scheltema RA, Watson DG. Metabolomic profiling using Orbitrap Fourier transform mass spectrometry with hydrophilic interaction chromatography: a method with wide applicability to analysis of biomolecules. Rapid Commun Mass Spectrom [Internet]. 2008 Jun 30;22(12):1912–8.

129. Fenn JB, Mann M, Chin-kai M, Shek-fu W, Whitehouse CM. Electrospray Ionization for Mass Spectrometry of Large Biomolecules. Science (80-). 1989;246(4926).

130. Dettmer K, Aronov PA, Hammock BD. Mass spectrometry-based metabolomics. Mass Spectrom Rev. 2007;26(1):51–78.

131. Patel KN, Patel JK, Patel MP, Rajput GC, Patel HA. Introduction to hyphenated

techniques and their applications in pharmacy. Pharm Methods [Internet]. 2010 Oct;1(1):2–13.

132. Hemström P, Irgum K. Hydrophilic interaction chromatography. J Sep Sci [Internet]. 2006 Aug;29(12):1784–821.

133. Jandera P. Stationary and mobile phases in hydrophilic interaction chromatography: a review. Anal Chim Acta [Internet]. 2011 Apr 29;692(1–2):1–25.

134. Dempster AJ. A new Method of Positive Ray Analysis. Phys Rev [Internet]. 1918 Apr 1;11(4):316–25.

135. Kamleh MA, Dow JAT, Watson DG. Applications of mass spectrometry in metabolomic studies of animal model and invertebrate systems. Briefings Funct Genomics Proteomics [Internet]. 2008 Dec 12;8(1):28–48.

136. Makarov A, Denisov E, Kholomeev A, Balschun W, Lange O, Strupat K, et al. Performance Evaluation of a Hybrid Linear Ion Trap/Orbitrap Mass Spectrometer. Anal Chem [Internet]. 2006 Apr 1;78(7):2113–20.

137. Katajamaa M, Miettinen J, Oresic M. MZmine: toolbox for processing and visualization of mass spectrometry based molecular profile data. Bioinformatics [Internet]. 2006 Mar 1;22(5):634–6.

138. Scheltema RA, Jankevics A, Jansen RC, Swertz MA, Breitling R. PeakML/mzMatch: A File Format, Java Library, R Library, and Tool-Chain for

Mass Spectrometry Data Analysis. Anal Chem [Internet]. 2011 Apr 1;83(7):2786–93.

139. Creek DJ, Jankevics A, Burgess KE V., Breitling R, Barrett MP. IDEOM: an Excel interface for analysis of LC–MS-based metabolomics data. Bioinformatics [Internet]. 2012 Apr 1;28(7):1048–9.

140. Grainger D. MegavariateStatisticsmeetsHighData-densityAnalyticalMethods: TheFutureofMedicalDiagnostics? 2003;1:1–6.

141. Eriksson L, Byrne T, Johansson E, Trygg J, Vikström C. Multi- and megavariate data analysis : basic principles and applications [Internet]. 3rd ed. Sweden; 2013. 503 p.

142. Xi B, Gu H, Baniasadi H, Raftery D. Statistical Analysis and Modeling of Mass Spectrometry-Based Metabolomics Data. In: Methods in molecular biology (Clifton, NJ) [Internet]. 2014. p. 333–53.

143. Prelorendjos A. Multivariate Analysis of Metabonomic Data. PhD, Strat. 2014;

144. Kirwan GM, Johansson E, Kleemann R, Verheij ER, Wheelock ÅM, Goto S, et al. Building Multivariate Systems Biology Models. Anal Chem [Internet]. 2012 Aug 21;84(16):7064–71.

145. Yamamoto H, Yamaji H, Abe Y, Harada K, Waluyo D, Fukusaki E, et al. Dimensionality reduction for metabolome data using PCA, PLS, OPLS, and RFDA with differential penalties to latent variables. Chemom Intell Lab Syst

[Internet]. 2009 Oct 15;98(2):136–42.

146. Trygg J, Holmes E, Lundstedt T. Chemometrics in Metabonomics. J Proteome Res [Internet]. 2007 Feb;6(2):469–79.

147. Goodacre R. Metabolomics of a Superorganism. J Nutr [Internet]. 2007 Jan 1;137(1):259S–266S.

148. Triba MN, Le Moyec L, Amathieu R, Goossens C, Bouchemal N, Nahon P, et al. PLS/OPLS models in metabolomics: the impact of permutation of dataset rows on the K-fold cross-validation quality parameters. Mol Biosyst [Internet]. 2015 Jan;11(1):13–9.

149. Wheelock ÅM, Wheelock CE. Trials and tribulations of 'omics data analysis: assessing quality of SIMCA-based multivariate models using examples from pulmonary medicine. Mol Biosyst [Internet]. 2013 Nov;9(11):2589.

150. Eriksson L, Trygg J, Wold S. CV-ANOVA for significance testing of PLS and OPLS® models. J Chemom [Internet]. 2008 Nov 1;22(11–12):594–600.

151. Zhang P, Chen J, Wang Y, Huang Y, Tian Y, Zhang Z, et al. Discovery of Potential Biomarkers with Dose- and Time-Dependence in Cisplatin-Induced Nephrotoxicity Using Metabolomics Integrated with a Principal Component-Based Area Calculation Strategy. Chem Res Toxicol [Internet]. 2016 May 16;29(5):776–83.

152. Laboratories S research. Human Pulmonary Artery Smooth Muscle Cells.

sciencell research laboratories.

153. Zhang T, Watson DG, Wang L, Abbas M, Murdoch L, Bashford L, et al. Application of Holistic Liquid Chromatography-High Resolution Mass Spectrometry Based Urinary Metabolomics for Prostate Cancer Detection and Biomarker Discovery. Agoulnik IU, editor. PLoS One [Internet]. 2013 Jun 18;8(6):e65880.

154. Creek DJ, Jankevics A, Breitling R, Watson DG, Barrett MP, Burgess KE V. Toward Global Metabolomics Analysis with Hydrophilic Interaction Liquid Chromatography–Mass Spectrometry: Improved Metabolite Identification by Retention Time Prediction. Anal Chem [Internet]. 2011 Nov 15;83(22):8703–10.

155. Xia J, Sinelnikov I V., Han B, Wishart DS. MetaboAnalyst 3.0—making metabolomics more meaningful. Nucleic Acids Res [Internet]. 2015 Jul 1;43(W1):W251–7.

156. Chong I-G, Jun C-H. Performance of some variable selection methods when multicollinearity is present. Chemom Intell Lab Syst [Internet]. 2005 Jul 28;78(1–2):103–12.

157. Efron B, Gong G. A Leisurely Look at the Bootstrap, the Jackknife, and Cross-Validation. Am Stat [Internet]. 1983 Feb;37(1):36.

158. Humbert M, Sitbon O, Chaouat A, Bertocchi M, Habib G, Gressin V, et al.

Survival in Patients With Idiopathic, Familial, and Anorexigen-Associated Pulmonary Arterial Hypertension in the Modern Management Era. Circulation [Internet]. 2010 Jul 13;122(2):156–63.

159. McLaughlin V V, Archer SL, Badesch DB, Barst RJ, Farber HW, Lindner JR, et al. ACCF/AHA 2009 expert consensus document on pulmonary hypertension a report of the American College of Cardiology Foundation Task Force on Expert Consensus Documents and the American Heart Association developed in collaboration with the American College of. J Am Coll Cardiol. 2009;53(17):1573–619.

160. Raphael C, Briscoe C, Davies J, Ian Whinnett Z, Manisty C, Sutton R, et al. Limitations of the New York Heart Association functional classification system and self-reported walking distances in chronic heart failure. Heart [Internet]. 2007 Apr 1;93(4):476–82.

161. Simonneau G, Gatzoulis MA, Adatia I, Celermajer D, Denton C, Ghofrani A, et al. Updated Clinical Classification of Pulmonary Hypertension. J Am Coll Cardiol [Internet]. 2013 Dec 24;62(25):D34–41.

162. Gopal DM, Santhanakrishnan R, Wang Y-C, Ayalon N, Donohue C, Rahban Y, et al. Impaired right ventricular hemodynamics indicate preclinical pulmonary hypertension in patients with metabolic syndrome. J Am Heart Assoc [Internet]. 2015 Mar 10;4(3):e001597.

163. Lai Y-C, Tabima DM, Dube JJ, Hughan KS, Goncharov DA, Vanderpool RR, et al. SIRT3-AMPK Activation by Nitrite and Metformin Improves Hyperglycemia and Normalizes Pulmonary Hypertension Associated with Heart Failure with Preserved Ejection Fraction (PH-HFpEF). Circulation [Internet]. 2016 Jan 26;133(8):CIRCULATIONAHA.115.018935.

164. Wallace DC. Diseases of the Mitochondrial DNA. Annu Rev Biochem [Internet]. 1992 Jun 28;61(1):1175–212.

165. Maxwell SR, Thomason H, Sandler D, Leguen C, Baxter MA, Thorpe GH, et al. Antioxidant status in patients with uncomplicated insulin-dependent and non-insulin-dependent diabetes mellitus. Eur J Clin Invest [Internet]. 1997 Jun;27(6):484–90.

166. Baynes JW. Role of oxidative stress in development of complications in diabetes. Diabetes [Internet]. 1991 Apr;40(4):405–12.

167. Masella R, Di Benedetto R, Varì R, Filesi C, Giovannini C. Novel mechanisms of natural antioxidant compounds in biological systems: involvement of glutathione and glutathione-related enzymes. J Nutr Biochem [Internet]. 2005 Oct;16(10):577–86.

168. Whiting PH, Kalansooriya A, Holbrook I, Haddad F, Jennings PE. The relationship between chronic glycaemic control and oxidative stress in type 2 diabetes mellitus. Br J Biomed Sci [Internet]. 2008;65(2):71–4.

169. Sundaram RK, Bhaskar A, Vijayalingam S, Viswanathan M, Mohan R, Shanmugasundaram KR. Antioxidant status and lipid peroxidation in type II diabetes mellitus with and without complications. Clin Sci (Lond) [Internet]. 1996 Apr;90(4):255–60.

170. Hakki Kalkan I, Suher M. The relationship between the level of glutathione, impairment of glucose metabolism and complications of diabetes mellitus. Pakistan J Med Sci [Internet]. 2013 Jul;29(4):938–42.

171. Wiseman H. Vitamin D is a membrane antioxidant. Ability to inhibit iron-dependent lipid peroxidation in liposomes compared to cholesterol, ergosterol and tamoxifen and relevance to anticancer action. FEBS Lett. 1993 Jul 12;326(1–3):285–8.

172. Wiseman H. Vitamin D is a membrane antioxidant. Ability to inhibit iron-dependent lipid peroxidation in liposomes compared to cholesterol, ergosterol and tamoxifen and relevance to anticancer action. FEBS Lett [Internet]. 1993 Jul 12;326(1–3):285–8.

173. Taheri E, Djalali M, Djazayeri A, Qorbani M, Rajab A, Larijani B, et al. Vitamin D status and its association with antioxidant profiles in diabetic patients: A cross-sectional study in Iran. Indian J Med Sci [Internet]. 2013;67(1):29.

174. Shen Z, Zhang X, Tang J, Kasiappan R, Jinwal U, Li P, et al. The coupling of epidermal growth factor receptor down regulation by 1alpha,25-

dihydroxyvitamin D3 to the hormone-induced cell cycle arrest at the G1-S checkpoint in ovarian cancer cells. Mol Cell Endocrinol [Internet]. 2011 May 16;338(1–2):58–67.

175. Fedirko V, Bostick RM, Long Q, Flanders WD, McCullough ML, Sidelnikov E, et al. Effects of Supplemental Vitamin D and Calcium on Oxidative DNA Damage Marker in Normal Colorectal Mucosa: A Randomized Clinical Trial. Cancer Epidemiol Biomarkers Prev [Internet]. 2010 Jan 1;19(1):280–91.

176. Virtamo J, Rapola JM, Ripatti S, Heinonen OP, Taylor PR, Albanes D, et al. Effect of Vitamin E and Beta Carotene on the Incidence of Primary Nonfatal Myocardial Infarction and Fatal Coronary Heart Disease. Arch Intern Med [Internet]. 1998 Mar 23;158(6):668.

177. Sacco M, Pellegrini F, Roncaglioni MC, Avanzini F, Tognoni G, Nicolucci A, et al. Primary prevention of cardiovascular events with low-dose aspirin and vitamin E in type 2 diabetic patients: results of the Primary Prevention Project (PPP) trial. Diabetes Care [Internet]. 2003 Dec;26(12):3264–72.

178. Chae CU, Albert CM, Moorthy M V., Lee I-M, Buring JE. Vitamin E Supplementation and the Risk of Heart Failure in Women. Circ Hear Fail [Internet]. 2012 Mar 1;5(2):176–82.

179. Schieber M, Chandel NS. ROS Function in Redox Signaling and Oxidative Stress. Curr Biol [Internet]. 2014 May 19;24(10):R453.

180. Heart Outcomes Prevention Evaluation Study Investigators, Yusuf S, Dagenais G, Pogue J, Bosch J, Sleight P. Vitamin E Supplementation and Cardiovascular Events in High-Risk Patients. N Engl J Med [Internet]. 2000 Jan 20;342(3):154–60.

181. Gæde P, Vedel P, Larsen N, Jensen GVH, Parving H-H, Pedersen O. Multifactorial Intervention and Cardiovascular Disease in Patients with Type 2 Diabetes. N Engl J Med [Internet]. 2003 Jan 30;348(5):383–93.

182. Lonn E, Yusuf S, Hoogwerf B, Pogue J, Yi Q, Zinman B, et al. Effects of vitamin E on cardiovascular and microvascular outcomes in high-risk patients with diabetes: results of the HOPE study and MICRO-HOPE substudy. Diabetes Care [Internet]. 2002 Nov;25(11):1919–27.

183. Skyrme-Jones RA, O'Brien RC, Berry KL, Meredith IT. Vitamin E supplementation improves endothelial function in type I diabetes mellitus: a randomized, placebo-controlled study. J Am Coll Cardiol [Internet]. 2000 Jul;36(1):94–102.

184. Beckman JA, Goldfine AB, Gordon MB, Garrett LA, Keaney JF, Creager MA. Oral antioxidant therapy improves endothelial function in Type 1 but not Type 2 diabetes mellitus. Am J Physiol Circ Physiol [Internet]. 2003 Dec;285(6):H2392–8.

185. Gaede P, Poulsen HE, Parving HH, Pedersen O. Double-blind, randomised

study of the effect of combined treatment with vitamin C and E on albuminuria in Type 2 diabetic patients. Diabet Med [Internet]. 2001 Sep;18(9):756–60.

186. Alipui C, Ramos K, Tenner TE. Alterations of rabbit aortic smooth muscle cell proliferation in diabetes mellitus. Cardiovasc Res [Internet]. 1993 Jul;27(7):1229–32.

187. Oikawa S, Hayasaka K, Hashizume E, Kotake H, Midorikawa H, Sekikawa A, et al. Human arterial smooth muscle cell proliferation in diabetes. Diabetes [Internet]. 1996 Jul;45 Suppl 3:S114-6.

188. Yoo HJ, Yu SH, Cho YJ, Nam HW, Kang DH. Effects of Homocysteine and Hyperglycemia on the Proliferation of Aortic Vascular Smooth Muscle Cells of Obese Type 2 Diabetes Rat. Ann Geriatr Med Res [Internet]. 2017 Jun 30;21(2):78.

189. Mitsuhashi T, Morris RC, Ives HE, Ives HE. 1,25-dihydroxyvitamin D3 modulates growth of vascular smooth muscle cells. J Clin Invest [Internet]. 1991 Jun;87(6):1889–95.

190. Carthy EP, Yamashita W, Hsu A, Ooi BS. 1,25-Dihydroxyvitamin D3 and rat vascular smooth muscle cell growth. Hypertens (Dallas, Tex 1979) [Internet]. 1989 Jun;13(6 Pt 2):954–9.

191. Boscoboinik D, Szewczyk A, Hensey C, Azzi A. Inhibition of cell proliferation by

alpha-tocopherol. Role of protein kinase C. J Biol Chem [Internet]. 1991 Apr 5;266(10):6188–94.

192. Labudzynskyi DO, Zaitseva O V, Latyshko N V, Gudkova OO, Veliky MM. VITAMIN D3 CONTRIBUTION TO THE REGULATION OF OXIDATIVE METABOLISM IN THE LIVER OF DIABETIC MICE. Ukr Biochem J [Internet]. 87(3):75–90.

193. Kono K, Fujii H, Nakai K, Goto S, Kitazawa R, Kitazawa S, et al. Anti-Oxidative Effect of Vitamin D Analog on Incipient Vascular Lesion in Non-Obese Type 2 Diabetic Rats. Am J Nephrol [Internet]. 2013;37(2):167–74.

194. Greń A. Effects of Vitamin E, C and D Supplementation on Inflammation and Oxidative Stress in Streptozotocin-Induced Diabetic Mice. Int J Vitam Nutr Res [Internet]. 2013 Jun;83(3):168–75.

195. Gavazza M, Catalá A. The effect of alpha-tocopherol on the lipid peroxidation of mitochondria and microsomes obtained from rat liver and testis. Mol Cell Biochem [Internet]. 2001 Sep;225(1-):121–8.

196. Archer SL, Weir EK, Wilkins MR. Basic science of pulmonary arterial hypertension for clinicians: new concepts and experimental therapies. Circulation. 2010 May 11;121(18):2045–66.

197. Monnier L, Mas E, Ginet C, Michel F, Villon L, Cristol J-P, et al. Activation of Oxidative Stress by Acute Glucose Fluctuations Compared With Sustained

Chronic Hyperglycemia in Patients With Type 2 Diabetes. JAMA. 2006 Apr 12;295(14):1681.

198. Sochor M, Gonzalez AM, McLean P. Regulation of alternative pathways of glucose metabolism in rat heart in alloxan diabetes: changes in the pentose phosphate pathway. Biochem Biophys Res Commun. 1984 Jan 13;118(1):110–6.

199. Anderson EJ, Kypson AP, Rodriguez E, Anderson CA, Lehr EJ, Neufer PD. Substrate-Specific Derangements in Mitochondrial Metabolism and Redox Balance in the Atrium of the Type 2 Diabetic Human Heart. J Am Coll Cardiol. 2009 Nov 10;54(20):1891–8.

200. Andreyev AY, Kushnareva YE, Starkov AA. Mitochondrial metabolism of reactive oxygen species. Biochemistry (Mosc). 2005 Feb;70(2):200–14.

201. Sekhar R V, McKay S V, Patel SG, Guthikonda AP, Reddy VT, Balasubramanyam A, et al. Glutathione synthesis is diminished in patients with uncontrolled diabetes and restored by dietary supplementation with cysteine and glycine. Diabetes Care [Internet]. 2011 Jan;34(1):162–7.

202. Reis GS, Augusto VS, Silveira APC, Jordão AA, Baddini-Martinez J, Poli Neto O, et al. Oxidative-stress biomarkers in patients with pulmonary hypertension. Pulm Circ [Internet]. 2013 Dec;3(4):856–61.

203. Zhao Y, Peng J, Lu C, Hsin M, Mura M, Wu L, et al. Metabolomic

heterogeneity of pulmonary arterial hypertension. PLoS One. 2014;9(2):e88727.

204. Helkin A, Stein JJ, Lin S, Siddiqui S, Maier KG, Gahtan V. Dyslipidemia Part 1—Review of Lipid Metabolism and Vascular Cell Physiology. Vasc Endovascular Surg. 2016 Feb 16;50(2):107–18.

205. Whiley L, Sen A, Heaton J, Proitsi P, García-Gómez D, Leung R, et al. Evidence of altered phosphatidylcholine metabolism in Alzheimer's disease. Neurobiol Aging. 2014 Feb;35(2):271–8.

206. Hong JH, Kang JW, Kim DK, Baik SH, Kim KH, Shanta SR, et al. Global changes of phospholipids identified by MALDI imaging mass spectrometry in a mouse model of Alzheimer's disease. J Lipid Res. 2016 Jan;57(1):36–45.

207. Gaudin M, Panchal M, Auzeil N, Duyckaerts C, Brunelle A, Laprévote O, et al. Choline-containing phospholipids in microdissected human Alzheimer's disease brain senile plaque versus neuropil. Bioanalysis. 2012 Sep;4(17):2153–9.

208. Steen Steenken* † and, Jovanovic‡ S V. How Easily Oxidizable Is DNA? One-Electron Reduction Potentials of Adenosine and Guanosine Radicals in Aqueous Solution. J Am Chem Soc. 1997;119(3):617–8.

209. Erlinge D. Extracellular ATP: A Growth Factor for Vascular Smooth Muscle Cells. Gen Pharmacol Vasc Syst. 1998 Jul 1;31(1):1–8.

210. Buse MG. Hexosamines, insulin resistance, and the complications of diabetes: current status. Am J Physiol Endocrinol Metab. 2006 Jan;290(1):E1–8.

211. Copeland RJ, Bullen JW, Hart GW. Cross-talk between GlcNAcylation and phosphorylation: roles in insulin resistance and glucose toxicity. Am J Physiol Endocrinol Metab. 2008 Jul;295(1):E17-28.

212. Hira HS, Samal P, Kaur A, Kapoor S. Plasma level of hypoxanthine/xanthine as markers of oxidative stress with different stages of obstructive sleep apnea syndrome. Ann Saudi Med. 2014 Aug;34(4):308–13.

213. Cofta S, Wysocka E, Piorunek T, Rzymkowska M, Batura-Gabryel H, Torlinski L. Oxidative stress markers in the blood of persons with different stages of obstructive sleep apnea syndrome. J Physiol Pharmacol. 2008 Dec;59 Suppl 6:183–90.

214. Sada K, Nishikawa T, Kukidome D, Yoshinaga T, Kajihara N, Sonoda K, et al. Hyperglycemia Induces Cellular Hypoxia through Production of Mitochondrial ROS Followed by Suppression of Aquaporin-1. PLoS One [Internet]. 2016;11(7):e0158619.

215. Nyengaard JR, Ido Y, Kilo C, Williamson JR. Interactions between hyperglycemia and hypoxia: implications for diabetic retinopathy. Diabetes [Internet]. 2004 Nov;53(11):2931–8.

216. Chung SSM, Ho ECM, Lam KSL, Chung SK. Contribution of polyol pathway to

diabetes-induced oxidative stress. J Am Soc Nephrol [Internet]. 2003 Aug;14(8 Suppl 3):S233-6.

217. Ramasamy R, Yan SF, Schmidt AM. Methylglyoxal Comes of AGE. Cell [Internet]. 2006 Jan 27;124(2):258–60.

218. Xiao H, Gu Z, Wang G, Zhao T. The Possible Mechanisms Underlying the Impairment of HIF-1α Pathway Signaling in Hyperglycemia and the Beneficial Effects of Certain Therapies. Int J Med Sci [Internet]. 2013;10(10):1412–21.

219. WELSH DJ, SCOTT P, PLEVIN R, WADSWORTH R, PEACOCK AJ. Hypoxia Enhances Cellular Proliferation and Inositol 1,4,5-Triphosphate Generation in Fibroblasts from Bovine Pulmonary Artery But Not from Mesenteric Artery. Am J Respir Crit Care Med [Internet]. 1998 Dec 14;158(6):1757–62.

220. WELSH DJ, PEACOCK AJ, MacLEAN M, HARNETT M. Chronic Hypoxia Induces Constitutive p38 Mitogen-activated Protein Kinase Activity That Correlates with Enhanced Cellular Proliferation in Fibroblasts from Rat Pulmonary But Not Systemic Arteries. Am J Respir Crit Care Med [Internet]. 2001 Jul 15;164(2):282–9.

221. Welsh DJ, Scott PH, Peacock AJ. p38 MAP kinase isoform activity and cell cycle regulators in the proliferative response of pulmonary and systemic artery fibroblasts to acute hypoxia. Pulm Pharmacol Ther [Internet]. 2006 Apr;19(2):128–38.

222. Yan L-J. Pathogenesis of chronic hyperglycemia: from reductive stress to oxidative stress. J Diabetes Res [Internet]. 2014;2014:137919.

223. Peiró C, Romacho T, Azcutia V, Villalobos L, Fernández E, Bolaños JP, et al. Inflammation, glucose, and vascular cell damage: the role of the pentose phosphate pathway. Cardiovasc Diabetol [Internet]. 2017;16(1):25.

224. Obrosova IG, Minchenko AG, Vasupuram R, White L, Abatan OI, Kumagai AK, et al. Aldose reductase inhibitor fidarestat prevents retinal oxidative stress and vascular endothelial growth factor overexpression in streptozotocin-diabetic rats. Diabetes [Internet]. 2003 Mar;52(3):864–71.

225. Koya D, King GL. Protein kinase C activation and the development of diabetic complications. Diabetes [Internet]. 1998 Jun;47(6):859–66.

226. Wendt T, Harja E, Bucciarelli L, Qu W, Lu Y, Rong LL, et al. RAGE modulates vascular inflammation and atherosclerosis in a murine model of type 2 diabetes. Atherosclerosis [Internet]. 2006 Mar;185(1):70–7.

227. Huijberts MS, Wolffenbuttel BH, Boudier HA, Crijns FR, Kruseman AC, Poitevin P, et al. Aminoguanidine treatment increases elasticity and decreases fluid filtration of large arteries from diabetic rats. J Clin Invest [Internet]. 1993 Sep;92(3):1407–11.

228. Zhang M, Kho AL, Anilkumar N, Chibber R, Pagano PJ, Shah AM, et al. Glycated Proteins Stimulate Reactive Oxygen Species Production in Cardiac

Myocytes. Circulation [Internet]. 2006 Mar 7;113(9):1235–43.

229. Beisswenger PJ, Howell SK, Nelson RG, Mauer M, Szwergold BS. Alpha-oxoaldehyde metabolism and diabetic complications. Biochem Soc Trans [Internet]. 2003 Dec;31(Pt 6):1358–63.

230. Rosca MG, Mustata TG, Kinter MT, Ozdemir AM, Kern TS, Szweda LI, et al. Glycation of mitochondrial proteins from diabetic rat kidney is associated with excess superoxide formation. Am J Physiol Physiol [Internet]. 2005 Aug;289(2):F420–30.

231. Rosca MG, Monnier VM, Szweda LI, Weiss MF. Alterations in renal mitochondrial respiration in response to the reactive oxoaldehyde methylglyoxal. Am J Physiol Physiol [Internet]. 2002 Jul;283(1):F52–9.

232. Chen YQ, Su M, Walia RR, Hao Q, Covington JW, Vaughan DE. Sp1 sites mediate activation of the plasminogen activator inhibitor-1 promoter by glucose in vascular smooth muscle cells. J Biol Chem [Internet]. 1998 Apr 3;273(14):8225–31.

233. VAUGHAN DE. PAI-1 and atherothrombosis. J Thromb Haemost. 2005 Aug 1;3(8):1879–83.

234. Inoguchi T, Battan R, Handler E, Sportsman JR, Heath W, King GL. Preferential elevation of protein kinase C isoform beta II and diacylglycerol levels in the aorta and heart of diabetic rats: differential reversibility to glycemic control

by islet cell transplantation. Proc Natl Acad Sci U S A [Internet]. 1992 Nov 15;89(22):11059–63.

235. Ramana K V, Friedrich B, Tammali R, West MB, Bhatnagar A, Srivastava SK. Requirement of aldose reductase for the hyperglycemic activation of protein kinase C and formation of diacylglycerol in vascular smooth muscle cells. Diabetes [Internet]. 2005 Mar 1;54(3):818–29.

236. Shiba T, Inoguchi T, Sportsman JR, Heath WF, Bursell S, King GL. Correlation of diacylglycerol level and protein kinase C activity in rat retina to retinal circulation. Am J Physiol Metab [Internet]. 1993 Nov;265(5):E783–93.

237. Nobe K, Miyatake M, Nobe H, Sakai Y, Takashima J, Momose K. Novel diacylglycerol kinase inhibitor selectively suppressed an U46619-induced enhancement of mouse portal vein contraction under high glucose conditions. Br J Pharmacol [Internet]. 2004 Sep;143(1):166–78.

238. Law B, Fowlkes V, Goldsmith JG, Carver W, Goldsmith EC. Diabetes-induced alterations in the extracellular matrix and their impact on myocardial function. Microsc Microanal [Internet]. 2012 Feb;18(1):22–34.

239. Lu TT, Yan LG, Madri JA. Integrin engagement mediates tyrosine dephosphorylation on platelet-endothelial cell adhesion molecule 1. Proc Natl Acad Sci U S A [Internet]. 1996 Oct 15;93(21):11808–13.

240. Dempsey EC, McMurtry IF, O'Brien RF. Protein kinase C activation allows

pulmonary artery smooth muscle cells to proliferate to hypoxia. Am J Physiol [Internet]. 1991 Feb;260(2 Pt 1):L136-45.

241. Stancakova A, Civelek M, Saleem NK, Soininen P, Kangas AJ, Cederberg H, et al. Hyperglycemia and a Common Variant of GCKR Are Associated With the Levels of Eight Amino Acids in 9,369 Finnish Men. Diabetes [Internet]. 2012 Jul 1;61(7):1895–902.

242. Increased Myocardial Fatty Acid Metabolism in Patients With Type 1 Diabetes Mellitus. J Am Coll Cardiol [Internet]. 2006 Feb 7;47(3):598–604.

243. Visiedo F, Bugatto F, Sánchez V, Cózar-Castellano I, Bartha JL, Perdomo G. High glucose levels reduce fatty acid oxidation and increase triglyceride accumulation in human placenta. Am J Physiol Metab [Internet]. 2013 Jul 15;305(2):E205–12.

244. Larsen PJ, Tennagels N. On ceramides, other sphingolipids and impaired glucose homeostasis. Mol Metab [Internet]. 2014 Jun;3(3):252–60.

245. Galadari S, Rahman A, Pallichankandy S, Galadari A, Thayyullathil F. Role of ceramide in diabetes mellitus: evidence and mechanisms. Lipids Health Dis [Internet]. 2013 Jul 8;12:98.

246. Dudzinska W. Uridine correlates with the concentration of fructosamine and HbA1c in children with type 1 diabetes. Acta Paediatr [Internet]. 2011 May;100(5):712–6.

247. Cory JG, Sato A. Regulation of ribonucleotide reductase activity in mammalian cells. Mol Cell Biochem [Internet]. 1983;53–54(1–2):257–66.

248. Tuder RM, Davis LA, Graham BB. Targeting energetic metabolism: a new frontier in the pathogenesis and treatment of pulmonary hypertension. Am J Respir Crit Care Med [Internet]. 2012 Feb 1;185(3):260–6.

249. Rhodes CJ, Ghataorhe P, Wharton J, Rue-Albrecht KC, Hadinnapola C, Watson G, et al. Plasma Metabolomics Implicates Modified Transfer RNAs and Altered Bioenergetics in the Outcomes of Pulmonary Arterial Hypertension. Circulation [Internet]. 2017 Jan 31;135(5):460–75.

250. Abdelsalam A, Del Priore L, Zarbin MA. Drusen in age-related macular degeneration: pathogenesis, natural course, and laser photocoagulation-induced regression. Surv Ophthalmol [Internet]. 44(1):1–29.

251. Curcio CA, Presley JB, Malek G, Medeiros NE, Avery D V., Kruth HS. Esterified and unesterified cholesterol in drusen and basal deposits of eyes with age-related maculopathy. Exp Eye Res [Internet]. 2005 Dec;81(6):731–41.

252. Storti F, Raphael G, Griesser V, Klee K, Drawnel F, Willburger C, et al. Regulated efflux of photoreceptor outer segment-derived cholesterol by human RPE cells. Exp Eye Res [Internet]. 2017 Dec;165:65–77.

253. Biswas L, Zhou X, Dhillon B, Graham A, Shu X. Retinal pigment epithelium cholesterol efflux mediated by the 18 kDa translocator protein, TSPO, a

potential target for treating age-related macular degeneration. Hum Mol Genet [Internet]. 2017 Nov 15;26(22):4327–39.

254. Sheraidah G, Steinmetz R, Maguire J, Pauleikhoff D, Marshall J, Bird AC. Correlation between lipids extracted from Bruch's membrane and age. Ophthalmology [Internet]. 1993 Jan;100(1):47–51.

255. Spaide RF, Ho-Spaide WC, Browne RW, Armstrong D. Characterization of peroxidized lipids in Bruch's membrane. Retina [Internet]. 1999;19(2):141–7.

256. Holz FG, Sheraidah G, Pauleikhoff D, Bird AC. Analysis of lipid deposits extracted from human macular and peripheral Bruch's membrane. Arch Ophthalmol (Chicago, Ill 1960) [Internet]. 1994 Mar;112(3):402–6.

257. Bonsack F, Sukumari-Ramesh S. TSPO: An Evolutionarily Conserved Protein with Elusive Functions. Int J Mol Sci [Internet]. 2018 Jun 7;19(6).

258. Karamichos D, Zieske JD, Sejersen H, Sarker-Nag A, Asara JM, Hjortdal J. Tear metabolite changes in keratoconus. Exp Eye Res [Internet]. 2015 Mar 1;132:1–8.

259. Li M, Li H, Jiang P, Liu X, Xu D, Wang F. Investigating the pathological processes of rhegmatogenous retinal detachment and proliferative vitreoretinopathy with metabolomics analysis. Mol Biosyst [Internet]. 2014 Apr 1;10(5):1055.

260. Li X, Luo X, Lu X, Duan J, Xu G. Metabolomics study of diabetic retinopathy

using gas chromatography–mass spectrometry: a comparison of stages and subtypes diagnosed by Western and Chinese medicine. Mol Biosyst [Internet]. 2011 Jan 7;7(7):2228.

261. Chen L, Cheng C-Y, Choi H, Ikram MK, Sabanayagam C, Tan GSW, et al. Plasma Metabonomic Profiling of Diabetic Retinopathy. Diabetes [Internet]. 2016 Apr 1;65(4):1099–108.

262. Guo J, Yan T, Bi H, Xie X, Wang X, Guo D, et al. Plasma metabonomics study of the patients with acute anterior uveitis based on ultra-performance liquid chromatography–mass spectrometry. Graefe's Arch Clin Exp Ophthalmol [Internet]. 2014 Jun 8;252(6):925–34.

263. Howe C, Alshehri A, Muggeridge D, Mullen A, Boyd M, Spendiff O, et al. Untargeted Metabolomics Profiling of an 80.5 km Simulated Treadmill Ultramarathon. Metabolites [Internet]. 2018 Feb 13;8(1):14.

264. Miyamura N, Ogawa T, Boylan S, Morse LS, Handa JT, Hjelmeland LM. Topographic and age-dependent expression of heme oxygenase-1 and catalase in the human retinal pigment epithelium. Invest Ophthalmol Vis Sci [Internet]. 2004 May;45(5):1562–5.

265. Wyss M, Kaddurah-Daouk R. Creatine and Creatinine Metabolism. Physiol Rev [Internet]. 2000 Jul;80(3):1107–213.

266. Winkler BS, Arnold MJ, Brassell MA, Puro DG. Energy metabolism in human

retinal Müller cells. Invest Ophthalmol Vis Sci [Internet]. 2000 Sep;41(10):3183–90.

267. Kurihara T, Westenskow PD, Gantner ML, Usui Y, Schultz A, Bravo S, et al. Hypoxia-induced metabolic stress in retinal pigment epithelial cells is sufficient to induce photoreceptor degeneration. Elife [Internet]. 2016 Mar 15;5.

268. Rohrer B, Bandyopadhyay M, Beeson C. Reduced Metabolic Capacity in Aged Primary Retinal Pigment Epithelium (RPE) is Correlated with Increased Susceptibility to Oxidative Stress. In: Advances in experimental medicine and biology [Internet]. 2016. p. 793–8.

269. Tu LN, Zhao AH, Hussein M, Stocco DM, Selvaraj V. Translocator Protein (TSPO) Affects Mitochondrial Fatty Acid Oxidation in Steroidogenic Cells. Endocrinology [Internet]. 2016 Mar;157(3):1110–21.

270. Farooqui AA, Ong W-Y, Horrocks LA. Plasmalogens, Docosahexaenoic Acid and Neurological Disorders. In Springer, Boston, MA; 2003. p. 335–54.

271. Hoffman DR, Uauy R, Birch DG. Metabolism of omega-3 fatty acids in patients with autosomal dominant retinitis pigmentosa. Exp Eye Res [Internet]. 1995 Mar;60(3):279–89.

272. Krohne TU, Stratmann NK, Kopitz J, Holz FG. Effects of lipid peroxidation products on lipofuscinogenesis and autophagy in human retinal pigment

epithelial cells. Exp Eye Res [Internet]. 2010 Mar;90(3):465–71.

273. Farooqui AA, Horrocks LA, Farooqui T. Interactions between neural membrane glycerophospholipid and sphingolipid mediators: A recipe for neural cell survival or suicide. J Neurosci Res [Internet]. 2007 Jul 1;85(9):1834–50.

274. Fliesler SJ, Bretillon L. The ins and outs of cholesterol in the vertebrate retina. J Lipid Res [Internet]. 2010 Dec;51(12):3399–413.

275. Rodríguez IR, Larrayoz IM. Cholesterol oxidation in the retina: implications of 7KCh formation in chronic inflammation and age-related macular degeneration. J Lipid Res [Internet]. 2010 Oct 1;51(10):2847–62.

276. Kopitz J, Holz FG, Kaemmerer E, Schutt F. Lipids and lipid peroxidation products in the pathogenesis of age-related macular degeneration. Biochimie [Internet]. 2004 Nov;86(11):825–31.

277. Kaemmerer E, Schutt F, Krohne TU, Holz FG, Kopitz J. Effects of Lipid Peroxidation-Related Protein Modifications on RPE Lysosomal Functions and POS Phagocytosis. Investig Opthalmology Vis Sci [Internet]. 2007 Mar 1;48(3):1342.

278. Krohne TU, Holz FG, Kopitz J. Apical-to-Basolateral Transcytosis of Photoreceptor Outer Segments Induced by Lipid Peroxidation Products in Human Retinal Pigment Epithelial Cells. Investig Opthalmology Vis Sci

[Internet]. 2010 Jan 1;51(1):553.

279. Suzuki M, Kamei M, Itabe H, Yoneda K, Bando H, Kume N, et al. Oxidized phospholipids in the macula increase with age and in eyes with age-related macular degeneration. Mol Vis [Internet]. 2007 May 23;13:772–8.

280. Suzuki M, Tsujikawa M, Itabe H, Du Z-J, Xie P, Matsumura N, et al. Chronic photo-oxidative stress and subsequent MCP-1 activation as causative factors for age-related macular degeneration. J Cell Sci [Internet]. 2012 May 15;125(10):2407–15.

281. Sanvicens N, Cotter TG. Ceramide is the key mediator of oxidative stress-induced apoptosis in retinal photoreceptor cells. J Neurochem [Internet]. 2006 Sep;98(5):1432–44.

282. Laíns I, Kelly RS, Miller JB, Silva R, Vavvas DG, Kim IK, et al. Human Plasma Metabolomics Study across All Stages of Age-Related Macular Degeneration Identifies Potential Lipid Biomarkers. Ophthalmology [Internet]. 2018 Feb;125(2):245–54.

283. Steinberg RH. Interactions between the retinal pigment epithelium and the neural retina. Doc Ophthalmol [Internet]. 1985 Oct;60(4):327–46.

284. Farnoodian M, Halbach C, Slinger C, Pattnaik BR, Sorenson CM, Sheibani N. High glucose promotes the migration of retinal pigment epithelial cells through increased oxidative stress and PEDF expression. Am J Physiol Cell

Physiol [Internet]. 2016;311(3):C418-36.

285. Al-Hussaini H, Kilarkaje N. Effects of diabetes on retinal pigment epithelial cell proliferation and mitogen-activated protein kinase signaling in dark Agouti rats. Exp Toxicol Pathol [Internet]. 2015 Feb 1;67(2):117–24.

286. Aiello LP. The Potential Role of PKC β in Diabetic Retinopathy and Macular Edema. Surv Ophthalmol [Internet]. 2002 Dec 1;47:S263–9.

287. Fowler MJ. Microvascular and Macrovascular Complications of Diabetes. Clin Diabetes [Internet]. 2008 Apr 1;26(2):77–82.

288. Masuda T, Shimazawa M, Hara H. Retinal Diseases Associated with Oxidative Stress and the Effects of a Free Radical Scavenger (Edaravone). Oxid Med Cell Longev [Internet]. 2017;2017:9208489.

289. Ferrucci L, Cherubini A, Bandinelli S, Bartali B, Corsi A, Lauretani F, et al. Relationship of Plasma Polyunsaturated Fatty Acids to Circulating Inflammatory Markers. J Clin Endocrinol Metab [Internet]. 2006 Feb;91(2):439–46.

290. Ilkan Z, Akar FG. The Mitochondrial Translocator Protein and the Emerging Link Between Oxidative Stress and Arrhythmias in the Diabetic Heart. Front Physiol [Internet]. 2018;9:1518.

291. Li J, Papadopoulos V. Translocator protein (18kDa) as a pharmacological target in adipocytes to regulate glucose homeostasis. Biochem Pharmacol

[Internet]. 2015 Sep 1;97(1):99–110.

292. Feldman EL. Oxidative stress and diabetic neuropathy: a new understanding of an old problem. J Clin Invest [Internet]. 2003 Feb 15;111(4):431–3.

293. Wu Y, Tang L, Chen B. Oxidative Stress: Implications for the Development of Diabetic Retinopathy and Antioxidant Therapeutic Perspectives. Oxid Med Cell Longev [Internet]. 2014;2014:1–12.

294. Steinmetz PR, Balko C, Gabbay KH. The Sorbitol Pathway and the Complications of Diabetes. N Engl J Med [Internet]. 1973 Apr 19;288(16):831–6.

295. Oates PJ. Polyol pathway and diabetic peripheral neuropathy. Int Rev Neurobiol [Internet]. 2002;50:325–92.

296. Beisswenger PJ, Howell SK, Smith K, Szwergold BS. Glyceraldehyde-3-phosphate dehydrogenase activity as an independent modifier of methylglyoxal levels in diabetes. Biochim Biophys Acta [Internet]. 2003 Jan 20;1637(1):98–106.

297. Semba RD, Huang H, Lutty GA, Van Eyk JE, Hart GW. The role of O-GlcNAc signaling in the pathogenesis of diabetic retinopathy. Proteomics Clin Appl. 2014 Apr;8(3–4):218–31.

298. Costa G, Pereira T, Neto AM, Cristóvão AJ, Ambrósio AF, Santos PF. High glucose changes extracellular adenosine triphosphate levels in rat retinal

cultures. J Neurosci Res [Internet]. 2009 May 1;87(6):1375–80.

299. Xia J, Wang Z, Zhang F. Association between Related Purine Metabolites and Diabetic Retinopathy in Type 2 Diabetic Patients. Int J Endocrinol [Internet]. 2014;2014:651050.

300. Vindeirinho J, Costa GN, Correia MB, Cavadas C, Santos PF. Effect of Diabetes/Hyperglycemia on the Rat Retinal Adenosinergic System. Chidlow G, editor. PLoS One [Internet]. 2013 Jun 28;8(6):e67499.

301. Busik J V, Esselman WJ, Reid GE. Examining the role of lipid mediators in diabetic retinopathy. Clin Lipidol [Internet]. 2012 Dec 1;7(6):661–75.

302. Tikhonenko M, Lydic TA, Wang Y, Chen W, Opreanu M, Sochacki A, et al. Remodeling of Retinal Fatty Acids in an Animal Model of Diabetes: A Decrease in Long-Chain Polyunsaturated Fatty Acids Is Associated With a Decrease in Fatty Acid Elongases Elovl2 and Elovl4. Diabetes [Internet]. 2010 Jan 1;59(1):219–27.

303. Desjardins DM, Yates PW, Dahrouj M, Liu Y, Crosson CE, Ablonczy Z. Progressive Early Breakdown of Retinal Pigment Epithelium Function in Hyperglycemic Rats. Investig Opthalmology Vis Sci [Internet]. 2016 May 18;57(6):2706.

304. Diker-Cohen T, Koren R, Ravid A. Programmed cell death of stressed keratinocytes and its inhibition by vitamin D: The role of death and survival

signaling pathways. Apoptosis [Internet]. 2006 Apr 9;11(4):519–34.

305. Wang H, Hartnett ME. Regulation of signaling events involved in the pathophysiology of neovascular AMD. Mol Vis [Internet]. 2016;22:189–202.

306. Grinnan D, Farr G, Fox A, Sweeney L. The Role of Hyperglycemia and Insulin Resistance in the Development and Progression of Pulmonary Arterial Hypertension. J Diabetes Res [Internet]. 2016;2016:1–7.

307. Hwang NR, Yim S-H, Kim YM, Jeong J, Song EJ, Lee Y, et al. Oxidative modifications of glyceraldehyde-3-phosphate dehydrogenase play a key role in its multiple cellular functions. Biochem J [Internet]. 2009 Sep 25;423(2):253–64.

308. Gupte SA. Targeting the Pentose Phosphate Pathway in Syndrome X-related Cardiovascular Complications. Drug Dev Res [Internet]. 2010 May 1;71(3):161–7.

10 Appendices

10.1 Chapter 3

The diagram below illustrates the steps of data filtration

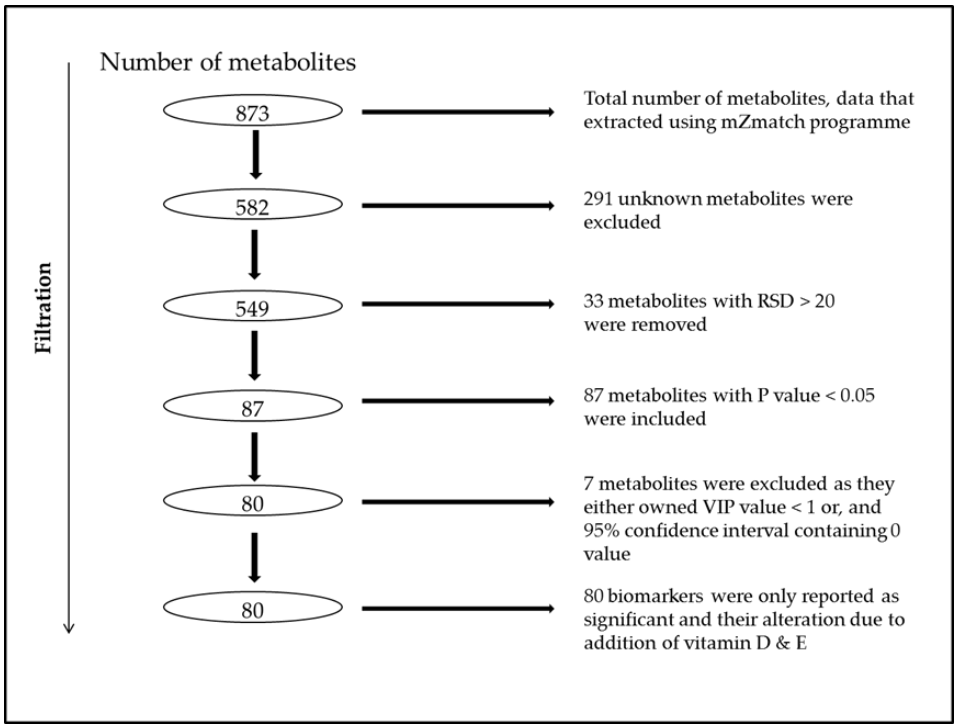

Figure S1: data filtration steps.

Table S1: metabolites differences of PASMCs among different pathways including amino acids, glycolysis, lipids and nucleotides.

Mass	RT	Met name	-/+	25mM/ 5mM glucose		Vit. D/25 mM glucose		Vit. E/25mM glucose	
				P.value	ratio	P.value	Ratio	P.value	ratio
Glutathione homeostasis									
230.019	16.7	Xylulose 5-phosphate *	-	<0.001	2.041	<0.001	0.520	0.153	0.726
232.035	16.4	Ribitol 5-phosphate	-	0.017	1.666	0.007	0.393	0.032	0.444
307.084	14.5	Glutathione	-	0.003	0.801	0.010	1.277	0.023	1.495
335.079	14.5	S-Formyl glutathione	+	0.007	1.290	<0.001	0.234	0.020	0.217
744.076	17.6	NADP+	-	0.031	0.719	0.216	1.156	0.719	1.122
745.085	18.4	NADPH	-	0.532	0.819	0.044	0.323	0.134	0.604
612.152	17.5	Glutathione disulphide *	-	0.025	1.417	0.011	0.606	0.965	1.044
Purines and pyrimidines									
111.043	10.4	Cytosine	-	0.206	1.084	0.004	0.635	0.006	0.679
136.038	10.2	Hypoxanthine *	+	0.009	1.221	<0.001	8.943	0.002	8.221
151.049	11.8	Guanine *	+	0.046	1.675	0.061	0.095	0.005	0.367
152.033	12.0	Xanthine *	-	0.473	1.374	0.603	1.209	0.625	1.225
158.044	14.7	Allantoin	-	0.033	0.535	0.099	0.460	0.132	0.542
168.028	13.6	Urate	-	0.979	0.992	0.127	0.396	0.168	0.502
244.070	9.9	Uridine *	-	0.002	1.584	<0.001	0.297	0.004	0.269
244.070	12.2	Pseudouridine	-	0.017	1.381	<0.001	0.337	0.279	0.408
268.081	11.0	inosine	+	0.154	0.381	0.083	4.940	0.173	8.201
324.036	17.4	UMP *	-	0.033	1.580	0.002	0.498	0.004	0.593
332.053	15.4	2'-Deoxyinosine 5'-monophosphate	+	0.032	0.598	0.138	1.422	0.300	1.244
347.063	14.3	AMP *	-	0.808	1.019	0.001	0.560	0.074	0.681

348.047	16.2	IMP	-	0.794	0.861	0.861	0.906	0.722	1.201
403.018	18.3	CDP	-	0.836	1.013	0.001	0.592	0.319	0.777
427.029	16.2	ADP *	+	0.699	1.039	0.009	0.718	0.457	0.828
482.985	21.1	CTP	-	0.161	0.894	0.002	0.447	0.089	0.580
483.969	20.2	UTP	-	0.310	0.870	<0.001	0.339	0.005	0.380
506.996	17.1	ATP *	+	0.010	0.858	<0.001	0.476	0.094	0.593
488.108	15.8	CDP-choline	-	0.014	0.694	0.623	1.035	0.151	1.381
537.076	17.6	CDP-ribitol	-	0.009	1.944	0.291	0.429	0.072	0.687
Glucose metabolism									
90.032	10.4	(R)-Lactate	-	0.304	1.384	0.004	0.459	0.087	0.581
87.010	8.8	Pyruvate *	-	0.098	1.076	0.431	0.971	0.351	1.147
116.011	15.8	Fumarate *	-	0.023	1.286	<0.001	0.303	0.009	0.429
118.027	16.4	Succinate *	-	0.339	1.191	0.278	0.708	0.496	0.754
134.022	17.4	(S)-Malate *	-	0.034	1.171	0.015	0.660	0.019	0.763
169.989	16.3	DL-Glyceraldehyde 3-phosphate	-	0.022	5.157	0.397	0.911	0.657	0.889
169.989	17.3	Dihydroxyacetone phosphate	-	0.001	4.408	0.018	0.816	0.199	0.686
192.019	19.6	Citrate *	-	0.018	0.763	0.272	0.077	0.534	0.006
196.058	14.4	Gluconic acid	-	0.005	1.364	<0.001	0.199	<0.001	0.267
260.030	17.8	Glucose 6-phosphate*	-	0.004	1.230	0.158	0.738	0.279	0.783
260.030	16.8	Glucose 1-phosphate *	-	0.041	2.055	0.017	0.686	0.204	0.792
260.030	17.2	Fructose 6-phosphate*	-	0.009	2.37	0.012	0.81	0.077	1.08
289.033	17.2	Sedoheptulose 7-phosphate	-	0.040	2.119	0.896	0.992	0.671	1.098
318.030	16.4	Octulose 8-phosphate	-	<0.001	1.229	0.008	0.261	0.052	0.436
566.055	17.4	UDP-glucose	-	0.012	1.312	<0.001	0.507	0.056	0.693
580.035	20.7	UDP-glucoronate	-	0.082	1.170	<0.001	0.443	0.028	0.502

663.109	14.4	NAD+ *	-	0.151	1.005	<0.001	0.571	0.636	0.044
665.125	14.1	NADH *	-	0.016	1.177	0.021	0.818	0.385	0.851
666.222	18.0	Maltotetraose (Cellotetraose)	-	<0.001	4.581	0.035	0.824	0.622	0.938
809.120	13.0	Acetyl-CoA *	-	0.165	1.127	0.284	0.702	0.604	0.840
828.275	18.5	Maltopentaose	-	0.053	6.750	0.775	0.979	0.662	1.148
320.051	17.5	Octulose 8-phosphate	-	<0.001	4.441	0.008	1.607	0.152	1.719
350.062	17.7	Nonulose 9-phosphate	-	<0.001	893.963	0.053	1.279	0.097	1.620
Fatty acids and Lipids									
101.024	13.3	Acetoacetate *	+	0.007	1.266	0.228	0.924	0.410	0.868
214.193	3.8	[FA (13:0)] tridecanoic acid	-	0.040	0.805	0.013	1.994	0.021	1.764
216.136	7.4	[FA (11:0/2:0)] Undecane dioic acid	-	0.003	0.778	0.074	0.901	0.077	0.894
228.209	3.7	Tetra decanoic acid	-	0.017	0.587	0.016	1.751	0.029	1.809
238.157	3.8	7-Oxo-11E,13-Tetradecadienoic acid	-	0.040	1.291	0.482	0.935	0.761	0.973
242.225	3.7	Pentadecanoic acid	-	0.049	0.673	0.018	1.880	0.046	1.739
256.240	3.7	Hexadecanoic acid	-	0.009	0.773	0.143	1.563	0.016	2.111
270.256	3.7	[FA (17:0)] heptadecanoic acid	-	0.023	0.581	0.005	1.712	0.039	1.941
280.240	3.7	Linoleic acid	-	0.474	1.132	0.024	1.749	0.064	1.843
284.272	3.7	Octadecanoic acid	-	0.021	0.682	0.213	1.547	0.040	2.016
298.287	3.6	Nonadecanoic acid	-	0.005	0.714	0.005	1.727	0.026	2.154
308.272	3.7	Eicosadienoic acid	-	0.911	1.011	0.014	1.630	0.042	1.803
312.303	3.6	Phytanic acid	-	0.002	0.666	0.029	1.682	0.035	1.918
332.272	3.6	Docosatetraenoic acid	-	0.009	1.330	<0.001	4.742	0.001	5.234
334.287	3.7	13,16,19-Docosatrienoic acid	-	0.356	1.174	0.001	2.165	0.023	2.771
340.334	3.6	Docosanoic acid	-	0.005	0.686	0.038	1.632	0.145	1.220
366.350	3.6	Nervonic acid	-	0.032	0.774	0.011	0.779	0.169	0.739

767.115	7.5	CoA	-	0.007	0.762	0.154	0.744	0.263	0.725
410.243	4.3	PA(16:0/0:0)	-	0.047	0.871	0.005	0.788	0.197	0.797
436.259	4.2	LysoPA(18:1(9Z)/0:0)	-	0.015	0.828	<0.001	0.584	0.022	0.590
453.285	4.2	LysoPE(0:0/16:0)	+	0.035	0.747	0.010	0.481	0.029	0.585
479.301	4.2	LysoPE(0:0/18:1(11Z))	-	0.004	0.739	<0.001	0.329	<0.001	0.370
497.275	4.0	PS(16:0/0:0)	-	0.003	0.713	0.096	0.868	0.330	0.833
523.291	3.9	PS(18:1(9Z)/0:0)	-	0.009	0.861	<0.001	0.335	0.009	0.389
525.307	3.9	PS(18:0/0:0)	-	0.005	0.826	<0.001	0.467	0.016	0.541
545.275	3.9	PS(20:4/0:0)	-	0.015	1.335	0.723	1.037	0.563	1.127
556.280	3.7	PG(22:6(4Z,7Z,10Z,13Z,16Z,19Z)/0:0)	-	0.022	1.206	<0.001	0.402	0.021	0.516
569.276	3.9	PS(22:6(4Z,7Z,10Z,13Z,16Z,19Z)/0:0)	-	0.042	0.753	0.193	0.186	0.004	0.256
572.296	4.0	PI(16:0/0:0)	-	0.012	0.852	<0.001	0.262	0.001	0.271
596.296	4.0	PI(18:2(9Z,12Z)/0:0)	-	0.037	0.754	0.001	0.412	0.021	0.369
600.328	4.0	LPI(18:0/0:0)	-	0.047	0.950	<0.001	0.209	0.002	0.223
620.296	4.0	PI(20:4(5Z,8Z,11Z,14Z)/0:0)	-	0.011	0.874	<0.001	0.482	0.032	0.514
698.489	3.8	PA(14:1(9Z)/22:2(13Z,16Z))	-	0.001	0.732	0.001	0.579	<0.001	0.430
700.505	3.7	PA(18:0/18:2(9Z,12Z))	-	0.007	0.769	0.046	0.852	0.001	0.588
720.494	3.5	PG(16:0/16:1(9Z))	-	0.026	1.539	0.044	0.843	0.293	0.809
731.546	3.8	PC(14:0/18:1(11Z))	-	0.897	0.917	0.001	0.429	0.001	0.355
805.561	3.7	PC(16:0/22:6(4Z,7Z,10Z,13Z,16Z,19Z))	-	0.810	1.019	<0.001	0.448	<0.001	0.404
755.546	3.7	PC(14:0/20:3(5Z,8Z,11Z))	-	0.028	0.670	0.078	0.143	0.082	0.160
779.546	3.8	PC(14:0/22:5(4Z,7Z,10Z,13Z,16Z))	-	0.659	1.064	0.001	0.394	0.001	0.404
783.505	3.5	PS(16:0/20:4(5Z,8Z,11Z,14Z))	-	0.041	1.308	0.007	1.586	0.133	1.176
820.526	3.4	PG(18:1(11Z)/22:6(4Z,7Z,10Z,13Z,16Z,19Z))	-	0.001	0.688	<0.001	0.175	<0.001	0.176
846.542	3.4	PG(20:2(11Z,14Z)/22:6(4Z,7Z,10Z,13Z,16Z,19Z))	-	0.021	0.805	0.020	0.810	0.105	0.700

856.510	3.5	PI(14:1(9Z)/22:4(7Z,10Z,13Z,16Z))	-	0.028	0.627	0.289	0.382	0.004	0.382
Carnitines									
231.147	8.4	Isobutyryl-L-carnitine	-	0.956	0.994	<0.001	0.002	<0.001	0.002
245.162	5.2	Isovalerylcarnitine	-	0.217	1.012	<0.001	0.001	<0.001	0.001
397.319	4.3	trans-Hexadec-2-enoylcarnitine	+	0.036	1.336	0.017	0.687	0.143	0.828
413.314	4.5	3-Hydroxy-9-hexadecenoylcarnitine	+	0.374	0.003	<0.001	1654	<0.001	1637
425.350	4.3	Oleoylcarnitine	+	0.018	1.283	0.006	0.500	0.023	0.547
Amino acids									
103.063	15.7	4-Aminobutanoate	+	0.030	1.194	0.001	1.410	0.038	1.635
117.079	12.2	5-Aminopentanoate	+	0.015	1.213	<0.001	0.271	0.004	0.339
146.106	25.2	Lysine*	+	0.044	1.133	0.091	0.866	<0.001	0.412
218.127	14.4	N2-(D-1-Carboxyethyl)-L-lysine	+	0.002	1.535	<0.001	0.240	0.005	0.336
119.058	15.0	L-Threonine	-	0.626	1.085	0.009	0.556	0.049	0.591
125.014	15.9	Taurine	-	0.058	1.107	<0.001	0.227	0.002	0.276
132.053	15.9	L-Asparagine	+	0.074	0.798	<0.001	0.216	0.001	0.240
132.090	23.8	D-Ornithine	+	0.549	0.988	0.021	0.365	0.026	0.379
133.037	15.8	Aspartate *	-	0.007	0.707	<0.001	0.289	0.004	0.374
147.050	15.4	Glutamate	-	0.024	1.453	0.078	0.83	0.154	1.10
89.047	15.2	L-Alanine	-	0.482	1.108	<0.001	0.258	0.001	0.279
204.090	11.8	L-Tryptophan*	-	0.008	1.152	0.059	0.852	0.112	0.471
174.112	26.6	L-arginine	-	0.035	1.141	0.020	0.861	0.002	0.723
115.063	12.9	L-proline	+	0.001	1.212	0.036	0.936	0.131	1.052
161.069	15.6	N-Methyl-L-glutamate	+	0.021	1.182	<0.001	0.390	0.004	0.386
131.069	14.9	Creatine	-	0.925	0.965	0.001	0.374	0.005	0.488
175.100	16.1	L-Citrulline*	-	<0.001	0.832	0.011	0.87	0.002	0.55

155.070	15.8	L-Histidine*	-	0.004	0.774	0.632	0.94	0.087	0.71

(*) means that metabolite matches standard retention time

10.2 Chapter 4

Table S2: metabolic different between HHG and NHG

Mass	RT	Metabolite name	HHG/NHG	
			p-value	ratio
Miscellaneous				
245.16	5.2	Isovalerylcarnitine	0.026	1.55
201.17	7.7	Caproylcholine	0.006	1.48
93.06	25.9	N-Methylpyridinium	0.047	1.22
256.11	7.3	Xenognosin A	0.009	1.22
125.05	9.4	N-Ethylmaleimide	0.025	1.12
130.07	15.1	Casein K	0.016	0.68
130.07	12.7	(R)-piperazine-2-carboxylate	0.004	0.60
309.11	14.1	O-Acetylneuraminic acid	0.030	0.38
Amino acids				
133.04	15.9	Aspartate	<0.001	0.70
132.05	15.9	Asparagine	0.036	0.78
123.99	15.2	Phosphonoacetaldehyde	0.012	0.49
129.04	10.8	4-Oxoproline	0.045	0.45
113.06	9.6	Creatinine	0.039	0.39
113.05	10.2	1-Pyrroline-2-carboxylate	<0.001	0.28
115.06	12.9	Proline	0.010	0.77
174.11	26.9	Arginine	0.046	0.44
132.09	23.8	Ornithine	0.036	0.40
307.08	4.6	Glutathione	0.030	1.41
612.15	17.5	Glutathione disulphide	<0.001	2.23
117.05	16.2	Guanidinoacetate	0.021	0.51
105.04	16.4	Serine	0.036	0.66
119.06	15.0	Threonine	0.018	0.60
144.09	13.4	isoglutamine	0.044	0.80
258.09	10.8	(1-Ribosylimidazole)-4-acetate	0.028	0.17
129.08	12.7	Pipecolate	0.017	0.63
193.07	4.6	Phenylacetylglycine	0.015	0.42
205.07	8.3	Indole lactate	0.030	0.44
176.09	13.4	Serotonin	0.023	0.43
208.08	10.8	Kynurenine	0.011	0.42
117.06	10.2	Indole	0.014	0.41
204.09	11.8	Tryptophan	0.016	0.50
181.07	13.4	Tyrosine	0.040	0.48
131.09	10.8	Leucine	0.033	0.45

131.09	11.3	Isoleucine	0.038	0.49
117.08	12.7	Valine	0.022	0.41
Glycolysis				
255.71	7.5	CoA	0.015	1.94
260.03	17.9	Glucose 1-phosphate	0.047	0.65
196.06	14.5	Mannonate	0.047	1.44
230.02	16.7	Xylulose 5-phosphate	0.014	0.77
342.12	16.4	Cellobiose	0.022	1.94
335.08	14.6	S-Formylglutathione	0.007	1.42
743.08	17.6	NADP+	0.001	0.64
Fatty acids and lipids				
450.33	4.0	3alpha,7alpha,12alpha-Trihydroxy-5beta-cholestanoate	0.027	0.74
499.30	4.1	Taurodeoxycholate	0.021	0.45
449.31	4.3	Chenodeoxyglycocholate	0.009	0.43
515.29	4.4	Taurocholate	0.018	0.40
216.04	14.9	2-C-Methyl-D-erythritol 4-phosphate	0.043	0.48
779.53	3.9	MIPC-assay	0.004	0.76
254.22	3.8	(9Z)-Hexadecenoic acid	0.035	0.73
240.25	3.9	Hexadecanal	0.009	1.34
332.27	3.7	[FA (22:4)] 7Z,10Z,13Z,16Z-docosatetraenoic acid	0.004	1.47
216.14	7.5	[FA (11:0/2:0)] Undecanedioic acid	0.001	1.37
296.27	7.4	18:1(13Z)(17Me)	0.037	1.31
384.36	3.6	Mycolipanolic acid (C24)	0.002	1.26
244.20	3.8	2S-Hydroxytetradecanoic acid	0.025	0.74
240.21	3.8	[FA dimethyl(13:0)] 2,5-dimethyl-2E-tridecenoic acid	0.006	0.73
240.17	3.9	7-oxo-11E-Tetradecenoic acid	0.027	0.72
242.19	3.8	[FA oxo(14:0)] 3-oxo-tetradecanoic acid	0.017	0.71
296.24	3.8	(9Z,12Z)-(8S)-Hydroxyoctadeca-9,12-dienoic acid	0.016	0.67
214.16	4.0	3-Oxododecanoic acid	0.020	0.64
216.17	4.0	12-Hydroxydodecanoic acid	0.019	0.57
389.26	3.7	[FA (18:0)] N-(9Z-octadecenoyl)-taurine	0.006	0.49
356.05	7.5	2-Hydroxy-1,3-dimethoxy-8,9-methylenedioxycoumestan	0.042	0.38
672.47	3.8	[GP (16:0/18:2)] 1-hexadecanoyl-2-(9Z,12Z-octadecadienoyl)-sn-glycero-3-phosphate	0.004	0.80
646.46	3.8	[GP (14:0/18:1)] 1-tetradecanoyl-2-(9Z-octadecenoyl)-sn-glycero-3-phosphate	0.002	0.78
644.44	3.8	PA(12:0/20:2(11Z,14Z))	0.037	0.69
698.49	3.8	PA(14:1(9Z)/22:2(13Z,16Z))	<0.001	0.69
479.34	7.4	[PC (16:1)] 1-(11Z-hexadecenyl)-sn-glycero-3-phosphocholine	0.003	1.80
809.59	4.2	[PC (16:0/22:4)] 1-hexadecanoyl-2-(7Z,10Z,13Z,16Z-	0.041	1.73

		docosatetraenoyl)-sn-glycero-3-phosphocholine		
857.59	3.7	PC(20:2(11Z,14Z)/22:6(4Z,7Z,10Z,13Z,16Z,19Z))	0.014	1.70
765.57	3.7	PC(18:3(6Z,9Z,12Z)/P-18:1(11Z))	0.003	1.54
795.58	3.7	PC(15:0/22:4(7Z,10Z,13Z,16Z))	0.016	1.25
481.35	4.4	[PC (16:2)] 1-hexadecyl-sn-glycero-3-phosphocholine	0.016	1.23
465.32	4.2	[PC (15:1)] 1-(1Z-pentadecenyl)-sn-glycero-3-phosphocholine	0.014	1.16
451.31	4.3	[PC (14:1)] 1-(1E-tetradecenyl)-sn-glycero-3-phosphocholine	0.030	1.15
493.32	4.2	LysoPC(16:1(9Z))	0.023	0.89
467.30	4.4	[PC (14:0)] 1-tetradecanoyl-sn-glycero-3-phosphocholine	0.029	0.75
481.32	4.3	[PC (15:0)] 1-pentadecanoyl-sn-glycero-3-phosphocholine	0.008	0.75
751.55	3.7	[PE (18:1/20:4)] 1-(1Z-octadecenyl)-2-(5Z,8Z,11Z,14Z-eicosatetraenoyl)-sn-glycero-3-phosphoethanolamine	0.014	1.54
751.55	4.4	PE(20:3(5Z,8Z,11Z)/P-18:1(11Z))	0.042	1.53
723.52	4.4	PE(18:3(6Z,9Z,12Z)/P-18:1(9Z))	0.039	1.48
723.52	3.7	PE(18:3(6Z,9Z,12Z)/P-18:1(11Z))	0.017	1.38
749.54	3.7	PE(20:4(5Z,8Z,11Z,14Z)/P-18:1(11Z))	0.018	1.30
501.29	7.4	LysoPE(0:0/20:4(8Z,11Z,14Z,17Z))	0.039	1.12
437.29	4.3	[PE (16:1)] 1-(1Z-hexadecenyl)-sn-glycero-3-phosphoethanolamine	0.048	1.10
527.30	4.2	LysoPE(0:0/22:5(4Z,7Z,10Z,13Z,16Z))	0.004	0.88
479.30	4.3	LysoPE(0:0/18:1(11Z))	0.002	0.77
481.32	7.4	LysoPE(0:0/18:0)	0.007	0.76
453.28	4.2	LysoPE(0:0/16:0)	0.027	0.75
503.30	4.2	LysoPE(0:0/20:3(11Z,14Z,17Z))	0.022	0.71
715.52	3.8	PE(14:0/20:2(11Z,14Z))	0.026	0.69
451.27	4.4	LysoPE(0:0/16:1(9Z))	0.004	0.68
499.27	4.3	LysoPE(0:0/20:5(5Z,8Z,11Z,14Z,17Z))	0.032	0.66
763.52	3.7	[PE (16:0/22:6)] 1-hexadecanoyl-2-(4Z,7Z,10Z,13Z,16Z,19Z-docosahexaenoyl)-sn-glycero-3-phosphoethanolamine	0.002	0.66
737.50	3.7	PE(14:0/22:5(4Z,7Z,10Z,13Z,16Z))	<0.001	0.53
706.52	3.5	PG(O-16:0/16:1(9Z))	0.024	2.13
870.54	3.5	PG(22:6(4Z,7Z,10Z,13Z,16Z,19Z)/22:4(7Z,10Z,13Z,16Z))	0.046	1.22
842.51	3.5	PG(20:4(5Z,8Z,11Z,14Z)/22:6(4Z,7Z,10Z,13Z,16Z,19Z))	0.040	1.20
510.30	3.7	[PG (18:1)] 1-(9E-octadecenoyl)-sn-glycero-3-phospho-(1'-sn-glycerol)	<0.001	0.73
884.54	3.6	PI(16:0/22:5(4Z,7Z,10Z,13Z,16Z))	0.050	0.78
600.33	4.0	[PI (18:0)] 1-octadecanoyl-sn-glycero-3-phospho-(1'-myo-inositol)	0.004	0.77

620.30	4.0	[PI (20:4)] 1-(5Z,8Z,11Z,14Z-eicosatetraenoyl)-sn-glycero-3-phospho-(1'-myo-inositol)	0.004	0.76
808.51	3.6	PI(16:0/16:1(9Z))	0.022	0.71
596.30	4.0	PI(18:2(9Z,12Z)/0:0)	0.002	0.60
586.31	4.0	PI(17:0/0:0)	0.004	0.58
572.30	4.1	[PI (16:0)] 1-hexadecanoyl-sn-glycero-3-phospho-(1'-myo-inositol)	<0.001	0.56
644.30	4.0	PI(22:6(4Z,7Z,10Z,13Z,16Z,19Z)/0:0)	0.019	0.49
488.11	15.8	CDP-choline	0.008	1.65
105.08	11.1	Diethanolamine	0.002	0.60
257.10	14.5	sn-glycero-3-Phosphocholine	0.002	1.71
811.54	4.8	PS(18:0/20:4(5Z,8Z,11Z,14Z))	0.025	1.86
811.54	3.6	[PS (18:0/20:4)] 1-octadecanoyl-2-(5Z,8Z,11Z,14Z-eicosatetraenoyl)-sn-glycero-3-phosphoserine	0.023	1.57
783.51	3.6	[PS (16:0/20:4)] 1-hexadecanoyl-2-(5Z,8Z,11Z,14Z-eicosatetraenoyl)-sn-glycero-3-phosphoserine	0.005	1.36
525.31	4.0	[PS (18:0)] 1-octadecanoyl-sn-glycero-3-phosphoserine	0.001	0.81
569.28	3.9	PS(22:6(4Z,7Z,10Z,13Z,16Z,19Z)/0:0)	0.009	0.70
304.24	7.5	Acutilol A	0.041	1.44
312.23	3.8	[FA (18:2)] 13S-hydroperoxy-9Z,11E-octadecadienoic acid	0.002	0.75
228.17	42.1	7-methoxy-4E-dodecenoic acid	0.027	0.82
330.24	4.0	[FA trihydroxy(18:1)] 9S,12S,13S-trihydroxy-10E-octadecenoic acid	0.019	0.52
379.25	4.5	[SP] Sphing-4-enine-1-phosphate	0.004	2.16
299.28	7.4	[SP] Sphing-4-enine	0.005	1.56
229.24	7.4	[SP (14:0)] 1-deoxy-tetradecasphinganine	0.021	1.11
430.31	4.0	[ST (2:0)] 22S,25S-furospirost-5-en-3beta,26-diol	0.008	0.62
Co-factors and nucleotides				
354.06	5.9	Phenolsulfonphthalein	0.033	0.37
664.09	15.0	Deamino-NAD+	0.021	1.30
123.03	8.0	Nicotinate	0.006	0.44
149.07	11.3	7-Methyladenine	0.011	0.47
151.05	12.6	Guanine	0.009	1.60
135.05	7.5	Adenine	0.016	1.29
111.04	10.4	Cytosine	0.014	0.70
126.04	12.3	Thymine	0.012	0.67

10.3 Chapter 5

Table S3: Comparison of metabolite changes between KT and KC, WT/WC, KT/WT, or KC/WC. KT: TSPO knockout cells with the treatment of oxLDL; KC: TSPO knockout cells without the treatment of oxLDL; WT: Wildtype cells with the treatment of oxLDL; WC: Wildtype cells without the treatment of oxLDL. (m/z) is the mass divided by charge number

Mass (m/z)	RT(min)	Putative metabolite	+/-	KT/KC		WT/WC		KT/WT		KC/WC	
Arginine/creatine metabolism				P value	Ratio	P value	Ratio	P value	Ratio	P value	Ratio
89.05	14.3	sarcosine *	+	0.003	2.75	0.001	2.58	0.012	1.55	0.098	1.45
113.06	15.3	Creatinine*	-	0.002	2.68	0.004	3.36	0.044	1.73	0.005	2.17
115.06	13.4	Proline *	-	0.012	1.36	0.012	1.66	0.114	1.16	0.037	1.42
123.99	12.2	Phosphonoacetaldehyde	+	0.972	0.95	0.047	0.81	0.179	0.86	0.19	0.73
131.07	14.2	Creatine *	+	0.007	3.39	<0.001	4.69	0.001	1.74	0.033	2.41
174.11	26.5	Arginine *	+	0.041	0.69	0.04	0.73	0.049	0.71	0.054	0.75
132.05	15	Asparagine *	+	0.002	0.65	0.014	0.64	0.046	1.27	0.055	1.25
189.06	14.1	N-Acetyl-L-glutamate	-	0.086	2.17	0.001	2.92	0.012	2.24	0.046	3.02
211.04	15.1	Phosphocreatine*	+	<0.001	2.9	<0.001	7.43	0.002	1.37	<0.001	3.5
Histidine/lysine metabolism											
156.05	11	4-Imidazolone-5-propanoate	+	0.03	1.52	0.01	1.67	0.615	0.94	0.833	1.03
159.09	9.3	5-Acetamidopentanoate	+	0.264	0.13	0.043	0.03	0.063	0.84	0.267	0.21
190.06	16.6	N-Carbamyl-L-glutamate *	-	0.001	1.75	<0.001	1.87	<0.001	1.66	0.002	1.77
188.12	11.6	N6-Acetyl-L-lysine *	+	0.256	1.18	0.016	1.65	0.002	0.58	0.263	0.8
Glycolysis											
88.02	8.3	Pyruvate *	-	0.004	0.69	0.001	0.64	0.043	1.22	0.039	1.12
92.05	10.1	Glycerol	-	0.287	0.14	0.035	0.07	0.426	1.04	0.418	0.47

168.99	16.2	Glyceraldehyde 3-P*	-	0.002	1.668	0.031	1.409	<0.001	3.009	<0.001	2.542
182.08	13.6	Mannitol	-	0.696	0.98	0.011	1.57	0.126	1.17	0.002	1.87
185.99	17.2	3-Phosphoglycerate	-	0.03	0.76	0.004	0.81	0.008	1.37	0.005	1.45
260.03	16.8	Glucose 1-phosphate *	-	0.015	1.09	0.042	1.58	0.144	1.07	0.043	1.55
260.03	17.2	Fructose 6-phosphate *	-	0.566	0.94	0.003	1.21	0.047	1.15	0.013	1.48
340	18.5	D-Fructose 1,6-bisphosphate*	-	0.042	1.27	0.039	1.49	0.023	1.63	<0.001	1.92
TCA cycle											
118.03	13.9	Succinate *	-	0.029	1.24	0.18	0.81	0.002	0.67	0.003	0.44
132.01	16.3	Oxaloacetate *	-	0.234	1.01	<0.001	1.21	<0.001	0.86	0.008	1.03
174.02	18.4	cis-Aconitate*	-	0.002	1.44	0.038	1.2	0.003	1.54	0.002	1.28
192.03	18.5	Citrate *	-	0.008	0.85	0.004	0.78	<0.001	1.91	<0.001	1.74
Glutathione homeostasis											
230.02	15.7	Ribose 5-phosphate *	-	0.012	1.24	0.003	1.3	<0.001	1.95	<0.001	2.05
276.02	18	6-Phospho-D-gluconate	-	0.048	1.31	0.013	1.52	0.006	1.28	0.038	1.49
307.083	14.1	Glutathione*	+	0.08	1.61	0.43	1.3	0.77	1.03	0.64	0.83
612.63	17.3	Glutathione disulphide *	-	0.005	2.44	0.031	1.84	0.011	2.23	0.036	1.68
745.09	17.3	NADPH *	+	0.003	1.23	0.03	1.16	0.001	1.35	0.007	1.27
Indicators of oxidative stress											
136.04	9.8	Hypoxanthine *	+	0.573	0.83	0.755	1.03	0.03	1.54	0.059	1.91
152.03	11.2	Xanthine*	-	0.003	0.59	0.002	0.53	0.004	1.57	0.019	1.43
155.07	14.2	Histidine *	+	0.024	1.3	0.015	1.18	0.026	1.19	0.333	1.08
168.03	12.6	Urate*	-	<0.001	1.57	0.021	2.3	0.102	0.61	0.03	0.89
226.106	15.2	carnosine	+	0.06	1.14	0.1	1.32	0.047	1.33	0.01	1.5
240.122	13.6	homocarnosine	+	0.04	1.22	0.28	0.88	0.011	1.85	0.01	1.34
Taurine/cysteine metabolism											

109.02	14.7	Hypotaurine	+	0.217	1.17	0.016	1.38	0.433	0.97	0.392	1.15
105.04	15.5	Serine *	-	0.014	0.75	0.016	0.71	0.605	0.97	0.435	0.92
125.014	15	taurine	+	0.44	0.95	0.62	1.02	0.019	1.17	0.03	1.26
125.999	11	Hydroxyethansulphonate	-	0.004	1.47	0.006	1.72	0.335	0.93	0.42	1.09
147.05	10.5	O-Acetyl-L-serine	-	0.002	1.7	0.005	2.51	0.313	0.9	0.128	1.33
153.01	14.4	3-Sulfino-L-alanine	-	<0.001	2.9	0.005	2.34	0.001	1.4	0.419	1.12
169	15.8	Cysteic Acid	-	0.001	2.92	<0.001	3.87	0.022	1.49	0.001	1.97
Pyrimidines and purines											
111.04	11.4	Cytosine *	+	0.954	0.97	0.049	0.79	0.001	0.46	0.004	0.38
114.04	12	5,6-Dihydrouracil	+	0.029	0.47	0.008	0.5	0.994	1.02	0.768	1.09
125.06	7.4	5-Methylcytosine	+	0.012	0.58	0.009	0.54	0.435	0.97	0.561	0.9
126.04	12.6	Thymine *	+	<0.001	1.91	0.011	1.4	<0.001	1.48	0.332	1.08
128.06	14.3	5,6-Dihydrothymine	+	<0.001	2.38	0.001	2.59	0.001	1.76	0.003	1.91
146.07	14.7	Glutamine *	+	0.051	0.71	0.007	0.67	0.001	1.39	0.126	1.31
244.11	15.1	dihydrothymidine	+	0.016	1.6	0.013	1.65	0.051	1.26	0.142	1.3
268.08	10.4	Inosine	-	0.001	1.2	0.291	0.95	0.022	0.9	0.001	0.72
Fatty acids biosynthesis and conjugates											
102.07	12.8	Pentanoate	+	0.255	0.21	0.003	0.17	0.003	0.57	0.183	0.46
144.12	4.2	[FA (8:0)] octanoic acid	-	0.596	0.89	0.008	1.38	0.025	0.84	0.235	1.29
146.09	4.5	hydroxy-heptanoic acid	-	0.077	1.49	0.002	1.52	0.739	1.04	0.853	1.06
174.13	7.3	hydroxy-nonanoic acid	-	0.294	1.17	0.02	1.49	0.106	0.77	0.857	0.98
224.14	3.8	[FA] Methyl jasmonate	-	0.008	2.24	0.001	1.91	0.062	1.45	0.159	1.23
228.14	4.2	Traumatic acid	-	0.004	1.54	0.033	1.25	0.172	1.1	0.294	0.9
228.17	3.9	oxo-tridecanoic acid	-	0.307	1.22	0.028	0.74	0.078	1.43	0.263	0.86
240.17	4	oxo-Tetradecenoic acid	-	0.002	5.85	0.003	4.76	0.256	1.24	0.888	1.01

n

242.19	3.8	oxo-tetradecanoic acid	-	0.014	1.7	0.014	1.69	0.009	1.26	0.27	1.25
246.15	4.6	3-Hydroxydodecanedioicacid	-	<0.001	6.37	0.001	4.76	0.145	1.37	0.721	1.03
278.22	3.5	octadecatrienoic acid	+	<0.001	4.73	0.032	3.03	0.077	0.67	0.092	0.43
284.27	3.6	Octadecanoic acid	-	0.347	1.15	0.041	0.66	0.016	1.97	0.302	1.12
308.27	3.6	Eicosadienoic acid	-	0.853	1.02	0.007	0.83	0.787	0.98	0.107	0.8
312.23	3.8	13S-hydroperoxy-9Z,11E-octadecadienoic acid	-	0.005	3.55	0.015	3.08	0.514	1.11	0.992	0.96
312.27	3.5	oxo-nonadecanoic acid	+	0.011	1.69	0.005	2.04	0.081	1.37	0.009	1.66
328.24	3.6	Docosahexaenoic acid	-	0.492	0.91	0.018	0.69	0.015	1.68	0.08	1.27
330.24	4.1	trihydroxyoctadecenoic acid	-	<0.001	26	<0.001	13.58	0.014	1.47	0.356	0.77
340.3	3.5	oxo-heneicosanoic acid	+	0.005	2.26	0.003	2.39	0.032	1.4	0.085	1.48
368.22	4.2	Prostaglandin G2	-	<0.001	>1000	<0.001	>1000	0.039	1.25	ND	1
Carnitines											
203.12	10.2	O-Acetylcarnitine	+	0.029	1.3	0.028	1.42	0.647	1.04	0.263	1.14
231.15	7.9	O-Butanoylcarnitine	+	0.011	0.12	0.001	0.19	0.005	0.32	0.125	0.5
399.33	4.2	L-Palmitoylcarnitine	+	<0.001	7.4	0.002	12.62	0.348	0.69	0.449	1.19
425.35	4.2	Oleoylcarnitine	+	0.004	2.26	0.012	2.78	0.648	0.89	0.547	1.09
427.37	4.1	Stearoylcarnitine	+	0.001	5.57	0.001	7.96	0.6	0.87	0.446	1.24
Energy metabolism											
347.06	13.4	AMP*	+	<0.001	1.46	<0.001	1.49	0.154	1.05	0.123	1.07
427.03	15.1	ADP *	-	0.237	1.1	0.026	1.23	0.102	1.18	0.002	1.33
443.02	18.2	GDP *	-	0.075	1.33	0.018	1.81	0.748	1.03	0.047	1.41
507	16.7	ATP *	-	0.006	1.18	0.008	1.34	0.145	1.1	0.004	1.25
522.99	19.8	GTP*	-	0.05	1.28	0.08	1.3	0.13	1.11	0.43	1.12
665.12	13.1	NADH *	-	0.005	1.41	0.004	1.6	0.383	1.08	0.018	1.23

o

Sphingolipids											
273.27	5.2	Hexadecasphinganine	+	<0.001	23.71	<0.001	35.73	0.197	0.76	0.403	1.15
299.28	7.3	Sphingenine	+	0.372	0.78	<0.001	0.8	0.001	1.75	0.053	1.78
327.31	4	N,N-Dimethylsphing-4-enine	+	0.006	2.65	0.003	2.34	0.613	0.92	0.22	0.81
329.33	4.8	dimethylaminooctadecanediol	+	0.003	2.15	0.002	1.91	0.016	1.62	0.016	1.44
535.5	3.7	Cer (d18:2/16:0)	-	0.091	1.4	0.004	2.5	0.139	0.71	0.138	1.26
537.51	3.6	Cer (18:1 16:0)	+	0.204	1.25	0.002	1.78	0.002	0.56	0.192	0.79
699.57	3.7	Glucosylceramide (d18:1/16:0)	-	0.585	1.12	0.01	1.22	0.628	0.94	0.69	1.03
730.6	3.8	SM(d18:1/18:0)	+	0.493	1.1	0.048	1.36	0.114	0.78	0.738	0.97
809.67	3.7	Glucosylceramide (d18:1/24:1)	-	0.024	0.69	0.012	0.61	0.428	0.93	0.207	0.83
Glycerophospholipids											
105.08	19	diethanolamine	+	0.376	0.76	0.044	0.5	0.569	0.85	0.056	0.56
410.24	4.3	LPA 16:0	-	0.002	2.25	0.031	2.04	0.018	1.61	0.134	1.46
437.29	4.2	LPE 16:0 ether	-	0.002	2.06	0.005	1.97	0.001	2	0.009	1.91
438.27	4.1	LPA 18:0	-	0.001	2.74	0.014	2.31	0.015	1.31	0.588	1.1
453.29	4.3	LPE 16:0	+	0.106	2.05	<0.001	2.89	<0.001	1.53	0.205	2.16
481.35	4.3	Lyso PC 16:2	+	0.194	8.27	<0.001	10.21	0.177	0.82	0.436	1.02
495.33	4.3	LPC 16:0	+	0.059	2.23	0.002	3.65	0.026	1.4	0.112	2.29
509.38	4.2	Lyso PC 18:0 ether	+	0.195	7.88	<0.001	5.04	0.03	0.62	0.307	0.39
523.36	4.2	LPC 18:0	+	0.005	3.74	0.001	4.92	0.573	1.14	0.172	1.5
676.54	3.7	PA O-18:0/17:0	+	<0.001	5.7	0.002	5.19	0.761	1.03	0.886	0.94
678.48	3.5	LPG 30:1 ether	-	0.001	2.64	0.01	2.17	0.111	1.41	0.154	1.16
680.5	3.5	PG 30:0	-	<0.001	4.38	0.008	2.4	0.213	1.26	0.039	0.69
694.48	3.5	PG 30:0	-	0.002	0.46	0.013	0.54	0.008	1.87	0.003	2.22
720.49	3.5	PG 32:1	-	0.008	0.56	0.03	0.65	0.013	1.72	0.005	2

722.51	3.5	PG 32:0	-	0.003	0.49	0.004	0.64	0.001	1.79	0.002	2.32
734.55	3.5	LPG 34:1 ether	-	<0.001	2.38	0.025	1.66	0.56	1.06	0.084	0.74
771.54	3.8	PS 36:3 ether	-	0.05	34.24	0.12	>1000	0.32	2.52	0.37	>1000
773.54	3.6	PE 40:7 ether	-	0.017	0.75	0.001	0.64	0.538	1.06	0.068	0.9
773.557	3.7	PS 36:2 ether	+	0.06	139.3	0.12	19.83	0.19	1.05	0.85	0.15
776.56	3.5	PG 36:1	-	0.071	2.07	0.011	1.79	<0.001	1.23	0.965	1.07
783.58	3.7	PC 36:3	+	<0.001	2.25	<0.001	2.29	0.145	1.12	0.001	1.14
785.52	3.5	PS 36:3	-	<0.001	2.44	0.002	3.01	0.07	0.78	0.855	0.96
797.56	3.7	PS 38:4 ether	+	<0.001	>1000	<0.001	>1000	0.014	1.14	*ND	1
799.57	3.7	PS 38:3 ether	+	<0.001	9.45	<0.001	9.86	0.355	1.08	0.477	1.13
815.57	3.5	PS 38:2	-	0.01	0.66	0.035	0.79	0.052	0.77	0.277	0.92
817.58	3.5	PS 38:1	-	0.042	0.74	0.003	0.74	0.025	0.81	0.08	0.81
831.58	3.7	PC 40:7	+	0.001	0.47	0.05	0.61	0.181	1.2	0.037	1.56
843.6	3.5	PS 40:2	-	0.003	0.52	0.001	0.62	0.017	0.67	0.027	0.81
858.53	3.5	PI 36:4	-	0.002	2.24	<0.001	2.41	0.008	1.36	0.037	1.46
859.61	3.7	PC 42:7	+	0.015	0.55	0.007	0.52	0.1	1.22	0.44	1.16
866.51	3.4	PG 44:12	-	0.003	0.54	0.014	0.66	0.005	1.51	0.006	1.84
871.63	3.5	PS 42:2	-	0.001	0.3	<0.001	0.4	<0.001	0.6	0.127	0.81
879.59	3.6	PI 36:0	+	0.157	0.57	0.038	0.65	0.001	0.4	0.045	0.45
900.57	3.5	PI 17:0/22:4	-	0.013	0.77	0.003	0.7	0.164	1.1	0.895	1.01
Miscellaneous											
100.05	4.4	glutaraldehyde	-	0.839	1.01	0.002	0.66	<0.001	1.77	0.336	1.15
172.01	13.8	sn-glycerol-1-phosphate	-	0.088	1.52	0.003	2.22	0.08	1.29	0.04	1.88
179.08	10.7	D-Glucosamine or isomer	-	0.634	1.11	0.043	1.42	0.723	0.96	0.152	1.23
187.1	13.3	5-guanidino-3-methyl-2-oxo-	+	0.007	0.46	0.031	0.5	<0.001	3.02	0.008	3.3

		pentanoate									
466.311	3.5	Cholesterolsulfate	-	<0.001	3.47	<0.001	3.49	0.82	1.04	0.75	1.05

(*) means that metabolite matches standard retention time

r

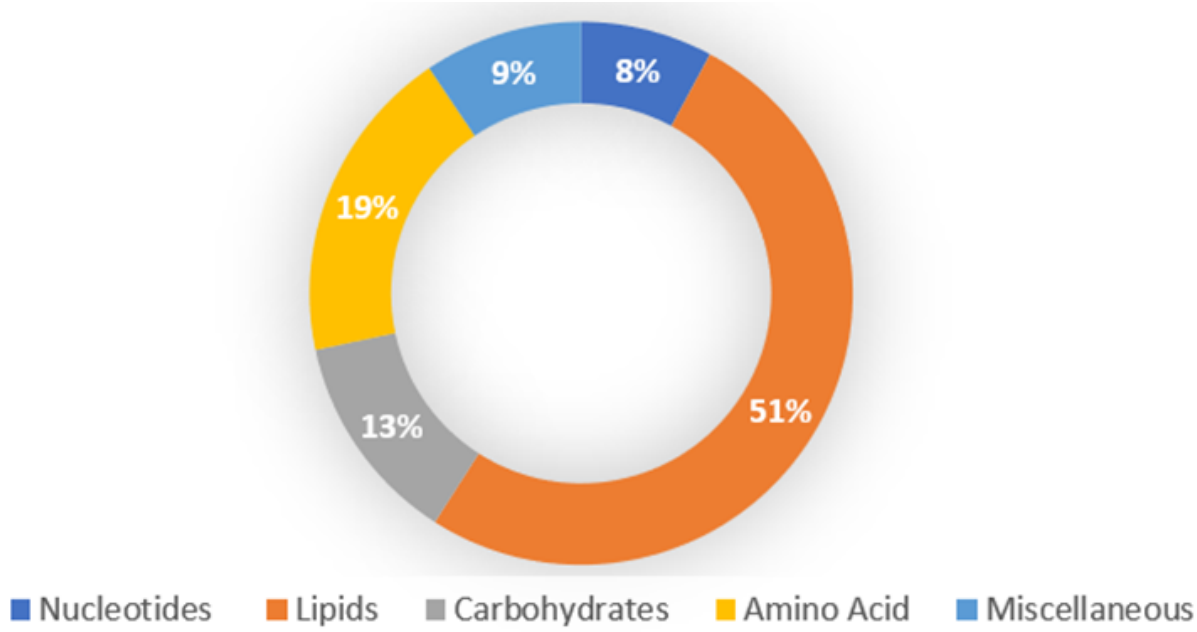

Figure S2.: Overview of the implication of different pathway to all significantly affected metabolites. Lipid pathway is the most influenced pathway while nucleotides were the least.

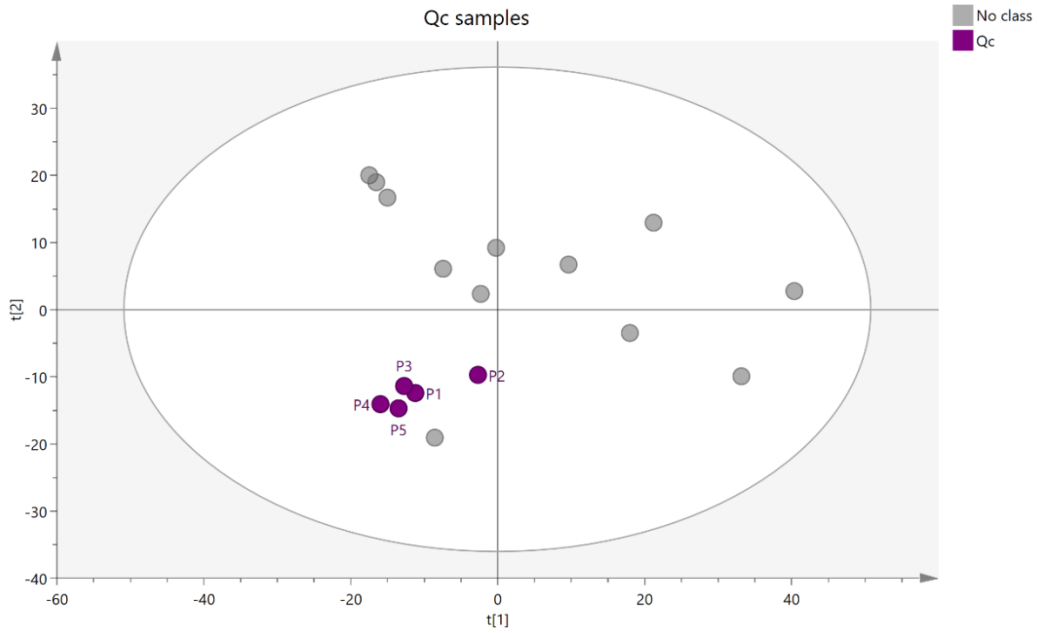

Figure S3: Principle component analysis (PCA) score plot for quality control (QC) (pooled) cell extract samples of wildtype and *TSPO* knockout RPE cells. P1, P2, P3, P4 and P5 are pooled (QC) sample runs throughout the experiment and reflect the goodness of device sensitivity.

10.4 Chapter 6

Table S4: Comparison of metabolite changes between normal, high glucose and high glucose with vitamin D RPE cells.

Mass	RT	Putative metabolite	Ratio hg/lg	p hg-lg	Ratio D/hg	p D/hg
Amino acids						
203.12	10.93	O-Acetylcarnitinez	4.58	<0.001	1.03	0.875
226.11	16.02	Carnosine *	1.93	<0.001	0.84	0.018
123.99	15.24	Phosphonoacetaldehyde	2.01	0.004	0.67	0.009
216.11	12.42	gamma-Glutamyl-gamma-aminobutyraldehyde	0.76	0.024	1.13	0.128
240.12	14.34	Homocarnosine	2.54	0.007	0.98	0.920
132.05	12.74	N-Carbamoylsarcosine	0.63	0.049	0.79	0.181
211.04	15.80	Phosphocreatine *	0.54	0.034	1.10	0.462
115.06	12.98	Proline *	3.07	<0.001	1.05	0.692
126.12	11.07	1-5-diazabicyclononane	2.51	0.001	0.85	0.500
245.15	16.40	beta-Alanyl-L-arginine	1.59	0.036	1.05	0.590
217.14	22.59	beta-Alanyl-L-lysine	2.44	0.018	1.06	0.781
87.03	15.72	2-Aminoacrylate	0.52	0.017	1.09	0.542
174.11	26.54	Arginine *	0.27	0.001	1.80	0.034
132.09	24.76	Ornithine *	1.36	0.006	0.92	0.138
301.06	15.85	N-Acetyl-D-glucosamine 6-phosphate *	26.67	<0.001	1.18	0.311
307.08	14.31	Glutathione *	0.73	0.027	0.83	0.326
612.15	17.47	Glutathione disulphide *	1.28	0.049	1.01	0.873
129.04	16.47	5-Oxoproline	2.05	<0.001	0.89	0.013

178.04	17.16	Cys-Gly	2.19	0.006	0.88	0.506
101.08	13.39	Betaine aldehyde	1.95	0.004	0.89	0.394
141.02	16.33	Ethanolamine phosphate	53.44	<0.001	0.88	0.325
119.06	14.93	Threonine	1.41	0.016	0.86	0.213
258.09	10.86	(1-Ribosylimidazole)-4-acetate	1.15	0.025	0.93	0.387
156.05	11.83	4-Imidazolone-5-propanoate	3.84	<0.001	1.04	0.677
140.06	10.03	Methylimidazoleacetic acid	1.77	0.011	0.94	0.005
138.04	11.53	Urocanate	0.57	0.030	1.04	0.260
203.08	15.87	N2-Acetyl-L-aminoadipate	15.71	<0.001	1.13	0.450
283.05	15.85	N2-Acetyl-L-aminoadipyl-delta-phosphate	26.61	<0.001	1.22	0.268
145.11	13.41	4-Trimethylammoniobutanoate	2.38	0.001	0.91	0.280
159.09	12.93	5-Acetamidopentanoate	2.02	0.005	0.89	0.382
161.11	13.40	Carnitine *	1.89	0.007	0.90	0.366
218.13	14.43	N2-(D-1-Carboxyethyl)-L-lysine	5.83	0.000	1.03	0.758
188.12	12.93	N6-Acetyl-L-lysine	1.86	<0.001	0.93	0.633
101.05	15.40	1-Aminocyclopropane-1-carboxylate	0.82	0.005	1.13	0.099
219.07	14.73	O-Succinyl-L-homoserine	9382.43	0.000	1.14	0.646
474.96	12.69	Adenylylselenate	1.28	0.029	0.85	0.232
254.06	16.57	5-Glutamyl-taurine	2.30	0.003	1.35	0.012
149.05	8.27	4-Hydroxymandelonitrile	3.42	0.003	0.79	0.306
186.02	15.07	Maleylpyruvate	0.30	0.004	1.55	0.010
158.06	9.58	2-Isopropylmaleate	0.58	0.004	0.95	0.639
Sugar metabolites						
614.15	15.88	CMP-N-acetylneuraminate	2.40	0.004	1.06	0.617
607.08	15.85	UDP-N-acetyl-D-glucosamine *	29.46	<0.001	1.21	0.187

b

256.00	20.22	Ascorbate 6-phosphate	5.48	<0.001	0.89	0.013
586.35	4.09	6,8a-Seco-6,8a-deoxy-5-oxoavermectin ''2a'' aglycone	0.36	0.007	0.93	0.597
529.09	15.41	dTDP-3-amino-2,3,6-trideoxy-D-threo-hexopyranos-4-ulose	0.49	0.016	1.14	0.459
168.02	17.16	Butanoylphosphate	1.61	<0.001	0.75	0.137
202.10	13.68	Proclavaminic acid	0.72	0.028	1.13	0.736
330.26	3.54	Taxa-4(20),11(12)-dien-5alpha-yl acetate	2.29	0.008	0.99	0.941
262.05	15.90	D-Mannitol 1-phosphate	11193.26	0.000	1.24	0.124
605.08	19.09	GDP-mannose	2.22	0.014	1.26	0.094
179.08	14.03	Galactosamine	3.86	0.000	0.74	0.007
809.13	12.69	Acetyl-CoA *	1.17	0.002	0.96	0.173
260.03	17.53	Glucose 6-phosphate *	5.38	<0.001	1.13	0.016
665.12	14.00	NADH *	3.00	0.002	1.04	0.727
663.11	14.35	NAD+ *	1.85	0.010	1.01	0.886
506.99	17.23	ATP *	2.24	<0.001	0.90	0.026
427.03	15.1	ADP *	1.64	0.013	1.06	0.743
580.03	20.21	UDP-glucuronate	5.43	0.002	1.17	0.248
566.05	17.20	UDP-glucose	4.41	0.001	1.03	0.992
290.04	16.95	Sedoheptulose 7-phosphate	4.79	<0.001	1.02	0.816
214.02	17.41	2-Deoxy-D-ribose 1-phosphate	16.68	0.044	1.09	0.527
745.09	17.80	NADPH *	0.89	0.008	1.11	0.010
342.12	16.29	Cellobiose	0.76	0.030	1.07	0.796
222.07	17.62	Cystathionine	2.49	0.023	1.19	0.446
Lipids						
691.55	3.87	PC(o-14:0/16:0)	0.45	0.007	1.07	0.756
436.26	7.64	Stearoylglycerone phosphate	0.31	0.010	1.37	0.345

851.58	3.51	[SP] (3'-sulfo)Galbeta-Cer(d18:0/2-OH-20:0)	2.61	0.010	1.21	0.513
376.30	3.54	3alpha-Hydroxy-5beta-cholanate	2.12	0.009	0.94	0.626
216.04	15.06	2-C-Methyl-D-erythritol 4-phosphate	1.58	0.006	0.72	0.008
338.32	4.11	[FA (22:0)] 13Z-docosenoic acid	0.68	0.002	1.03	0.906
328.24	3.53	Docosahexaenoicacid	2.61	0.003	1.02	0.970
368.37	3.63	Tetracosanoic acid	0.51	<0.001	1.26	0.009
318.26	3.52	3alpha-Hydroxy-5beta-pregnane-20-one	1.73	0.006	1.01	0.992
728.58	3.93	SM(d18:1/18:1(11Z))	1.65	0.037	1.11	0.439
617.48	6.10	[SP (16:0)] N-(hexadecanoyl)-sphing-4-enine-1-phosphate	2.50	0.003	0.39	0.001
393.40	3.75	cholest-5-en-3beta-ol(d7)	1.97	0.006	1.46	0.047
688.51	3.61	[GL (20:4/22:6)] 1-(5Z,8Z,11Z,14Z-eicosatetraenoyl)-2-(4Z,7Z,10Z,13Z,16Z,19Z-docosahexaenoyl)-sn-glycerol	0.81	0.013	1.51	0.003
648.51	3.62	[GL (8:0/8:0)] 1-(8-[5]-ladderane-octanoyl)-2-(8-[3]-ladderane-octanyl)-sn-glycerol	0.54	0.024	0.98	0.896
602.53	3.62	[GL methyl(15:0/8:0)] 1-(14-methyl-pentadecanoyl)-2-(8-[3]-ladderane-octanyl)-sn-glycerol	0.48	0.006	1.16	0.259
550.50	3.58	1-O-(1Z-Tetradecenyl)-2-(9Z-octadecenoyl)-sn-glycerol	0.57	0.022	1.36	0.029
254.22	3.81	(9Z)-Hexadecenoic acid	0.61	0.005	0.98	0.549
228.21	3.89	Tetradecanoic acid	0.60	<0.001	1.04	0.425
240.25	4.32	Hexadecanal	0.68	0.018	1.18	0.205
226.19	3.83	(9Z)-Tetradecenoic acid	0.46	0.005	1.02	0.900
304.24	3.68	[FA (20:4)] 5Z,8Z,11Z,14Z-eicosatetraenoic acid	1.55	0.002	1.00	0.978
332.27	3.55	[FA (22:4)] 7Z,10Z,13Z,16Z-docosatetraenoic acid	1.89	0.010	0.97	0.804
282.26	7.63	[FA (7:2/11:0)] 11-Cycloheptylundecanoic acid	0.34	0.006	1.19	0.434
284.24	3.59	[FA methoxy(16:1)] 2-methoxy-5Z-hexadecenoic acid	0.41	0.008	1.43	0.003
270.26	7.60	[FA methyl(16:0)] 3-methyl-hexadecanoic acid	0.59	0.033	1.17	0.348

d

284.27	3.96	[FA methyl(17:0)] 10-methyl-heptadecanoic acid	0.68	0.025	1.73	0.017
284.27	7.64	[FA methyl(17:0)] 15-methyl-heptadecanoic acid	0.42	0.013	1.15	0.555
340.30	3.60	[FA oxo(21:0)] 2-oxo-heneicosanoic acid	1.39	0.038	1.33	0.010
256.24	7.63	[FA trimethyl(13:0)] 4,8,12-trimethyl-tridecanoic acid	0.42	0.017	1.06	0.789
334.29	3.58	13,16,19-Docosatrienoic acid	2.16	<0.001	1.02	0.909
268.24	7.54	16:1(6Z)(15Me)	0.54	0.020	1.10	0.224
280.24	7.60	16:2(2E,4E)(4Me,6Me[S])	0.36	0.006	1.00	0.976
290.22	3.56	16:4(2E,4E,8E,10E)(7Me[R],9Me,14Me[R])	1.72	0.004	1.01	0.931
310.29	7.61	20:1(7Z)	0.35	0.004	1.06	0.718
268.24	3.57	omega-Cyclohexylundecanoic acid	0.68	0.015	1.01	0.947
240.25	7.64	11E-Hexadecen-1-ol	0.56	0.002	1.22	0.024
226.23	3.76	Pentadecanal	1.97	0.003	0.91	0.613
389.26	3.68	[FA (18:0)] N-(9Z-octadecenoyl)-taurine	0.08	<0.001	1.27	0.008
391.28	3.67	[FA (18:0)] N-octadecanoyl-taurine	0.18	<0.001	1.11	0.317
253.24	3.76	Palmitoleamide	0.62	0.002	1.36	0.017
410.24	4.33	LPA(0:0/16:0)	0.43	0.003	1.21	0.175
436.26	4.30	LPA(0:0/18:1(9Z))	0.42	0.002	1.22	0.216
436.26	3.62	LPA(18:1(9Z)/0:0)	0.72	0.023	1.16	0.142
434.24	4.28	LPA(18:2(9Z,12Z)/0:0)	0.39	0.006	1.10	0.698
646.46	3.89	[GP (14:0/18:1)] 1-tetradecanoyl-2-(9Z-octadecenoyl)-sn-glycero-3-phosphate	0.70	0.013	1.05	0.615
620.44	3.90	[GP (15:0/15:0)] 1,2-dipentadecanoyl-sn-glycero-3-phosphate	0.66	0.048	1.05	0.555
410.24	3.91	[GP (16:0)] 1-hexadecanoyl-2-sn-glycero-3-phosphate	0.76	0.033	1.00	0.971
672.47	3.87	[GP (16:0/18:2)] 1-hexadecanoyl-2-(9Z,12Z-octadecadienoyl)-sn-glycero-3-phosphate	0.76	0.038	1.02	0.859
616.41	3.88	PA(12:0/18:2(9Z,12Z))	0.85	0.025	1.06	0.668

614.39	3.87	PA(12:0/18:3(6Z,9Z,12Z))	0.61	0.011	1.04	0.929
632.44	3.88	PA(12:0/19:1(9Z))	0.66	0.031	1.00	0.969
642.43	3.92	PA(12:0/20:3(8Z,11Z,14Z))	1.37	0.047	0.94	0.510
618.43	3.91	PA(13:0/17:1(9Z))	0.64	0.018	1.09	0.543
698.49	3.83	PA(14:1(9Z)/22:2(13Z,16Z))	0.76	0.002	0.96	0.455
462.27	4.29	PA(20:2(11Z,14Z)/0:0)	0.35	<0.001	1.33	0.040
460.26	4.15	PA(20:3(8Z,11Z,14Z)/0:0)	0.50	<0.001	1.08	0.229
482.24	3.53	PA(22:6(4Z,7Z,10Z,13Z,16Z,19Z)/0:0)	2.51	0.003	0.99	0.898
467.30	4.48	[PC (14:0)] 1-tetradecanoyl-sn-glycero-3-phosphocholine	0.13	<0.001	1.76	0.065
677.50	3.91	[PC (14:0/14:0)] 1,2-ditetradecanoyl-sn-glycero-3-phosphocholine	0.58	0.024	0.99	0.984
705.53	3.87	[PC (14:0/16:0)] 1-tetradecanoyl-2-hexadecanoyl-sn-glycero-3-phosphocholine	0.68	0.042	1.06	0.561
703.52	3.89	[PC (14:0/16:1)] 1-tetradecanoyl-2-(9Z-hexadecenoyl)-sn-glycero-3-phosphocholine	0.73	0.045	0.92	0.234
731.55	4.46	[PC (14:0/18:1)] 1-tetradecanoyl-2-(9Z-octadecenoyl)-sn-glycero-3-phosphocholine	0.37	0.020	1.40	0.242
481.32	4.45	[PC (15:0)] 1-pentadecanoyl-sn-glycero-3-phosphocholine	0.21	0.001	1.68	0.017
745.56	4.22	[PC (15:0/18:1)] 1-pentadecanoyl-2-(9Z-octadecenoyl)-sn-glycero-3-phosphocholine	0.35	0.003	1.96	0.084
743.55	3.78	[PC (15:0/18:2)] 1-pentadecanoyl-2-(9Z,12Z-octadecadienoyl)-sn-glycero-3-phosphocholine	0.73	0.009	1.05	0.566
495.33	3.92	[PC (16:0)] 1-hexadecanoyl-sn-glycero-3-phosphocholine	0.64	0.001	1.04	0.215
813.62	4.51	[PC (16:0/22:2)] 1-hexadecanoyl-2-(13Z,16Z-docosadienoyl)-sn-glycero-3-phosphocholine	0.35	0.017	1.59	0.129
493.32	7.64	[PC (16:1)] 1-(9E-hexadecenoyl)-sn-glycero-3-phosphocholine	0.36	0.002	1.63	0.034
785.59	3.78	[PC (18:1/18:1)] 1-(9Z-octadecenoyl)-2-(9Z-octadecenoyl)-sn-glycero-3-phosphocholine	0.74	0.010	0.98	0.722
493.32	4.46	LysoPC(16:1(9Z))	0.12	<0.001	1.82	0.018

509.35	4.26	LysoPC(17:0)	0.56	0.012	1.41	0.199
523.36	4.45	LysoPC(18:0)	0.25	0.009	1.77	0.072
521.35	7.65	LysoPC(18:1(9Z))	0.32	0.021	1.40	0.324
727.52	3.86	PC(14:0/18:3(6Z,9Z,12Z))	1.92	0.011	0.83	0.109
757.56	3.80	PC(14:0/20:2(11Z,14Z))	0.71	0.005	1.00	0.964
755.55	3.81	PC(14:0/20:3(5Z,8Z,11Z))	0.79	<0.001	1.01	0.676
785.59	4.48	PC(14:0/22:2(13Z,16Z))	0.37	0.015	1.37	0.258
689.50	3.86	PC(14:1(9Z)/15:0)	0.54	<0.001	1.08	0.296
701.50	3.89	PC(14:1(9Z)/16:1(9Z))	1.45	0.050	0.97	0.754
757.56	4.49	PC(14:1(9Z)/20:1(11Z))	0.36	0.020	1.37	0.297
783.58	3.82	PC(14:1(9Z)/22:2(13Z,16Z))	0.65	0.013	1.03	0.759
813.62	3.73	PC(14:1(9Z)/24:1(15Z))	0.63	0.002	1.17	0.043
741.53	4.50	PC(15:0/18:3(6Z,9Z,12Z))	0.32	0.008	1.56	0.053
739.52	3.76	PC(15:0/18:4(6Z,9Z,12Z,15Z))	0.48	0.005	1.32	0.065
771.58	3.79	PC(15:0/20:2(11Z,14Z))	0.72	0.002	0.99	0.894
769.56	3.78	PC(15:0/20:3(5Z,8Z,11Z))	0.71	0.012	1.08	0.290
765.53	3.74	PC(15:0/20:5(5Z,8Z,11Z,14Z,17Z))	0.58	0.009	1.08	0.527
801.62	3.86	PC(15:0/22:1(13Z))	0.65	0.034	0.92	0.581
799.61	3.74	PC(15:0/22:2(13Z,16Z))	0.78	0.004	1.03	0.665
745.60	3.80	PC(16:0/P-18:0)	0.49	0.014	1.24	0.284
717.53	4.50	PC(16:1(9Z)/15:0)	0.38	0.019	1.48	0.215
811.61	3.73	PC(16:1(9Z)/22:2(13Z,16Z))	0.81	0.049	1.11	0.133
841.65	3.74	PC(16:1(9Z)/24:1(15Z))	0.57	0.010	1.30	0.046
743.55	4.50	PC(18:2(9Z,12Z)/15:0)	0.35	0.012	1.53	0.111
863.64	3.72	PC(18:4(6Z,9Z,12Z,15Z)/24:1(15Z))	0.57	0.003	1.11	0.387

823.65	3.72	PC(22:2(13Z,16Z)/P-18:1(11Z))	1.57	0.005	1.10	0.553
795.58	4.53	PC(22:4(7Z,10Z,13Z,16Z)/15:0)	0.48	0.047	1.41	0.207
439.31	4.32	PC(O-12:0/O-1:0)	0.48	0.009	1.50	0.032
883.53	3.54	PS(22:4(7Z,10Z,13Z,16Z)/22:6(4Z,7Z,10Z,13Z,16Z,19Z))	5.47	0.002	1.12	0.580
453.29	3.80	[PE (16:0)] 1-hexadecanoyl-sn-glycero-3-phosphoethanolamine	0.69	0.028	1.16	0.237
437.29	4.46	[PE (16:1)] 1-(1Z-hexadecenyl)-sn-glycero-3-phosphoethanolamine	0.36	0.044	1.59	0.145
481.32	7.64	[PE (18:0)] 1-octadecanoyl-sn-glycero-3-phosphoethanolamine	0.39	0.007	1.27	0.288
751.55	3.70	[PE (18:1/20:4)] 1-(1Z-octadecenyl)-2-(5Z,8Z,11Z,14Z-eicosatetraenoyl)-sn-glycero-3-phosphoethanolamine	1.69	0.001	1.24	0.042
453.29	4.48	LysoPE(0:0/16:0)	0.19	<0.001	1.31	0.249
479.30	4.26	LysoPE(0:0/18:1(11Z))	0.34	<0.001	1.15	0.319
479.30	7.64	LysoPE(18:1(11Z)/0:0)	0.23	0.002	1.14	0.444
715.52	3.85	PE(14:0/20:2(11Z,14Z))	0.66	0.016	0.92	0.467
713.50	3.87	PE(14:0/20:3(5Z,8Z,11Z))	0.71	0.001	1.04	0.631
463.27	4.38	PE(17:2(9Z,12Z)/0:0)	0.23	<0.001	1.38	0.033
797.59	3.75	PE(18:1(11Z)/22:2(13Z,16Z))	0.75	0.005	0.95	0.423
723.52	3.72	PE(18:3(6Z,9Z,12Z)/P-18:1(11Z))	1.61	0.004	1.03	0.532
721.51	3.74	PE(18:4(6Z,9Z,12Z,15Z)/P-18:1(11Z))	1.50	0.042	1.14	0.436
749.54	3.72	PE(20:4(5Z,8Z,11Z,14Z)/P-18:1(11Z))	1.70	0.001	1.11	0.159
822.54	3.53	[PG (18:0/22:6)] 1-octadecanoyl-2-(4Z,7Z,10Z,13Z,16Z,19Z-docosahexaenoyl)-sn-glycero-3-phospho-(1'-sn-glycerol)	1.56	0.028	0.98	0.809
746.51	3.55	PG(16:0/18:2(9Z,12Z))	0.31	<0.001	1.05	0.864
742.48	3.55	PG(16:1(9Z)/18:3(6Z,9Z,12Z))	0.58	0.040	0.85	0.408
768.49	3.53	PG(16:1(9Z)/20:4(5Z,8Z,11Z,14Z))	0.76	0.006	1.18	0.476
826.57	3.53	PG(18:0/22:4(7Z,10Z,13Z,16Z))	1.46	0.023	1.05	0.688
820.53	3.52	PG(18:1(11Z)/22:6(4Z,7Z,10Z,13Z,16Z,19Z))	1.70	0.018	1.03	0.885

h

790.48	3.54	PG(18:3(6Z,9Z,12Z)/20:5(5Z,8Z,11Z,14Z,17Z))	2.58	0.003	1.05	0.946
848.56	3.52	PG(20:1(11Z)/22:6(4Z,7Z,10Z,13Z,16Z,19Z))	2.24	0.006	1.02	0.893
846.54	3.53	PG(20:2(11Z,14Z)/22:6(4Z,7Z,10Z,13Z,16Z,19Z))	1.89	0.010	1.05	0.775
534.30	3.53	PG(20:3(8Z,11Z,14Z)/0:0)	1.63	0.038	0.95	0.748
844.53	3.53	PG(20:3(8Z,11Z,14Z)/22:6(4Z,7Z,10Z,13Z,16Z,19Z))	2.88	0.001	1.07	0.760
842.51	3.53	PG(20:4(5Z,8Z,11Z,14Z)/22:6(4Z,7Z,10Z,13Z,16Z,19Z))	4.74	<0.001	0.94	0.615
556.28	3.52	PG(22:6(4Z,7Z,10Z,13Z,16Z,19Z)/0:0)	2.29	0.008	1.16	0.290
840.49	3.53	PG(22:6(4Z,7Z,10Z,13Z,16Z,19Z)/20:5(5Z,8Z,11Z,14Z,17Z))	5855.10	0.000	0.97	0.782
870.54	3.52	PG(22:6(4Z,7Z,10Z,13Z,16Z,19Z)/22:4(7Z,10Z,13Z,16Z))	5.16	<0.001	1.10	0.715
866.51	3.52	PG(22:6(4Z,7Z,10Z,13Z,16Z,19Z)/22:6(4Z,7Z,10Z,13Z,16Z,19Z))	5.62	0.001	1.11	0.625
706.51	3.56	PG(O-16:0/16:1(9Z))	0.69	0.034	1.49	0.039
572.30	4.12	[PI (16:0)] 1-hexadecanoyl-sn-glycero-3-phospho-(1'-myo-inositol)	0.24	<0.001	1.27	0.259
600.33	4.06	[PI (18:0)] 1-octadecanoyl-sn-glycero-3-phospho-(1'-myo-inositol)	0.44	0.006	1.22	0.225
879.58	3.62	[PI (18:0/18:0)] 1,2-di-(9Z-octadecenoyl)-sn-glycero-3-phospho-(1'-myo-inositol)(ammonium salt)	0.41	0.002	1.20	0.324
598.31	7.64	[PI (18:1)] 1-(9Z-octadecenoyl)-sn-glycero-3-phospho-(1'-myo-inositol)	0.24	0.005	1.08	0.794
620.30	3.67	[PI (20:4)] 1-(5Z,8Z,11Z,14Z-eicosatetraenoyl)-sn-glycero-3-phospho-(1'-myo-inositol)	0.48	0.001	1.08	0.676
832.51	3.63	PI(14:0/20:3(8Z,11Z,14Z))	0.39	<0.001	0.99	0.820
864.57	3.60	PI(14:0/22:1(11Z))	0.57	0.013	1.70	0.004
808.51	3.64	PI(16:0/16:1(9Z))	0.21	<0.001	1.19	0.082
836.54	3.62	PI(16:0/18:1(11Z))	0.41	0.005	1.31	0.008
834.52	3.62	PI(16:0/18:2(9Z,12Z))	0.23	<0.001	1.16	0.161
833.52	3.61	PI(16:0/18:2)-Na	0.67	0.022	1.14	0.174
862.56	3.61	PI(16:0/20:2(11Z,14Z))	0.46	0.003	1.19	0.179
860.54	3.61	PI(16:0/20:3(5Z,8Z,11Z))	0.34	0.004	1.27	0.024

882.53	3.60	PI(16:0/22:6(4Z,7Z,10Z,13Z,16Z,19Z))	0.36	<0.001	1.22	0.005
900.57	3.60	PI(17:0/22:4(7Z,10Z,13Z,16Z))	0.43	0.006	1.32	0.326
914.59	3.59	PI(18:0/22:4(10Z,13Z,16Z,19Z))	0.55	0.022	1.21	0.383
596.30	4.08	PI(18:2(9Z,12Z)/0:0)	0.29	<0.001	1.28	0.280
626.34	4.00	PI(20:1(11Z)/0:0)	0.38	<0.001	1.25	0.039
584.33	4.10	PI(P-18:0/0:0)	0.12	<0.001	1.32	0.276
446.06	16.88	CDP-ethanolamine	3.68	<0.001	0.92	0.496
149.11	9.40	Triethanolamine	0.67	0.001	0.92	0.386
761.52	3.62	[PS (16:0/18:1)] 1-hexadecanoyl-2-(9Z-octadecenoyl)-sn-glycero-3-phosphoserine	0.67	0.045	1.28	0.059
763.54	3.55	PS(16:0/18:0)	0.28	0.009	1.17	0.413
787.53	3.62	PS(18:0/18:2(9Z,12Z))	0.60	0.008	1.31	0.025
867.60	3.56	PS(20:0/22:4(7Z,10Z,13Z,16Z))	1.85	0.020	1.25	0.034
857.52	3.56	PS(20:3(8Z,11Z,14Z)/22:6(4Z,7Z,10Z,13Z,16Z,19Z))	18177.80	0.000	1.06	0.944
546.46	3.63	[PR] bacteriohopane-32,33,34,35-tetrol	0.27	<0.001	1.98	0.040
278.22	3.64	[FA (18:3)] 6Z,9Z,12Z-octadecatrienoic acid	0.58	0.009	1.09	0.548
280.24	3.54	Linoleate	0.60	0.021	1.01	0.982
217.13	9.58	O-Propanoylcarnitine	0.58	0.002	1.03	0.874
700.55	3.94	SM(d16:1/18:1)	1.97	<0.001	1.07	0.311
810.66	3.87	SM(d18:2/24:1)	1.51	0.005	1.13	0.003
390.31	3.54	[ST (3:0/3:0)] (5Z,7E)-A-dinor-(1,2)-(9,10)-diseco-5,7,10(19)-cholestatriene-1,2,25-triol	2.56	0.011	1.05	0.847
317.29	7.72	[SP hydrox] 4-hydroxysphinganine	2.95	0.009	1.21	0.298
699.56	3.64	Glucosylceramide (d18:1/16:0)	4.24	0.013	1.50	0.002
316.24	3.55	[ST hydrox] 3beta-hydroxypregn-5-ene-20-one	1.53	0.012	1.03	0.846
102.03	13.40	Acetoacetate *	1.87	0.002	1.01	0.970

Nucleotides						
347.06	17.29	3'-AMP	1.37	<0.001	0.99	0.888
443.02	19.00	GDP *	2.07	0.015	0.95	0.646
151.05	12.60	Guanine *	0.32	0.006	0.95	0.810
363.06	17.37	Guanosine 3'-phosphate	0.81	0.035	1.07	0.888
136.04	10.29	Hypoxanthine *	0.62	0.003	0.81	0.036
268.08	11.06	Inosine *	0.60	0.002	1.02	0.976
152.03	3.88	Xanthine *	0.43	0.011	1.21	0.570
522.99	20.64	GTP	2.66	0.004	0.98	0.809
323.05	16.85	3'-CMP	3.53	0.005	1.11	0.925
324.04	17.41	UMP *	4.29	<0.001	1.04	0.961
128.06	14.99	5,6-Dihydrothymine	0.49	0.006	1.04	0.759
482.98	19.36	CTP *	1.57	0.014	1.08	0.668
243.09	12.08	Cytidine *	0.17	0.001	1.05	0.962
228.07	8.21	Deoxyuridine	1.55	0.034	0.74	0.032
324.04	20.21	Pseudouridine 5'-phosphate	5.64	0.001	0.88	0.515
126.04	12.68	Thymine *	2.11	0.010	0.76	0.033
114.04	12.72	5,6-Dihydrouracil	0.57	0.003	0.86	0.272